Cellular response to PorA-Loop4-derived peptides of *Neisseria meningitidis*

RININTA FIRDAUS
BSc. MSc.

Thesis submitted to University of Nottingham for the degree of Doctor of Philosophy

APRIL 2019

Molecular Bacteriology and Immunology Group
School of Life Sciences
University of Nottingham

Declaration

With exception of reference to other people's work, which has been duly acknowledge, I declare that the work presented in this thesis is the result of my own research and has not been submitted in any form for the award of a higher education degree elsewhere.

……..

(26/04/2019)

Rininta Firdaus
PhD Student
Molecular Bacteriology and Immunology Group
School of Life Sciences
University of Nottingham

This thesis is dedicated to the memories of my father,
Achmadhy Bambang Soedinarto (1952-2016),
who always believed in my ability to be successful in academia.
You are gone, but your belief in me has made this journey possible.

Acknowledgements

First and foremost, all praise and thanks are due to Allah, the Most Gracious, and the Most Merciful for all his blessings and for making me able to go through this PhD journey and write this thesis.

I would like to thank my supervisors, Dr. Karl Wooldridge and Dr. Neil Oldfield for giving me the opportunity to carry out my PhD studies in the Molecular Bacteriology and Immunology Group (MBIG). Without their support, patience and guidance, this study would not have been completed. I would also like to thank my internal and external assessors, Dr. Alan Cockayne and Dr. Darryl Hill for their comments and suggestions to improve this study.

I gratefully acknowledge the financial support provided by Lembaga Pengelola Dana Pendidikan (Indonesian Endowment Fund for Education) and the Faculty of Pharmacy Pancasila University, who have funded my PhD study at the University of Nottingham.

A big thank you to all past and present members of MBIG: Sozan Qarani, Mahab Al Jannat, Osman Dufailu, Banan Atwah, Iyelola Turner, Shoma Dutta, who always shared their time for helping me in the office and lab. I am grateful to all my friends, Denny Vitasari, Wahyu Utami, Raras Tyasnurita, and Dewi Yunita for your lovely company to get away from the stressful time. Also, I would like to thank all Indonesian members of PeDLN society as my family in Nottingham.

I would like to thank my family in Indonesia, Ibu Khusnawiyah, Iqbal Dwi Rahmanto, Nenden Ditta Suparman, Kaerul Triramadhan, Arifah Anggai, Ladzan Nurul Fathi, Alinka Safiya Alesha, and Emak Temu. They have been with me at every turn. They always give me support and encouragement during the tough times although we were in different time zones and continents. Without them, I would not be able to complete this PhD.

Finally, I would also offer my regards to all of those who supported me in any respect during the completion of the thesis.

Table of Contents

List of Figures

List of Tables

Abbreviations

Δ	(Delta) Deleted/missing
°C	Degrees Celsius
µg	Microgram
µl	Microlitre
µm	Micromètre
µM	Micromolar
1-AKP	1-Azakenpaullone
37LRP	37-kDa laminin receptor precursor
4CMenB	Assigned name to the new Serogroup B vaccine
67LR	67-kDa laminin receptor
x g	Times gravity
ACT	Adenylate cyclase toxin
aka	Also known as
ANOVA	Analysis of variance
App	Adhesion and penetration protein
ATP	Adenosine triphosphate
ATM	Ataxia-telangiectasia-mutated
ATR	Ataxia and rad3 related
Aβ	Amyloid beta
Bad	Bcl-2-associated death promoter
BBB	Blood brain barrier
BCIP	5-bromo-4-chloro-3-indolyl phosphate
Bcl-2	B-cell lymphoma 2
BHI	Brain-heart infusion
BiP	Binding immunoglobin protein
bp	Base pair
BrdU	Bromodeoxyuridine
BSA	Bovine serum albumin
ca.	Approximately
CAK	CDK activating kinase
CAMP	Cationic antimicrobial peptide
cAMP	Cyclic adenosine monophosphate
CbpA	Choline-binding protein A
CD	Cluster of differentiation
CDC	Cell division cycle

CDK	Cyclin-dependent kinase
cDNA	Complementary DNA
CDT	Cytolethal distending toxin
CEACAM	Carcinoembryonic antigen-related cell adhesion molecule
cfu	Colony forming unit
cgMLST	Core genome MLST
CIF	Cycle inhibiting factor
Cip	CDK interacting protein
CKI	CDK inhibitors
cm	Centimetre
CNF1	Cytotoxic necrotising factor 1
CNS	Central nervous system
CO_2	Carbon dioxide
c-Raf	cellular Raf gene
CRM1	Chromosomal maintenance 1
CSF	Cerebrospinal Fluid
C_T	Cycle threshold
CTA	Cholera Toxin A subunit
CTB	Cholera Toxin B subunit
CTX	Cholera Toxin
DAPI	4’,6-diamidino-2-phenylindole
DMSO	Dimethyl sulfoxide
DNA	Deoxyribonucleic acid
Dyrk1B	Dual specificity tyrosine-phosphorylation-regulated kinase 1B
e.g.	For example
E3	Ubiquitin ligase
ECM	Endothelial cell medium
ECM	Extracellular matrix
EDD4	E3 isolated by differential display
EDTA	Ethylenediaminetetraacetic acid
Edu	5-ethynyl-2'-deoxyuridine
EHEC	Enterohemorrhagic *E. coli*
ELISA	Enzyme-linked immunosorbent assay
eIF2α	Eukaryotic Initiation Factor 2α
EPEC	Enteropathogenic *E. coli*
Erk	Extracellular signal-regulated kinase
ET	Edema toxin, a subunit of anthrax toxin
et al	And others

EU	Endotoxin unit
FAK	Focal adhesion kinase
FBS	Fetal bovine serum
FI	Faraday isolator
fHbp	Factor H binding protein
FOXO	Fork head box class O
Gal	Galectin
GAPDH	Glyceraldehyde 3-phosphate dehydrogenase
GM1	Monosialotetrahexosylganglioside
GPCR	G-protein coupled receptor
GSK-3β	Glycogen synthase kinase 3 beta
GTP	Guanosine triphosphate
h	Hour
H_2O	Dihydrogen oxide
HBMEC	Human brain microvascular endothelial cell
HCT116	Human colon carcinoma cells
HDAC	Histone deacetylases
HeLa	Immortal cervical cancer cell line from Henrietta Lacks
HEp-2	Human epithelial type 2
Hep3b	Human hepatoma cell line 3b
HmbR	Haemoglobin-binding receptors
HMW	Higher molecular weight
HpuA/B	Haemoglobin-haptoglobin utilisation protein A/B
HRP	Horse radish peroxidase
HrpA	Hemagglutinin/haemolysin related protein A
HSP90	Heat shock protein 90
HSPG	Heparin sulphate proteoglycan
HUS	Haemolytic uremic syndrome
IAP	Inhibitor of apoptosis
i.e.	In other words
IgA1/G	Immunoglobuline A1/G
IL-1/6/8/10	Interleukine 1/6/8/10
IMD	Invasive meningococcal disease
INK4	Inhibitor CDK4
JNK	c-Jun N-terminal kinase
kDa	Kilo Dalton
Kip	Kinase inhibitory protein
LAMP1	Lysosome-associated membrane protein 1

LAMR	Laminin receptor
LbpA/B	Lactoferrin-binding receptors A/B
LEF-1	Lymphoid Enhancer Binding Factor 1
LOS	Lipooligosaccharide
LT	Lethal toxin, a subunit of anthrax toxin
M	Molar
mAb	Monoclonal antibody
MAP	Mitogen activated protein
MAPK	MAP kinases
Mat-1	Ménage à trois-1
MDA	Meningococcal disease associated
MEK	MAPK/Erk Kinase
MenA/B/C	Meningococci serogroup A/B/C
MenACWY	Meningococci serogroup A, C, W, and Y
min	Minute
ml	Millilitre
MLEE	Multi-locus enzyme electrophoresis
MLST	Multi-locus sequence typing
mm	Millimetre
MOI	Multiplicity of infection
MR	Mannose receptor
mRNA	Messenger RNA
MRF	Meningitis Research Foundation
MspA	Meningococcal serine protease
mTORC2	Mammalian target of rapamycin Complex 2
MyD88	Myeloid differentiation primary response 88
Myt1	Myelin transcription factor 1
NadA	Neisserial adhesin A
NBT	Nitro blue tetrazolium
NF-κB	Nuclear factor kappa-light-chain-enhancer of activated B cells
ng	Nanogram
NHBA	Neisseria heparin binding antigen
NhhA	Neisseria hia homologue A
NLS	Nuclear localisation signal
nm	Nanometre
nM	Nano molar
NSCLC	Non-small cell lung cancer
nt	Nucleotide

Oca	Oligomeric coiled-coil
OD	Optical density
OMP	Outer membrane protein
OmpP2	OMP P2
OMV	Outer membrane vesicle
Opa/Opc	Opacity protein A/C
p	Phosphorylated
p	Probability value
P70-S6	Ribosomal protein S6 kinase beta-1
P90RSK	Protein 90 ribosomal s6 kinase
pAb	Polyclonal antibody
PAFr	Platelet-activating factor receptor
Par3/6	Partitioning defective 3/6 homolog
PBS	Phosphate Buffered Saline
PBS-T	PBS supplemented with 0.05% (v/v) Tween 20
PCR	Polymerase Chain Reaction
PDK	Pyruvate dehydrogenase kinase
PEA-15	Phosphoprotein enriched in astrocytes 15
PERK	Protein kinase R (PKR)-like endoplasmic reticulum kinase
PFGE	Pulsed-Field Gel Electrophoresis
PH	Pleckstrin homology
PHLPP	PH domain and Leucine rich repeat Protein Phosphatases
PI3K	Phosphoinositide 3-kinase
PilQ	Secretin of type IV pili
PIP2	Phosphatidylinositol (3,4)-biphosphate
PIP3	Phosphatidylinositol (3,4,5)-triphosphate
PKA/PKC	Protein Kinase A/C
PorA/B	Porin A/B
PP1	Protein phosphatase 1
PP2A	Protein phosphatase 2A
PrP^{sc}	Scarpie prion protein
PTEN	Phosphatase and tensin homolog
PVL	Panton–Valentine leukocidin
qRT PCR	Quantitative Real-Time PCR
R	Restriction
Rb	Retinoblastoma
RBC	Red blood cell
rCbpA	Recombinant CbpA

RIN	RNA integrity number
RIPA	Radio immunoprecipitation assay
rLR	Recombinant 37LRP
RNA	Ribonucleic acid
ROS	Reactive oxygen species
rPilQ	Recombinant PilQ
rpm	Revolutions per minute
rPorA	Recombinant PorA
RPKM	Reads Per Kilobase of transcript per Million mapped reads
RPSA	Ribosomal Protein SA
RQ	Relative quantification
rRNA	Ribosomal RNA
RS3	Repeated DNA sequence
RT	Room temperature
RTK	Receptor tyrosine kinase
s	Second
S	Svedberg Units
SBR	Small basic repeats
SCF	Complex Skp, Cullin, F-box containing complex
SD	Standard Deviation
SDS	Sodium dodecyl sulphate
SDS-PAGE	SDS–polyacrylamide gel electrophoresis
Ser	Serine
siRNA	Small interfering RNA
SMD	Systemic meningococcal disease
Src	Sarcoma
ST	Sequence Type
STEC	Shiga Toxin-producing *E. coli*
SUMO	Small ubiquitin-like modifier
SubAB	Subtilase AB
TbpA/B	Transferrin-binding receptors A/B
TBS	Tris Buffered Saline
TBS-T	TBS supplemented with 0.1% (v/v) Tween 20
TfR1	Transferrin receptor 1
TGF	Transforming growth factor
Thr	Threonine
TIMAP	TGF-β inhibited membrane associated protein
TLR2	Toll like receptor 2

TMD	Transmembrane domain
TNF-α	Tumour necrosis factor alpha
TPS	Two partner secretion
Tyr	Tyrosine
V	Volt
VacA	Vacuolating cytotoxin
VDAC	Voltage-dependent anion channel
VEE	Venezuelan equine encephalitis
w/v	Weight/volume
WHO	World Health Organization
Wnt	Wingless-related integration site
XTT	2,3-Bis-(2-Methoxy-4-Nitro-5-Sulfophenyl)-2H-Tetrazolium-5-Carboxanilide

List of presentations

Poster presentations

Rininta Firdaus, Neil J. Oldfield, and Karl G. Wooldridge. Fourth Extracellular Loop of Meningococcal PorA Causes Altered Expression of G_1 Cell Cycle Regulators in Human Brain Microvascular Endothelial Cells. Presented at Microbiology Society Annual Conference. 3-6th of April **2017**, Edinburgh, UK.

Rininta Firdaus, Neil J. Oldfield, and Karl G. Wooldridge. Fourth Extracellular Loop of Meningococcal PorA Causes Altered Expression of G_1 Cell Cycle Regulators in Human Brain Microvascular Endothelial Cells. Presented at School of Life Science PGR Symposium, 13-14th July **2017**, Nottingham, UK.

Rininta Firdaus, Neil J. Oldfield, and Karl G. Wooldridge. Meningococcal PorA-Loop4 induces G_1 Cell Cycle Arrest through the Akt Signalling Pathway. Presented at The Australian Society for Microbiology Meeting. 1-4th of July **2018**, Brisbane, Australia.

Oral presentations

Rininta Firdaus, Neil J. Oldfield, and Karl G. Wooldridge. Cellular response to PorA Loop4-derived peptide of Neisseria meningitidis. Presented at School of Life Science PGR Symposium, 11-12th July **2018**, Nottingham, UK.

Rininta Firdaus, Neil J. Oldfield, and Karl G. Wooldridge. Extracellular Loop4 of meningococcal outer membrane protein PorA induces a G_1 cell cycle arrest through the Akt signalling pathway. Presented at 5th Midlands Molecular Microbiology Meeting (M4), 13-14th of September **2018**, Warwick, UK.

Rininta Firdaus, Neil J. Oldfield, and Karl G. Wooldridge. PorA-Loop4 derived peptides of *Neisseria meningitidis* cause a G_1 cell cycle arrest through the Akt signalling pathway in human brain microvascular endothelial cells. Presented at Microbiology Society Annual Conference, 8-9th of April **2019**, Belfast, UK.

Abstract

Neisseria meningitidis (the meningococcus) is a major meningitis-causing bacterium and is known for its ability to breach the blood-brain barrier (BBB). Meningococci bind to the Laminin receptor (LAMR) on the surface of the vascular endothelium, which is part of the BBB. In a previous study, the meningococcal surface proteins PorA and PilQ were identified as the bacterial ligands responsible for binding and, subsequently, the LAMR-binding moiety of PorA was localised to its fourth extracellular loop (PorA-Loop4). PorA preferentially targets the 37 kDa laminin receptor precursor (37LRP) rather than the 67 kDa laminin receptor form (67LR) on the cell surface. It was confirmed that the PorA:37LRP interaction is mediated by PorA-Loop4 as deletion of this loop abrogates recruitment of 37LRP under meningococcal colonies. Using a cyclised peptide corresponding to PorA-Loop4 from *N. meningitidis* MC58, the PorA-Loop4:37LRP interaction induced specific cellular responses in human brain microvascular endothelial cells (HBMECs) including G_1-phase cell cycle arrest. The interaction of PorA-Loop4:37LRP was cytostatic, not cytotoxic. Flow cytometric analysis indicated that the treatment of HBMECs with PorA-Loop4 for 24 h caused a significant reduction of cells at S-phase and a corresponding increase in the G_1 population.

Based on these results, it is hypothesised that PI3K/Akt pathway was affected by the interaction resulting in G_1 arrest. The current study aimed to investigate the perturbations of key proteins' expression and activation involved in the PI3K/Akt pathway (including Akt, GSK-3β, Cyclin D1, and CDK4) after the treatment of PorA-Loop4 peptide in HBMECs.

The work indicated that PorA-Loop4 caused perturbations of Cyclin D1/CDK4 as cell cycle regulators at G_1 phase. Transcriptome analysis using qRT-PCR showed that treatment of HBMECs with PorA-Loop4 peptide for 2, 4, 8, or 24 h increased gene expression of CDK4, and decreased expression of Cyclin D1. Immunoblotting confirmed these results as the 24 h-treatment of PorA-Loop4 peptide caused the downregulation of Cyclin D1 and the upregulation of pCDK4 (Thr172).

PorA-Loop4 caused a blockade of PI3K/Akt signalling. Using ZSTK474 as a PI3K inhibitor, we observed that the effect of PorA-Loop4 on Cyclin D1 and pCDK4 (Thr172) was PI3K-dependent at both mRNA and protein levels.

Exposure of HBMECs to PorA-Loop4 peptide caused a downregulation of pAkt (Ser473) and an upregulation of pGSK-3β (Ser9) at the protein level 24 h post treatment. The upregulation of pGSK-3β (Ser9) was dependent to Akt, and the downregulation of Cyclin D1 was independent of GSK-3β.

Using the whole bacterial cells of *N. meningitidis* wild-type MC58 and its mutants lacking of PorA-Loop4, PorA, and/or PilQ, the role of PorA-Loop4, PorA and PilQ in influencing the PI3K/Akt pathway were investigated. Similar perturbations of pAkt (Ser473), pGSK-3β (Ser9), Cyclin D1, and pCDK4 (Thr172) occurred in PorA-Loop4 peptide treated cells and wild-type infected cells while the abrogation of the PorA-Loop4 erased the perturbations in HBMECs. Both PorA and PilQ have significant roles in the perturbation of pAkt (Ser473), pGSK-3β (Ser9), and Cyclin D1. However, the upregulation of pCDK4 (Thr172) was mediated by Loop4, not by other parts of the PorA, nor by PilQ.

Confocal microscopy showed the localisation of pAkt (Ser473), pGSK-3β (Ser9), Cyclin D1, and pCDK4 (Thr172) in the uninfected, wild-type-infected, and PorA-Loop4 mutant-infected HBMECs. The pAkt (Ser473), pGSK-3β (Ser9), Cyclin D1 were localised mainly in the cytoplasm, while the pCDK4 (Thr172) was localised in cytoplasmic and nuclear regions. Confocal microscopy confirmed the immunoblotting results, as the diffuse pattern of pAkt (Ser473), pGSK-3β (Ser9), Cyclin D1, and pCDK4 (Thr172) in the wild-type infected cells were in contrast with the uninfected and the PorA-Loop4 mutant infected cells.

In summary, PorA-Loop4 causes the perturbation of PI3K/Akt pathway via Akt/GSK-3β/Cyclin D1/CDK4. The data presented in this thesis has extended knowledge of meningococcal-host pathogen interaction. A thorough understanding of PorA-Loop4 interaction with LAMR and its effect in the PI3K/Akt pathway may provide another strategy for the development of interventions against the meningococcus and perhaps other Gram-negative pathogens.

Chapter 1 - General Introduction

1.1 Characteristics of *Neisseria meningitidis*

1.1.1 The genus *Neisseria*

Neisseria is a genus member of family Neisseriaceae. It includes at least 25 species based on 16S rRNA analysis (Hung and Christodoulides, 2013). The genus was named after Albert Neisser who observed *Neisseria gonorrhoeae* in urethral exudates from patients with gonorrhoea in 1879 (Neisser, 1879). Eight years later Weichselbaum isolated the *Neisseria meningitidis* from cerebrospinal fluid (CSF) of patients with 'epidemic cerebrospinal meningitis' (Weichselbaum, 1887).

N. meningitidis and *N. gonorrhoeae* are genetically closely related human-restricted pathogens, colonising the mucosal surfaces of the human nasopharynx and urogenital tract, respectively (Tønjum, 2005). Other Neisseria species are commensals in mammalian and/or non-mammalian hosts, which might under certain conditions give rise to opportunistic infections. Human commensals of *Neisseria* species include *Neisseria lactamica* (Hollis et al., 1969), *Neisseria animaloris* (Ganiere et al., 1995), *Neisseria bacilliformis* (Han et al., 2006), *Neisseria cinerea* (Knapp et al., 1984), *Neisseria elongata* (Bovre and Holten, 1970), *Neisseria flavescens* (Branham et al., 1930), *Neisseria mucosa* (Veron et al., 1959), *Neisseria polysaccharea* (Riou and Guibourdenche, 1987), *Neisseria sicca* (Shaw, 1932), *Neisseria subflava* (Benson et al., 1928), *Neisseria zoodegmatis* (Ganiere et al., 1995), *Neisseria weaveri* (Andersen et al., 1993).

1.1.2 *Neisseria meningitidis*

N. meningitidis (the meningococcus) is a Gram-negative, oxidase and catalase positive, non-spore forming, aflagellate, aerobic bacterium, often found in a diplococcus form, and is approximately 0.8 μm in diameter. The meningococcus can be grown *in vitro* on enriched media including blood, chocolate, modified New York City medium, and Muller-Hinton agar at 35-37°C, 5-10% CO_2, and pH 7-7.4 (Ala'Aldeen and Turner, 2006). On blood agar, meningococcal colonies are round, smooth, moist, glistening, convex, grey and unpigmented; while on chocolate agar they appear as large, colourless-to-grey, opaque colonies (Centers for Disease Control and Prevention, 2011a).

1.1.3 Classification of *Neisseria meningitidis*

The polysaccharide capsule (Figure 1.1), which is a phase-variable structure present on the external face of the outer membrane, is commonly used to differentiate meningococci into serogroups, traditionally via the use of monoclonal antibodies Up to 13 serogroups have been described (A, B, C, E, H, I, K, L, W, X, Y, Z, and Z') but most meningococcal disease is caused by strains belonging to six serogroups (A, B, C, W, X, and Y) (Branham, 1953). The chemical structures of the capsule polysaccharides from these six serogroups are presented in Table 1.1.

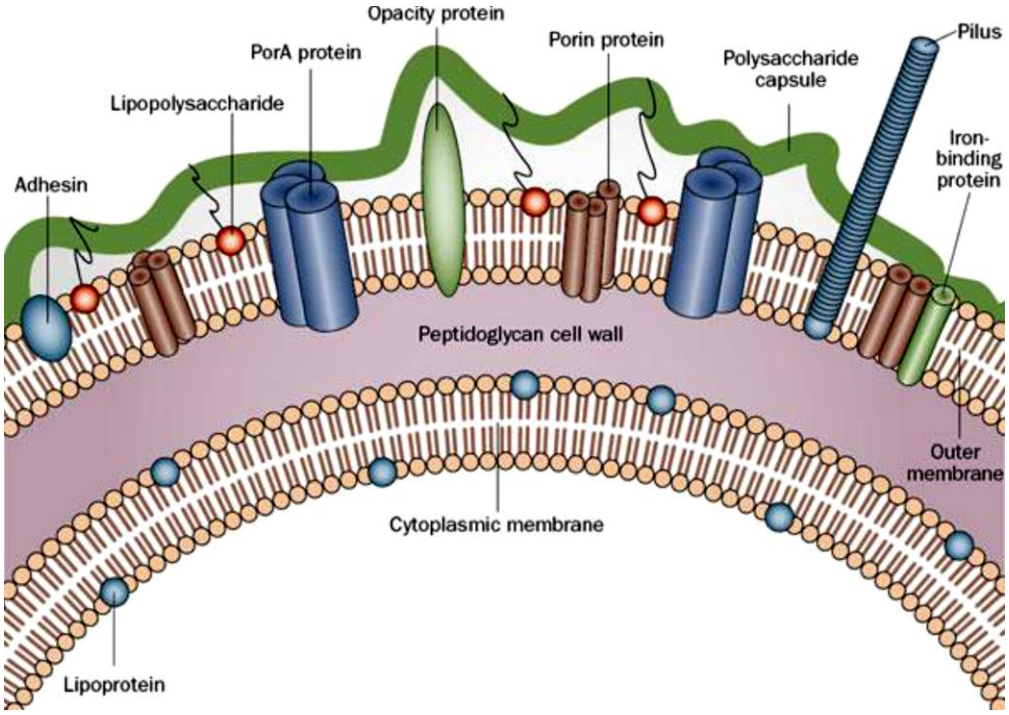

Figure 1.1: Envelope structure of the meningococcus. The bacteria are encapsulated with a polysaccharide capsule. The outer membrane contains numerous surface proteins and structures including adhesins, porins, type IV pili, opacity proteins, and iron-binding proteins. The figure is reproduced from (Pollard, 2011).

Table 1.1: Chemical structures of the important capsules of meningococci (Virji, 2009).

Capsule	Structure	Features
A	(α1–6)-N-acetyl-mannosamine-1-phosphate	Disease-associated, non-sialic acid polymer
B	(α2–8)-N-acetylneuraminic acid	Homopolymer of sialic acid; mimics structures present on neuronal cell adhesion molecules; poor immunogen
C	(α2–9)-N-acetylneuraminic acid	Homopolymer of sialic acid; immunogenic
W	6-D-Gal(α1–4)-N-acetylneuraminic acid	Heteropolymer; contains sialic acid
X	(α1–4)-N-acetyl-D-glucosamine 1-phosphate	Homopolymer of sialic acid
Y	6-D-Glc(α1–4)-N-acetylneuraminic acid	Heteropolymer; contains sialic acid

Further serology-based characterisation of meningococcal strains, such as serotyping, serosubtyping, and immunotyping is based on the variants of surface antigens PorB, PorA, and lipooligosaccharide (LOS), respectively (Rosenstein et al., 2001). So far, meningococci have been classified into over 20 different serotypes and serosubtypes (Ala'Aldeen and Turner, 2006), and 12 immunotypes (Zhu et al., 2002). An example of nomenclature based on the serological typing of *N. meningitidis* strain H44/76 is B:15:P1.7,16:L3,7,9 which denotes serogroup B, serotype 15, serosubtype 7 and 16, and immunotype 3, 7, and 9 (Jolley et al., 2007).

However, serogrouping fails to characterise meningococcal strains which lack the capsule (termed as 'non-groupable') (Dolan-Livengood et al., 2003). Also, the high frequency of phase and antigenic variation of surface antigens reduces the reliability of the serological classification of meningococci. Therefore, molecular typing has been developed for identifying closely related strains, strains with the potential to cause outbreaks, predicting vaccine coverage, and understanding the genetic structure of circulating meningococcal strains (Rouphael and Stephens, 2012). Available techniques for molecular typing are pulsed-field gel electrophoresis (PFGE) (Bevanger et al., 1998), multilocus enzyme electrophoresis (MLEE) (Weis and Lind, 1998), multilocus sequence typing

(MLST) (Maiden et al., 1998), multiplex PCR (Zhu et al., 2012), oligonucleotide microarrays (Bannister et al., 2018), and whole-genome sequencing (Tettelin et al., 2000).

MLST has been used as a molecular typing method of meningococci (Jolley et al., 2018, Maiden et al., 1998). The DNA sequences of seven DNA fragments (433-501bp) amplified from housekeeping genes (*abcZ*, *adk*, *aroE*, *fumC*, *gdh*, *pdhC*, *pgm*) are utilised in this technique (Birtles et al., 2005). Each sequence is assigned an allele number, and the combination of alleles is used to define the sequence type (ST) of each isolate. The database of the sequence types (STs) and the genome diversity of meningococci are available online (http://pubmlst.org/) where MLST schemes and isolate data of a wide range of prokaryotic and eukaryotic genomes are hosted (Jolley et al., 2018). Some STs in the database have been termed as 'hyper-invasive lineages'; isolates belonging to these STs are responsible for most cases of the disease worldwide (Vogel, 2010). Increasingly MLST based on seven DNA sequences is being superseded by core genome MLST (cgMLST) analysis which offers greater resolution (Bratcher et al., 2014).

1.2 Clinical manifestations of invasive meningococcal disease (IMD)

Meningococci in the bloodstream and CSF cause the life-threatening disease termed as 'invasive meningococcal disease' (IMD) (Leggiadro et al., 1989) or systemic meningococcal disease (SMD) (Bovre et al., 1983). There are four classes of IMD: (1) fulminant sepsis (septic shock without meningitis) (2) meningitis with septic shock (3) meningitis without septic shock, and (4) meningococcemia without shock/meningitis (Brandtzaeg and van Deuren, 2012). Fulminant sepsis is the most severe, while meningococcemia without shock/meningitis is the mildest IMD. The clinical manifestation is influenced by factors such as age, host co-factors, host immune-system, and stage of the disease (Stephens, 2009). Early common symptoms of IMD are very similar to those resulting from many self-limiting viral illnesses, i.e. headache, fever, nausea, and stiff neck, photophobia, and rash; thus recognising IMD during its early stages is very challenging. After displaying these non-specific symptoms, around 60% of patients with IMD develop meningitis, up to 20% progress to sepsis, or a combination of both clinical conditions can be experienced (Stephens et al., 2007, Theilen et al., 2008).

1.2.1 Meningococcal sepsis

Non-blanching rash, known as purpura, is a common symptom of sepsis, which may proceed to other symptoms of meningitis including convulsions/seizures (Brandtzaeg, 2006, Brandtzaeg and van Deuren, 2012). Meningococcal sepsis is further classified into transient, chronic and fulminant forms. The transient form is characterised by fever and non-specific rash, which can both disappear within 2-5 days without treatment (Stephens et al., 2007). The chronic form is rarely developed and is clinically associated with intermittent fever, arthralgia, signs of vasculitis, and a non-specific maculopapular rash. These symptoms might fade for days or reappear (Harwood et al., 2005, Stephens et al., 2007) . The fulminant form occurs when meningococci proliferate rapidly in the bloodstream and reach the concentration of 10^5-10^8 ml^{-1} bacteria and 10^1-10^3 EU ml^{-1} LOS (Brandtzaeg et al., 1989, Brandtzaeg et al., 2001, Hackett et al., 2002, Bjerre et al., 2003, Øvstebø et al., 2004, Brandtzaeg, 2006, Stephens et al., 2007). If the LOS level in plasma passes 8–10 EU ml^{-1}, 95% of patients will develop persistent septic shock and seizures for more than 24 h (Brandtzaeg et al., 1989, Brandtzaeg, 2006, Brissac et al., 2012). The accumulation of invasive meningococci and their endotoxin in the bloodstream will induce an overwhelming immune response, resulting in generalised pathology of the microvascular endothelium, which in turn leads to progressive circulatory collapse, severe coagulopathy and severe depression of myocardial function, all of which contribute towards multi-organ failure and may lead to death (Pathan et al., 2003).

1.2.2 Meningococcal meningitis

Meningitis is an acute inflammation of the meninges – the membrane surrounding the brain and spinal cord. It is caused by bacterial, fungal and viral infections. Three major pathogenic bacteria which can cause meningitis are *N. meningitidis*, *Streptococcus pneumoniae*, and *Haemophilus influenzae* (Brouwer et al., 2010, van Sorge and Doran, 2012). Other known bacteria causing meningitis are group B Streptococci, *Listeria monocytogenes, Escherichia coli* K1 (Dawson et al., 1999, Nigrovic et al., 2008, Brouwer et al., 2010, Thigpen et al., 2011, van Sorge and Doran, 2012), and *Mycobacterium tuberculosis* (Manuel L et al., 1997, Békondi et al., 2006, Swe et al., 2008, van Sorge and Doran, 2012). *N. meningitidis, S. pneumoniae,* and *H. influenzae* are the most common causes of childhood

meningitis (Turk, 1984, Saarinen et al., 1995, Ramsay et al., 1997, Corless et al., 2001), while in adults *N. meningitidis* is the second commonest cause after *S. pneumoniae* (Stephens et al., 2007, Hoffman and Weber, 2009). Meningitis caused by *E. coli* K1 is usually associated with neonates (Houdouin et al., 2008, Nudelman and Tunkel, 2009, Croxen and Finlay, 2010, van de Beek et al., 2010, Mittal et al., 2011).

High loads of meningococci and high levels of endotoxin in the bloodstream may result in increased concentrations of the inflammatory factors including TNFα, IL-1, IL-6 and IL-8 (Waage et al., 1987, Waage et al., 1989, Ohga et al., 1994, De Smedt et al., 1996, Kolb-Maurer et al., 2001). The inflammatory process extends throughout the meninges which causes meningitis. Developing meningitis without septic shock is the most common clinical presentation associated with IMD; more than 60% of patients in industrialised countries develop this condition, while in developing countries this percentage can be even higher (Stephens et al., 2007).

Symptoms of meningococcal meningitis are generally similar to meningococcal sepsis. In adults, meningitis is clinically characterised by a sudden fever accompanied by a headache and neck stiffness. Other symptoms that a patient can experience include nausea, vomiting, photophobia and altered mental status (van de Beek et al., 2004). In infants and young children, meningitis might cause non-specific symptoms including poor feeding, irritability, a high pitched cry and a bulging fontanelle (Nadel and Kroll, 2007). Nowadays, the overall mortality rate associated with IMD is 10-15% due to early diagnosis and management (Sharip et al., 2006, Rouphael and Stephens, 2012). Unfortunately, around 25% of meningococcal disease survivors develop marked morbidity including limb loss, hearing loss, cognitive dysfunction, visual impairment, educational difficulties, developmental delays, motor nerve deficits, seizure disorders, or behavioural problems (Edwards and Baker, 1981, Kirsch et al., 1996, Rosenstein et al., 2001, Rouphael and Stephens, 2012).

1.2.3 Other clinical manifestations

In addition to sepsis and meningitis, meningococci are able to cause other clinical manifestations such as sore throat, meningoencephalitis, chronic meningococcaemia, pneumonia, septic arthritis, pericarditis, myocarditis, endocarditis, conjunctivitis, panophthalmitis, genitourinary tract infection, pelvic infection, peritonitis, and proctitis (Oldfield and

Ala'Aldeen, 2012). The clinical picture can progress from one end of the spectrum to the other during the course of the disease.

1.3 Epidemiology of IMD

Epidemics of IMD have occurred worldwide for decades. Places with high population density (e.g. university halls, dormitories, hajj-pilgrimage areas) might contribute to the transmission and spread of meningococci because of the prolonged contact between residents (World Health Organization, 2015a). Uncontrolled and fast transmission between hosts could produce local epidemics, in those populations. Although rates of asymptomatic carriage could be high, disease rates are relatively low (approximately 1-1000 per 100,000 population) (Caugant and Maiden, 2009). The conversion from harmless bacteria into pathogens is further explained in section 1.5.

In 2004, WHO reported that there are 1.2 million cases of bacterial meningitis per year, 170,000 of which are fatal (Beaglehole et al., 2004, van Sorge and Doran, 2012). While in 2014, there was a decline to approximately 15,000 suspected cases of bacterial meningitis globally (World Health Organization, 2015b), including 1,304 deaths (World Health Organization, 2014), these mainly occurred in the meningitis belt of sub-Saharan Africa (World Health Organization, 2015b). Effective vaccines and advanced therapeutic interventions have reduced the numbers of fatal cases. Still, several countries reported meningitis epidemics in 2014 such as Benin, Ethiopia, Gambia, Ghana, Nigeria and Guinea (World Health Organization, 2015b).

The worldwide distribution of meningococcal serogroups causing disease is presented in Figure 1.2. Serogroup A and, to a lesser extent, serogroup C have caused major outbreaks in the 'African meningitis belt' (Greenwood et al., 1987, Greenwood, 1999, World Health Organization, 2006, Stephens et al., 2007). Serogroup A also caused epidemics across China and Russia but have recently been replaced by localised disease due to serogroups B and C (Rouphael and Stephens, 2012). Serogroup B overall has a lower incidence compared to serogroup A. However, it is the most important cause of endemics in developed countries with significant morbidity and mortality. Serogroup W has been associated with meningococcal disease among pilgrims of Hajj in Saudi Arabia (Dull et al., 2005). Return of the pilgrims to their home country might be associated with

the spread of serogroup W throughout the world (Hahne et al., 2002, Lingappa et al., 2003, Wilder-Smith et al., 2003). Serogroup X and Y do not cause major outbreaks. However, serogroup Y remains the cause of 26% of the total meningococcal disease in the US (Cohn et al., 2010, Rosenstein et al., 1999, Centers for Disease Control and Prevention, 1993). Also, isolates of serogroup Y have been recorded in Europe, Latin America, and Israel (Rouphael and Stephens, 2012).

Figure 1.2: Worldwide serogroup distribution of meningococcal disease (Rouphael and Stephens, 2012). Serogroup A and C are the cause of major outbreaks of meningococcal disease in Africa, while serogroup B and C are the predominant strains in Europe, Australia, and America. Serogroup A cause epidemics in Russia and China, while serogroup B cause epidemics in New Zealand. Serogroup W has been associated with meningococcal disease among pilgrims of Hajj in Saudi Arabia. Serogroup X and Y do not cause major outbreaks. Serogroup Y has been recorded mostly in the USA.

The United Kingdom is one of the developed countries with the highest incidence of meningococcal disease (Maiden et al., 2002, Hill et al., 2015). In England, 755 cases of IMD were reported to the National Public Health England Meningococcal Reference Unit during 2017/2018, similar to the 748 cases reported in 2016/2017 (Public Health England, 2018). Overall IMD incidence in 2017/2018 has remained stable at one per 100,000. Serogroup B (54% of all cases) was the dominant cause, followed by serogroups W (24%), Y (12%), and C (8%). Cases of serogroup W in 2017/2018 have decreased by 14% since the previous year. However, cases of serogroup Y

have increased by 10%. Adults aged 25 years and older accounted for most cases of serogroup Y.

1.4 Treatment and prevention of IMD

Treatment and prevention strategies for IMD should ideally be developed based on the pathophysiology, symptoms, and mechanisms of the disease in the human body. Treatment should begin as soon as possible, even before confirmation of the bacterial species involved. Samples from suspected patients could be retrieved from CSF, blood, skin lesion, or throat fluid, which can then be examined by basic methods (e.g. gram staining, agar culture) or molecular methods (e.g. PCR) (Miller et al., 2018). IMD is commonly treated with antibiotics including penicillin, cephalosporins, aminoglycosides, and quinolones (Tunkel et al., 2004, Van de Beek et al., 2006, Brouwer et al., 2010, van de Beek et al., 2012). Sulfonamides are no longer used following the identification of sulfadiazine-resistant meningococci (Millar et al., 1963, Fiebelkorn et al., 2005).

For the prevention of disease, four kinds of vaccines are available to protect against meningococcal infections including (1) polysaccharide, (2) polysaccharide-protein conjugate-based, (3) vaccines based on outer membrane vesicles (OMVs), and (4) vaccines based on OMPs.

The first vaccines developed against meningococci incorporated the capsular polysaccharides of serogroups A, C, Y, and W (Goldschneider et al., 1969, Gotschlich et al., 1969, Griffiss et al., 1981, Hankins et al., 1982). These vaccines were effective in providing serogroup-specific protection in adults. However, they were short-lived and they were ineffective in young children (Gold et al., 1975, Robbins, 1978, Jennings, 1983).

More recently, conjugated vaccines were developed to provide longer-term protection through the induction of immunological memory (Keyserling et al., 2005, Lewis et al., 2009, Tan et al., 2010, Bröker et al., 2011, Gasparini and Panatto, 2011). The examples of the developed conjugated vaccine are MCC (for MenC strains) (Miller et al., 2001) and MenAfrivac (for MenA strains) (Bilukha and Rosenstein, 2005, LaForce and Okwo-Bele, 2011). MCC and MenAfriVac contain polysaccharides conjugated to tetanus or diphtheria toxoid as a carrier (Miller et al., 2001, LaForce and Okwo-Bele, 2011). These vaccines work both directly and indirectly to protect the population. Directly, the MCC and MenAfriVac provide immunological memory and protection to each vaccinated individual.

Indirectly, mass vaccination induces a 'herd immunity' in which people who have not been vaccinated are also protected from IMD. The protection occurs because there has been a significant drop in the population-wide carriage. Both effects will significantly reduce the incidence of IMD where it has been adopted.

Another type of meningococcal vaccine is exemplified by the quadrivalent MenACWY vaccines (e.g. Menactra®, Nimentrix®, Menveo®), which are given in the USA to adolescents at high risk of IMD (Centers for Disease Control and Prevention, 2011b). They have also been used in the UK for close contacts of an IMD patient with MenACWY or administered to travellers going to regions of the world where MenACW or Y is endemic. Since 2015, MenACWY is routinely given to UK adolescents to combat the rise of MenW (Public Health England, 2015). There were also worries that immunity gained from childhood MenC has waned in adolescents; thus, the MenACWY vaccines also acts as a MenC booster.

Development of vaccines against MenB has been the most challenging. The MenB capsule consists of (α2→8)-linked polysialic acid, a structure which is also found on some human neural-cells (Nedelec et al., 1990, Finne et al., 1987). Thus, OMV vaccines have been developed based on the fact that the meningococcus produces and releases vesicles composed of OMPs, LOS, lipids, and periplasmic components. The first generation OMV vaccines against MenB primarily contained the meningococcal porins PorA and PorB as antigenic components (Fredriksen et al., 1991, Sierra et al., 1991, Boslego et al., 1995). PorA is a very abundant meningococcal OMP but is highly-variable among isolates. Thus, OMV (PorA)-based vaccines are serosubtype-specific and ineffective against heterologous invasive strains. Second generation OMV vaccines have been developed to increase coverage. For example, Claassen et al. genetically engineered meningococcal strains to express six PorA variants to produce hexavalent PorA vaccines (Claassen et al., 1996).

One recently developed vaccine against MenB is 4CMenB that was licensed by GlaxoSmithKline by the name of Bexsero® (Gorringe and Pajon, 2012). It contains four recombinant antigen components: factor H binding protein (fHbp), Neisserial adhesin A (NadA), Neisseria heparin binding Antigen (NHBA), and OMVs from a New Zealand epidemic strain (including PorA P1.4) (Gorringe and Pajon, 2012). Clinical trials showed that 4CMenB gave significant immunological responses among infants (Gorringe and Pajon, 2012). In the UK, Bexsero is now part of the infant immunisation

schedule. However, it is anticipated that the vaccine may need further improvement, possibly with additional components, because of its limited predicted protection against only ca. 78% of European invasive MenB strains (Vogel et al., 2013).

Also, a recombinant fHbp-based vaccine against MenB was approved by European Medicines Agency in May 2017 (European Medicines Agency, 2017). The recombinant vaccine includes two clones of fHbp representing two major classes of fHbp circulating in Europe. Pfizer licensed it under the name Trumenba® (McNeil et al., 2013). It is indicated for individuals from 10 through 25 years of age. Targeting teenagers and adolescents for vaccination would significantly reduce the meningococcal carriage and transmission as these age groups has the pivotal role in the epidemiology of meningococcal disease (Vetter et al., 2016).

1.5 Meningococcal pathogenesis

Meningococcal pathogenesis, particularly the factors enabling the capacity to progress from harmless commensal residing in the nasopharynx into a pathogen, is not fully understood. The environmental conditions facilitating exposure and acquisition, the bacterial genetics influencing the virulence of the organism, and the host susceptibility favouring bacterial acquisition, colonisation, invasion, and survival are all factors which contribute to the development of invasive disease from meningococcal infection (Rouphael and Stephens, 2012).

Meningococci are spread from one person to another by direct contact or via respiratory droplets (DeVoe, 1982, Caugant et al., 2007). The bacteria first colonise the human upper respiratory tract mucosa to establish a carrier state and, in some cases, may progress to meningococcal disease. During the carriage stage in the nasopharynx, co-colonisation with pathogenic and non-pathogenic bacteria may lead to horizontal genetic exchange and recombination events, which may result in the emergence of new meningococcal clones expressing one or more capsular polysaccharide to evade the host immune defences (Feil et al., 1999, Yazdankhah and Caugant, 2004). Moreover, new successful clones might be capable of wide global dissemination and could be associated with explosive epidemics of invasive disease (Caugant et al., 1986, Read, 2014). Transmissibility is essential in the life cycle of meningococci (Yazdankhah and Caugant, 2004).

The stages of meningococcal pathogenesis throughout the human body are illustrated in Figure 1.3 (Virji, 2009). After adhesion and colonisation in the nasopharynx, the bacteria may invade the epithelial barrier via transcytosis or through phagocytes. Then, the bacteria can translocate into the blood vessels, survive host-immune defences, proliferate, and disseminate throughout the body. After reaching the capillaries, meningococci bind to the vascular endothelium via type IV pili. Invasion into CSF via transcytosis and the paracellular route is the last stage of pathogenesis.

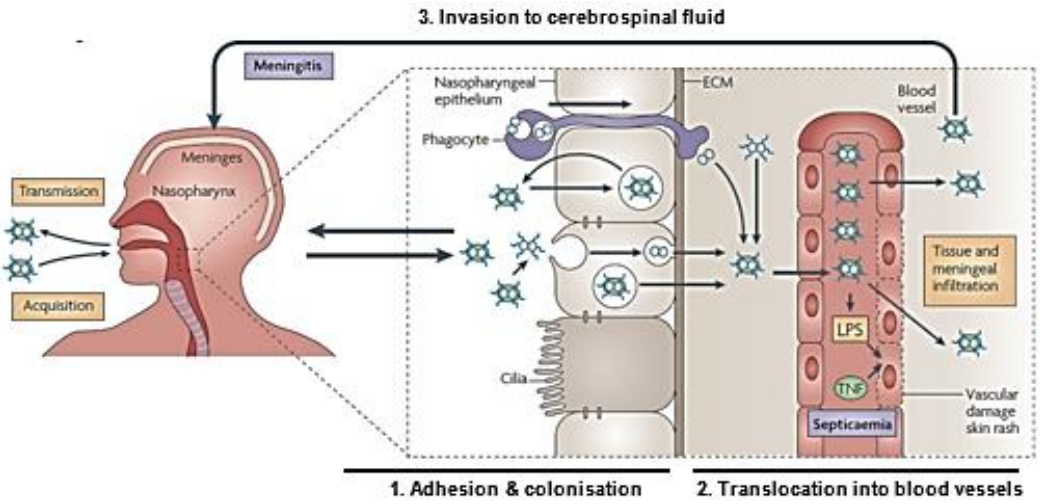

Figure 1.3: Stages in the pathogenesis of *N. meningitidis*. Meningococci may be acquired through the inhalation of respiratory droplets. The organism establishes intimate contact with non-ciliated mucosal epithelial cells of the upper respiratory tract, where it may enter the cells briefly before migrating back to the apical surfaces of the cells for transmission to a new host. Asymptomatic carriage is common in healthy adults in which bacteria that enter the body by crossing the epithelial barrier are eliminated. Besides transcytosis, *N. meningitidis* can cross the epithelium either directly following damage to the monolayer integrity or through phagocytes in a 'Trojan horse' manner. In susceptible individuals, once in the bloodstream, *N. meningitidis* may survive, multiply rapidly and disseminate throughout the body and the brain. Meningococcal passage across the brain vascular endothelium (or the epithelium of the choroid plexus) may then occur, resulting in infection of the meninges and the cerebrospinal fluid. The figure is reproduced from (Virji, 2009).

1.5.1 Adhesion and colonisation

Meningococci utilise adhesins to attach to ligands distributed on the surfaces of different human cells. Type IV pili, autotransporters, and various

adhesins facilitate contact of bacteria with host cells (Table 1.2). The Type IV pili establish the initial contact with non-ciliated mucosal epithelial cells at the upper respiratory tract (Stephens et al., 1983, Virji, 2009). During this stage, the meningococcal capsule hampers intimate adhesion; thereby it is downregulated via phase variation (Hammerschmidt et al., 1996a, Hammerschmidt et al., 1996b, Deghmane et al., 2002). Loss of the capsule facilitates meningococcal attachment, microcolony formation, and the carriage state at human mucosal surfaces (Bartley et al., 2013, Tzeng et al., 2016). Other surface structures, including pili, are also subject to phase variation, as well as post-translational modification, which allows dissociation of the meningococci from bacterial aggregates to the new colonisation sites, also migration across the epithelium (Chamot-Rooke et al., 2011).

Table 1.2: Adhesion and invasion proteins, modified from Virji, (2009).

Proteins	Properties	Features	Function	Targets	Receptors	References
Type IV pili	15-20 kDa subunits	Polymeric fibres; phase and antigenically variable	Adhesion and invasion	Human epithelial cells, endothelial cells and RBC	CD46	(Kallstrom et al., 1997)
					PAFr	(Jen et al., 2013)
					β-adrenergic receptor	(Coureuil et al., 2010)
					CD147	(Bernard et al., 2014)
PorA (with Type IV pili 'PilQ')	45 kDa	OMP	Adhesion and invasion	Human epithelial and endothelial cells	LAMR/Gal-3	(Orihuela et al., 2009, Alqahtani et al., 2014)
Opa	24–35 kDa; heat modifiable	Eight-stranded β-barrel; phase and antigenically variable	Adhesion and invasion	Human epithelial cells and fibronectin	CEACAMs	(Chen and Gotschlich, 1996, Virji et al., 1996, Muenzner et al., 2000)
					HSPG	(Chen et al., 1995, Van Putten and Paul, 1995, Virji et al., 1999)
					ECM and integrins	(Duensing and van Putten, 1998)
Opc	24–35 kDa; heat modifiable	Ten-stranded β-barrel; phase variable	Adhesion and invasion	Human epithelial cells, endothelial cells, activated vitronectin and fibronectin	ECM, integrins	(Virji et al., 1994, Unkmeir et al., 2002)
					HSPG	(De Vries et al., 1998, Prince et al., 2002)
NhhA	57 kDa	Trimeric autotransporter; *Haemophilus influenzae* Hsf/Hia homologue	Adhesion	Human epithelial cells	Laminin and HSPG	(Scarselli et al., 2006)
App	160 kDa	Autotransporter; *H. influenzae* Hap homologue	Adhesion and spread	Human epithelial cells	MR, TfR1	(Serruto et al., 2003, Khairalla et al., 2015)
HrpA (TPS)	180 kDa	*Bordetella pertussis* FHA homologue	Adhesion?	Some human epithelial cell lines	Unknown	(Tala et al., 2008)
NadA	38 kDa	Trimeric Autotransporter belonging to Oca family; phase variable	Adhesion and invasion	Human epithelial cells	β1 integrin	(Nagele et al., 2011)
					HSP90	(Capecchi et al., 2005)
MspA	157 kDa	Autotransporter; secreted; phase variable	Adhesion	Human epithelial and endothelial cells (when expressed by *E. coli*)	MR, TfR1	(Turner et al., 2006, Oldfield et al., 2013, Khairalla et al., 2015)

Retracting pili induce twitching motility that allows the meningococci to move along the epithelial mucosa until the bacteria come into intimate contact with specific receptors. Alqahtani et al. showed that Galectin-3 (Gal-3) and laminin receptor precursor (37LRP) on the surface of the host cell build a complex interaction with Type IV pili, meningococcal outer membrane protein PorA and LOS to enhance adherence to the epithelium (Alqahtani et al., 2014).

Trimeric autotransporters, NhhA and NadA, are also involved in the bacterial-host cell close association. NadA forms stable trimers on the bacterial surface which promotes adherence and invasion to epithelial cells (Capecchi et al., 2005). Interestingly, NadA binds to human cytoplasmic chaperone Hsp90 (Heat shock protein 90), and the purified Hsp90 was shown to inhibit NadA-mediated adhesion and invasion *in vitro* (Montanari et al., 2012). NhhA also aids adhesion by binding to the extracellular matrix proteins of the epithelial cells heparin sulphate and laminin (Scarselli et al., 2006). NhhA affects the host immune system by promoting the apoptosis of macrophages and affecting the differentiation of monocytes, which sustain asymptomatic colonisation (Wang et al., 2016a).

App and MspA, chymotrypsin-like serine proteases, were also reported to function as adhesins (Turner et al., 2006, Serruto et al., 2003). The proteins might remain temporarily associated with the cell surface before they are released. Heterologous expression of App and MspA in *E. coli* mediated adhesion of the bacteria to epithelial cells and endothelial cells, and this function was confirmed in *N. meningitidis* (Serruto et al., 2003, Turner et al., 2006). The capsule did not appear to limit App's adhesin function, suggesting that the protein extends beyond the capsule to interact with its receptor on the Chang epithelial cells (Serruto et al., 2003).

After the initial adhesion with diverse adhesins, meningococci continue to proliferate to form small micro-colonies. The close adherence of meningococci to host epithelial cells leads to the formation of cortical plaques (Doulet et al., 2006, Stephens et al., 2007). The intimate association generates specific signals and events, which eventually trigger the formation and extension of epithelial cell pseudopodia that engulf the meningococcus. The intimate association is mediated by the meningococcal opacity proteins Opa and Opc, which interact with CD66/CEACAMs and integrin receptors, respectively, which are both found on the surface of the epithelial cells (Virji et al., 1994). However, CEACAMs are also found on other type of cells including endothelial cells and cells of the immune system.

1.5.2 Bacteraemia

Following the successful traversal of the nasopharyngeal mucosa, meningococci disseminate to sub-epithelial tissues from where they may gain access to the bloodstream. Meningococci must first evade human host defences, especially from phagocytes and the complement system, to survive in the bloodstream. Transient bacteraemia is expected when meningococci are faced with an effective immune response; however, if the latter is compromised, then meningococcal sepsis can be established (Hung and Christodoulides, 2013). To maintain bacterial survival, meningococci utilise a wide range of virulence factors. Functions of virulence factors involved in bacteraemia are summarised in Table 1.3.

Table 1.3: Functions of virulence factors involved in bacteraemia.

Virulence Factors	Function	References
Capsule	- Protects against complement - Prevents phagocytosis - Resists temperature increases during inflammation - Provides resistance to antimicrobial peptides and antibiotics	(Hammerschmidt et al., 1996b, Kahler et al., 1998)
Type IV pili	- Adhere to human vessels and trigger vascular damage - Adhere to endothelial cells leading to reshaping of the host cell plasma membrane with the formation of filopodia-like petrusions	(Imhaus and Dumenil, 2014)
LOS/Endotoxin	- Lipid A induces a release of cytokines (IL-1, IL-6, and TNF-α), chemokines, reactive oxygen species (ROS), and nitric oxides; thus, it leads to necrosis of tissues	(Zughaier et al., 2007)
	- Prevent the binding of dendritic cells by modification of its structure	(Kurzai et al., 2005)
Factor H Binding Protein (fHbp)	Binds to human fH and down-regulates complement pathway in host innate immunity	(Hammerschmidt et al., 1996b, Kahler et al., 1998, Madico et al., 2006, Welsch and Ram, 2008)
Iron acquiring proteins - TbpA/B - LbpA/B - HpuA/B and HmbR	Acquire iron from human blood iron-containing proteins including: - Transferrin, - Lactoferrin - Haemoglobin	(Irwin et al., 1993) (Pettersson et al., 1994) (Stojiljkovic et al., 1995)
FetA/FrpB	Binds to TonB siderophores secreted by other bacteria (e.g. *E. coli*)	(van der Ley et al., 1996)
IgA Protease	- Cleaves host immunoglobulin IgA - Hampers phagosome maturation via degrading lysosome-associated membrane proteins (LAMP1)	(Hopper et al., 2000)
NalP	Cleaves human complement C3 and degrades human C3b, helps the bacteria evading the innate immune system	(Del Tordello et al., 2014)
PorB	- Binds to human fH - down-regulates complement pathway *in vivo*	(Lewis et al., 2014)

The meningococcal capsules provide protection against complement-mediated bacterial killing and phagocytosis (Hammerschmidt et al., 1996b, Kahler et al., 1998). Based on the study by Spinosa et al., the meningococcal capsule also promoted intracellular survival in HeLa, HEp-2, or Chang conjunctiva cells (Spinosa et al., 2007). The encapsulated bacteria had an increased resistance to cationic antimicrobial peptides (CAMPS), while the non-capsulated bacteria were more susceptible to defensins, cathelicidins, protregins, and polymyxin B, which are used as model compounds to define the mechanism of action of CAMPs.

Similarly, shedding of outer membrane blebs, which are rich in bacterial endotoxin and outer membrane proteins (OMPs), allows diversion of antibodies and complement components away from the surfaces of intact bacteria. Survival of intracellular *Neisseria* is also influenced by the expression of IgA1 protease that hampers phagosome maturation via degrading lysosome-associated membrane protein 1 (LAMP1) (Hopper et al., 2000).

To survive the iron-limited environment in the bloodstream, meningococci express surface receptors including haemoglobin-binding receptors (HmbR and HpuA/HpuB) (Stojiljkovic et al., 1995, Lewis et al., 1997), transferrin-binding receptors (TbpA/TbpB) (Irwin et al., 1993), and lactoferrin-binding receptors (LbpA/LbpB) (Pettersson et al., 1994, Pettersson et al., 1998, Prinz et al., 1999), which are respectively assigned to hijack iron from human haemoglobin, transferrin and lactoferrin. Also, meningococci obtain iron from siderophores produced by other bacteria, for example the siderophore enterochelin, which is bound by the TonB-dependent outer membrane protein FetA/FrpB (Pettersson et al., 1995, van der Ley et al., 1996, Perkins-Balding et al., 2004). These iron uptake systems would support the growth and proliferation.

1.5.3 Traversing the blood-brain barrier

After invasion of the epithelial mucosa and circulation in the bloodstream, meningococci encounter the endothelium of the Blood Brain Barrier (BBB). Meningitis can occur if the bacteria disrupt this structure and enter the CSF. However, the BBB contains unique endothelial cells which prohibit the free exchange of molecules. The molecule transport pathways via tight junctions and enzymatic pathways are strictly limited in BBB. Thus, interactions between meningococci and the endothelium are complex. Until now, researchers are still answering questions regarding these interactions, especially the signalling pathways initiated and mechanisms of bacterial uptake.

The bacterial proteins involved in these interactions seem similar to those mediating bacterial interactions with the nasopharyngeal mucosa, in which the type IV pili, Opa, and Opc are the major adhesins that mediate adhesion to endothelial cells (Virji, 2009). The Type IV pili recruit the Par3/Par6/PKCzeta polarity complex which is essential in the establishment of eukaryotic cell polarity and the formation of intercellular junctions (Coureuil et al., 2009). The interaction between the pili and the polarity complex leads to the formation of ectopic intercellular junctional domains at the site of bacteria-host cell interaction and a subsequent depletion of junctional proteins at the cell-cell interface with opening of the intercellular junctions of the brain-endothelial interface.

Then, meningococci hijack the β2-adrenoceptor/β-Arrestin pathway to cross the brain endothelium by confining β-arrestin-interacting partners, such as the Src tyrosine kinase and junctional proteins, under the meningococcal colonies (Coureuil et al., 2010). Cytoskeletal reorganisation mediated by β-arrestin-activated Src stabilises bacterial adhesion to endothelial cells, whereas β-arrestin-dependent delocalisation of junctional proteins results in anatomical gaps used by bacteria to penetrate into tissues. In addition, meningococcal infection cause the brain endothelial cells to produce metalloproteinase-8, which disrupts the tight junction protein occludin leading to a subsequent BBB breakdown (Schubert-Unkmeir et al., 2010).

Meningococcal infection also impacts on the restoration of endothelial barrier. The bacteria modulate and interfere with the host cell cycle progression that is crucial to the growth of new endothelial cells and preservation of its barrier function. The opacity proteins have been reported

to trigger the accumulation of cells in the S phase of the endothelial cell cycle via p21 and Cyclin G2 (Oosthuysen et al., 2016).

1.6 Meningococcal porins

One major group of OMPs involved in the pathogenesis of *N. meningitidis* are the porins. These trimeric proteins are the most abundant proteins in the outer membrane of meningococci and are important as virulence factors and antigens for vaccines and therapeutics (Naumann et al., 1999, Achouak et al., 2001, Galdiero et al., 2003, Galdiero et al., 2012). The main function of meningococcal porins is to form channels in the outer membrane that are essential for the exchange of ions and small molecules between the bacterial periplasm and the external milieu. Two major classes of meningococcal porins are PorA (class I) and PorB (class II/III). Class II and III proteins are produced by two alleles of the single-copy PorB locus (Minetti et al., 1998).

PorA (*ca*. 45 kDa) contains 16 transmembrane β-strands and eight surface-exposed loops (Figure 1.4) (Derrick et al., 1999). Loop 1 and Loop 4 are the largest and most variable loops in PorA among different meningococcal strains (van der Ley et al., 1991).

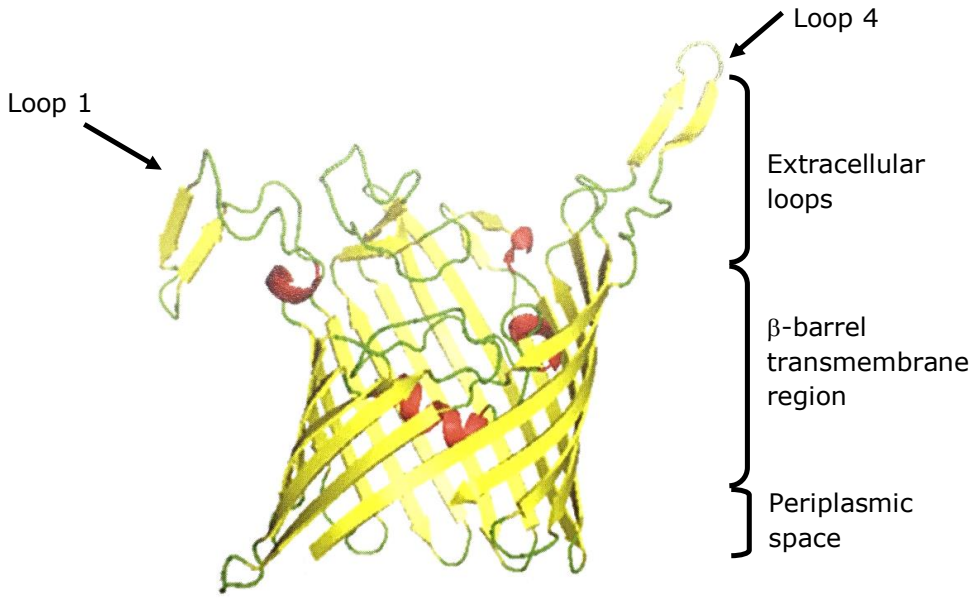

Figure 1.4: Ribbon diagram of the tertiary structure of PorA derived from *N. meningitidis* MC58 (Vassey, 2014). The model shows a classic β-barrel structure in the membrane (yellow), helix-turn-helix in PorA (red), and eight extracellular loops (green). Loop 1 (left) and loop 4 (top right) are the most prominent loops on the surface.

The variation of both loops is the basis of classification schemes as determined by both serological and DNA sequence-based schemes. PorB (*ca.* 33 kDa) has a similar loop structure to PorA, although they have different roles and characteristics in the pathogenesis of meningococci.

PorB has been reported to promote adhesion to host cells, translocate to mitochondria and affect host cell signalling. Muller et al. reported that PorB initiates the release of intracellular calcium and induces apoptosis via translocation to the host mitochondria (Muller et al., 1999). However, Massari et al. contradicted the previous report with the finding that PorB binds to mitochondrial porin voltage-dependent anion channel (VDAC) without an apoptotic effect, resulting in cell survival and activation of B cells (Massari et al., 2003). The immune stimulation by PorB was Toll-like receptor 2 (TLR-2) and MyD88 dependent (Massari et al., 2002). PorB binds directly to TLR2/TLR1 heterodimer and activates NF-κB (Massari et al., 2006). Although NF-κB is involved in the regulation of Bcl-XL and inhibitors of apoptosis (IAPs) in the intrinsic pathway (Nagata, 1997, Chen et al., 2000, Bernal-Mizrachi et al., 2006), the antiapoptotic effect of PorB was independent of TLR-2 and NF-κB (Massari et al., 2010). In addition, PorB has been shown to regulate the alternative complement pathway via binding to human factor H (Lewis et al., 2014).

Unlike PorB, PorA has not been reported to translocate from the bacterial membrane. PorA is not expressed by gonococci, suggesting a specific role in the life cycle of meningococci which may have implications for its pathogenesis. The loops of PorA are frequently recognised by human antibodies in convalescent patients. Thus, OMV vaccines have been produced based on porins (van der Ley et al., 1991). These loops are subject to variation by changing the length of the sequence via point mutations, insertions, and deletions in the gene encoding PorA resulting in changes in the protein structure and expression; they can also lead to attenuation in antibody binding. PorA expression is influenced by phase variation, which can lower expression rates during long-term persistent meningococcal carriage; such changes will become subjects to antibody-mediated selection (Alamro et al., 2014). It leads to host persistence, allowing the bacteria to establish a commensal relationship within the human host. Phase variation of PorA might also impact on the effectiveness of PorA-based vaccines.

Reported strains of meningococci with a *porA* deletion were rare. Van der Ende et al. found that *porA* deletions in H44/76 and H355 strains were

probably caused by recombination between RS3 core sequences (Van der Ende et al., 1999). RS3 contains nine direct and inverted repeats, which share a common 6-bp core sequence, 5'-ATTCCC-3' or 5'-GGGAATS' (Haas and Meyer, 1986). The deletion of *porA* occurred via recombination between homologous regions of 116 bp upstream and downstream of *porA*.

Our group's previous studies showed that PorA (via Loop4) binds to the non-integrin laminin receptor (LAMR) in human microvascular endothelial cells (Orihuela et al., 2009, Abouseada et al., 2012). A recent paper confirmed these findings, as NMB1429 (aka PorA) was reported as part of the surface HBMEC interactome of *Neisseria meningitidis* (Kanova et al., 2018). Both meningococcal PorA and PilQ are able to engage LAMR in HBMECs (Orihuela et al., 2009). However, not only meningococcal PorA binds to LAMR but also pneumococcal CbpA and OmpP2 of *H. influenzae* (Orihuela et al., 2009). Binding of these three major bacterial pathogens to LAMR reveals the importance of LAMR as a receptor for pathogens which target the central nervous system (CNS).

1.7 Human non integrin laminin receptor (LAMR) as the cellular receptor for meningococcal adhesins

LAMR is a cell-surface receptor, important for many fundamental cellular processes. It was first identified in 1983 as a 67-kDa protein (67LR) that binds to immobilised laminin-1 (Lesot et al., 1983, Malinoff and Wicha, 1983, Rao et al., 1983, Orihuela et al., 2009, Abouseada et al., 2012). Later, Rao et al. reported that the protein might arise from a 37-kDa precursor (37LRP) based on SDS-PAGE results (Rao et al., 1989). The ribbon diagram of both 67LR and 37LRP is presented in Figure 1.5. LAMR is equivalent to laminin binding protein p40, part of the 40S ribosome. Thus, it is also known as ribosomal protein SA (RPSA) (Tohgo et al., 1994).

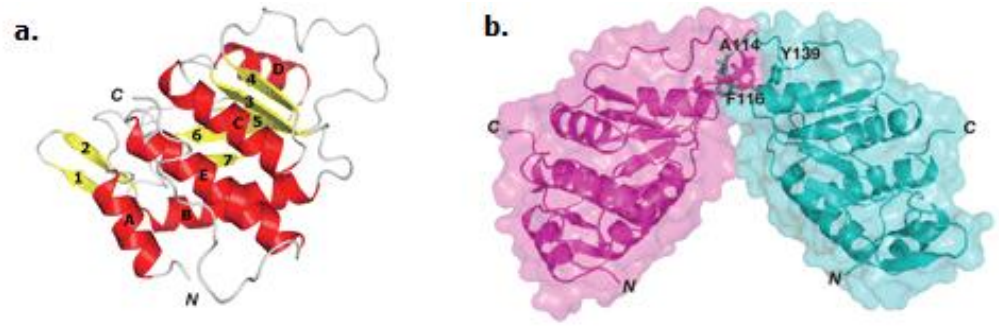

Figure 1.5: Crystal structure of LAMR (Jamieson et al., 2008). (a) Ribbon diagram of (a) 37 kDa LAMR (37LRP) with α helices colored red (A-E) and β strands colored yellow (1-7). (b) 67LR structure built from homodimer interaction of 37LRP (magenta) with another 37-LRP molecule (cyan). Residues in the dimer interface are labeled. The crystallographic two-fold axis is vertical.

1.7.1 The molecular structure of LAMR

LAMR is encoded in humans by the RPSA gene (NCBI Gene ID: 3921, Accession No.: AC_000135). The gene is a 5,833-bp stretch along chromosome location 3p22.2 consisting of seven exons and six introns (Jackers et al., 1996). The human RPSA gene produces a final mRNA of 1,155 nucleotides (Accession No.: NM_002295) or a 1,109-nucleotide variant with an alternative 5′ exon prior to the start codon (NM_001012321) (Satoh et al., 1992). The open reading frame of 855 bases encodes a 295-amino acid protein termed 37LRP (Wewer et al., 1986, Castronovo et al., 1991).

37LRP was originally presumed to be a precursor to 67LR based on two studies. The first study found the conversion of 37LRP to a higher molecular weight (HMW) 67-kDa form using pulse-chase radiolabelled cells to monitor the transition over time (Castronovo et al., 1991). The second attempt to solidify a precursor relationship comes from a study hypothesising that fatty acid acylation of 37LRP may be required for the transition to the HMW form (Buto et al., 1998).

As the understanding of the receptor has grown, more evidence has suggested a more complex relationship between 37LRP and 67LR. Buto et al. proposed that LAMR is possibly a heterodimer between 37LRP and Galectin-3 (Buto et al., 1998), which is supported by the findings that lectin epitopes are present in LAMR, laminin recognition by LAMR is lactose dependent, and LAMR can be eluted from laminin-affinity chromatography columns by lactose (Castronovo et al., 1991). The hypothesis was confirmed

by our group's findings of a heterodimeric form of LAMR consisting of 37LRP and Galectin-3 (Alqahtani et al., 2014).

Later studies showed that more possible forms of LAMR are present in human cells. DiGiacomo and Meruelo suggested that there are possibly seven different LAMR species in the cell including (1) intracellular LAMR (37 kDa), (2) extracellular peripheral membrane LAMR (67 kDa) capable of independently binding laminin, (3) extracellular peripheral membrane LAMR (37 kDa) supporting integrin laminin binding, (4) LAMR (67 kDa) membrane-associated via the properties of a homo- or heteromer, (5) LAMR (67 kDa) with hypothetical transmembrane domain (TMD), (6) shed LAMR (67 kDa), and (7) intracellular small ubiquitin-like modifier (SUMO)ylated LAMR (53 kDa) (shown in Figure 1.6) (DiGiacomo and Meruelo, 2015). LAMR has been localised to the membrane, ribosomes, cytoplasm, and nucleus.

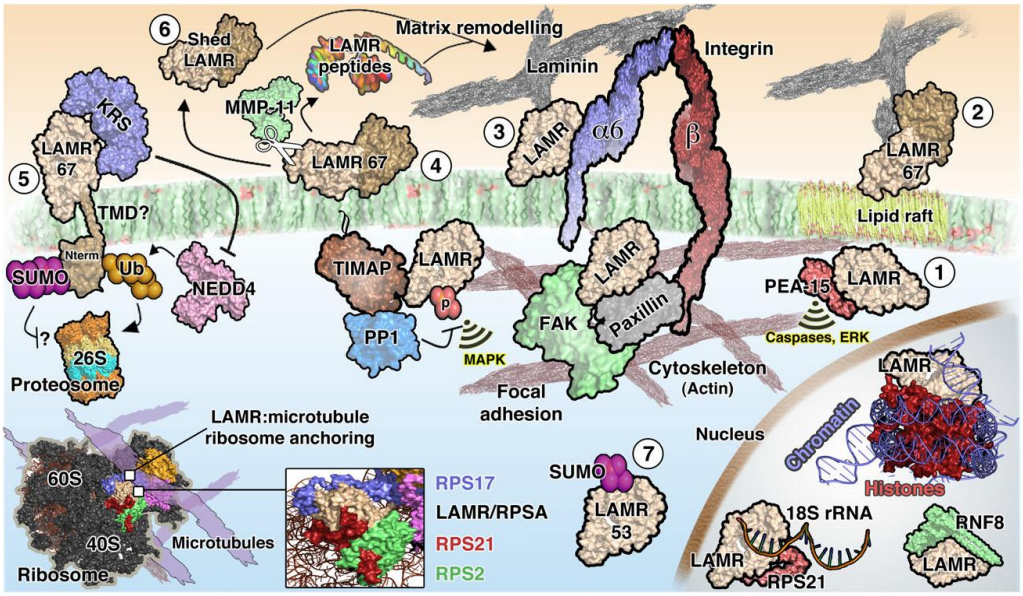

Figure 1.6: Cellular Biology Overview of LAMR/RPSA. Several possible LAMR species are depicted including (1) intracellular LAMR; (2) extracellular peripheral membrane 67LR capable of independently binding laminin; (3) extracellular peripheral membrane 37LRP supporting integrin laminin binding; (4) 67LR membrane association via the properties of a homo- or heteromer; (5) 67LR with hypothetical transmembrane domain (TMD). It is unclear how LAMR membrane presence is dynamically regulated by intracellular proteins in the absence of a TMD; (6) shed 67LR and (7) intracellular SUMOylated LAMR. Ribosomal, cytoskeletal and nuclear localisations of LAMR in addition to its presence at focal adhesions are also depicted. All protein-protein contacts represent experimentally demonstrated interactions. Signalling indications (yellow) represent preliminary evidence for signalling cascades involving LAMR. Because of ambiguity in the data, the subcellular locations of each protein are not necessarily accurate and represent only predictions based on available evidence. Similarly, the species of LAMR (i.e. 37/67 kDa) depicted for each function is not meant to suggest exclusivity or a definitive understanding of the relevant molecule(s). This figure is reproduced from (DiGiacomo and Meruelo, 2015).

In addition to 37LRP and 67LR, LAMR appears to have the 53-kDa (SUMO)ylated form after cellular stress or a particular signalling stimulus (Golebiowski et al., 2009, Manza et al., 2004). Previously, it was predicted that SUMO oligomers might build 67LR and larger species (Digiacomo et al., 2015). However, a recent report suggested that SUMOylation is not associated with the 67LR formation (Umbaugh and Figueiredo, 2018).

1.7.2 The cellular function of LAMR

In addition to laminin binding, LAMR has been shown to be involved in ribosomal biogenesis and translation, pre-RNA processing, cellular migration, invasion, cytoskeleton reorganisation, as well as chromatin and histone binding (DiGiacomo and Meruelo, 2015). The effects of reduced LAMR expression are known to include: decreases in viability (Scheiman et al., 2010a), reduction in proliferation and induction of G_1 arrest (Satoh et al., 1999, Scheiman et al., 2010b), attenuation of protein synthesis (Scheiman et al., 2010b), disruption of pre-rRNA processing (O'Donohue et al., 2010), and reduced adhesive and migratory ability (Venticinque et al., 2011).

These phenotypes were confirmed by our group in a previous study (Vassey, 2014). Exposure of HBMECs to PorA-Loop4, the meningococcal ligand of 37LRP, caused a significant change to the cellular actin cytoskeleton in the immunofluorescent microscopy images. Flow cytometric analysis indicated that the PorA-Loop4 peptide caused G_1 arrest. Using the Roche XCELLigence system, the treatment of HBMECs with PorA-Loop4 peptide resulted in a reduction of cellular impedance in a dose-dependent manner, indicating a change in cellular adhesion. The cell migration was also inhibited by the PorA-Loop4 in wound healing assay.

LAMR binds to laminin in the basement membrane. The 67LR mainly interacts with laminin-1 (Sasaki et al., 2004). At least three regions of the C-terminal domain of 67LR are known to be involved in laminin binding: (1) the most C-terminal 53 amino acids containing four acidic TEDWS repeats, (2) a putative helical stretch between amino acids 205-229; and (3) a heparan sulfate-dependent laminin-binding region from amino acids 161-180 (Figure 1.7) (Kazmin et al., 2000). The LAMR-laminin interaction affects intracellular laminin signalling. In the cytoplasm, LAMR was shown to co-localise with actin, focal adhesion kinase (FAK) and paxillin: all crucial cytoskeletal rearrangement participants in laminin signalling (Venticinque et al., 2011).

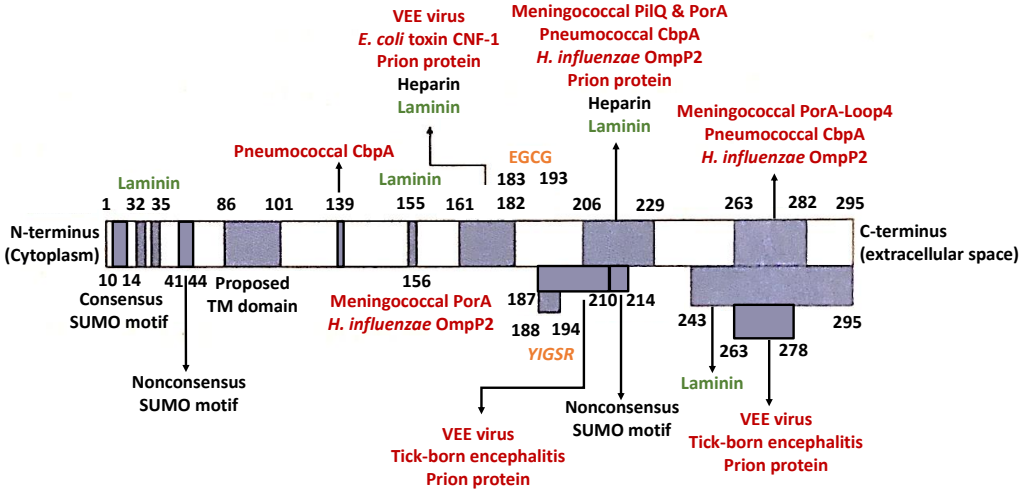

Figure 1.7: The main functional regions of human LAMR. Blue boxes represent the specific binding domains of LAMR ligands with amino acids positions indicated numerically. Binding sites identified for known LAMR targeting pathogens (red), natural ligands/LAMR binding peptides (orange), and laminin binding sites (green). Functional domains identified from a combination of published literature and homology modelling (*italics*). TM: transmembrane, CbpA: Choline-binding protein A, OmpP2: Outer membrane protein P2, VEE: Venezuelan equine encephalitis, EGCG: green tea polyphenol epigallocatechin-3-gallate (anti-cancer properties working through LAMR as receptor) (Umeda et al., 2008), *YIGSR* homology domain: the binding site for the minimal ligand sequence of laminin required for interaction with LAMR (Di Giovanni et al., 2012), SUMO: small ubiquitin-like modifier LAMR, consensus SUMO motif: a SUMO motif observed in all mammalian species, nonconsensus SUMO motif: identified in *H. sapiens* 37LRP sequence (Umbaugh and Figueiredo, 2018). This image is modified from Vassey, (2014) and Qarani, (2015).

37LRP is a part of the ribosome component defined as p40 (Tohgo et al., 1994). The function of LAMR ribosomal incorporation is not known outside the observation that it is important for protein synthesis and ribosome biogenesis (Malygin et al., 2011). The N-terminal domain of 37LRP is sufficient for ribosomal binding (Scheiman et al., 2010a), while the C-terminal (210-295) region is co-opted for binding additional proteins, stabilising binding or interacting with rRNA (Malygin et al., 2011). In a recent report, the lysine residues within putative SUMO motifs of 37LRP (Figure 1.7) appeared to alter steady-state levels of pre and/or mature rRNA levels (Umbaugh and Figueiredo, 2018).

The nucleolar localisation of 37LRP was noted early, but the functional implications are still not clear. It is not clear if the SUMO modification of LAMR plays a role in nuclear import, a common function of SUMOylation

(Chen et al., 2013, DiGiacomo and Meruelo, 2016). The presence of LAMR in the nucleus is explained by its association with nucleolar pre-40S ribosomes and small nucleolar ribonucleoproteins (O'Donohue et al., 2010). 37LRP also potentially interacts with chromatin and histones (H2A, H2B, and H4) (Kinoshita et al., 1998, O'Donohue et al., 2010).

LAMR is also reported to mediate intracellular signalling. LAMR was identified interacting with TGF-inhibited membrane-associated protein (TIMAP) and Protein phosphatase 1 (PP1) (Kim et al., 2005a), representing one possible mechanism leading to downstream effects. TIMAP and PP1 have been linked to the regulation of 67LR phosphorylation and GSK-3β signalling (Kim et al., 2005a, Li et al., 2007a). In addition, LAMR might alter the MAPK pathway based on a report that the lower LAMR levels gave an increase of phosphorylated ERK, JNK and p38 (Givant-Horwitz et al., 2004). Laminin-induced signals also might lead to the phosphorylation of phosphoprotein enriched in astrocytes 15 (PEA-15), an adaptor protein that binds LAMR (Formisano et al., 2012). Phosphorylation of PEA15 leads to activation of the ERK cascade as well as blockage of caspase activation, linking LAMR to laminin pro-survival signalling.

1.7.3 LAMR association with human disease

LAMR has been associated with several diseases including neoplastic and metastatic cancers, neurodegenerative diseases, several developmental aberrations, and certainly microbial infections.

LAMR has mostly been studied for its overexpression in malignant cancerous cells. Tumour progression might be associated with LAMR's ribosomal functions (Scheiman et al., 2010b, DiGiacomo and Meruelo, 2016). It has been investigated as a prognostic marker in solid and haematological malignancies (Martignone et al., 1993, Ménard et al., 1998, Friedrichs et al., 2008). The receptor is mainly associated with breast carcinomas, colorectal carcinomas and lymphomas (Martignone et al., 1993, Colnaghi, 1994, Carbone et al., 1995, Sanjuan et al., 1996, Tagliabue and Pastorino, 1996, Viacava et al., 1997), but gastric (d'Errico et al., 1991), ovarian (Van den Brule et al., 1994), lung (Satoh et al., 1992, Pellegrini et al., 1994), thyroid (Basolo et al., 1996, Montuori et al., 1999), prostate (Waltregny et al., 1997), laryngeal (Zhou et al., 2006), and renal/adrenal tumours (Zelle-Rieser et al., 2001) have also been investigated in addition to mesotheliomas, melanomas, leukaemias, astrocytomas,

hepatocarcinomas, and the various metastatic sites of these cancers (DiGiacomo and Meruelo, 2015).

Neurodegenerative diseases and developmental aberrations are related to the interaction between LAMR and prions (DiGiacomo and Meruelo, 2015). Prions are misfolded proteins responsible for neurodegenerative diseases in animals and humans. LAMR is the receptor responsible for the binding and internalisation of the protease-resistant infectious form of prions PrP^{sc} (Simoneau et al., 2003). The PrP^{sc} form of prions is the pathological molecule in bovine spongiform encephalopathy (mad cow disease) in bovids and Creutzfeldt-Jakob disease in humans (Rieger et al., 1999). LAMR also has been suggested to be involved in the development of Alzheimer's disease because of the commonalities of amyloid beta (Aβ), an etiological agent in Alzheimer's disease, with prion proteins and the association of PrP^{sc} in Aβ-related pathology (Da Costa Dias et al., 2011). LAMR was reported to contain irregular oxidative modifications in proteomics investigation of the brains of Alzheimer's disease model mice (Shin et al., 2004). Modulation of LAMR affected the Aβ cytotoxicity (Da Costa Dias et al., 2013), and its release from cells (Jovanovic et al., 2014).

LAMR has been reported as the receptor for numerous microbial pathogens including viruses, protozoa, and bacteria (details in Section 1.7.4). LAMR has been shown to interact with viruses including Sindbis (Wang et al., 1992, Strauss et al., 1994), Venezuelan equine encephalitis (Ludwig et al., 1996), Dengue (Thepparit and Smith, 2004), Adeno-associated (Akache et al., 2006), West Nile (Bogachek et al., 2008), Tick-borne encephalitis (Protopopova et al., 1999), and Japanese encephalitis viruses (Thongtan et al., 2012). LAMR might enhance the cell surface interaction of the parasitic protozoan *Toxoplasma gondii* (Furtado et al., 1992).

1.7.4 Roles of LAMR in bacterial infection

All reports to date on the roles of LAMR in bacterial infection are related to bacterial meningitis. Chung et al. and Kim et al. studied LAMR as a cellular target for *E. coli* K1 cytotoxic necrotising factor 1 (CNF1) (Chung et al., 2003, Kim et al., 2005b). Binding of CNF1 to LAMR activates Rho GTPases, which triggers cytoskeletal rearrangements and enhances bacterial uptake in human brain microvascular endothelial cells (HBMECs).

In 2009, Orihuela et al. reported LAMR as a common receptor for pneumococcal CbpA, meningococcal PilQ and PorA, and OmpP2 of *H. influenzae* on the surface of HBMECs (Orihuela et al., 2009). The carboxyl terminus of LAMR appeared to be a likely common recognition site for these adhesins. Further studies by Abouseada et al. described meningococcal PorA-Loop4 and OmpP2-loop2 of *H. influenzae* as critical domains for LAMR binding (Abouseada et al., 2012). Residues 198-208 within PorA-Loop4 and residues 91-99 within OmpP2-loop2 were essential for optimal binding to LAMR. Subsequently, Alqahtani et al. showed evidence that PorA preferentially targets the 37LRP isoform of LAMR (Alqahtani et al., 2014). The binding region of PorA-Loop4 on 37LRP was in the region of amino acids 263-282 on the C-terminal end of the protein (Alqahtani et al., 2014, Qarani, 2015). These findings suggest an important role for PorA-Loop4 in the host-pathogen interaction. An illustration of the interaction between 37LRP and meningococcal adhesins including PorA is presented in Figure 1.8.

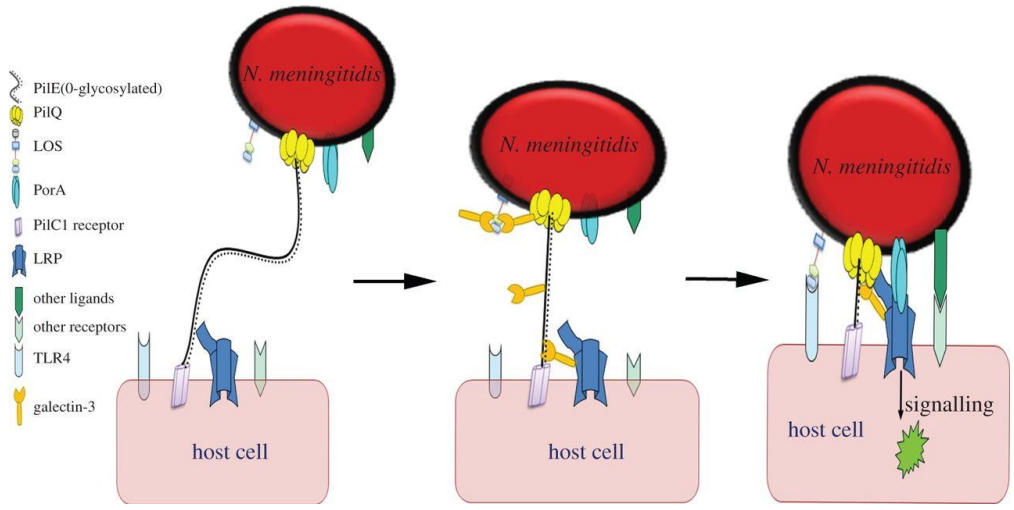

Figure 1.8: Illustration of meningococcal binding to host cells using surface ligands (Alqahtani et al., 2014). Initial contact mediated by PilC1, which binds its putative receptor, followed by 37LRP/Gal-3-PilE binding, which strengthens the initial contact, and pilus retraction, which brings the two cells closer together. Decametric PilQ on the meningococci surface binds to both 37LRP and Gal-3, establishes intimate contact, strengthens interactions, and triggers host cell signalling events.

Meningococcal PorA not only facilitates bacterial binding to the surface of host cells but also likely alters host cell signalling leading to an alteration in the host cell cycle. Recently, a study by Vassey suggested that binding of PorA-Loop4 to 37LRP led to a cellular response including (1)

bacterial cellular invasion, (2) inhibition of cellular migration, and (3) G_1-phase cell cycle arrest (Vassey, 2014).

The reduced expression of LAMR affected the association and invasion of *N. meningitidis* MC58 with HBMECs. The LAMR siRNA treatment for 48 h caused 20% reduction of meningococcal association and 40% reduction of meningococcal invasion (Vassey, 2014). Further experiments showed that the recruitment of 67LR to *N. meningitidis* MC58 was not affected by deletion of PorA-Loop4 (Vassey, 2014). However, the ability of this mutant to recruit and bind 37LRP under its colonies was significantly reduced by 20% ($p \leq 0.001$). It showed that the meningococcal invasion in HBMECs was established by the PorA-Loop4:37LRP interaction.

The interaction of PorA-Loop4 with epithelial cells affected cellular migration. Using a wound healing assay, treatment of Human Colon Carcinoma Cells (HCT116) with PorA-Loop4 peptide significantly inhibited cell migration at all-time points between 16 - 60 h compared to the untreated (or scrambled peptide) control (Vassey, 2014). HCT116 were chosen as a model in the wound healing assay to replace HBMECs. The size of HBMECs were too large (50-100 µm diameter) and HBMECs closed the wound gap (ca. 400 µm) very quickly. In preliminary experiments, the wound gap was made larger but could no longer be visualised with the available microscope (Vassey, 2014).

Using a ClickiT Edu proliferation assay, addition of PorA-Loop4 peptide to HBMECs, HCT116 cells or Human Pharyngeal Carcinoma cells (Detroit 562) reduced the number of cells in S-phase by 24%, 10%, and 11%, respectively, suggesting the cells may have entered a cell cycle arrest (Vassey, 2014). Later, the results from BrdU incorporation assays (cell cycle analysis via flow cytometry) confirmed that the PorA-Loop4 treated cells showed a significant increase in the proportion of cells at the G_1 checkpoint: 23%, 10% and 8% of HBMEC, HCT116 and Detroit 562 cells, respectively, were arrested at this stage in the cell cycle (Vassey, 2014).

Evidence for PorA-Loop4 inducing a G_1 arrest via its interaction with LAMR is supported by the role of the laminin receptor in regulating the host cell cycle. 37LRP is essential for viability of HeLa and Hep3b epithelial cells (Kaneda et al., 1998, Susantad and Smith, 2008). Also, Scheiman et al. reported that the deletion of 75 amino acids at the C-terminal end of 37LRP affected host cell proliferation causing a G_1 arrest in epithelial cells (Scheiman et al., 2010b). However, more investigation of the downstream

signalling events following PorA-Loop4 binding are required to confirm the mechanism/pathways involved which result in the G_1 arrest.

1.8 Mammalian Cell Cycle

Cell division and proliferation are the essential functions of a living organism in order to maintain growth, development and tissue maintenance. Initially, cell division consists of two stages: mitosis (nuclear division), and interphase (interlude between two M phases). Mitosis was further divided into prophase, metaphase, anaphase, and telophase. The interphase was then carefully observed under the microscope and classified into G_1 (first gap phase characterised by cell growth), S (DNA replication), and G_2 (second gap phase in which cells are prepared for division) (Figure 1.9) (Pardee et al., 1978). Together, these phases form a cell cycle or a cell-division cycle leading to duplication of DNA (DNA replication) and segregation of replicated chromosomes into two separate cells.

Cells in G_1 may enter a resting state called G_0 before they are committed to DNA replication in the restriction (R) point (Baserga, 1976, Prescott, 1976, Pardee et al., 1978, Vermeulen et al., 2003). Cells in G_0 account for the major part of the non-growing, non-proliferating cells in the human body. The G_0 cells can be stimulated by mitogenic signals to re-enter the cell cycle.

Progression through the cell cycle is controlled mainly by the cyclins and their partner molecules, cyclin-dependent kinases (CDKs) (Vermeulen et al., 2003, Weinberg, 2014). Each cyclin binds and activates a specific CDK to form a Cyclin-CDK complex that modulates the cell cycle machinery (Figure 1.9). Other proteins also regulate the cell cycle including CDK inhibitors (CKIs), CDK substrates (i.e. retinoblastoma protein (pRb), Wee1, Myt1, Cdc25, microtubules, vimentin), and checkpoint regulators (i.e.. p53, ataxia-telangiectasia-mutated (ATM), ataxia and rad3 related (ATR), DNA-dependent protein kinase) (Vermeulen et al., 2003).

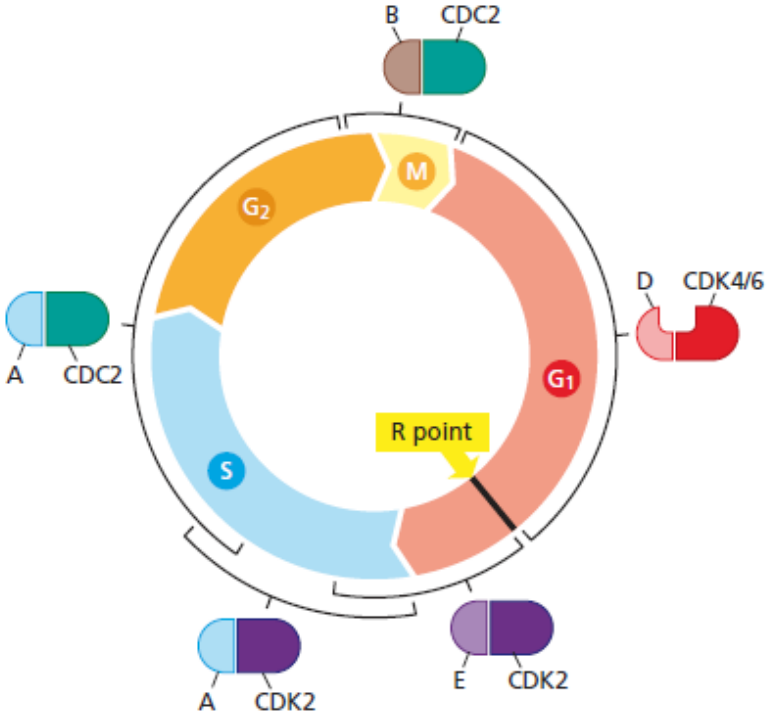

Figure 1.9: Pairing of cyclins with cyclin-dependent kinases to control human cell cycle (Weinberg, 2014). Each type of cyclin pairs with a specific cyclin-dependent kinase (CDK) or set of CDKs. The D-type cyclins (D1, D2, and D3) bind CDK4 or CDK6, the E-type (E1 and E2) bind CDK2, the A-type cyclins (A1 and A2) bind CDK2 or CDC2, and the B-type cyclins (B1 and B2) bind CDC2. The brackets indicate the periods during the cell cycle when these various Cyclin–CDK complexes are active.

1.8.1 Cyclin Dependent Kinases (CDKs)

The CDKs are a family of serine/threonine kinases which are activated at specific points of the cell cycle. The active CDKs induce downstream processes by phosphorylating selected proteins (Morgan, 1995, Pines, 1995, Vermeulen et al., 2003). So far, nine CDKs have been identified, and of these five are active during the cell cycle, i.e. during G_1 (CDK4, CDK6 and CDK2), S (CDK2), G_2 and M (CDK1 also known as CDC2) (Figure 1.9, Table 1.4). A complex of CDK7 and Cyclin H acts as CDK Activating Kinase (CAK) at all cell cycle phase (Fisher and Morgan, 1994, Vermeulen et al., 2003). The remaining CDKs have not yet been shown to have a crucial role in normal cell cycle progression (Rickert et al., 1996, Vermeulen et al., 2003). CDK protein levels remain stable during the cell cycle, in contrast to their activating proteins, the cyclins.

Table 1.4: Cyclin-CDK complexes are activated at specific points of the cell cycle (Vermeulen et al., 2003).

CDK	Cyclin	Cell cycle phase activity
CDK4	Cyclin D1, D2, D3	G_1 phase
CDK6	Cyclin D1, D2, D3	G_1 phase
CDK2	Cyclin E	G_1/S phase transition
CDK2	Cyclin A	S phase
CDK1 (CDC2)	Cyclin A	G_2/M phase transition
CDK1 (CDC2)	Cyclin B	M phase
CDK7*	Cyclin H*	all cell cycle phases

*CDK Activating Kinase (CAK)

CDK levels remain constant throughout the cell cycle and most regulation is post-translational (Morgan, 1995, Arellano and Moreno, 1997). In general, there are four major regulatory mechanisms of CDKs: 1) most CDKs require binding to cyclins to become active; 2) CDK activity is inhibited by binding of CKIs; 3) phosphorylation of conserved residues in the ATP-binding pocket of the CDK inhibits its activity; and 4) phosphorylation of a conserved residue in the T-loop of CDKs is required for the activation of most CDKs (Liu and Kipreos, 2000-2003). CAK phosphorylates CDK1, CDK2, and CDK4 at threonine 161, threonine 160, and threonine 172, respectively. The phosphorylation by CAK induces conformational changes and enhance the binding of cyclins (Jeffrey et al., 1995, Paulovich and Hartwell, 1995, Vermeulen et al., 2003). Loss of CAK activity leads to a cell cycle arrest (Larochelle et al., 1998).

1.8.2 Cyclins

Cyclins are a group of proteins that are classified based on the existence of a conserved 100 amino acid structure named 'cyclin box' (Hadwiger et al., 1989, Weinberg, 2014). All cyclins contain a similar tertiary structure of two compact domains of 5 α helices (Brown et al., 1995). The first of which is the conserved cyclin box, outside of which cyclins are divergent. The cyclin box is involved in the binding and functional activation of CDKs (Hadwiger et al., 1989, Weinberg, 2014).

The protein levels of cyclins oscillate during the cell cycle (Evans et al., 1983, Pines, 1991, Vermeulen et al., 2003). Different cyclins are required at different phases of the cell cycle (Table 1.4), thus, the cyclin genes are

expressed periodically at certain phases. However, Cyclin D differs from other cyclins as it is synthesised as long as extracellular signals and growth factor stimulations persist (Weinberg, 2014).

Sixteen cyclins have been identified but only five cyclins are cell-cycle related (Okamoto and Beach, 1994, Rickert et al., 1996, Peng et al., 1998, Vermeulen et al., 2003). Each of the Cyclin D proteins (Cyclin D1, Cyclin D2, and Cyclin D3) forms a complex with CDK4 or CDK6 to enter the G_1 phase and regulate the cell cycle before the R point (Sherr, 1994, Weinberg, 2014). Another G_1 cyclin is Cyclin E which binds to CDK2 to regulate the progression from G_1 to S phase (Ohtsubo et al., 1995, Vermeulen et al., 2003). During S phase, the progression is regulated by Cyclin A-CDK2 complex (Girard et al., 1991, Walker and Maller, 1991, Vermeulen et al., 2003). In late G_2, Cyclin A binds to CDK1 to promote entry into M phase. Mitosis is further regulated by Cyclin B-CDK1 complex (King et al., 1994, Arellano and Moreno, 1997, Vermeulen et al., 2003).

The collapse of cyclin levels is required to enter another phase of the cell cycle. Ubiquitins rapidly degrade the cyclins at each checkpoint of the cell cycle (Weinberg, 2014). The ubiquitin binds to a cyclin at destruction-box motif or PEST sequence (segment rich in proline (P), glutamic acid (E), serine (S) and threonine (T) residues), and leads to a proteolytic breakdown in the proteasomes (Glotzer et al., 1991, Rechsteiner and Rogers, 1996, Vermeulen et al., 2003, Weinberg, 2014).

1.8.3 CDK inhibitors (CKIs)

CDK activity can be counteracted by CKIs which bind to CDK alone (Carnero and Hannon, 1998) or to the Cyclin-CDK complex (Polyak et al., 1994, Harper et al., 1995, Lee et al., 1995, Hengst and Reed, 1998). CKIs consist of INK4 family and Cip/Kip family (Sherr and Roberts, 1995). The INK4 family consists of p15 (INK4b), p16 (INK4a), p18 (INK4c), and p19 (INK4d). Each INK4 binds to CDK4 or CDK6 and forms a stable complex before cyclin binding (Carnero and Hannon, 1998). The Cip/Kip family consists of p21 (Waf1, Cip1), p27 (Cip2), and p57 (Kip2). These inhibitors inactivate the Cyclin-CDK complexes (Polyak et al., 1994, Harper et al., 1995, Lee et al., 1995, Hengst and Reed, 1998). The Cip/Kip family is also involved in the regulation of transcription, apoptosis, and cytoskeleton (Wang et al., 1997, Nagahara et al., 1998, Coqueret, 2003, Besson et al., 2004). CKIs are regulated by both internal and external signals. Each CKI is induced by different stimuli (Figure 1.10).

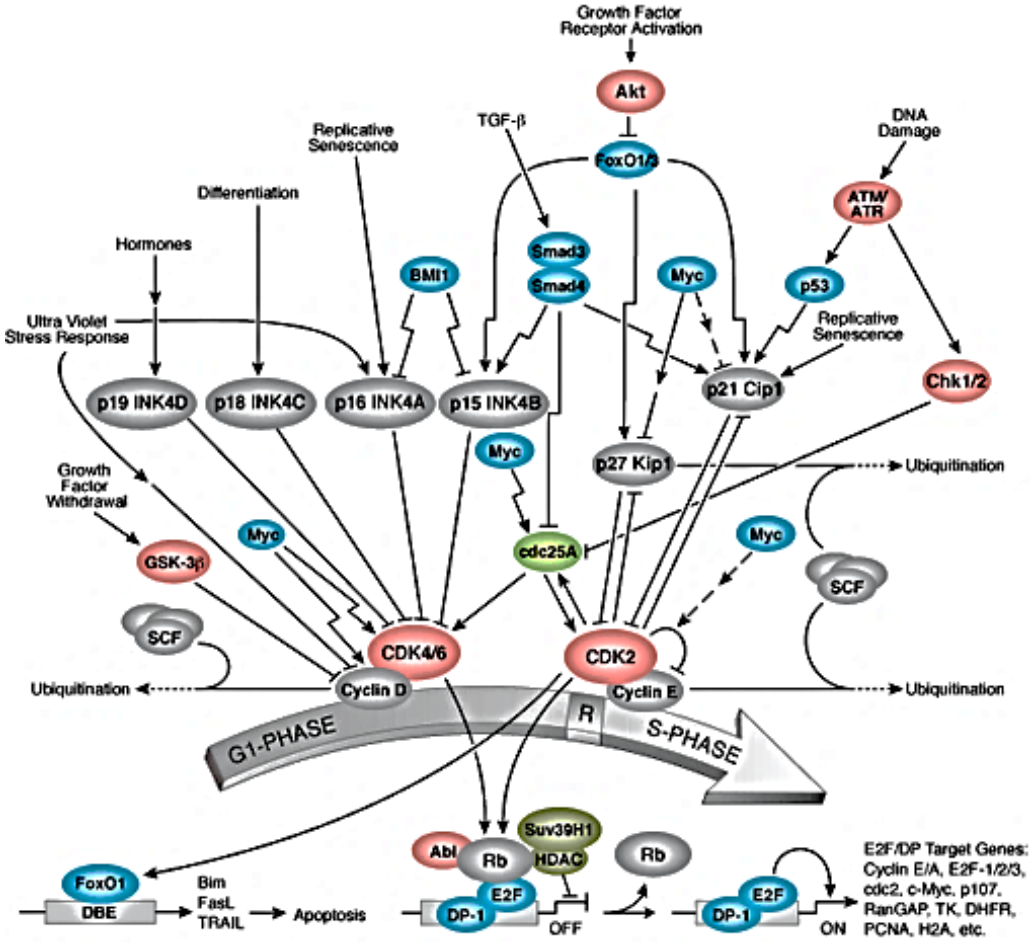

Figure 1.10: Schematic representation of the Cell Cycle G_1/S Checkpoint. The primary G_1/S cell cycle checkpoint controls the commitment of eukaryotic cells to transition through the G_1 phase to enter into the DNA synthesis S phase. Two cell cycle kinase complexes, Cyclin D-CDK4/6 and Cyclin E-CDK2, work in concert to relieve inhibition of a dynamic transcription complex that contains the retinoblastoma protein (Rb) and E2F. In G_1-phase uncommitted cells, hypo-phosphorylated Rb binds to the E2F-DP1 transcription factors forming an inhibitory complex with HDAC to repress key downstream transcription events. Commitment to enter S-phase occurs through sequential phosphorylation of Rb by Cyclin D-CDK4/6 and Cyclin E-CDK2 that dissociates the HDAC-repressor complex, permitting transcription of genes required for DNA replication (Cell Signaling Technology, 2012).

1.8.4 CDK substrates

When CDK is active, target proteins become phosphorylated on CDK consensus sites, resulting in changes that are physiologically relevant for cell cycle progression. The most frequently studied CDK target is pRb, the substrate of Cyclin D-CDK4/6 and Cyclin E-CDK2 complexes (Vermeulen et

al., 2003). The two complexes work in concert to relieve inhibition of a dynamic transcription complex that contains the retinoblastoma protein (Rb) and E2F (Figure 1.10).

In G_1-phase uncommitted cells, hypo-phosphorylated Rb binds to the E2F-DP1 transcription factors forming an inhibitory complex with histone deacetylases (HDAC) to repress key downstream transcription events (van den Heuvel and Dyson, 2008, Cell Signaling Technology, 2012). During early G_1, the Cyclin D-CDK4/6 complex phosphorylates pRb and this leads to disruption of HDAC and release of E2F-DP1, which positively regulate the transcription of genes whose products are required for S phase progression, including Cyclin A and Cyclin E (Buchkovich et al., 1989, Kato et al., 1993, Brehm et al., 1998). The Cyclin E-CDK2 complex maintains the hyper-phosphorylated state of pRb for the remainder of the cell cycle.

1.8.5 Signalling pathways that control cell proliferation

Control of cell proliferation generally occurs during G_1 phase when multiple signals, ranging from growth factors to DNA damage, influence the decision to enter S phase. Hence, G_1 regulators are linked with a diverse set of pathways controlling differentiation, cell quiescence, senescence, and responses to a variety of stresses. Once the cell enters the R point, the cells will undergo an intracellular autonomous program which is independent of extracellular growth factors.

The Cyclin D1 transcription is activated by the canonical Ras–Raf–MEK–ERK mitogen-activated protein kinase (MAPK) pathway (Morrison, 2012). The pathway stimulates the transcription factors, Jun and Fos, which bind to an AP1 site in the Cyclin D1 promoter (Albanese et al., 1995). The Cyclin D1 gene (*CCND1*) is also induced by other signalling pathways including mitogen-stimulated Rac and NF-κB signalling, cytokine signalling, signalling by receptors for extracellular matrix (ECM) proteins (e.g. integrins), and the Wnt and Notch pathways (Kopan, 2012, Nusse, 2012). Multiple transcription factors regulate the *CCND1*, including Jun, Fos, STAT3, β-catenin, and NF-κB (Duronio and Xiong, 2013).

The protein level of Cyclin D1 must be high during G_1 phase, but then must be suppressed to low level during S phase for efficient DNA synthesis (Yang et al., 2006b). The Cyclin D1 degradation at the S phase is related to the phosphorylation at Thr286 and Thr288 by active GSK-3β and Dyrk1B, respectively (Diehl et al., 1998, Zou et al., 2004). Phosphorylated Cyclin D1 is exported from the nucleus to the cytoplasm by the nuclear exportin CRM1

(Alt et al., 2000). In the cytoplasm, phosphorylated Cyclin D1 is degraded by the 26S proteasome system after ubiquitination catalysed by SCF complex (Figure 1.10) (Lin et al., 2006). The active GSK-3β also phosphorylates β-catenin in the cytoplasm. Phosphorylated β-catenin is degraded, resulting in the inhibition of transcription of target genes such as *CCND1* and *c-myc* (Takahashi-Yanaga and Sasaguri, 2008).

PI3K/Akt pathway regulates the G_1 phase through inhibition of GSK-3β (Hemmings and Restuccia, 2012, Duronio and Xiong, 2013). In the presence of growth factor, Akt phosphorylates GSK-3β at Ser9 (Frame et al., 2001, Beurel et al., 2015). The phosphorylation at this site inactivate GSK-3β, and prevents GSK-β to bind Cyclin D1 causing the Cyclin D1 degradation. The growth factor withdrawal reactivates GSK-3β to phosphorylate Cyclin D1, which leads to its rapid ubiquitination and proteasomal degradation (Figure 1.10).

1.9 Hypothesis and aims of the study

The PI3K/Akt pathway is important for regulating the human cell cycle at G_1 phase. It also influences cellular quiescence, proliferation and longevity, and is known to be essential for cell survival by reducing apoptosis. Akt, a key protein in the pathway, has been reported to be down-regulated by up to 76% during meningococcal infection (Schubert-Unkmeir et al., 2007). Also, Akt controls GSK-3β, a kinase which has been reported to be regulated by the interaction of TIMAP and PP1 to LAMR on the inner membrane (Kim et al., 2005a). Based on these reports and the finding that the interaction of PorA-Loop4:37LRP was cytostatic, not cytotoxic (Vassey, 2014), it is hypothesised that PI3K/Akt pathway was affected by the PorA-Loop4:37LRP interaction resulting in G_1 arrest. The aim of this study is to investigate the perturbations of expression of key proteins involved in the PI3K/Akt pathway (including CDK4, Cyclin D1, GSK-3β, and Akt) after the treatment of HBMECs with PorA-Loop4.

Chapter 2 - Materials and Methods

2.1 Bacterial strains and culture conditions

Neisseria meningitidis serogroup B, strain MC58 (B:15:P1.7.16b) was the wild-type meningococcal strain used throughout the study (Tettelin et al., 2000). All Neisseria strains were cultured on chocolate horse blood agar (Oxoid, Hampshire, UK) at 37°C in an atmosphere of 5% CO_2. When grown in suspension, all meningococcal strains were grown in brain-heart infusion (BHI) broth (Oxoid) at 37°C with agitation at 200 rpm. A list of bacterial strains used in these studies is shown in Table 2.1.

Table 2.1: List of bacterial strains which have been used in this study.

Bacteria/Strain	Description	Source / Reference
N. meningitidis MC58	Wild-type serogroup B strain	(Tettelin et al., 2000)
N. meningitidis MC58 ΔPorA-Loop4	*porA-Loop4* (*porA*$^{\Delta 197\text{-}210}$) deletion mutant	(Abouseada et al., 2012)
N. meningitidis MC58 ΔPorA	*porA* deletion mutant replaced with an omega cassette	(Abouseada et al., 2012)
N. meningitidis MC58 ΔPorA-Loop4 ΔPilQ	Double mutants of *porA-Loop4* and *pilQ*	(Abouseada et al., 2012)
N. meningitidis MC58 ΔPorA ΔPilQ	Double mutants of *porA* and *pilQ*	(Abouseada et al., 2012)

2.2 Synthetic peptides, antibodies, and inhibitors

Peptides used in this study were synthetic loops with sequence matching the *N. meningitidis* PorA VR2 (PorA-Loop4) from strain MC58. The sequence of the peptide was C-PIQNSKSAYTPAYYTKNTNNNLTLVPAVVGKP GS-C. The peptides were synthesised commercially by Alta Bioscience (Brimingham, UK) and PepMic (Suzhou, China). The polypeptide chains have been cyclised by the addition of cysteine residues on either end, to mimic the native structure of the extracellular loops. The peptides were high purity grade (>95%).

For immunoblotting and immunofluorescence, antibodies used are presented in Table 2.2, and inhibitors in Table 2.3.

Table 2.2: List of antibodies used in this study.

Name	Protein Target	Supplier	Class	Host
A-7	37LRP	Santa Cruz	Monoclonal	Mouse
PA5-64482	Phospho-CDK4 (Thr172)	Thermo Fisher Scientific	Polyclonal	Mouse
92G2	Cyclin D1	Cell Signaling Technology	Monoclonal	Rabbit
N1C3	Cyclin D1	GeneTex	Polyclonal	Rabbit
D3A4	Phospho-GSK3β (Ser9)	Cell Signaling Technology	Monoclonal	Rabbit
193H12	Phospho-Akt (Ser473)	Cell Signaling Technology	Monoclonal	Rabbit
N3C2	Akt	GeneTex	Polyclonal	Rabbit
H-2	α-actinin	Santa Cruz	Monoclonal	Mouse
P1.16	PorA-Loop4	NIBSC	Monoclonal	Mouse
Anti-PorA	PorA	In-house	Polyclonal	Rabbit
Anti-PilQ	PilQ	In-house	Polyclonal	Rabbit
NA931	Anti-Mouse IgG HRP	GE Healthcare	Polyclonal	Sheep
NA934	Anti-Rabbit IgG HRP	GE Healthcare	Polyclonal	Donkey
A32734	Anti-Rabbit IgG Alexa Fluor 680	Molecular Probes (Invitrogen)	Polyclonal	Goat
A3562	Anti-Mouse IgG–Alkaline Phosphatase	Sigma-Aldrich	Polyclonal	Goat
A3687	Anti-Rabbit IgG–Alkaline Phosphatase	Sigma-Aldrich	Polyclonal	Goat

Table 2.3: List of inhibitors used in this study.

Inhibitor name	Target	Supplier
ZSTK474	PI3K	Cell Signaling Technology
1-Azakenpaullone	GSK3β	Sigma-Aldrich
MK-2206	Akt	reSource

Unless otherwise stated, details of commonly used buffers, solutions, and reagents can be found in Appendix I.

2.3 Enzyme-linked immunosorbent assay (ELISA)

Covalink ELISA plates (Nunc, Fisher Scientific) were coated with synthetic peptides (1-10 µg ml^{-1}) in 0.1 M sodium carbonate-bicarbonate buffer pH 9 (Appendix I). In each well, 100 µl of coating solution was added and incubated overnight at 4°C. Wells were washed three times using Phosphate Buffered Saline (PBS, 200 µl $well^{-1}$) supplemented with 0.05% (v/v) Tween 20 (PBS-T) (Appendix I). Non-specific protein interactions were blocked with 100 µl of 1% (w/v) BSA/PBS-T for 1 h at room temperature (RT). Blocking buffer was decanted, and 100 µl of recombinant 37-LRP (rLR) (5-10 µg ml^{-1} in PBS) were added and incubated at 4°C overnight. The rLR was provided by Dr Sozan Qarani which was expressed in *E. coli* BL21 (DE3) (pLysS) containing pET28/LAMR and purified under denatured conditions (Qarani, 2015). The plate was washed five times with 200 µl of PBS-T. Then, 100 µl of the diluted primary antibody (A-7, Santa Cruz, 1:1000, 0.2 µg ml^{-1})) was added and incubated for 1 h at RT. The plate was washed a further five times, 100 µl of the diluted alkaline phosphatase secondary antibody (1:10,000, 0.4 µg ml^{-1}) added, and incubated for 1 h at RT. Plates were washed five times, and 100 µl of phosphatase substrate (BCIP: 0.15 mg ml^{-1}; NBT: 0.3 mg ml^{-1}, Sigma-Aldrich) was added. The OD of the developer colour change was read with an ELISA plate reader (Biotek EL 800, Biotek Instruments, Vermont, USA) at an absorbance of 405 nm. Data were collected from three independent experiments and statistically analysed with GraphPad Prism 7.

2.4 Human brain microvascular endothelial cell culture

Human brain endothelial cells (HBMECs; ScienCell Research Labs.) were cultured in complete medium containing Endothelial Cell Medium (ECM) supplemented with 5% (v/v) Fetal Bovine Serum (FBS), 1% (v/v) Penicillin/Streptomycin, and 1% (v/v) Endothelial Cell Growth Supplement (ScienCell Research Labs.). All cells were routinely maintained in the T-75 fibronectin-coated flask (Biocoat, BD Biosciences) at 37°C, 5% CO_2. Cells were passaged as required by washing in 10 ml of PBS (Gibco, Fisher Scientific), incubating in 2 ml of trypsin-EDTA 0.25% (w/v) (Sigma-Aldrich) for 5 min at 37°C, 5% CO_2, and adding complete medium up to 10 ml. HBMECs used in this study were immortalised cell lines with passage number ranging from 20 to 40. During experiments, HBMECs were seeded onto fibronectin-coated 6-well plates (Corning). Each well was coated with 1 ml of bovine fibronectin solution (Appendix I) and incubated at 37°C, 5% CO_2 for 1 h before seeding.

2.5 Association assay

Association assays were performed essentially as previously described (Oldfield et al., 2007). HBMECs were seeded into the fibronectin-coated plates and incubated for 24 h at 37°C, 5% CO_2. Once confluent, cells were washed with PBS (1 ml $well^{-1}$). Cells were infected with bacteria at a multiplicity of infection (MOI) 100 and left to associate for 8 h at 37°C, 5% CO_2. After 1 h incubation, the bacterial suspension was discarded and changed with new medium.

Starting inocula were retrospectively confirmed by serial dilution (10^{-1} to 10^{-7}) and plating onto Chocolate agar (Oxoid). Colony forming unit (cfu) were determined by plating 10 µl spots from the diluted suspensions, and incubating the plates overnight at 37°C, 5% CO_2.

To assess the association of meningococcal cells with the HBMECs, the infected monolayers were washed four times with PBS. For SDS-PAGE and immunoblotting, the cells were removed in 133 µl of SDS-sample buffer (Appendix I), disrupted with a cell scraper, and transferred into Eppendorf tubes. The cell suspension was boiled (100°C, 10 min) in a heat block and cells were lysed using sonicator. The supernatant was separated from the cell debris by centrifugation at 14,000 *x g* for 30 min at 4°C. For immunofluorescence, the infected monolayers were fixed with 1 ml of 4%

(w/v) paraformaldehyde (Appendix I) at RT for 10 min before proceeding to immunofluorescence steps.

2.6 The viability of HBMECs in the presence of inhibitors

Viability tests were performed to define the effective concentrations of the inhibitors before quantification of mRNA/protein expression. HBMECs (10^6 cells $well^{-1}$) were treated with various concentrations of inhibitors dissolved in DMSO for 24 h at 37°C, 5% CO_2. Cells were then washed with PBS (1 ml $well^{-1}$) and detached with trypsin-EDTA 0.25% (w/v) (200 µl $well^{-1}$). Detached cells were centrifuged, resuspended in 500 µl of PBS and stained with 500 µl of 0.4% (w/v) Trypan blue solution (Sigma-Aldrich) before being counted in a haemocytometer. Cell viability (%) was determined by comparing treated and untreated cells.

2.7 Quantification of gene expression

2.7.1 Treatment of cells with peptides and inhibitors

HBMECs in the assay plate were treated with 50 µM of PorA-Loop4 peptides for 0, 2, 4, 8, and 24 h. Cells were also treated with PBS (as solvent for PorA-Loop4 peptide) in complete medium as the untreated control.

2.7.2 Extraction of total RNA

The cells were washed twice with 1 ml $well^{-1}$ serum free ECM medium (Sciencell Research Labs.) and detached with trypsin-EDTA 0.25% (w/v) (200 µl $well^{-1}$). The number of cells (10^6 cells $well^{-1}$) was determined using a haemocytometer. The total RNA was extracted using the RNeasy® Mini Kit (Qiagen) according to the manufacturer's instructions. The quality of RNA samples was verified by measuring the optical density (OD, 260/280) absorption ratio using a Nanodrop ND-1000 spectrophotometer (NanoDrop Technologies). The remaining DNA was removed using Optizyme™ Recombinant DNase I (Fisher Scientific) at 37°C for 30 min. RNA was cleaned and concentrated using the RNeasy MinElute Cleanup Kit (Qiagen) according to the manufacturer's instructions. The quantity and OD 260/280 ratio of the clean RNA was again measured using NanoDrop.

2.7.3 Quality assessment of the RNA

The RNA template was qualitatively assessed using an Agilent 2100 Bioanalyzer with RNA 6000 Pico LabChip Kit (Agilent Technologies). The gel images, electrophoregrams, and RNA integrity number (RIN) were measured to evaluate the quality and integrity of the total RNA. RNA with the 28S/18S ratio in a range between 1.8-3.2 and RIN above 8.7 was used as a template for cDNA synthesis.

2.7.4 cDNA synthesis

cDNA was synthesised from 0.5 µg RNA of each sample using High Capacity cDNA Reverse Transcription Kit (Thermo Fisher Scientific) according to manufacturer's instructions. The quantity and OD 260/280 ratio of the cDNA were measured using Nanodrop.

2.7.5 qRT PCR

Quantitative Real-Time PCR (qRT PCR) was performed using AB7500 Real-time PCR system (Applied Biosystems) and Power SYBR® Green PCR Master Mix (Applied Biosystems) according to the manufacturer's instructions. Primers specific to the genes being tested (CDK4 and Cyclin D1) and the housekeeping gene (GAPDH) are shown in Table 2.4. To test PCR efficiency, a standard curve was generated with a serial ten-fold dilution of a known amount of HBMEC cDNA using 100 nM of forward and reverse primers. A standard curve was plotted for GAPDH, CDK4, and Cyclin D1 using template dilution versus C_T and ΔC_T values. The qPCR reaction mixture (10 µl total volume) consisted of 1 µl of cDNA (50 ng μl^{-1}), 5 µl of Power SYBR® Green PCR Master Mix (2x), 100 nM of forward and reverse primers and H_2O. Cycling was initiated at 95°C for 2 min, followed by 40 cycles of 95°C for 15 s and 60°C for 60 s. Samples were run in triplicate, and relative expression of CDK4 and Cyclin D1 were normalised to GAPDH as a housekeeping gene. The expression quantification of CDK4 and Cyclin D1 was relative to the untreated HBMECs and was determined by the $\Delta\Delta C_T$ method (Livak and Schmittgen, 2001).

Table 2.4: Primers for qRT PCR used in this study.

Gene Name (GeneBank Accession No.)		Primer Sequence (5′ – 3′)	Nucleotide Position
CDK4	Forward	AGTGTGAGAGTCCCCAATGG	398-456
(NM_000075.3)	Reverse	CGAACTGTGCTGATGGGAAG	
Cyclin D1	Forward	CCGTCCATGCGGAAGATC	304-378
(M64349)	Reverse	GAAGACCTCCTCCTCGCACT	
GAPDH	Forward	CAACGTGTCAGTGGTGGACC	817-896
(AF261085)	Reverse	CCTGCTTCACCACCTTCTTG	

2.7.6 Data analysis ($\Delta\Delta C_T$ method)

The $\Delta\Delta C_T$ method for real-time relative quantitative PCR with power SYBR Green detection was used to estimate the relative gene expression of CDK4 and Cyclin D1 in HBMECs. Analysis of real-time PCR amplification data was performed using 7500 v 2.3 software (Applied Biosystems). First, the average of C_T value from the housekeeping gene and the gene being tested was calculated from each treated sample and the untreated control. Then, the differences between the C_T values of the housekeeping gene and the gene being tested were calculated (ΔC_T). The differences of ΔC_T from the treated samples and the untreated were measured ($\Delta\Delta C_T$). Since all calculations are in logarithm base 2, the value of $2^{-\Delta\Delta C_T}$ was measured from each sample to get the expression fold change.

2.8 Quantification of protein expression

In general, protocols overviewed in Figure 2.1 were performed to analyse the protein expression level in HBMECs. HBMECs were treated with peptide and/or inhibitors, lysed, and analysed for protein expression based on protocols in Section 2.8.1 to 2.8.5 (Figure 2.1 A). Lysates from infected cells (Section 2.5) were also analysed based on protocols from Section 2.8.3 to 2.8.5 (Figure 2.1 B).

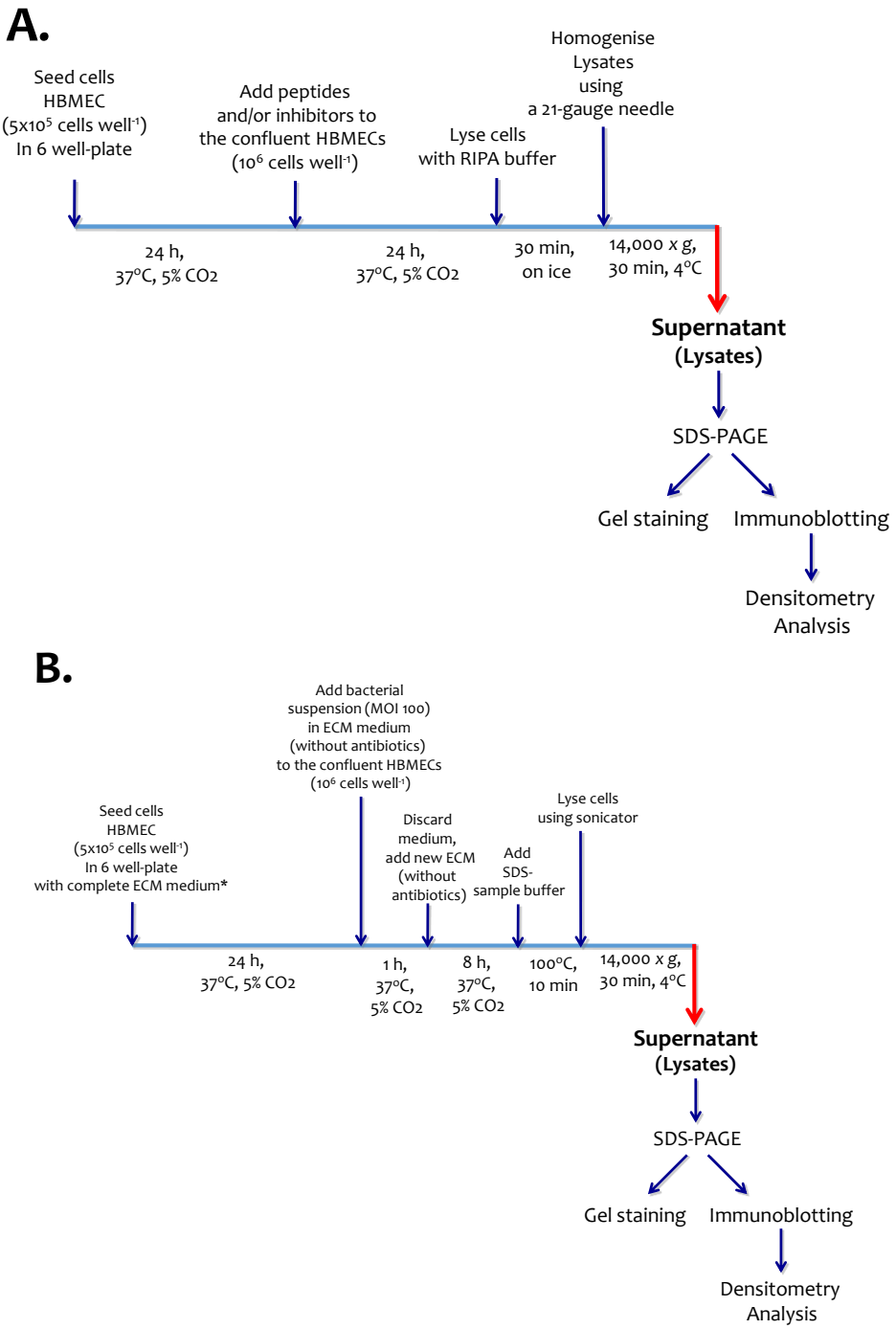

Figure 2.1: Protocol overview for analysing protein expression in the HBMECs. (A) HBMECs were treated with peptide and/or inhibitors, lysed with RIPA buffer, homogenised using a 21-gauge needle, and analysed for protein expression based on SDS-PAGE, immunoblotting, and densitometry analysis. (B) HBMECs were infected with bacterial suspension (MOI 100) and lysed with SDS-sample buffer. The cell aggregates were further lysed using sonicator. The lysates were also analysed for protein expression based on SDS-PAGE, immunoblotting, and densitometry analysis. *Endothelial Cell Medium (ECM) supplemented with 5% (v/v) Fetal Bovine Serum (FBS), 1% (v/v) Penicillin/ Streptomycin, and 1% (v/v) Endothelial Cell Growth Supplement.

2.8.1 Treatment of cells with peptides and inhibitors

HBMECs in the assay plate were treated with 50 μM of PorA-Loop4 peptides, inhibitors (at various effective concentrations), and a combination of both PorA-Loop4 peptide and each inhibitor, in complete ECM medium for 24 h at 37°C, 5% CO_2. Cells were also treated with PBS and DMSO (as solvents for PorA-Loop4 peptide and inhibitors, respectively) in complete medium as the untreated control.

2.8.2 Preparation of cell lysates

Following the treatments of cells with peptides or inhibitors, the culture medium was discarded. One ml of cold RIPA buffer (Sigma-Aldrich) supplemented with PhosSTOP (Rochhe), and c0mplete Mini EDTA-free protease inhibitor cocktail (Roche) (Appendix I) was added to the cells. The plates were then placed on ice for 30 min. The cells were scraped; the lysates were collected in microfuge tubes and passed through a 21-gauge needle to break up the cell aggregates. The lysates were cleared by centrifugation at 14,000 × *g* for 30 min at 4°C, and the supernatants (total cell lysate) were either used immediately or stored at -20°C.

2.8.3 SDS-PAGE

Protein samples were resolved by SDS-PAGE using the Bolt™ Mini Gel Tank system (Novex®, Life Technologies, ThermoFisher Scientific). Before loading the gels, 40 μl of samples were mixed with 10 μl of 5 x SDS-sample buffer (Appendix I) and then heated at 100°C for 5 min to denature the proteins. Typically, 10-20 μl of each sample was loaded into each well of 10% (w/v) acrylamide gels (Appendix I) alongside ColourPlus pre-stained protein ladder (New England Biolabs). The total running time was 1 h at 130V voltage. Proteins were visualised by staining with Coomassie Blue Staining Solution (Appendix I) for 1 h at RT, and then washed in destaining solution (Appendix I) overnight.

2.8.4 Immunoblotting

For immunoblot analysis, proteins in the gels were transferred to a nitrocellulose membrane (GE Healthcare) at 10 V for 30 min on a Trans-Blot Semi-Dry System (Bio-Rad). Membranes were blocked with 20 ml of 5% (w/v) BSA/Tris Buffered Saline supplemented with 0.1% (v/v) Tween 20 (TBS-T) (Appendix I) for 1 h at RT. Primary antibodies were diluted (1:1000)

in 20 ml of 5% (w/v) BSA/TBS-T, and incubated with the membranes at 4°C overnight. Membranes were washed (3 × 5 min) in 20 ml of TBS-T and subsequently probed with diluted secondary antibodies (1:10,000) in 5% (w/v) BSA/TBS-T for 1 h at RT. The membranes were washed (3 × 5 min) with 20 ml of TBS-T, before membranes were exposed to 10 ml Luminata™ Crescendo Western HRP Substrate (Millipore) for 5 min. The membranes were drained, wrapped in plastic, and scanned with C-Digit Blot Scanner (LI-COR Biosciences) to visualise the immunoreactive proteins.

Confirmation of the amount of protein loaded in each well was performed by stripping the blots and re-probing with anti-α-actinin. The membranes were washed with (3 × 5 min) with 20 ml of TBS-T before membranes were placed in 20 ml of Restore™ Western Blot Stripping Buffer (ThermoFisher Scientific) for 30 min at RT. The membranes were re-washed in TBS-T, re-blocked with 5% (w/v) BSA/TBS-T, and re-probed with primary antibody against anti-α-actinin (H-2, Santa Cruz) using the same protocol as mentioned in the previous paragraph.

2.8.5 Image analysis

The bands in the scanned blots were quantified with Image J software (National Institutes of Health, USA). The area of each band was compared to the untreated sample (relative density). Then, the relative density of each sample was compared to the relative density of the loading control (adjusted density). The untreated samples were normalised to one, thus the adjusted density represents the fold change of each sample. Data were collected from three independent experiments.

2.9 Immunofluorescence

Cells were grown on acid-etched glass 11 mm coverslips (SLS, Nottingham, UK). The coverslips were soaked with 1 M HCl overnight and rinsed with H_2O and ethanol. Then, the dried coverslips were located in the 24-well plate and incubated with 300 µl of 1 µg ml^{-1} of bovine fibronectin solution (Appendix I) for at least 1 h. One hundred thousand cells were seeded into each well and incubated for 24 h at 37°C, 5% CO_2.

After association assay (Section 2.5), the cells were fixed with 300 µl of 4% (w/v) paraformaldehyde (Appendix I) for 10 min at RT, washed with PBS, and permeabilised with 0.1% (v/v) TX-100/1% (w/v) BSA in PBS (Appendix I) for 5 min at RT. Following 1 h incubation with 4% (w/v)

BSA/PBS-T (Appendix I) to reduce non-specific binding, cells were incubated with primary antibody at recommended dilution (mAb pAkt, 1:200; mAb pGSK-3β, 1: 200; pAb Cyclin D1, 1:500; pAb pCDK4, 1:300) and incubated overnight at 4°C. Cells were washed three times in 500 µl of PBS and incubated with conjugated secondary antibodies, anti-rabbit IgG Alexa 680 (1:100, Molecular Probes) in 4% (w/v) BSA/PBS-T for 24 h at 4°C. Coverslips were mounted with ProLong Gold anti-fade with DAPI (Invitrogen, UK), and images obtained by confocal microscope. For the co-localisation studies, samples stained for localisation of each protein individually were processed in parallel, and the fluorescence of the adjacent channels was monitored for spectral overlap.

2.10 Confocal microscopy

Images were acquired with Zen 2009 operating software on a Zeiss LSM 700 confocal microscope using a Plan-Apochromat 63x/1.40 Oil DIC M27 objective. Alexa 680 and DAPI were detected using 635 nm and 405 nm lasers, respectively. The image size was 1024 x 1024 with 8 average frames taken per line and a pinhole size of 1 Airy unit. All images were captured with the same laser gains, and zoom setting. Co-localisation analysis was carried out using the ZEN software (2011 Blue Edition) inbuilt function with a FI threshold of 50 and was not intensity weighted. Images were further processed by Image J and GIMP 2.10.

2.11 Statistical analysis

Data are represented as the mean + standard deviation (SD) unless otherwise stated. Statistical analysis was carried out to test the significance of the datasets. T-test was used for pair-wise analysis, ANOVA was used for datasets with multiple comparisons. All ANOVAs were applied post hoc. One-way ANOVA was used to consider one independent variable or factor. Dunnett's test was applied to compare every mean to a control mean, while Tukey's test was applied to compare every mean with every other mean. The significance is represented as the P value. All data were analysed using GraphPad Prism 7.

Chapter 3 - Effects of PorA-Loop4 on Cyclin D1 and CDK4 as cell cycle regulators in HBMECs

3.1 Introduction

In eukaryotic cells, cell cycle arrest usually happens when defects (e.g. DNA damage) are detected by checkpoint regulators (Bertoli et al., 2013). The cell cycle arrest occurs until the defects are repaired, or regulators may induce signals to cause apoptosis.

During infection, pathogenic bacteria interfere with the host signalling pathways regulating the cell cycle in order to survive and sustain colonisation (Nougayrede et al., 2005). The bacteria produce molecules that cause the cell cycle arrest through perturbation of specific regulators. *E. coli*, *Shigella dysenteriae*, *Campylobacter* spp., *Salmonella typhi*, *Haemophilus ducreyi*, *Helicobacter hepaticus* and *Actinobacillus actinomycetemcomitans* produce cytolethal distending toxin (CDT) to cause DNA damage and block the cell cycle at G_2 phase (De Rycke and Oswald, 2001). Enteropathogenic and enterohemorrhagic *E. coli* (EPEC and EHEC) use a type III secretion system (TTSS) to inject cycle inhibiting factor (CIF) into the host cytoplasm and trigger G_2 arrest associated with prevention of CDK1 activation (Marches et al., 2003). Fusobacterial immunosuppressive protein (FIP) from *Fusobacterium nucleatum* triggers G_1 arrest through perturbation of proliferating cell nuclear antigen (PCNA) expression (Shenker and Datar, 1995). Mycolactone secreted by *Mycobacterium ulcerans* induces cell cycle arrest in G_0–G_1 and eventually apoptosis (George et al., 1999).

Meningococci have been reported causing the perturbation of the host cell cycle. The previous study in our lab showed that the binding of meningococcal PorA-Loop4 to 37LRP on the cell surface leads to cellular responses including the G_1 arrest. The Click-iT EdU proliferation assay in a previous study suggested that the exposure of HBMECs to PorA-Loop4 peptide to HBMECs caused a decrease of cells in the S phase by 24% (Vassey, 2014). BrdU incorporation assays confirmed that the PorA-Loop4 treated cells showed a significant (23%) increase in the proportion of cells at the G_1 checkpoint ($p \leq 0.01$) (Vassey, 2014). Still, the effect of PorA-Loop4 to G_1 regulators had not been investigated.

The main regulators at early G_1 phase are Cyclin D1 and CDK4 (Table 1.4). Initially, the growth factors activate CDK4 by inducing Cyclin D1 to concentrations allowing it to overcome an inhibitory threshold imposed by INK4 inhibitory proteins (including p15, p16, p18, and p19) (Sherr, 1995, Bockstaele et al., 2006a). The INK4 proteins bind to the catalytic domain of the isolated CDK4, thus preventing cyclin association and activation (Hall et al., 1995, Sherr and Roberts, 1995, Pavletich, 1999). The Cyclin D1/CDK4 complex is further stabilised by p21 at the nucleus (Figure 3.1) (Bockstaele

et al., 2006a). Then, CAK phosphorylates CDK4 at Thr172 in its activation loop (Kato et al., 1994). CAK is a trimeric protein which consists of CDK7, Cyclin H, and Mat1. The activation of CDK4 complexed to Cyclin D1 leads to phosphorylation of pRb, DNA replication, and cell cycle progression from G_1 to S phase.

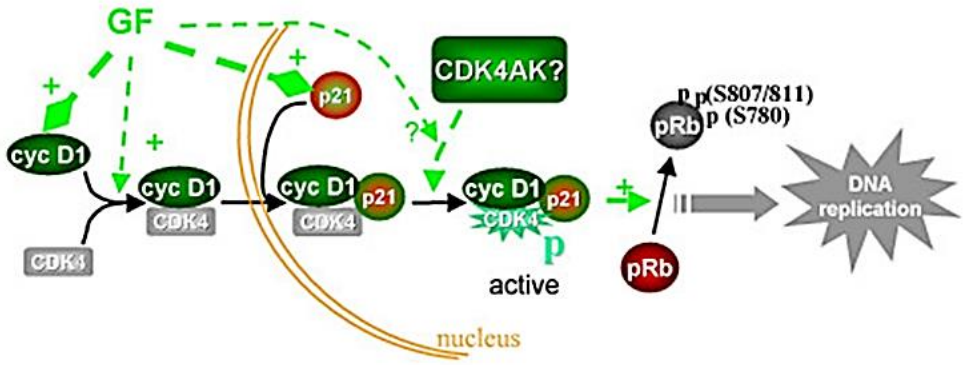

Figure 3.1: Schematic illustration of CDK4 regulation. Growth factors (GF) activate CDK4, mainly by inducing Cyclin D1 and also p21, which stabilises the Cyclin D1-CDK4 complex in the nucleus. Then, CAK (CDK4AK) phosphorylates CDK4 at Thr172 in its activation loop. Activation of CDK4 complexed to Cyclin D1 and p21 leads to phosphorylation in pRb which contributes to initation of DNA replication. Diamond arrowheads represent inductions; the other dashed arrows are activations (+). This figure is modified from Bockstaele et al., (2006a).

3.2 Aim

The aim of this chapter is to study the effect of PorA-Loop4 on the expression of Cyclin D1/CDK4 in HBMECs, which controls the transition of cells from G_1 to S phase. It is our aim to understand the effects of PorA-Loop4 on the expression of Cyclin D1/CDK4 at both the mRNA and protein levels. Perturbation of Cyclin D1/CDK4 expression would support the previous finding that the cyclised peptide of PorA-Loop4 caused the G_1 arrest. Also, it would provide evidence for the possible intracellular signalling pathways influenced by the interaction of PorA-Loop4 with 37LRP.

3.3 Confirmation of the binding interaction between the PorA-Loop4 peptide and recombinant laminin receptor (rLR)

Before investigating the expression of Cyclin D1/CDK4 in HBMECs, the cyclised synthetic peptide of PorA-Loop4 were tested for its capability to bind the rLR. The rLR was expressed and purified by Dr Sozan Qarani in a previous

study (Qarani, 2015). ELISA was used whereby the peptides were immobilised on a plate and then probed with the rLR. In each experiment, BSA coated wells were included to measure background levels of binding. Three parameters (incubation time, peptide concentration, rLR concentration) were optimised (Appendix II). The optimised conditions used in the subsequent experiments were 2 h incubation period with phosphatase substrate, 10 μg ml^{-1} of peptide, and 5 μg ml^{-1} of rLR. Figure 3.2 shows that the peptide of PorA-Loop4 used in this study bound to rLR. The absorbance from the PorA-Loop4 was significantly higher than the BSA ($p \leq 0.05$). The high variability between repeats occurred probably due to the use of different batches of PorA-Loop4 peptide (Alta bioscience and Pepmic) in this assay. The peptide from Pepmic was used to replace the finished batch from Alta bioscience. Change of supplier happened due to time and price considerations. Both batches have the same purity (>98%).

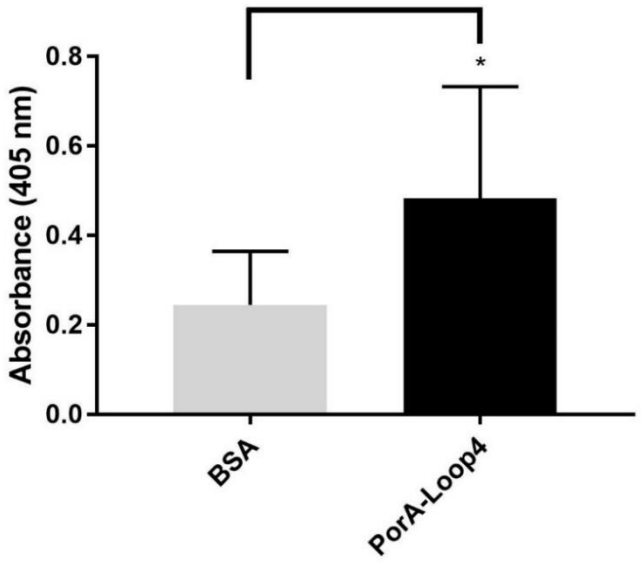

Figure 3.2: Synthetic cyclised peptide of PorA-Loop4 binds to recombinant laminin receptor (rLR). Microtitre plate wells were coated with peptide of the PorA-Loop4 and BSA. The concentrations of the coated proteins were all 10 μg ml^{-1}. The coated wells were incubated with the rLR (5 μg ml^{-1}) at 4°C overnight. The rLR was obtained from a previous study (Abouseada et al., 2012). Data represent mean + SD from three independent experiments (each carried out in triplicate). Statistical analysis was performed with t-test (*$p \leq 0.05$).

3.4 The mRNA levels of Cyclin D1 and CDK4 in PorA-Loop4-treated HBMECs

To investigate the effect of PorA-Loop4 peptide on the transcription of Cyclin D1 and CDK4, qRT PCR was carried out. The concentration of the peptide used in this study was previously optimised (Vassey, 2014). The cytotoxicity of the peptide to HBMEC was measured using the XTT cell viability kit. The addition of 1 ml of 50 μM PorA-Loop4 peptide to $1x10^6$ HBMECs had no effect on cell viability compared to the untreated cells (data not shown).

Before the main experiments, the total RNAs were extracted from monolayers of HBMECs treated with PorA-Loop4 peptide (50 μM) for 2, 4, 8, and 24 h. RNA quantity and the OD 260/280 ratio was assessed spectrophotometrically using NanoDrop® ND-1000 Spectrophotometer, which showed that all samples fell within 100-200 ng μl^{-1} and ratio of 2. The quality of extracted RNA was further confirmed by Agilent 2100 Bioanalyzer. The 28S/18S ratio of all samples were between 1.7-3.2, and the RIN values were 8.7-10 (Table 3.1) which are considered to reflect intact RNA (Fleige and Pfaffl, 2006, Imbeaud et al., 2005). Pseudo-gel images and chromatograms of the RNA samples are shown in Figure 3.3 and Appendix III, respectively.

Table 3.1: 28S/18s ratio and RIN values of RNA samples used in this study.

The values were obtained from the Agilent 2100 Bioanalyzer.

Incubation time (h)	Samples	Replicate	28S/18S ratio	RIN
0	Untreated	1	1.9	9.8
		2	1.8	9.9
		3	1.7	10
2	Untreated	1	2.1	9.6
		2	2.1	9.9
		3	1.9	8.7
	PorA-Loop4	1	2.5	9.3
		2	2.0	10
		3	1.9	10
4	Untreated	1	1.8	9.8
		2	2.7	10
		3	2.5	10
	PorA-Loop4	1	1.7	9.8
		2	2.8	10
		3	3.0	10
8	Untreated	1	1.7	9.6
		2	2.7	10
		3	2.9	10
	PorA-Loop4	1	2.3	10
		2	2.1	10
		3	3.2	10
24	Untreated	1	2.0	9.8
		2	2.2	10
		3	2.1	10
	PorA-Loop4	1	1.8	9.6
		2	2.6	10
		3	2.7	10

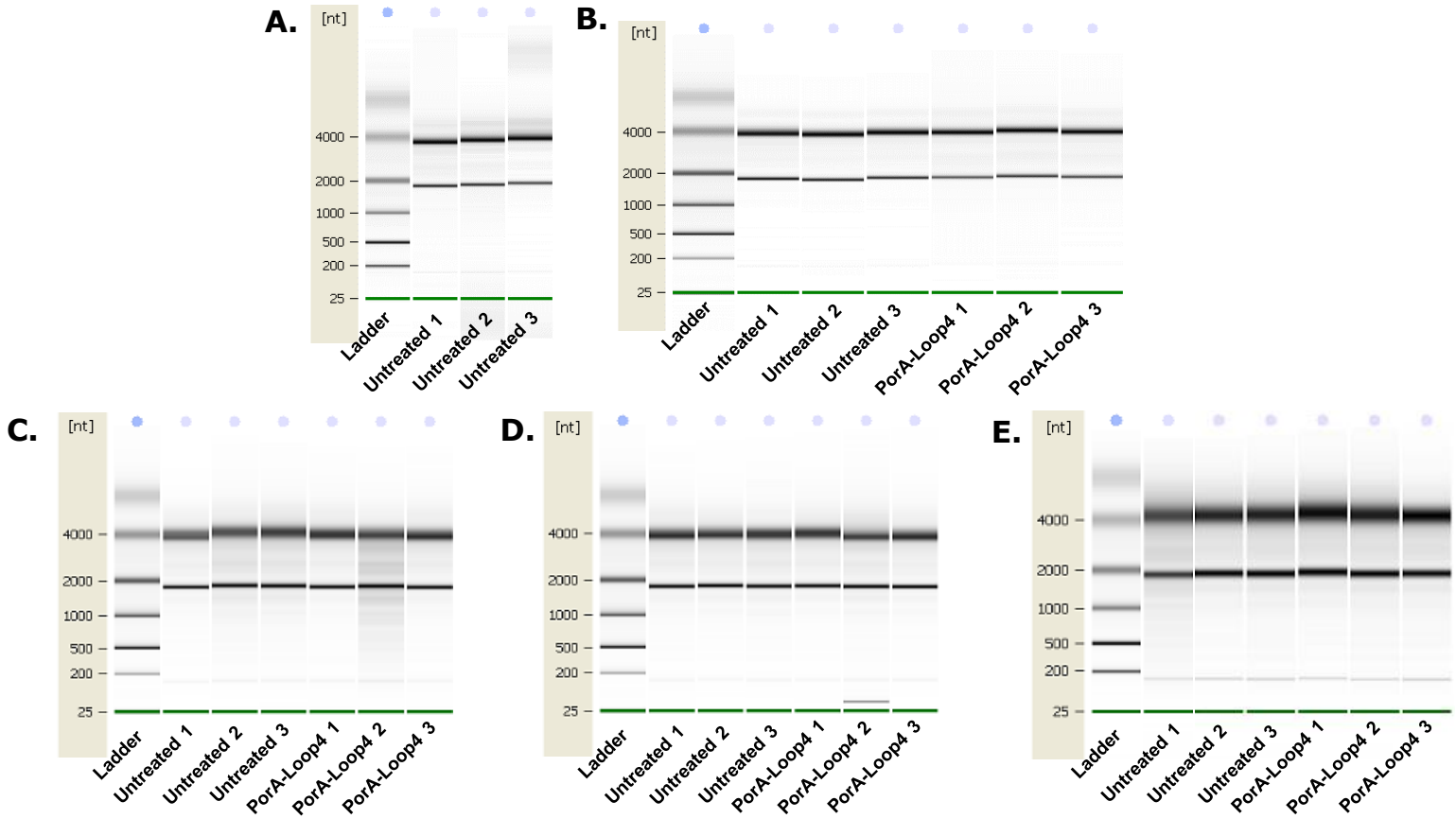

Figure 3.3: Pseudo-gel images of RNA samples produced using the Agilent 2100 Bioanalyzer. Figure A-E show quality of samples from HBMECs treated with PorA-Loop4 peptide and untreated controls for 0, 2, 4, 8, and 24h, respectively, from three independent experiments. Each RNA sample was extracted from 1 x 10^6 cells of HBMECs using RNeasy® Mini Kit (Qiagen). Bands at 2000 and 4000 nt represent 18S and 28S RNA, respectively.

Quantitative PCR (qPCR) was utilised to examine the effect of PorA-Loop4 peptide treatment of HBMECs on the transcription level of Cyclin D1 and CDK4 in time-dependent experiments. The ratios of gene expression levels were calculated using the $\Delta\Delta C_T$ method (Livak and Schmittgen, 2001).

To calculate relative transcriptional levels of the genes of interest using the $\Delta\Delta C_T$ method, the reaction efficiency of PCR was calculated. cDNA was used as a template to perform standard curves for Cyclin D1, CDK4, and GAPDH to examine the PCR efficiency and linearity of template amplification. As shown in Figure 3.4, the slope of standard curves was -3.364, -3.608 and -3.093 for Cyclin D1, CDK4, and GAPDH, respectively, revealing 98.27, 89.3, 110% efficient PCR amplification. Efficiencies between 90 and 110% are typically acceptable (Ruijter et al., 2009). The efficiency was calculated according to the following equation: $E= 1+10^{(-1/slope)} \times 100$. Figure 3.4 also demonstrates a linear correlation between the cDNA and C_T values. The correlation coefficients (R) were 0.9348, 0.9227, and 0.996 for Cyclin D1, CDK4, and GAPDH, respectively, confirming the amplification efficiency.

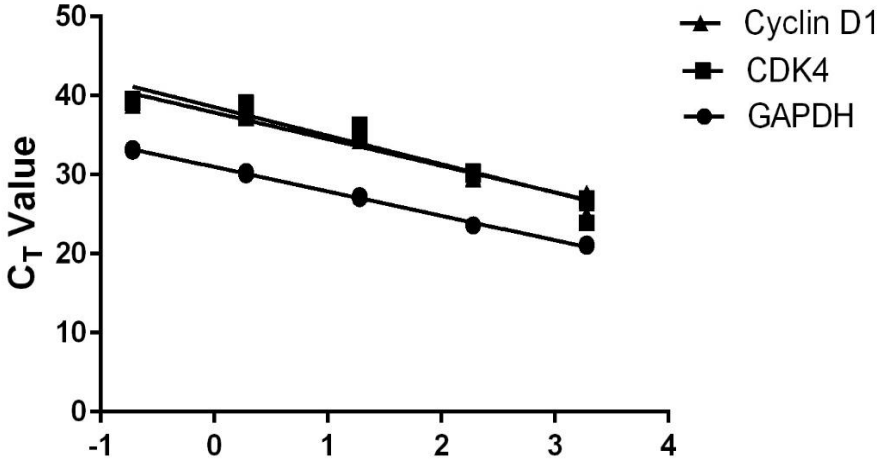

Figure 3.4: Standard curves for Cyclin D1, CDK4, and GAPDH to evaluate efficiency of qPCR. The diluted and undiluted cDNAs were used as templates for the amplification of Cyclin D1, CDK4, and GAPDH. The C_T values were plotted versus the log concentrations of cDNAs. Slopes of the standard curves were -3.364, -3.608 and -3.093 for Cyclin D1, CDK4, and GAPDH, respectively, revealing 98.27, 89.3, 110% efficient PCR amplification. While the correlation coefficients (R) were 0.9348, 0.9227, and 0.996 for Cyclin D1, CDK4, and GAPDH, respectively, confirming the amplification efficiency. Each point represents the mean of triplicate values for each Cyclin D1, CDK4, and GAPDH.

In addition, the $\Delta\Delta C_T$ method can be used when the amplification efficiencies of the target and reference genes are approximately equal. The assessment of the amplification efficiency can be measured by studying ΔC_T (C_T (Target)–C_T (Endogenous)) changes with different dilutions of cDNA. Close to identical efficiencies of the target (Cyclin D1 and CDK4) and reference gene (GAPDH) were observed, as indicated by slope values close to zero. As a result, the ΔC_T of Cyclin D1-GAPDH and the ΔC_T of CDK4-GAPDH was calculated and plotted versus log cDNA as shown in Figure 3.5. The slopes of the lines were -0.27 and -0.39, thus the $\Delta\Delta C_T$ method can be used to analyse the data.

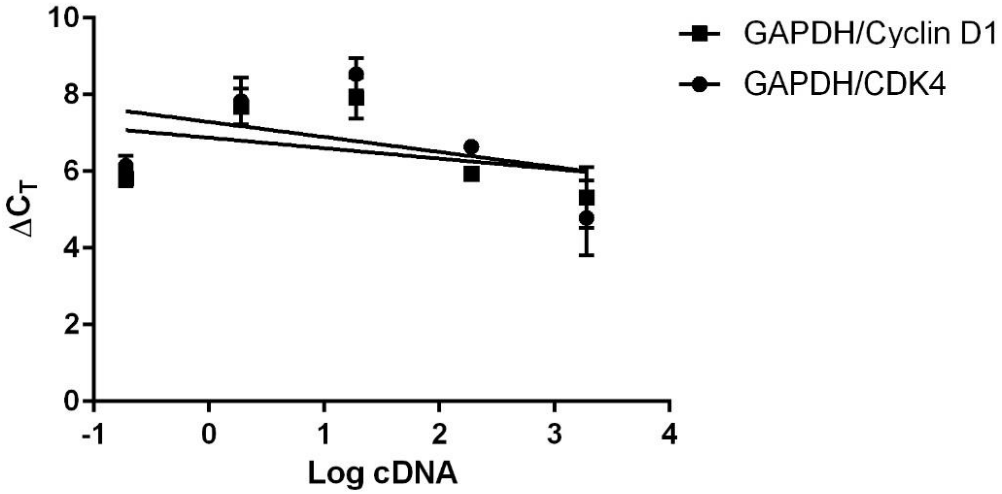

Figure 3.5: Validation of $2^{-\Delta\Delta C_T}$ method. The ΔC_T of Cyclin D1-GAPDH and the ΔC_T of CDK4-GAPDH were calculated and plotted versus log cDNA of HBMECs. The data fit using linear regression analysis (n=3). Slopes of the regression lines reflect the amplification efficiencies of the target genes (Cyclin D1 and CDK4) and reference gene (GAPDH). The $\Delta\Delta C_T$ method can be used when the slope values close to zero. The slopes of the regression lines were -0.27 and -0.39 for Cyclin D1-GAPDH and CDK4-GAPDH, respectively, confirming the almost equal efficiencies between the target and reference genes.

The graphs showing Cyclin D1 and CDK4 expression levels are shown in Figure 3.6. A reduction in Cyclin D1 expression was observed in cells treated with PorA-Loop4 for 2, 4, 8, and 24 h compared to the untreated controls. Meanwhile CDK4 expression was increased in cells treated with PorA-Loop4 peptide for 2, 4, 8, and 24 h compared to the untreated controls. These findings suggest that the treatment of HBMECs with PorA-Loop4 results in altered expression of Cyclin D1 and CDK4 at the transcriptional level.

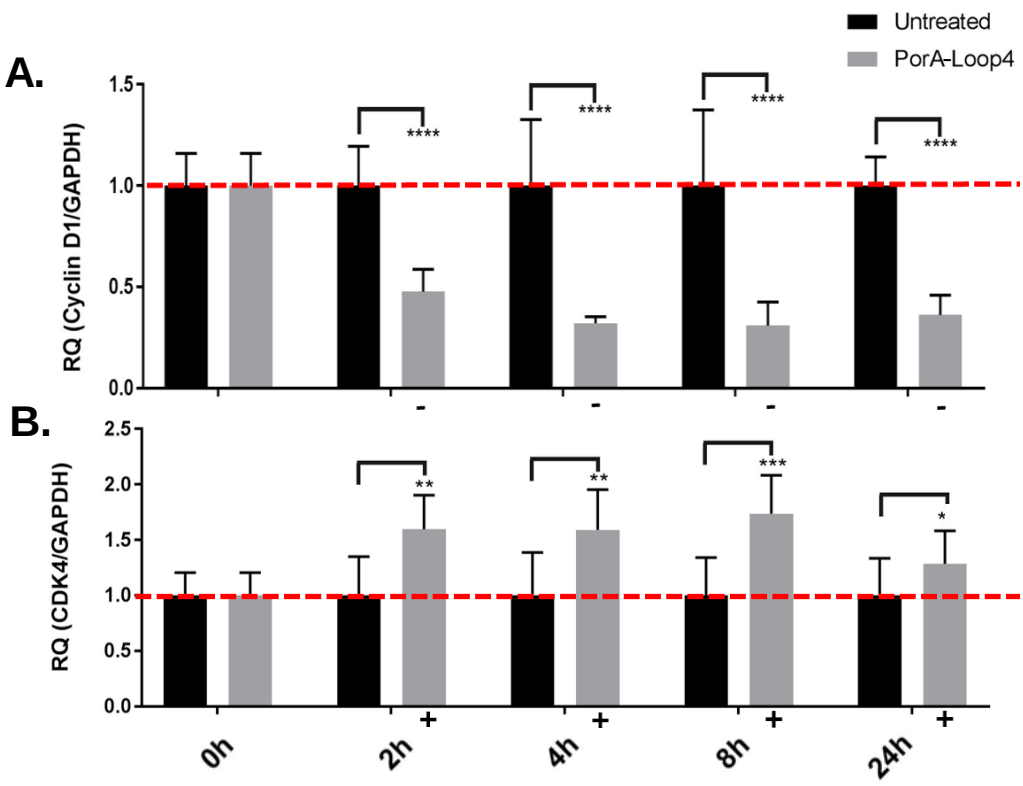

Figure 3.6: PorA-Loop4 peptide caused decreased expression of Cyclin D1 and increased expression of CDK4 at mRNA level. HBMECs (10^6 cells) were either left untreated or treated with cyclised peptide of PorA-Loop4 (50 µM) for 0-24 h incubation. RNA was extracted, cDNA was generated, and qRT PCR was performed to analyse mRNA expression. Bars represent RQ (relative quantification) mRNA expression ($2^{-\Delta\Delta C_T}$, fold change) of Cyclin D1 (Figure A) and CDK4 (Figure B) relative to GAPDH levels as the housekeeping gene. Data were normalised to the untreated cells. qRT PCR was performed in three independent experiments. Significant difference to the untreated controls (*p≤0.05, **p≤0.01, ***p≤0.001, ****p≤0.0001, unpaired Student's t-test).

3.5 Protein expression of Cyclin D1 and pCDK4 (Thr172) in PorA-Loop4-treated HBMECs

Immunoblot analysis was performed to quantify the protein expression levels of Cyclin D1 and pCDK4 (Thr172) in treated HBMECs. Before immunoblotting, cells were lysed and centrifuged to create clear whole cell lysates. Typically, 15-20 µl (5 µg) of each sample was loaded into each well of the acrylamide gels. First, the gels were stained with Coomassie Blue to confirm that equal amount of proteins loaded from each sample. The results of the stained gels are shown in Figure 3.7.

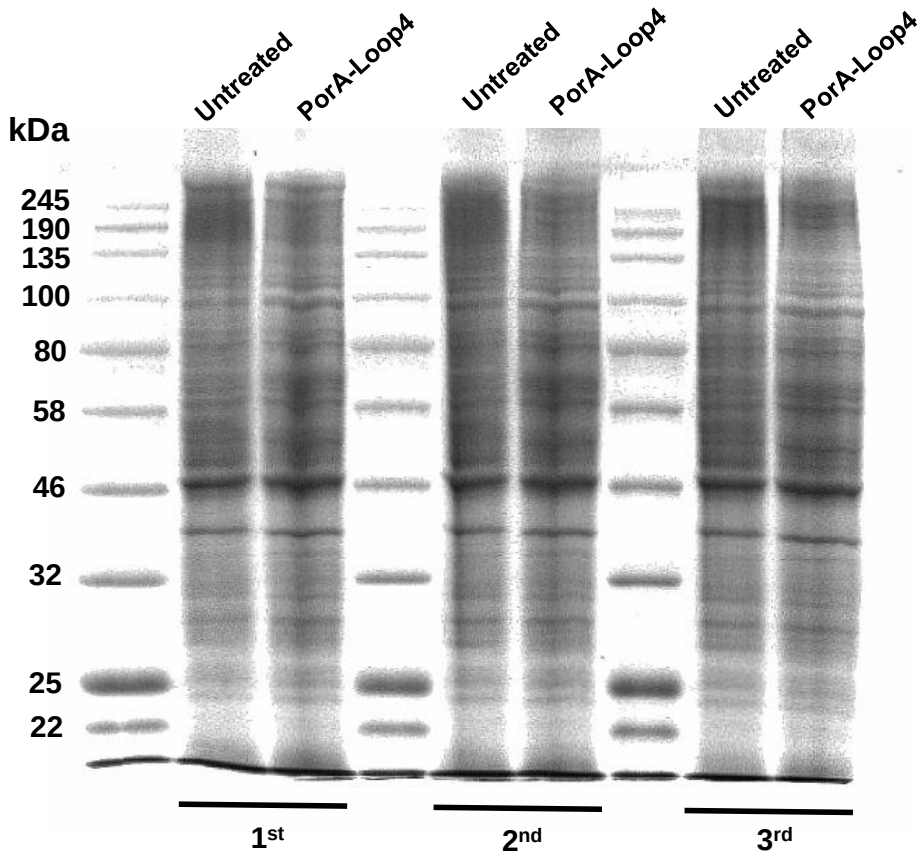

Figure 3.7: SDS-PAGE of whole lysates from PorA-Loop4 peptide treated HBMECs and untreated controls. Protein lysates (5 µg) were separated on 10% acrylamide gels. Samples were obtained from three independent experiments (1^{st}-3^{rd}).

The separated proteins were then transferred onto a nitrocellulose membrane and probed with anti-Cyclin D1, anti-phosphoCDK4 (Thr172), and anti-α-actinin (loading control). The blot images and densitometry analysis are shown in Figure 3.8. The treatment with PorA-Loop4 peptide resulted in changes in protein expression of Cyclin D1 and pCDK4. Specifically, the adjusted density of Cyclin D1 was 0.6 fold lower than the control, while the adjusted density of pCDK4 was 0.9 fold higher than the control. Cyclin D1 expression was significantly decreased in PorA-Loop4 treated cells compared to the control ($p \leq 0.05$), while a significant increase of pCDK4 (Thr172) was observed in the PorA-Loop4 treated cells compared to the control ($p \leq 0.0001$). PorA-Loop4 treated cells also caused the upregulation of CDK4 24 h post treatment (data not shown). The CDK4 expression was significantly increased in PorA-Loop4 treated cells compared to the control ($p \leq 0.01$).

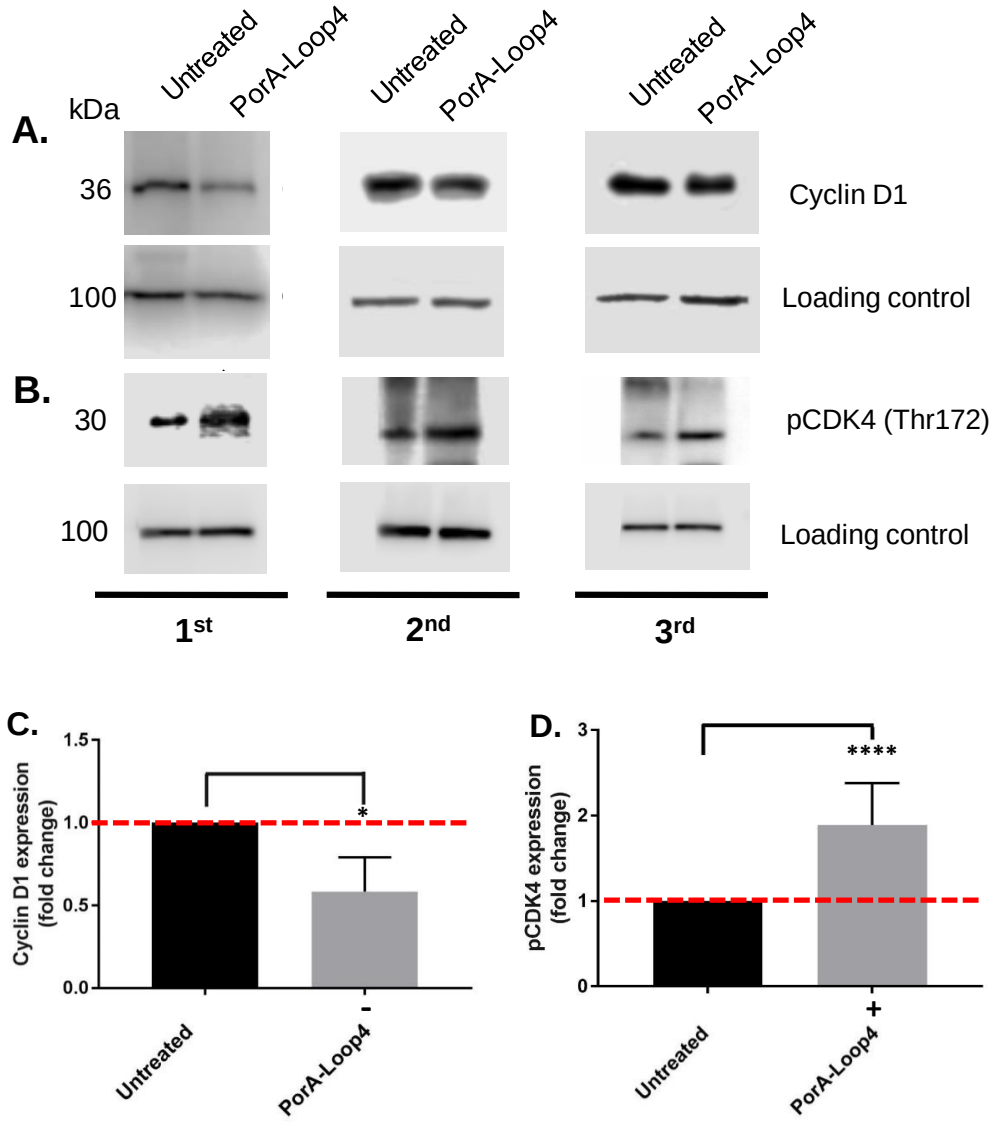

Figure 3.8: PorA-Loop4 peptide caused decreased expression of Cyclin D1 (Figure A and C) and increased level of pCDK4 (Thr172) (Figure B and D) at the protein level 24 h post treatment. HBMECs (10^6 cells) were either left untreated or treated with cyclised peptide of PorA-Loop4 (50 µM) for 24 h incubation. The cells were lysed with RIPA buffer and homogenised using a 21-gauge needle. The whole lysates were separated on 10% acrylamide gels and probed with anti-Cyclin D1 or anti-pCDK4 (Thr172). Figure A and B show immunoblot images from three independent experiments (1^{st}-3^{rd}), while Figure C and D show the densitometry analysis. Band intensities were quantified using Image J software. Alpha actinin was used as loading control in all immunoblots. All data were normalised to the untreated controls and adjusted to the loading control densities. Significant difference to the untreated controls (*p≤0.05, ****p≤0.0001, unpaired Student's t-test).

3.6 Discussion

The addition of PorA-Loop4 to HBMECs caused a significant reduction in the proportion of cells in S-phase and a corresponding increase in the proportion of cells in G_1, indicating a G_1 arrest (Vassey, 2014). To understand this finding, the full molecular mechanism of the cell cycle arrest should be elucidated. Expression analysis of cell-cycle checkpoint proteins, such as Cyclin D1 and CDK4, should provide an initial approach to understand the mechanism.

Work in this thesis used a similar PorA-Loop4 peptide to the one used in previous study (Vassey, 2014). A scrambled peptide was used by Vassey as negative control which consists of the same amino acids as the PorA-Loop4 peptide but in different sequences (Vassey, 2014). The scrambled peptide was not used in current study due to the solubility issues of the peptide. It was insoluble in DMSO and PBS.

The treatment of HBMECs with PorA-Loop4 peptide caused a decreased level of Cyclin D1 and an increased level of CDK4 at both the mRNA and protein level. The expressions at both levels were studied in view of the fact that genes with cell-cycle specific functions tended to have unstable mRNA and unstable protein (Kendrick, 2014). A change in mRNA expression is not always reflected by similar changes in protein expression due to the complexity of post-transcriptional mechanisms and post-translational modifications (Liu et al., 2016). In this study, however, changes in mRNA levels strongly correlated with the changes at the protein level.

Downregulation of Cyclin D1 at the mRNA and protein levels might lead to G_1 arrest. The lack of Cyclin D1 would be expected to influence the formation of the Cyclin D1/CDK4 complex, which is required for progression from G_1 to S phase in the cell cycle. Yet, the upregulation of pCDK4 (Thr172) caused by treatment with PorA-Loop4 raises many questions in regards to the G_1-arrest effects. pCDK4 (Thr172) complexed to Cyclin D1 causes phosphorylation of Rb and thus facilitates further cell signalling leading to cell cycle progression (Figure 3.1). However, a subsequent phosphorylation of Rb by Cyclin E/CDK2 complex is needed to fully dissociate Rb from the HDAC-repressor complex and to allow the cell cycle progression from G_1 to the S-phase. Future study in the downstream events of the G_1/S checkpoint signalling pathway (e.g. Cyclin E, CDK2, pRb and E2F) is needed to fully elucidate the G_1-arrest mechanism caused by the PorA-Loop4.

In addition, a second antibody was also used to detect the non-phosphorylated protein of CDK4 and that level of this form was also increased in the PorA-Loop4-treated cells. The upregulation of the total CDK4 indicates that PorA-Loop4 may cause perturbation on CAK which phosphorylates the CDK4 at Thr172. Future studies are needed to confirm this assumption.

Altered expression of cell cycle regulators following interaction with meningococci has also been noted by others. For example, recent work by von Papen showed that meningococcal infection from pathogenic and carriage isolates arrested epithelial cells (Detroit 562 and NP69) in G_1 phase at 24 h post-infection and caused decreased expression of Cyclin D1 and increased expression of Cyclin E and p21 at the protein level (von Papen et al., 2016). Another report stated that Opa and Opc of *N. meningitidis* strain MC58 caused the S-arrest in HBMECs and the upregulation of p21 and Cyclin G2 (Oosthuysen et al., 2016).

At the mRNA level, Schubert-Unkmeir et al. found that there were changes in HBMEC cell cycle regulators' expression in response to meningococcal infection (Schubert-Unkmeir et al., 2007). A two-fold increase in Cyclin D1, Cyclin D3 and CDKs 8 and 9 were reported after four hours of infection, indicating significant changes in the key cell cycle control molecules at the G_1 checkpoint in response to infection. Interestingly, they also confirmed a decrease in the expression of LAMR mRNA of 0.607 and 0.490 fold at 4 and 8 h post infection, respectively. The increased expression of Cyclin D1 in the study by Schubert-Unkmeir et al. seems contrary to our result. However, it should be noted that they used whole MC58 bacteria to infect the endothelial cells. The bacteria possess many surface molecules that interact with components of the host cell surface, each of which may potentially alter different pathways in the host cell, and thus cause different effects on the cell cycle regulators.

To gain a better understanding of the perturbation of the cell cycle regulators caused by the PorA-Loop4, the use of a whole PorA would be a good approach between peptide and whole bacteria. However, in a previous study by Vassey, difficulties were encountered in purifying recombinant PorA in a native conformation (Vassey, 2014). Approaches taken included expression of His-Tagged PorA in *E. coli* based systems, purification of PorA using the Invitrogen Membrane Max system, and ion-exchange and gel filtration chromatography. These methods were ineffective to obtain natively folded PorA with the necessary tertiary

structure in preparations that were sufficiently free of detergents. Later in this study (Chapter 5), whole cell *N. meningitidis* of strain MC58 and mutants derived from it lacking either PorA-Loop4 or PorA were used to confirm the results described in this chapter.

Other bacteria also manipulate the cell cycle as part of their strategy to colonise and infect host cells. Most use toxins to damage the DNA of host cells, and thus stimulate apoptosis. A closely related pathogen to meningococci, *Neisseria gonorrhoeae,* has been shown to modulate G_1 arrest through the decrease of Cyclin B1, Cyclin D1, and Cyclin E (Jones et al., 2007). Gonococci interfere with the host cell cycle via translocation of bacterial restriction endonucleases into the host cell nucleus where they cause double strand breaks in the DNA and thus prevent progression of the host cell cycle (Weyler et al., 2014).

Meningococci potentially dysregulate host cell processes during disease progression and/or commensal carriage to facilitate long term colonisation. The PorA-Loop4:37LRP interaction with the cells in the local micro-environment is likely to influence normal turnover and renewal of endothelium by stalling the cell cycle via altered expression of the cell cycle regulators, and ultimately allowing bacteria to initiate a sustained colonisation. Nougayrede et al. described bacterial toxins and effectors that modulate the eukaryotic cell cycle as cyclomodulins (Nougayrede et al., 2005). The data suggest that PorA-Loop4 is one such meningococcal cyclomodulin affecting the endothelial cell cycle, specifically by locking cells into the G_1 phase.

To study the whole mechanism of meningococcal PorA-Loop4 in triggering the G_1 arrest in HBMECs, the possible affected signalling pathway from the inner membrane to the nucleus should be explored. Since Cyclin D1 and CDK4 were involved in several pathways and the cell cycle arrest happened in the G_1 phase, it is hypothesised that the PorA-Loop4 acts via the PI3K/Akt pathway. The hypothesis is also based on some reports mentioned in Section 1.8. Thus, the perturbation of key proteins' expression in the PI3K/Akt pathway and the effect of associated inhibitors in the pathway were investigated in the following chapter.

Chapter 4 - Effects of PorA-Loop4 on Akt and GSK-3β as key proteins in the PI3K/Akt pathway

4.1 Introduction

The PI3K/Akt pathway is one of the intracellular signalling pathways regulating the human cell cycle, and is known to be essential for cell survival by reducing apoptosis (Chang et al., 2003). It also influences other cellular functions including glucose metabolism (Hu et al., 2016), neuronal function (Zhong, 2016), and cellular migration (Xue and Hemmings, 2013). In order to promote the transition from G_1 to S phase, the PI3K/Akt pathway involves some key proteins including PI3K, Akt, GSK, FOXO, p21, p27, Cyclin D and CDK4/6 (Figure 4.1).

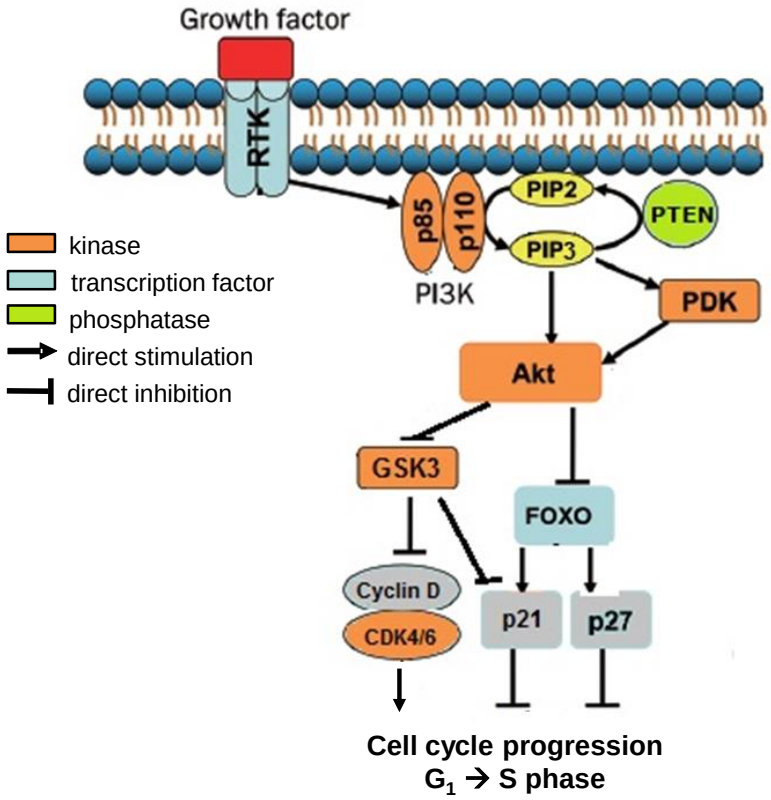

Figure 4.1: Schematic illustration of the PI3K/Akt pathway in the regulation of the human cell cycle. Binding of growth factor to its receptor activates phosphatidylinositol-4,5-bisphosphate 3-kinase (PI3K), an enzyme which catalyses phosphatidylinositol (3,4)-biphosphate (PIP2) into phosphatidylinositol (3,4,5)-triphosphate (PIP3). PIP3 activates protein kinase B (also known as Akt), localising it in the plasma membrane. Akt inhibits cell cycle regulators (p21 and p27) entering the nucleus, thus the cell cycle progresses. Akt also inhibits glycogen synthase kinase-3 (GSK3) which inhibits Cyclin D1 from making a complex with cyclin dependent kinase (CDK) 4/6. The CyclinD1/CDK4 complex is known to regulate the early G_1 phase of the cell cycle. This figure is modified from Kong and Yamori, (2010).

Phosphoinositide 3-kinases (PI3Ks) are a family of enzymes which phosphorylate the 3 position hydroxyl group of the inositol ring of phosphatidylinositol (Whitman et al., 1988). They are activated by a G protein-coupled receptor and a tyrosine kinase receptor (Leevers et al., 1999). Class 1 PI3K, in particular, consists of p85 regulatory subunit and p110 catalytic subunit (Carpenter et al., 1990). The p85 subunit contains SH2 and SH3 domains which allow PI3K to dock with phosphorylated tyrosine residues on other proteins (Lemmon and Schlessinger, 2010). The p110 subunit catalyses the conversion of PIP2 into PIP3 (Yu et al., 1998). The conversion is antagonised by PTEN which removes the phosphate group from the D3 position of the inositol ring of PIP3 (Maehama and Dixon, 1998). In the PI3K/Akt pathway, Akt and PDK bind to PIP3, although Akt also binds to the PIP2 at lower affinity (DiNitto and Lambright, 2006). The binding of Akt to PIP3 keeps the Akt and PDK in the plasma membrane.

Akt (also known as PKB) has three isoforms with different functions. Akt1 is the main isoform involved in the PI3K/Akt pathway (Cantley, 2004). It inhibits the apoptotic process via inhibition of Bad/Bcl-2 activity and degradation of p53. Akt1 also induces protein synthesis, and promotes cell proliferation. Akt2 has an important role in the insulin signalling pathways. The function of Akt3 is unclear but it appears to be predominantly expressed in brain, heart, and kidneys. In general, the protein structure of Akt contains three domains: (1) an amino-terminal pleckstrin homology domain (PH domain), (2) central kinase domain containing threonine residue Thr308, and (3) carboxyl-terminal regulatory domain (hydrophobic) containing serine residue Ser473 (Manning and Toker, 2017, Liao and Hung, 2010). The pleckstrin homology domain is a protein domain which binds to phosphatidylinositol lipids (PIP2 and PIP3) within biological membrane.

Inactive Akt primarily resides in the cytoplasm. The activation of Akt involves the PH-domain dependent membrane translocation step, followed by phosphorylation of Thr308 and Ser473 (Manning and Toker, 2017, Liao and Hung, 2010). After the stimulation of RTKs or GPCRs and PIP3 production at the plasma membrane, inactive Akt is recruited to the membrane. The three way interaction of Akt/PDK/PIP3 allows PDK1 to phosphorylate Akt at its Thr308 residue. It primes the phosphorylation at Ser473 caused by mTORC2 and marks the full activation of Akt (Manning and Toker, 2017, Jacinto et al., 2006). Signal termination is achieved by the PTEN, PP2A, and PHLPP protein phosphatases. PTEN reconverts PIP3 to PIP2, while PP2A and PHLPP2 dephosphorylates the Akt at Thr308 and Ser473,

respectively (Wlodarchak and Xing, 2016). The phosphorylated Akt is also partly ubiquitinated by E3 ligase EDD4 and degraded by the proteasome (Suizu et al., 2009).

The active Akt phosphorylates glycogen synthase kinase-3β (GSK-3β) at Ser9 (Cross et al., 1995) and FOXO transcription factor at two or three critical residues (Thr24, Ser253, and Ser316 in FoxO1a) (Tzivion et al., 2011). Phosphorylation at these sites is inhibitory and do not lead to activation of GSK-3β and FOXO. The inhibition of FOXO leads to downregulation of p21 and p27 (Hauck et al., 2007, Medema et al., 2000). The inhibition of p21 and p27 for nuclear localisation would facilitate the formation of Cyclin E/CDK2 complex which progresses the late G_1 phase to the S phase (Abukhdeir and Park, 2008).

GSK-3 is a kinase with over 100 known substrates involved in multiple signalling pathways (PI3K/Akt, mTOR, Wnt/β-catenin, MAPK/Erk, NF-κB, Hedgehog) (Jope and Johnson, 2004). It has two isoforms: GSK-3α and GSK-3β. The activity of GSK-3β in particular is regulated by the phosphorylation status of its tyrosine and serine residues. The activation requires the phosphorylation at Tyr216 in the activation loop (Lochhead et al., 2006). The Tyr phosphorylation was thought to be auto phosphorylation (Cole et al., 2004). However, phosphorylation by Src family tyrosine kinases has also been reported (Goc et al., 2014). Tyr216-phosphorylated GSK3β is constitutively active and is inactivated by phosphorylation at Ser9 by many protein kinases including Akt, PKA, P90RSK, PKC, and P70-S6 Kinase (Beurel et al., 2015, Jope and Johnson, 2004). Phosphorylated Ser9 self-associates in the primed-substrate binding pocket, hindering the binding of primed substrates, and thus diminishes primed-substrate phosphorylation by GSK-3β (Beurel et al., 2015).

4.2 Aim

In the previous chapter, exposure of HBMECs to PorA-Loop4 caused the perturbation of Cyclin D1 and CDK4 expression. The primary aim of this chapter is to investigate whether the perturbation of Cyclin D1 and CDK4 expression is associated with PI3K/Akt signalling. Another aim of this chapter is to investigate the effect of PorA-Loop4 on the expression and activation of pAkt (Ser473) and pGSK-3β (Ser9) as these two kinases regulate the PI3K/Akt signalling pathway. The final aim is to explore whether the perturbation of Cyclin D1 and GSK-3β expression caused by the PorA-Loop4

are dependent on, or influenced by, the activity of GSK-3β and Akt as upstream kinases in the PI3K/Akt pathway, respectively.

4.3 The effect of PorA-Loop4 on Cyclin D1 expression in the presence of PI3K inhibitor (ZSTK474)

To test our hypothesis that PorA-Loop4 causes the perturbation of Cyclin D1 and CDK4 expression via the PI3K/Akt pathway, the HBMECs were exposed to PorA-Loop4 in the presence of a PI3K inhibitor to determine any subsequent change in Cyclin D1 and CDK4 expression. If PorA-Loop4 works via PI3K, the PI3K inhibition would be predicted to prevent the perturbation of Cyclin D1 and CDK4 caused by the PorA-Loop4. ZSTK474, a PI3K inhibitor that acts through ATP-competition by binding at the ATP-binding pocket of PI3K Class I (Kong and Yamori, 2007, Kong and Yamori, 2010), was used to treat the HBMECs.

First, the effect of ZSTK474 on the viability of HBMECs were assessed by using trypan blue as a viability stain (Figure 4.2). The cells were treated with various concentrations of ZSTK474 as suggested by the manufacturer. The viability of HBMECs treated with the maximum suggested concentration for 24 h was 83.05% (~16.95% of dead cells), significantly different to the untreated controls ($p \leq 0.05$). The viability from 2 μM to the lowest concentration (0.1 μM) were not significantly different to the untreated controls ($p > 0.05$). In subsequent experiments, 2 μM and 0.1 μM ZSTK474 were used to treat the HBMECs.

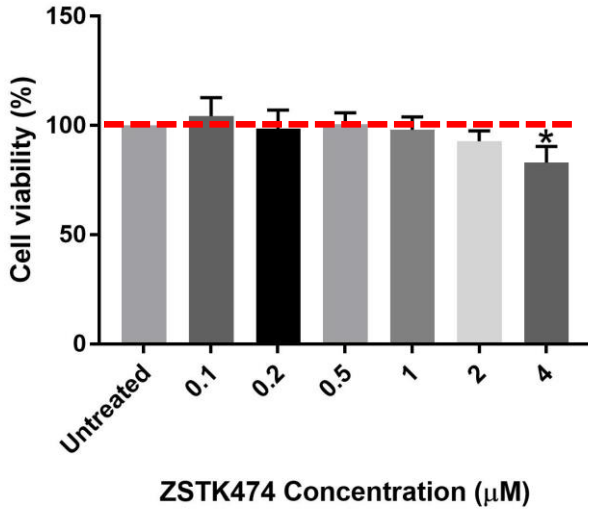

Figure 4.2: Effect of ZSTK474 on the viability of HBMECs. HBMECs (10^6 cells $well^{-1}$) were treated with various concentrations of ZSTK474 (0.1-4 μM) for 24h, and the number of viable cells counted in a haemocytometer. Trypan Blue was used to stain dead cells. Cell viability (%) was calculated by comparison of treated viable cells with the untreated controls. Data were presented as the mean + SD (n=3). Significant difference to the untreated controls (*p≤0.05, ANOVA Dunnet's test applied post hoc).

HBMECs were then treated either with PorA-Loop4 peptide (50 μM), ZSTK474 (2 μM), or a combination of PorA-Loop4 peptide and ZSTK474, for 2, 4, 8, 24 h. The treated cells and the untreated controls were lysed to extract the total RNA for the qRT PCR assays. The quality of extracted RNA was confirmed by Agilent 2100 Bioanalyzer. The RIN values, pseudo-image gels, and chromatograms from all samples used in this chapter are presented in Appendix IV. The 28S/18S ratio of all samples were between 1.7 and 3.5, and the RIN values were 8.2-10.

The qRT PCR system used in this chapter was the same as section 3.4. Figure 4.3 shows the Cyclin D1 mRNA expression levels from all samples. A reduction of Cyclin D1 was observed in PorA-Loop4-treated cells for 2, 4, 8, and 24 h compared to the untreated controls. The ZSTK474-treated cells also showed a reduction of Cyclin D1, and it was significantly lower than the Loop4-treated samples at 2 h post treatment (p≤0.01). However, Cyclin D1 expression in ZSTK474-treated cells showed a tendency to return back to initial levels from 4 to 24 h post treatment. Cyclin D1 expression in PorA-Loop4 and ZSTK474-treated cells was not significantly different from the ZSTK474-treated cells from 4 to 24 h post treatment (p>0.05).

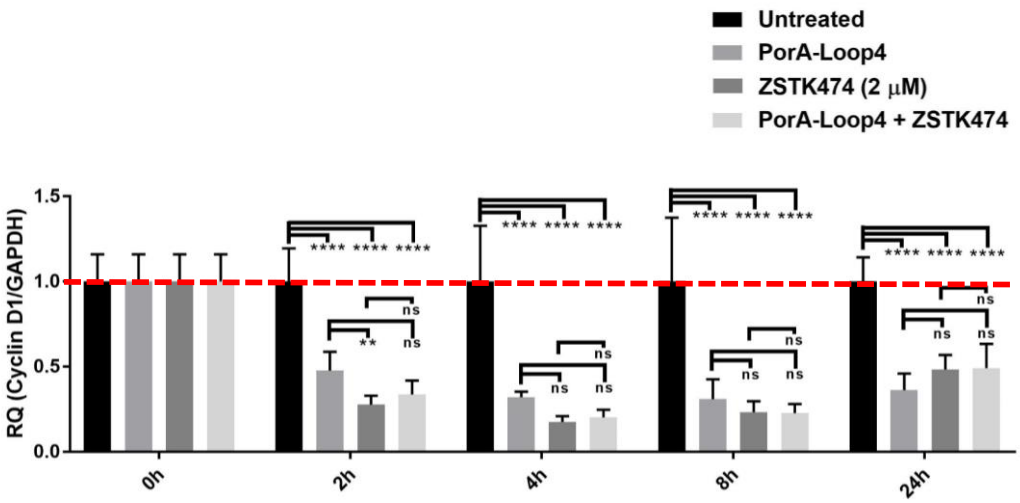

Figure 4.3: qRT PCR analysis of Cyclin D1 expression in treated-HBMECs. Bars represent RQ (relative quantification) mRNA expression ($2^{-\Delta\Delta C_T}$, fold changes) of Cyclin D1 in response to treatment with PorA-Loop4 (50 μM), ZSTK474 (2 μM), both PorA-Loop4 (50 μM) and ZSTK474 (2 μM), or in untreated controls. Data were adjusted for GAPDH levels, and normalised to the untreated cells. qRT PCR was performed in three independent experiments. Significant difference (**p≤0.01, ****p≤0.0001, ns: not significant, one-way ANOVA Tukey's test applied post hoc).

To study Cyclin D1 expression at the protein level, immunoblotting and densitometry analysis were performed with lysates from 24h post treated HBMECs. The lysates were loaded into acrylamide gels for either staining or immunoblotting with the anti-Cyclin D1. Figure 4.4 shows the stained gels that illustrating the equal amount of protein between samples used in this section.

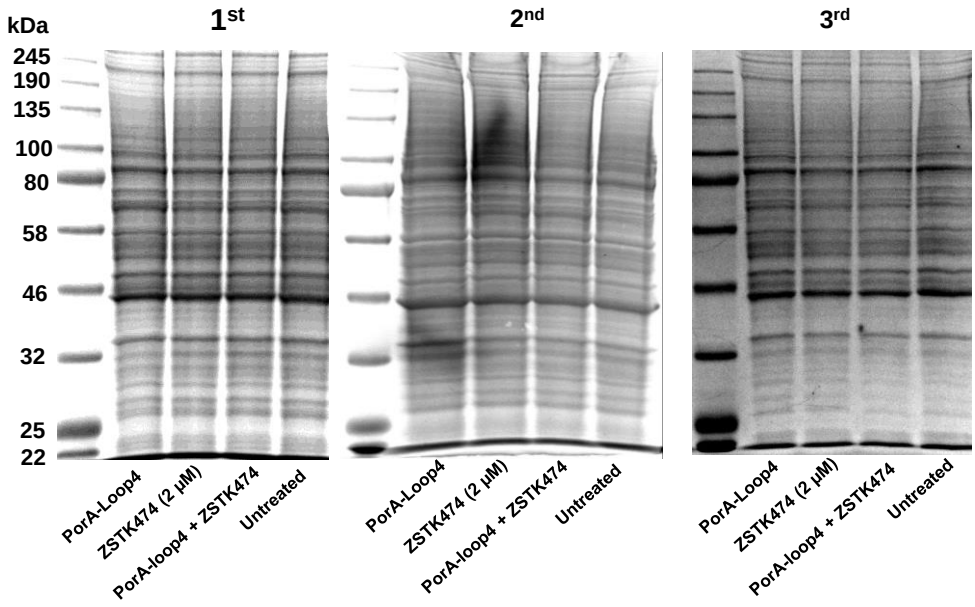

Figure 4.4: SDS-PAGE of lysates from the treated-HBMECs. The HBMECs were treated with PorA-Loop4 (50 μM), ZSTK474 (2 μM), both PorA-Loop4 (50 μM) and ZSTK474 (2 μM), or left untreated as controls. Protein lysates (5 μg) were separated on 10% acrylamide gels. Images were obtained from three independent experiments (1st-3rd).

Representative images of blots and the densitometry analysis of Cyclin D1 expression are presented in Figure 4.5. Overall, Cyclin D1 protein expression from all samples were similar to the Cyclin D1 mRNA expression. The PorA-Loop4-treated cells showed a lower expression of Cyclin D1 at the 24 h post treatment compared to the untreated controls. The ZSTK474-treated cells also showed the lower expression of Cyclin D1 than the untreated controls which was expected based on a previous report (Wang et al., 2016b). However, the ZSTK474-treated cells had a higher Cyclin D1 protein expression than the PorA-Loop4-treated cells, although the difference was not significiant. The combined PorA-Loop4 and ZSTK474-treated cells had the same level of Cyclin D1 expression as the ZSTK474 only-treated cells. Again there was a partial, but not statistically significant ($p>0.05$), recovery in Cyclin D1 protein expression in the presence of PorA-Loop4 and ZSTK474.

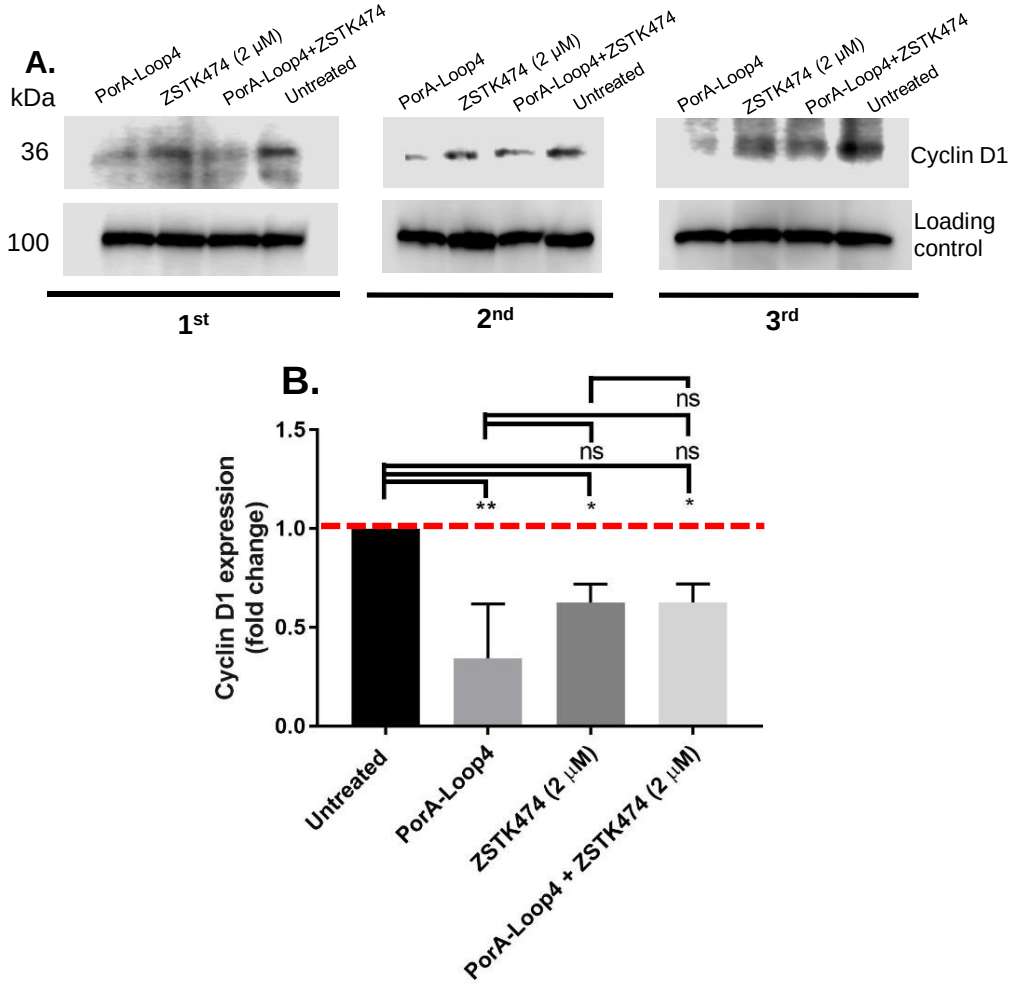

Figure 4.5: Immunoblot images (A) and densitometry analysis (B) of Cyclin D1 expression in treated-HBMECs. HBMECs were treated with PorA-Loop4 (50 μM), ZSTK474 (2 μM), both PorA-Loop4 (50 μM) and ZSTK474 (2 μM), or left untreated as controls**.** The HBMECs were lysed at 24 h post treatment. Representative images were obtained from three independent experiments (1^{st}-3^{rd}). Alpha actinin was used as loading control in all immunoblots. Band intensities were quantified by Image J software. All data were normalised to the untreated controls and adjusted to the loading control densities. Significant difference to the untreated controls (*$p \leq 0.05$, **$p \leq 0.01$, ns: not significant, one-way ANOVA Tukey's test applied post hoc).

The lowest suggested concentration of ZSTK474 (0.1 μM) was also used to treat the HBMECs. The stained gels are presented in Figure 4.6, while the blot images and densitometry analysis are presented in Figure 4.7. PorA-Loop4 caused the lower expression of Cyclin D1 compared to untreated cells. The Cyclin D1 expressions in the ZSTK474-treated cells was not significantly altered ($p>0.05$), which was also seen in the combined PorA-Loop4 and ZSTK474-treated cells. There was a significant recovery of Cyclin D1 expression in the combined PorA-Loop4 and ZSTK474-treated cells to the steady state level ($p\leq0.01$). The data suggest that the PI3K inhibitor prevents the PorA-loop4's effect on Cyclin D1 expression which means that PorA-Loop4 is dependent on PI3K for downregulating Cyclin D1.

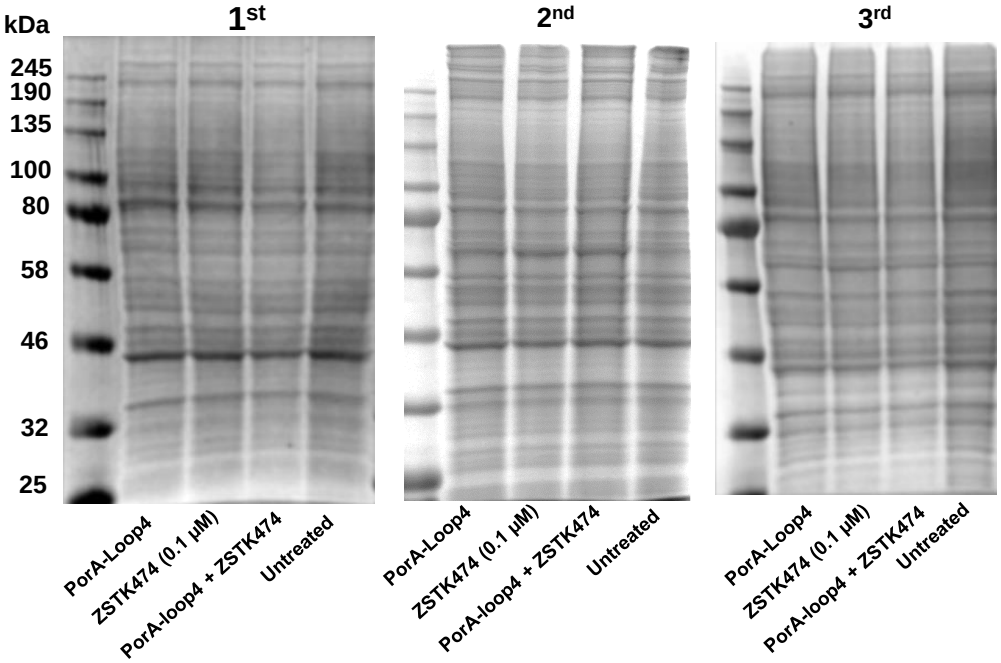

Figure 4.6: SDS-PAGE of whole lysates from HBMECs treated with PorA-Loop4 peptide and/or ZSTK474 (0.1 μM), and the untreated controls. Protein lysates (5 μg) were separated in 10% acrylamide gels. Images were obtained from three independent experiments (1^{st}-3^{rd}).

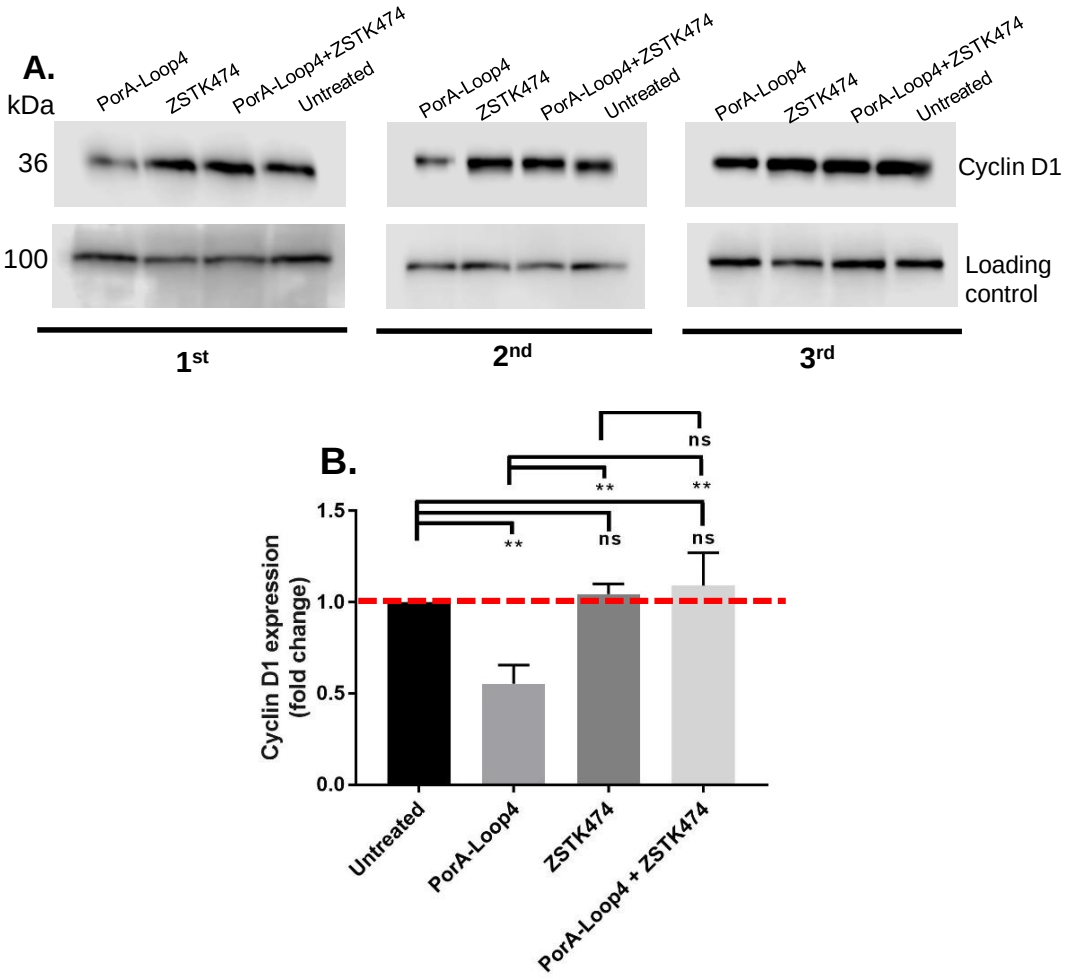

Figure 4.7: Immunoblot images (A) and densitometry analysis (B) of Cyclin D1 expression in treated-HBMECs. HBMECs were treated with PorA-Loop4 (50 μM), ZSTK474 (0.1 μM), both PorA-Loop4 (50 μM) and ZSTK474 (0.1 μM), or left untreated as controls**.** The HBMECs were lysed at 24 h post treatment. Representative images were obtained from three independent experiments (1^{st}-3^{rd}). Alpha actinin was used as loading control in all immunoblots. Band intensities were quantified by Image J software. All data were normalised to the untreated controls and adjusted to the loading control densities. Significant difference to the untreated controls (**$p \leq 0.01$, ns: not significant, one-way ANOVA Tukey's test applied post hoc).

4.4 The effect of PorA-Loop4 on CDK4 expression in the presence of PI3K inhibitor

The alteration in CDK4 expression caused by the PorA-Loop4 was also investigated for its dependency on PI3K activity. The lysates, qRT PCR, and immunoblot system used for this purpose were similar to the previous experiments in Section 4.3.

Figure 4.8 shows the qRT PCR analysis of CDK4 from the treated-HBMECs. PorA-Loop4 caused higher CDK4 expression than the untreated controls at 2-24 h post treatment. The CDK4 expression at 2-24 h post treatment was not significantly altered in the ZSTK474-treated cells ($p>0.05$). The combined PorA-Loop4 and ZSTK474-treated cells showed a higher CDK4 expression than the untreated controls at the 2 h, but the CDK4 expression went down gradually to the similar level of the untreated controls at 4-24 h post treatment.

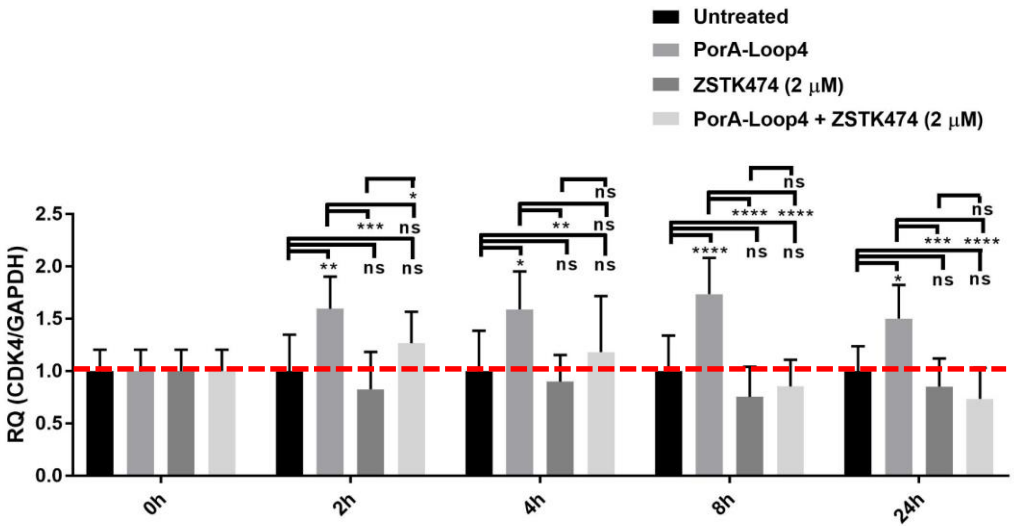

Figure 4.8: qRT PCR analysis of CDK4 expression in treated-HBMECs. Bars represent RQ (relative quantification) mRNA expression ($2^{-\Delta\Delta C_T}$, fold changes) of CDK4 in response to treatment with PorA-Loop4 (50 μM), ZSTK474 (2 μM), both PorA-Loop4 (50 μM) and ZSTK474 (2 μM), or in untreated controls. Data were adjusted for GAPDH levels, and normalised to the untreated cells. qRT PCR was performed in three independent experiments. Significant difference (*p≤0.05, **p≤0.01, ***p≤0.001, ****p≤0.0001, ns: not significant, one-way ANOVA Tukey's test applied post hoc).

Figure 4.9 shows the immunoblot images and the densitometry analysis of pCDK4 (Thr172) level in the treated-HBMECs. PorA-Loop4 caused upregulation of pCDK4 (Thr172) at 24 h post treatment. The protein level

was not significantly altered in the ZSTK474-treated cells and the combined PorA-Loop4 and ZSTK474-treated cells ($p>0.05$). The data suggest that in the presence of the PI3K inhibitor, PorA-Loop4 could not exert an effect on pCDK4 (Thr172) level, and so PorA-Loop4 may act via a PI3K activity-dependant upregulation of pCDK4 (Thr172).

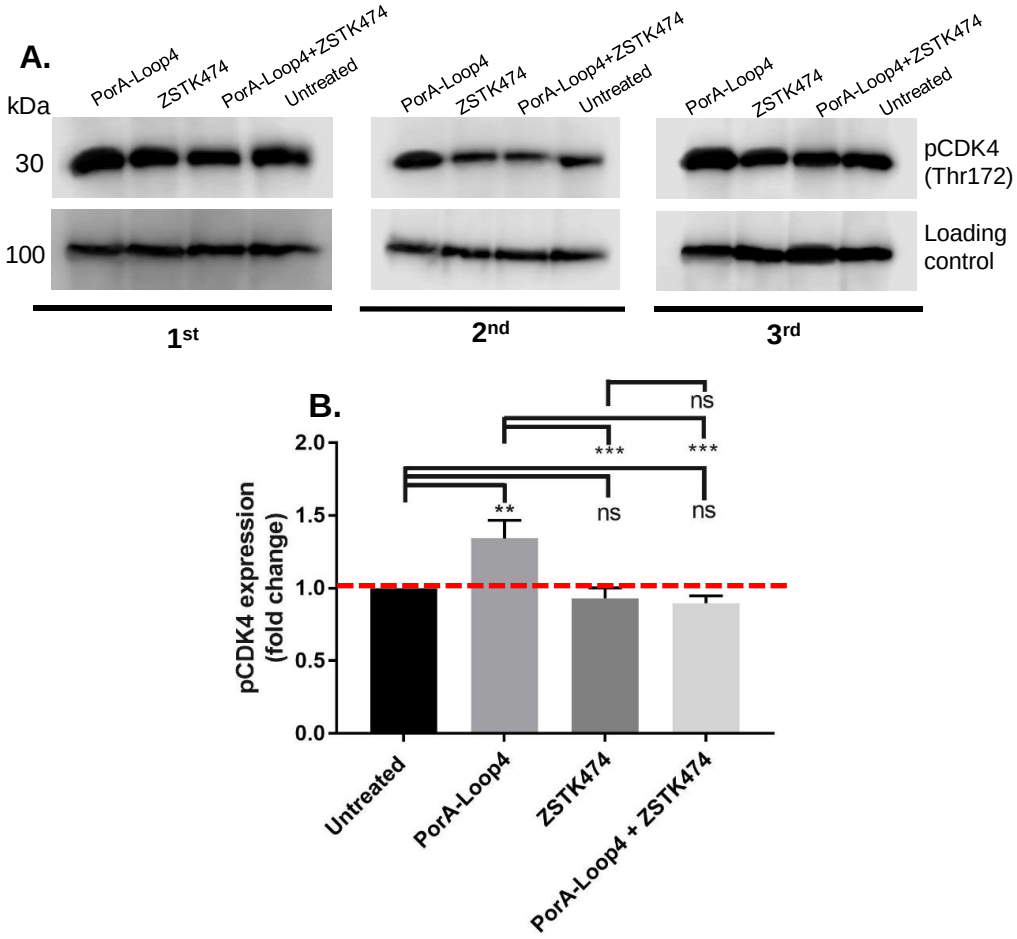

Figure 4.9: Immunoblot images (A) and densitometry analysis (B) of pCDK4 (Thr172) level in treated-HBMECs. HBMECs were treated with PorA-Loop4 (50 μM), ZSTK474 (2 μM), both PorA-Loop4 (50 μM) and ZSTK474 (2 μM), or left untreated as controls**.** The HBMECs were lysed at 24 h post treatment. Representative images were obtained from three independent experiments (1^{st}-3^{rd}). Alpha actinin was used as loading control in all immunoblots. Band intensities were quantified by Image J software. All data were normalised to the untreated controls and adjusted to the loading control densities. Significant difference to the untreated controls (**$p\leq0.01$, ***$p\leq0.001$, ns: not significant, one-way ANOVA Tukey's test applied post hoc).

4.5 The levels of pAkt (Ser473) and pGSK-3β (Ser9) in PorA-Loop4-treated HBMECs

After investigating PI3K's influence on the ability of PorA-Loop4 to alter Cyclin D1/CDK4 expression, perturbation of pAkt (Ser473) and pGSK-3β (Ser9) levels were checked in the PorA-Loop4-treated HBMECs. The lysates used in this experiment were the same as Section 3.5. Figure 4.10: and Figure 4.11 show the immunoblot analysis of pAkt (Ser473) and pGSK-3β (Ser9), respectively. PorA-Loop4 caused a decrease in the level of pAkt (Ser473), 0.5 times lower than in untreated controls at 24 h post-treatment ($p \leq 0.05$). In contrast, PorA-Loop4 caused an increase in pGSK-3β (Ser9) levels, 2.6 times higher than the untreated controls at 24 h post treatment ($p \leq 0.0001$).

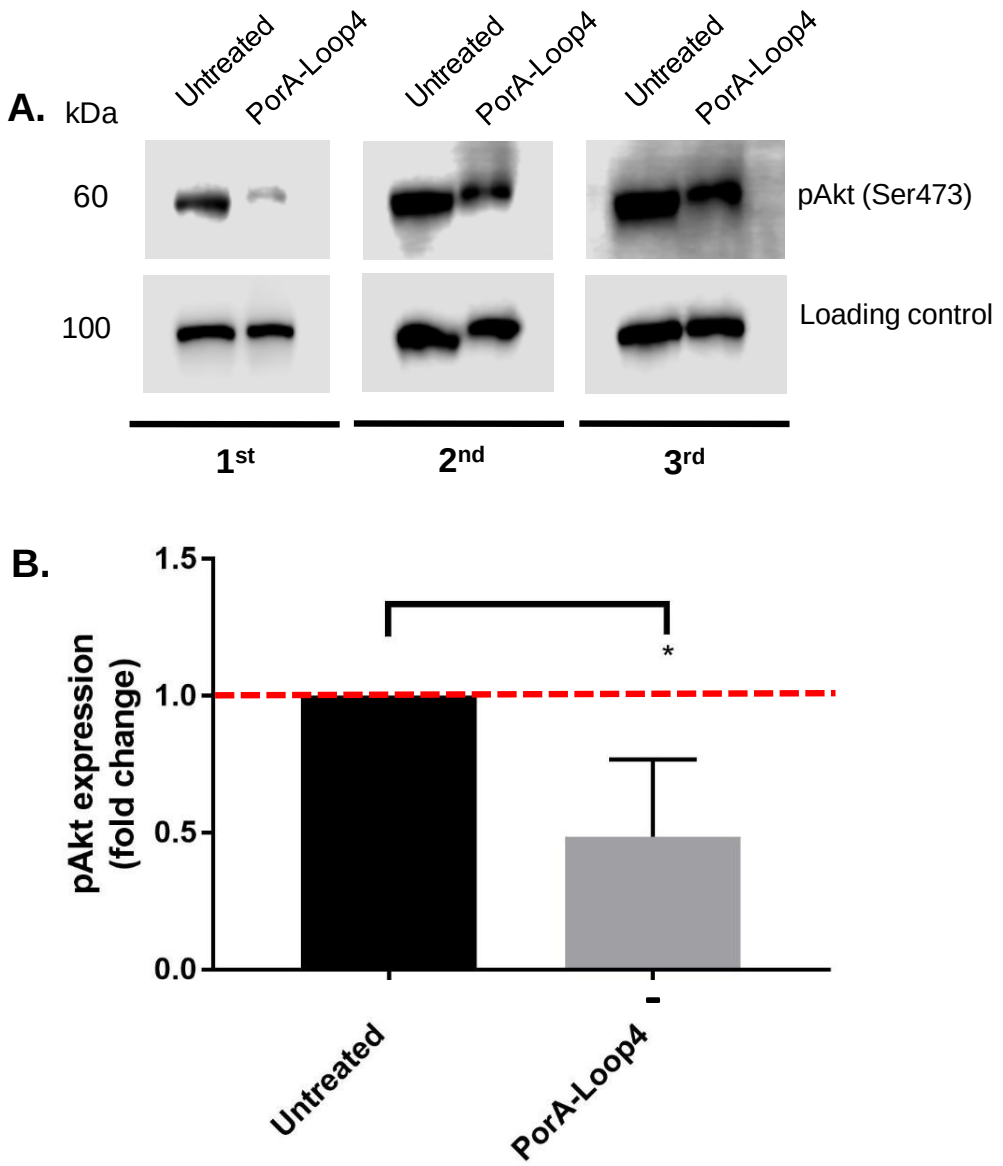

Figure 4.10: Exposure to 50 μM PorA-Loop4 resulted in decreased level of pAkt (Ser473) at 24 h post treatment. Panel A represents the immunoblot images from three independent experiments (1st-3rd), while Panel B represents the densitometry analysis. Alpha actinin was used as loading control in all immunoblots. Band intensities were quantified using Image J software. All data were normalised to the untreated controls and adjusted to the loading control densities. Significant difference to the untreated controls (*p≤0.05, unpaired Student's t-test).

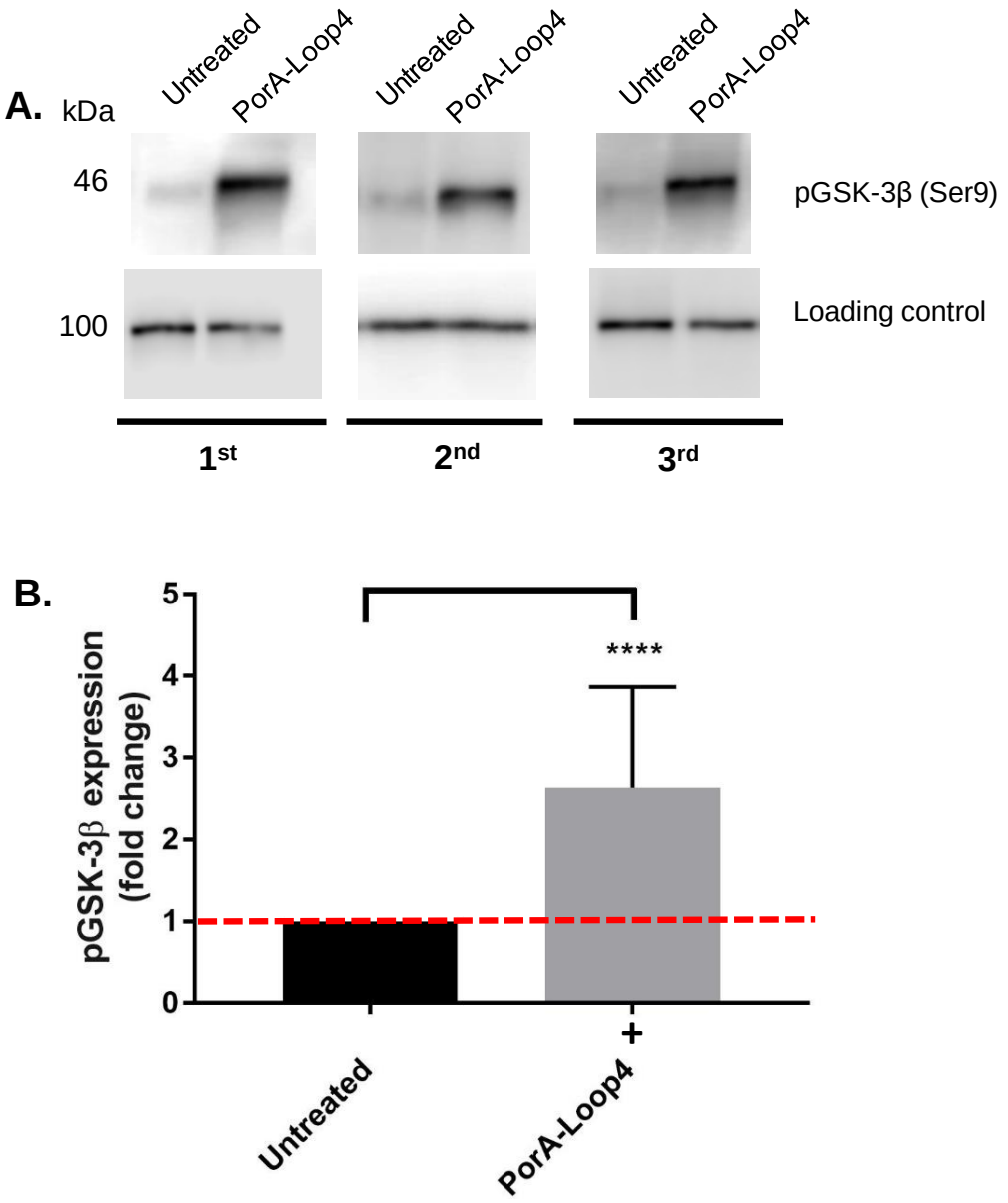

Figure 4.11: Exposure to 50 μM PorA-Loop4 resulted in increased level of pGSK-3β (Ser9) at 24 h post treatment. Panel A represents the immunoblot images from three independent experiments (1st-3rd), while Panel B represents the densitometry analysis. Alpha actinin was used as loading control in all immunoblots. Band intensities were quantified using Image J software. All data were normalised to the untreated controls and adjusted to the loading control densities. Significant difference to the untreated controls (****p≤0.0001, unpaired Student's t-test).

4.6 The effect of PorA-Loop4 on Cyclin D1 expression in the presence of GSK-3β inhibitor (1-Azakenpaullone)

The previous experiments showed that PorA-Loop4 caused the downregulation of Cyclin D1 24 h post treatment. Based on reports that GSK-3β regulates the degradation of Cyclin D1, work described in this section aimed to investigate whether the downregulation of Cyclin D1 caused by the Loop4 is dependent on GSK-3β. 1-Azakenpaullone (1-AKP, Sigma-Aldrich), a selective GSK-3β inhibitor with 100-fold less cross-reactivity against CDKs (Kunick et al., 2004) was used to treat the cells.

Figure 4.12 shows the effect of 1-AKP on the viability of HBMECs. HBMECs were treated with 1-AKP at various concentrations from 0.15 to 2.5 μM as suggested by the manufacturer. Exposure to higher concentrations of 1-AKP resulted in increased cell numbers as the GSK-3β inhibitor promotes cell proliferation (Stein et al., 2011, Mussmann et al., 2007). The minimum and maximum concentrations of 1-AKP (0.15 and 2.5 μM) were used to treat HBMECs.

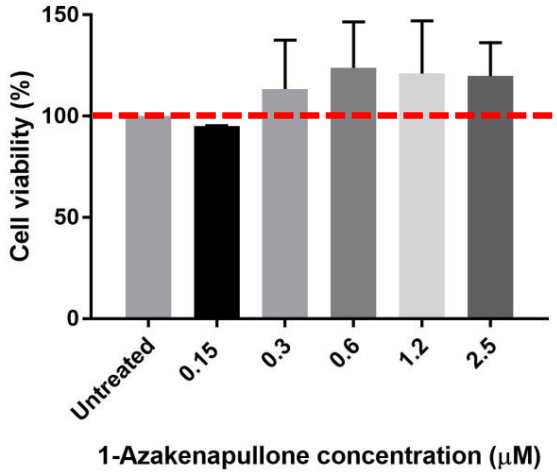

Figure 4.12: Effect of 1-AKP on the viability of HBMECs. HBMECs (10^6 cells $well^{-1}$) were treated with various concentration of 1-AKP (0.15-2.5 μM) for 24 h, and the number of viable cells counted in a haemocytometer. Trypan Blue was used to stain dead cells. Cell viability (%) was calculated by comparison of treated viable cells with controls (untreated cells). Data were presented as the mean + SD (n=3). The increase of viable cells treated with 0.3 – 2.5 μM of 1-AKP were not significant.

Figure 4.13 shows the stained gels of the lysates used for immunoblotting. It shows similar amount of proteins between samples. Figure 4.14 shows the immunoblotting analysis. The PorA-Loop4-treated cells showed decreased Cyclin D1 expression, similar to previous results in Section 3.5 and 4.3. The Cyclin D1 expression was not significantly altered in the 1-AKP-treated cells ($p>0.05$). PorA-Loop4 still caused the decrease of Cyclin D1 in the presence of minimum and maximum concentrations of 1-AKP indicating that PorA-Loop4 alters Cyclin D1 expression in a GSK-3β-independent manner.

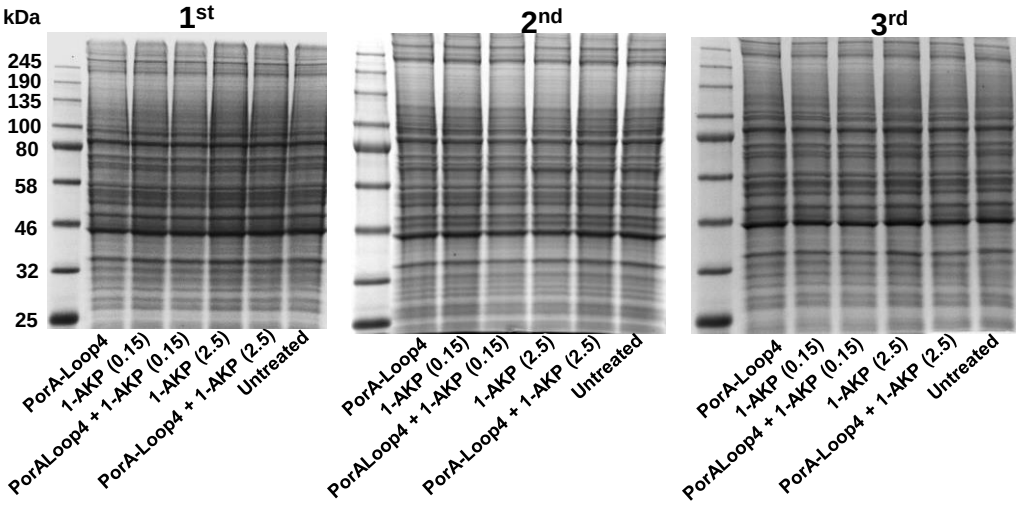

Figure 4.13: SDS-PAGE of whole lysates from HBMECs treated with PorA-Loop4 peptide (50 μM) and/or 1-Azakenapaullone (1-AKP, 0.15 and 2.5 μM), and the untreated controls. Protein lysates (5 μg) were separated on 10% acrylamide gels. Images were obtained from three independent experiments (1^{st}-3^{rd}).

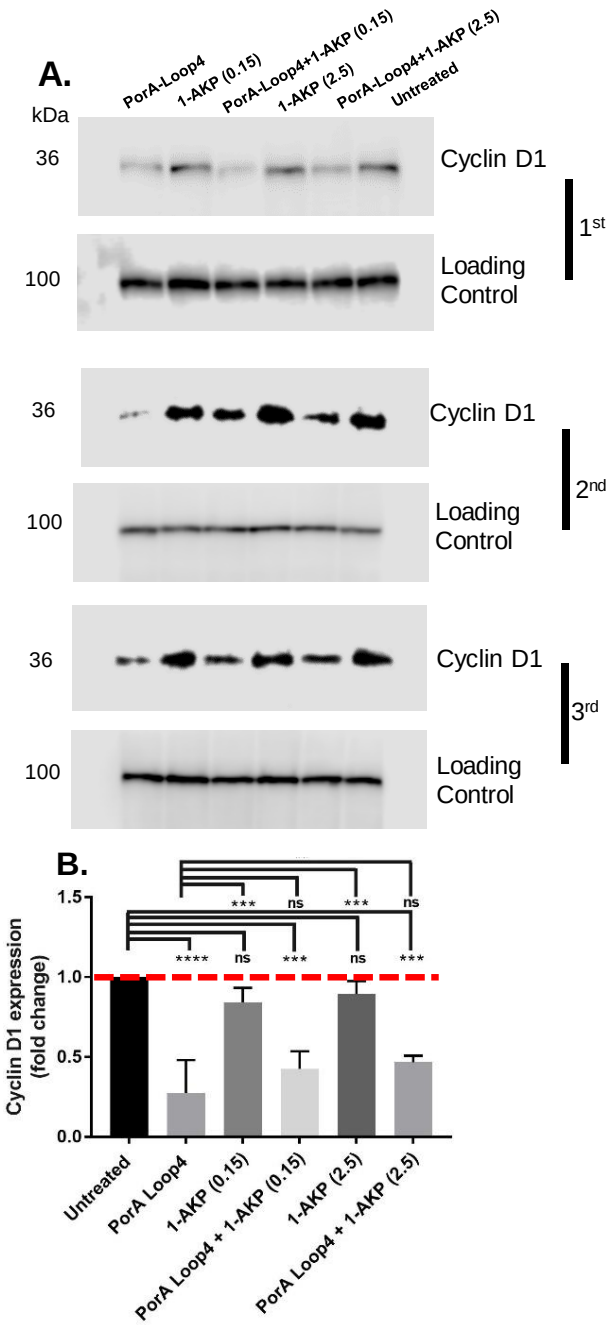

Figure 4.14: Immunoblot images (A) and densitometry analysis (B) of Cyclin D1 expression from treated-HBMECs. HBMECs were treated with PorA-Loop4 (50 μM), 1-AKP (0.15 μM), PorA-Loop4 and 1-AKP (0.15 μM), 1-AKP (2.5 μM), PorA-Loop4 and 1-AKP (2.5 μM), or left untreated as control. The HBMECs were lysed at 24 h post treatment. Representative images were obtained from three independent experiments (1^{st}-3^{rd}). Alpha actinin was used as loading control in all immunoblots. Band intensities were quantified by Image J software. All data were normalised to the untreated controls and adjusted to the loading control densities. Significant difference to the untreated controls (***$p \leq 0.001$, ****$p \leq 0.0001$, ns: not significant, one-way ANOVA Tukey's test applied post hoc).

4.7 The effect of PorA-Loop4 on pGSK-3β (Ser9) level in the presence of Akt inhibitor (MK2206)

Previous results showed that PorA-Loop4 caused an upregulation of pGSK-3β (Ser9) 24 h post treatment. Based on the fact that Akt phosphorylates GSK-3β at Ser9, work in this section aimed to investigate whether the upregulation of pGSK-3β (Ser9) caused by the Loop4 is dependent to the Akt activity. MK2206 (reSource), an allosteric Akt inhibitor, was used to prevent Akt-mediated phosphorylation of downstream signalling molecules (Hirai et al., 2010).

Figure 4.15 shows the effect of MK2206 on the viability of HBMECs. HBMECs were treated with MK2206 at various concentrations from 0.6 to 20 μM as suggested by the manufacturer. Higher concentrations of MK2206 caused lower cell viability as the inhibitor promotes apoptosis (Agarwal et al., 2014). The viability of HBMECs treated with the maximum concentration (20 μM) was 64%. Although the difference was not statistically significant compared to the untreated controls ($p>0.05$), it still caused cytotoxicity to HBMECs resulting in 36% cell death. Therefore, 0.6 and 10 μM MK2206 were used to treat the HBMECs in subsequent experiments.

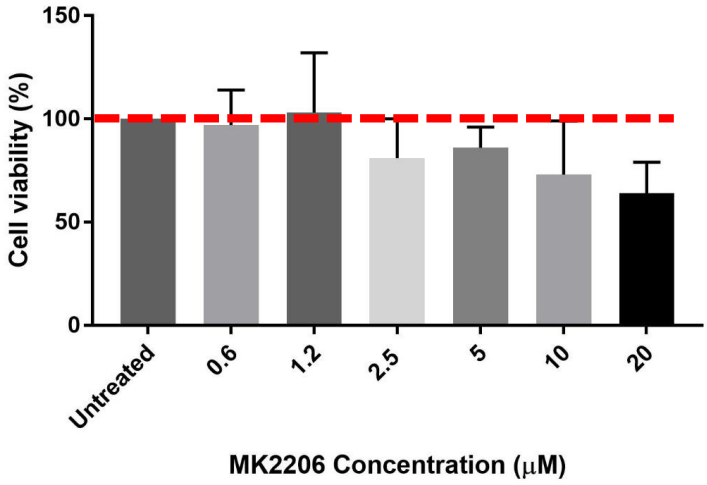

Figure 4.15: Effect of MK2206 on the viability of HBMECs. HBMECs (10^6 cells $well^{-1}$) were treated with various concentrations of MK2206 (0.6-20 μM) for 24 h, and the number of viable cells counted in a haemocytometer. Trypan Blue was used to stain dead cells. Cell viability (%) was calculated by comparison of treated viable cells with controls (untreated cells). Data were presented as the mean + SD (n=3). The decrease of viable cells treated with 2.5 – 20 μM of MK2206 were not significant.

Figure 4.16 shows the stained gels of the lysates used for immunoblotting. It shows similar amount of proteins between samples. Figure 4.17 shows the immunoblotting analysis. PorA-Loop4 caused the upregulation of pGSK-3β (Ser9) which is similar to previous results. The MK2206-treated cells showed a decrease of pGSK-3β (Ser9) level, which was expected corresponding to a previous report (Swiatkowski et al., 2017). The combined PorA-Loop4 and MK2206-treated cells also showed the decrease of pGSK-3β (Ser9) levels, although there was a small increase but not significant compared to the MK2206 only-treated cells ($p>0.05$). The presence of the inhibitor at 0.6 and 10 μM caused a large decrease in levels of pGSK-3β, but addition of PorA-Loop4 did not significantly increase pGSK-3β expression in MK2206-treated cells.

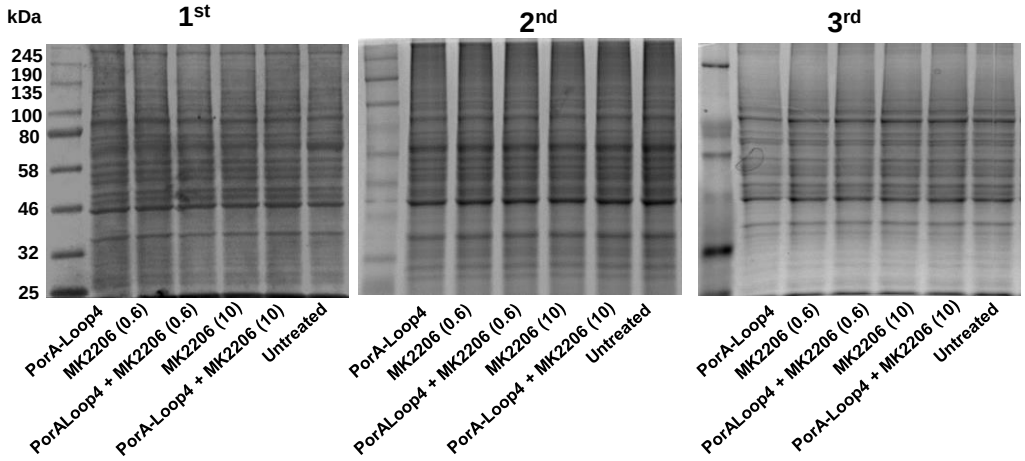

Figure 4.16: SDS-PAGE of whole lysates from HBMECs treated with PorA-Loop4 peptide and/or MK2206 (0.6 and 10 μM), and the untreated controls. Protein lysates (5 μg) were separated on 10% acrylamide gels. Images were obtained from three independent experiments (1st-3rd).

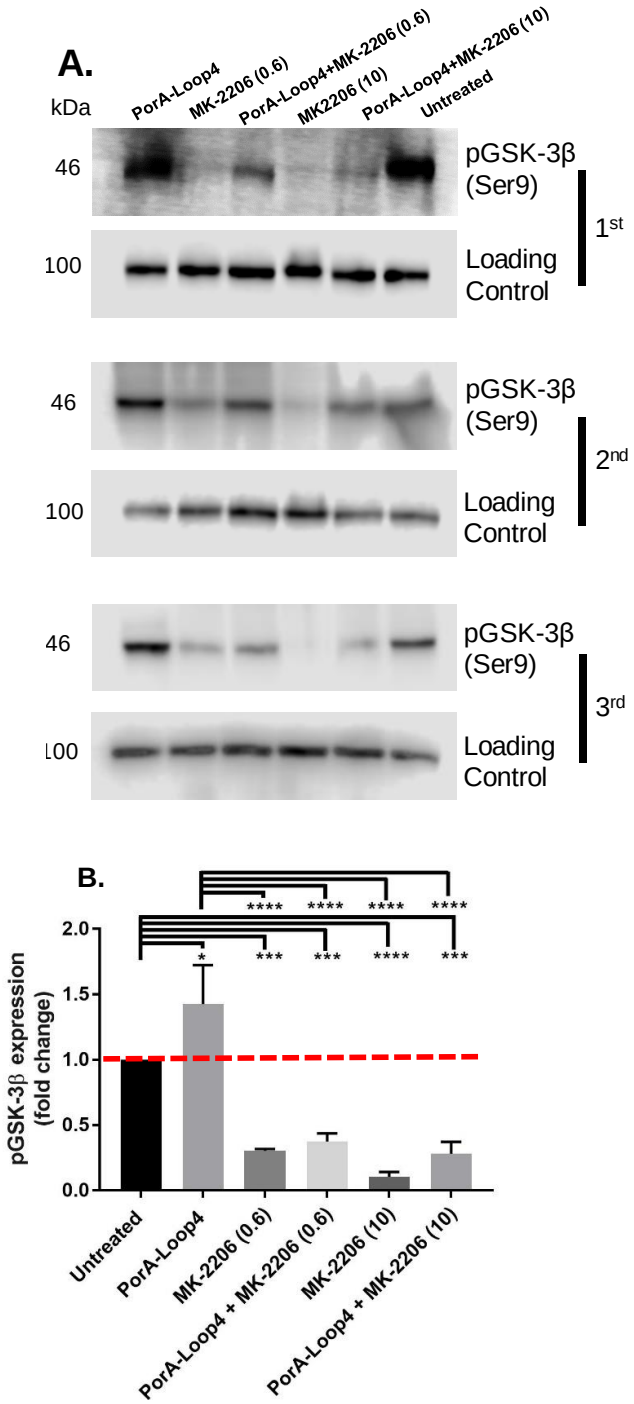

Figure 4.17: Immunoblot images (A) and densitometry analysis (B) of pGSK-3β (Ser9) level from treated-HBMECs. HBMECs were treated with PorA-Loop4 (50 μM), MK2206 (0.6 μM), PorA-Loop4 and MK2206 (0.6 μM), MK2206 (10 μM), PorA-Loop4 and MK2206 (10 μM), or left untreated as control. The HBMECs were lysed at 24 h post treatment. Representative images were obtained from three independent experiments (1st-3rd). Alpha actinin was used as loading control in all immunoblots. Band intensities were quantified by Image J software. All data were normalised to the untreated controls and adjusted to the loading control densities. Significant difference to the untreated controls (*p≤0.05, ***p≤0.001, ****p≤0.0001, ns: not significant, one-way ANOVA Tukey's test applied post hoc).

4.8 Discussion

In the previous chapter, it was shown that PorA-Loop4 caused perturbations in Cyclin D1 and pCDK4 (Thr172) protein expression, which might affect cell cycle progression from the G_1 phase. In this chapter, the hypothesis that the interaction of PorA-Loop4:37LRP on the surface of HBMECs cause the G_1 arrest via the PI3K/Akt signalling pathway was tested. PI3K activity was inhibited using ZSTK474, and the effect of PorA-Loop4 on Cyclin D1 and pCDK4 (Thr172) was shown to be PI3K-dependent (at both mRNA and protein levels).

Furthermore, the effect of the PorA-Loop4 on Akt and GSK-3β expression was studied as these proteins are the central kinases in the PI3K/Akt signalling pathway which regulate Cyclin D1 degradation at S phase. Akt-mediated phosphorylation of GSK-3β on Ser9 decreases its kinase activity for Thr286 of Cyclin D1, which consequently inhibits nuclear export and cytoplasmic proteasomal degradation of Cyclin D1 (Alao, 2007, Diehl et al., 1998). In the current study, the data suggest that the PorA-Loop4 caused the downregulation of pAkt (Ser473) and the upregulation of pGSK-3β (Ser9) at the protein levels in HBMECs.

The downregulation of pAkt (Ser473) was expected as the decrease in Akt would interfere with signal transduction to the downstream kinases in the pathway and potentially cause the cell cycle arrest. However, the upregulation of pGSK-3β (Ser9) raises many questions, as the decrease of pAkt (Ser473) might lead to reduced levels of phosphorylation of GSK-3β on Ser9. However, multiple signalling pathways feed into increasing the serine9-phosphorylation of GSK-3β, which can be mediated by PKA, PKC, p70-S6 kinase, and other kinases (Beurel et al., 2015). This suggests that PorA-Loop4 may not only affect the PI3K/Akt pathway, but also other signalling pathways causing the upregulation of pGSK-3β (Ser9).

Current work did not include the effect of PorA-Loop4 on the non-phosphorylated form of GSK-3β, or on pGSK-3β (Tyr216), which directly affects Cyclin D1. The pGSK-3β (Tyr216) partially induce the degradation of Cyclin D1 by phosphorylating Cyclin D1 on Thr286 (Zou et al., 2004, Diehl et al., 1998). Future study investigating the effect of PorA-Loop4 on non-phosphorylated GSK-3β and pGSK-3β (Tyr216) would fill gaps in the current findings. The PorA-Loop4 possibly upregulate the pGSK-3β (Tyr216) to cause the subsequent downregulation of Cyclin D1. The assessment of the non-phosphorylated form of GSK-3β would provide information about the total

protein expression and the ratio of each phosphorylated form could be assessed. It would provide a better perspective on how the PorA-Loop4 affects the post-translational modification of the GSK-3β.

The GSK-3β influence on the perturbation of Cyclin D1 was also investigated. The GSK-3β activity was inhibited using 1-AKP and it was shown that the PorA-Loop4 affected Cyclin D1 independently of GSK-3β. Previous reports suggested that GSK-3β has a limited role in cell cycle regulation of Cyclin D1 levels (Yang et al., 2006a), and degradation of Cyclin D1 might occur independently of phosphorylation of Thr286 by GSK-3β (Germain et al., 2000). Another kinase, such as Mirk/Dyrk1B, may serve to regulate Cyclin D1 stability in situations where GSK-3β activity is absent (Zou et al., 2004). Dyrk1B phosphorylates Cyclin D1 at Thr288, inducing nuclear export and degradation of Cyclin D1. Future studies investigating the effect of PorA-Loop4 to Mirk/Dyrk1B in particular, or the effect of PorA-Loop4 on cytoplasmic Cyclin D1 degradation would fill gaps in the current findings.

It was also shown that PorA-Loop4 was dependent on Akt to cause the upregulation of pGSK-3β (Ser9). This result confirms that PorA-Loop4 affects the PI3K/Akt pathway via Akt and GSK-3β. However, again the opposite effect caused by the PorA-Loop4 on pAkt (Ser473) and pGSK-3β (Ser9) would only be possible if PorA-Loop4 affects multiple pathways not only on the PI3K/Akt pathway. Possibly, PorA-Loop4 upregulates other kinases which phosphorylate the Ser9 of GSK-3β such that it would overcome the decreased kinase activity of Akt.

In addition, the inhibitor concentrations used to block Akt may have been too high. The concentrations were based on the suggestion from the manufacturers and the viability of the HBMECs at the suggested concentrations. The MK2206 at 0.6-10 μM decreased the GSK-3β at very low level. Use of lower concentrations of MK2206 which could block Akt activity without decreasing pGSK-3β (Ser9) expression would have been more appropriate to allow the importance of Akt in upregulation of pGSK-3β by PorA-Loop4 to be assessed. Testing of a wider range of concentrations would have also allowed confirmation of the dose-dependency of any effects seen.

Future studies may use alternative inhibitors to validate current results as the current inhibitors may cause off target effects. The off target effects may occur due to the conserved nature of the ATP-binding sites across the kinase family. Work in this chapter used ZSTK474 to inhibit PI3K Class I by binding to the ATP-pocket of the catalytic subunit p110 (Kong and Yamori, 2007, Kong and Yamori, 2010). ZSTK474 is a pan-PI3K inhibitor which blocks

all p110 isoforms, α, β, δ, and γ. The pan-PI3K inhibitor may cause off-target effects as each isoform is expressed differently, and it is associated with different stimuli and receptors (Wang et al., 2015). PI3Kα-selective inhibitors may be used in the future as they block the isoform α which plays essential roles in cell metabolism, growth, and proliferation. DW09849 would be a good alternative to ZSTK474 as the inhibitor was reported to block PI3K and cause G_1 arrest without killing cells *in vitro* (Liu et al., 2014)

1-AKP was used in the current study based on the fact that the kenpaullone derivative has an enhanced GSK-3β selectivity against CDK1 (Kunick et al., 2004). The inhibitor acts through ATP binding of GSK-3β which could potentially also cause off target effects as the ATP-pocket of GSK-3β is relatively similar to the structure of CDKs. Non ATP-competitive GSK-3β inhibitors (e.g. thiadiazolidinones analogues, tricantin, menzamin, quinolone) might be considered to be used in the future as these allosteric inhibitors bind to the sites that are highly conserved to GSK-3β but differ to other GSK-3 isoform or other kinases (Palomo et al., 2011, Pandey and DeGrado, 2016).

MK2206 was used in the current study to inhibit Akt based on previous report that it targets all three Akt isoforms and induce G_1 arrest (Hirai et al., 2010, Jiao et al., 2013). Current results may be validated by using an inhibitor that selectively targets Akt1. The Akt1 is the main isoform involved in the PI3K/Akt pathway. The Akt-1 inhibitor, A-674563, is a good candidate for future studies as the inhibitor inhibits the cell proliferation more effectively than MK2206 (Chorner and Moorehead, 2018). The MK2206 was not significantly induced the G_1 arrest in non-small cell lung cancer (NSCLC) cell lines (A549, A427, and NCI-H23 cells), while A-674563 still cause the G_1 arrest in these cell lines.

Bacterial pathogens have been reported to manipulate the host PI3K/Akt pathway to alter the host cytoskeleton and membrane, reinforce focal adhesions, and internalisation (Krachler et al., 2011). *Pseudomonas aeruginosa* subverts the PI3K/Akt pathway to gain entry from the apical surfaces of the host cells (Kierbel et al., 2007). PI3K/Akt activity is also important for the internalisation of *Staphylococcus aureus* in Bovine endothelial cells via phosphorylation of GSK-3α, GSK-3β, and NF-κB (Oviedo-Boyso et al., 2011). So far, limited reports have been published on the meningococcal alteration of PI3K/Akt/GSK-3β/Cyclin D1/CDK4 pathway. However, Lambotin et al. reported that meningococci hijack the PI3K/Rac1 signalling pathway via meningococcal LOS to facilitate the bacterial uptake

(Lambotin et al., 2005). Also, meningococcal infection caused a downregulation of Akt (Schubert-Unkmeir et al., 2007).

Work described in the next chapter would aim to extend the study by investigating the effect of the abrogation of PorA-Loop4 in meningococcus on the Akt/GSK-3β/Cyclin D1/CDK4 pathway using wild-type and PorA-Loop4 deficient meningococcal strains.

Chapter 5 – Effects of abrogation of PorA-Loop4 in intact cells on the ability of *N. meningitidis* to alter the PI3K/Akt pathway

5.1 Introduction

In addition to PorA, Orihuela et al. showed that meningococcal PilQ also binds LAMR of HBMECs (Orihuela et al., 2009). PilQ is an essential component of type IV pili, which play a key role in bacterial binding to epithelial and endothelial cells (Virji et al., 1993). PilQ influences host cell signalling by stimulating a calcium signal (Kallstrom et al., 1998). Structurally, N-terminal domain of PilQ contains 4 to 7 copies of octapeptides, PAKQQAAA, termed small basic repeats (SBRs) which appear to influence the pilus expression (Tonjum et al., 1998). The C-terminal domain of PilQ contains 13 β-strands, which are embedded in the outer membrane (Bitter et al., 1998). The C-domain of PilQ is responsible for secretin oligomer formation and is conserved in Gram negative bacteria (Genin and Boucher, 1994). PilQ subunits form dodecameric complex structures that are extremely stable at high temperature and in the presence of denaturing agents such as SDS. The PilQ complex forms a channel through which the moving pilus fiber is extended and retracted from the bacterial surface (Frye et al., 2006). MDAΦ, an 8 kb genomic island from certain hypervirulent lineages of the meningococcus, has the characteristics of a filamentous prophage which is secreted using PilQ (Meyer et al., 2016).

The deletion of PorA and PilQ abrogates recruitment of laminin receptor under meningococcal colonies. Synthetic peptides corresponding to PorA-Loop4 bound LAMR and could block LAMR-binding to bacterial ligands in a dose-dependent manner (Abouseada et al., 2012). When both *porA* and *pilQ* were inactivated in *N. meningitidis* MC58, recombinant LAMR (rLR) binding was significantly reduced compared to the wild type ($p \leq 0.01$) (Abouseada et al., 2012). Amino acids 197-210 (Loop4) of PorA confer the rLR-binding activity, as the MC58 mutant lacking these amino acids ($PorA^{\Delta 197-210}$) and PilQ failed to bind to rLR.

The abrogation of PorA-Loop4 and PilQ did not interfere with the expression of PorA or the ability of the protein to correctly localise to the meningococcal outer membrane (Abouseada et al., 2012). Immunoblot of cell fractions confirmed the presence of PorA in MC58 ΔPorA-Loop4 ΔPilQ at similar levels to PorA in MC58 wild-type in outer membrane-enriched sub-cellular fractions. In addition, a mouse monoclonal antibody directed against PorA-Loop1 (P1.7) bound to the surface of MC58 wild-type or MC58 ΔPorA-Loop4 ΔPilQ at similar levels as observed by confocal microscopy, but not to MC58 ΔPorA ΔPilQ.

Subsequently, Alqahtani et al. showed evidence that PorA preferentially targets the 37LRP isoform of LAMR in a dimer form with Gal-3 (Alqahtani et al., 2014). The binding region of PorA-Loop4 on 37LRP was in the region of amino acids 263-282 in the C-terminal end of the protein (Alqahtani et al., 2014, Qarani, 2015).

A study by Vassey also quantified the co-localisation of the wild-type strain *N. meningitidis* MC58 and MC58 ΔPorA-Loop4 in the HBMECs (Vassey, 2014). The analysis of immunofluorescence images showed that the wild-type strain were found to co-localise significantly more with 37LRP than 67LR (71% and 58%, respectively; $p \leq 0.0001$). Additionally, pre-incubation of HBMECs with 37LRP-specific antibody reduced invasion of the wild-type strain by 25%, whereas the 67LR-specific antibody had no effect. Quantification of the co-localisation coefficient showed that recruitment of 67LR to *N. meningitidis* MC58 was not affected by deletion of PorA-Loop4. However, the ability of this mutant to recruit and bind 37LRP under its colonies was significantly reduced ($p \leq 0.0001$). These findings suggest an important role of PorA-Loop4 in particular, in the host-pathogen interaction.

Bacterial porins have been known to play important roles in host-pathogen interactions and the surface exposed loops of porins facilitate the binding of the bacteria to the host cells. Recent studies have shown that these loops were involved in the binding and signalling during adhesion and internalisation. In *H. influenzae*, Vitiello et al. reported that Loop L7 of porin P2 induced the MEK1-MEK2/MAPK phosphorylation in human astroglioma cells (U87-MG) and upregulated the cellular adhesion molecules and IL-6 production (Vitiello et al., 2011). Similarly, in *E. coli,* loop 1, 2 and 3 of porin OmpA were shown to mediate entry of the bacteria to HBMEC via the host receptor cPLA2α (Maruvada and Kim, 2011). In the meningococcus, a study by Kattner et al. showed that loop7 of PorB (serogroup W) mediates the binding to TLR2 (Kattner et al., 2014).

The Meningitis Research Foundation UK has been collating a genome database for all meningococcal disease isolates in England, Wales and Northern Ireland. There are 1,381 meningococcal genomes in the database of 2010-2015 and of these, there are 132 unique PorA sequences. These sequences are used to identify and subgroup the meningococci.

Although PorA is highly variable among strains, interaction of PorA and LAMR is not specific to PorA subtype (Vassey, 2014). In a previous study, nine major whole PorA molecules expressed by invasive serogroup B meningococci in the UK (Pfizer), were tested for their ability to bind

recombinant LAMR in ELISA assays, and no significant differences in LAMR binding were observed ($p>0.05$) (Vassey, 2014). The nine PorA variants used in the study occurred in 41.99% of invasive meningococcal isolates subtyped in UK from 2010-2013. These variants differed in sequence in the variable region 1 (Loop1) as well as the variable region 2 (Loop4) suggesting a significance in the tertiary structure for protein-protein interactions with the host LAMR.

5.2 Aims

In previous chapters, exposure of HBMECs to the PorA-Loop4 peptide caused the perturbation on the pAkt (Ser473), pGSK-3β (Ser9), Cyclin D1, and pCDK4 (Thr172) expression in the PI3K/Akt signalling pathway. Given that PorA and PilQ are specific ligands of LAMR and play important roles in the host-pathogen interaction, the aim of this chapter is to investigate the effect of the abrogation of PorA-Loop4, PorA, PorA-Loop4 PilQ, and PorA PilQ on pAkt (Ser473), pGSK-3β (Ser9), Cyclin D1, and pCDK4 (Thr172) expression in HBMECs. It is also our aim to determine the localisation of pAkt (Ser473), pGSK-3β (Ser9), Cyclin D1, and pCDK4 (Thr172) with respect to adherent or internalised meningococci on HBMECs by confocal microscopy.

5.3 The protein expressions of pAkt (Ser473), pGSK-3β (Ser9), Cyclin D1, and pCDK4 (Thr172) in infected HBMECs

To study the effect of abrogation of PorA-Loop4, PorA, and PilQ on pAkt (Ser473), pGSK-3β (Ser9), Cyclin D1, and pCDK4 (Thr172) expression, HBMECs were infected with *N. meningitidis* wild-type MC58 and its isogenic strains of ΔPorA-Loop4, ΔPorA, ΔPorA-Loop4 ΔPilQ, and ΔPorA ΔPilQ. All strains were obtained from previous study (Abouseada, 2010). All mutants retained wild-type growth rates (data not shown).

First, the engineered mutations in the isolates from stocks were confirmed. Lysates of infected cells were separated by SDS-PAGE, transferred into a nitrocellulose membrane and probed with anti-PorA-Loop4 (P1.16), anti-PorA, and anti-PilQ. Colorimetric detection was used for this purpose. The blots were probed with secondary antibody conjugated to alkaline phosphatase and subsequently exposed with BCIP/NBT as the precipitating substrate. The blot images are presented in Figure 5.1.

The strains used were confirmed as ΔPorA-Loop4, ΔPorA, ΔPorA-Loop4 ΔPilQ, and ΔPorA ΔPilQ. Only wild-type sample showed band at *ca.* 42 kDa in the blot probed with anti-PorA-Loop4 (Figure 5.1 A). The wild type, ΔPorA-Loop4, and ΔPorA-Loop4 ΔPilQ showed bands at *ca.* 42 kDa in the blot probed with anti-PorA (Figure 5.1 B). These results were expected as the 42-kDa reactive protein agrees with the known molecular mass of PorA (Derrick et al., 1999).

The wild type, ΔPorA-Loop4, ΔPorA-Loop4, and ΔPorA showed bands at *ca.* 83 kDa in the blot probed with anti-PilQ (Figure 5.1 C) which is consistent with the expected size of the PilQ monomer (Collins et al., 2001). Three less abundant proteins of 72, 55, and 43 kDa reacted with the anti-PilQ antisera in extracts of ΔPorA-Loop4 and ΔPorA samples, and presumably represent degradation products of PilQ (Burkhardt et al., 2011). Other bands detected in extracts of ΔPorA-Loop4 ΔPilQ and ΔPorA ΔPilQ cells were non-specific proteins that reacted to the polyclonal anti-PilQ.

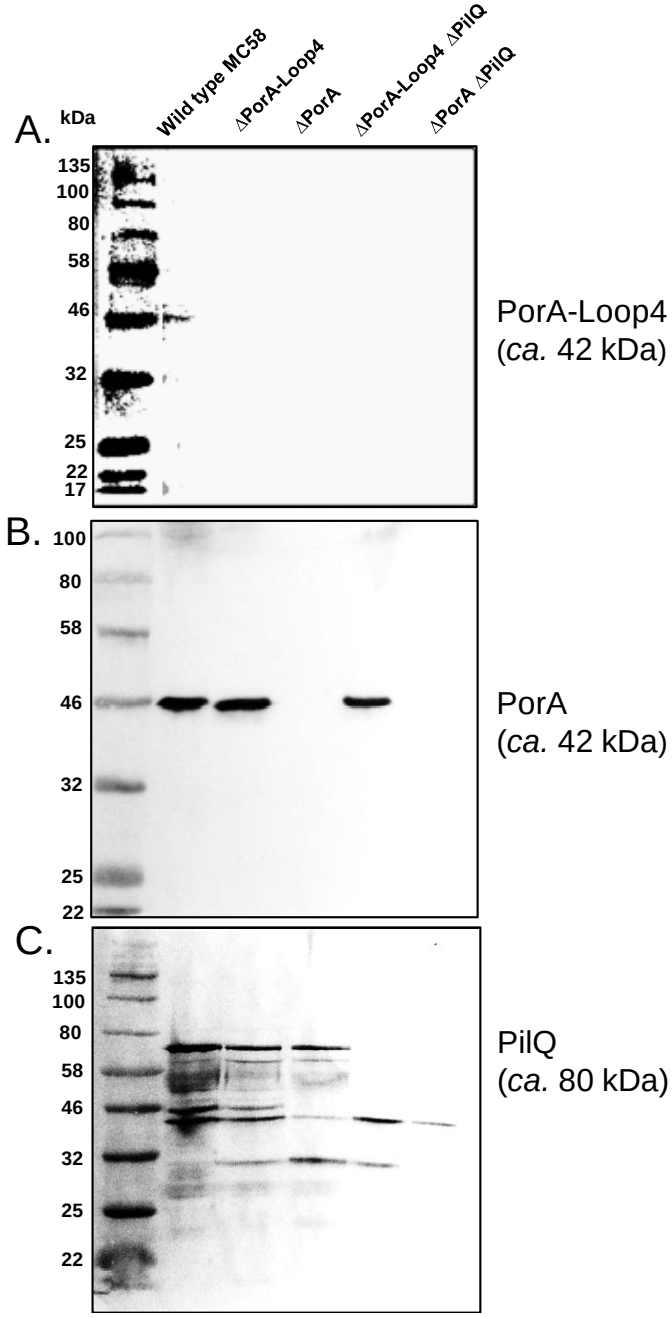

Figure 5.1: Immunoblot confirmation of isogenic strains of *N. meningitidis* MC58. Bacteria were grown overnight in BHI broth. Samples were lysed in sample buffer and then separated on a 10% Tris-Glycine SDS-PAGE. After transfer to nitrocellulose membrane, blots were probed with (A) anti-PorA-Loop4 (P1.16) (1:1000), (B) anti-PorA (1:1000) or (C) anti-PilQ (1:1000). Subsequent detection was carried out with anti-mouse IgG-alkaline phosphatase conjugate (1:10,000) or anti-rabbit IgG-alkaline phosphatase conjugate (1:10,000).

Immunoblotting and densitometry analysis were performed to study the perturbation of pAkt (Ser473), pGSK-3β (Ser9), Cyclin D1, and pCDK4 (Thr172) expression at the protein level. Lysates from the infected HBMECs were loaded onto acrylamide gels for either staining or immunoblotting with specific antibodies of each protein. Figure 5.2 shows the stained gels illustrating that approximately equal amount of protein were loaded for each samples used in this section. Representative images of blots and the densitometry analysis of pAkt (Ser473), pGSK-3β (Ser9), Cyclin D1, and pCDK4 (Thr172) expression are presented in Figure 5.3, Figure 5.4, Figure 5.5, Figure 5.6, respectively.

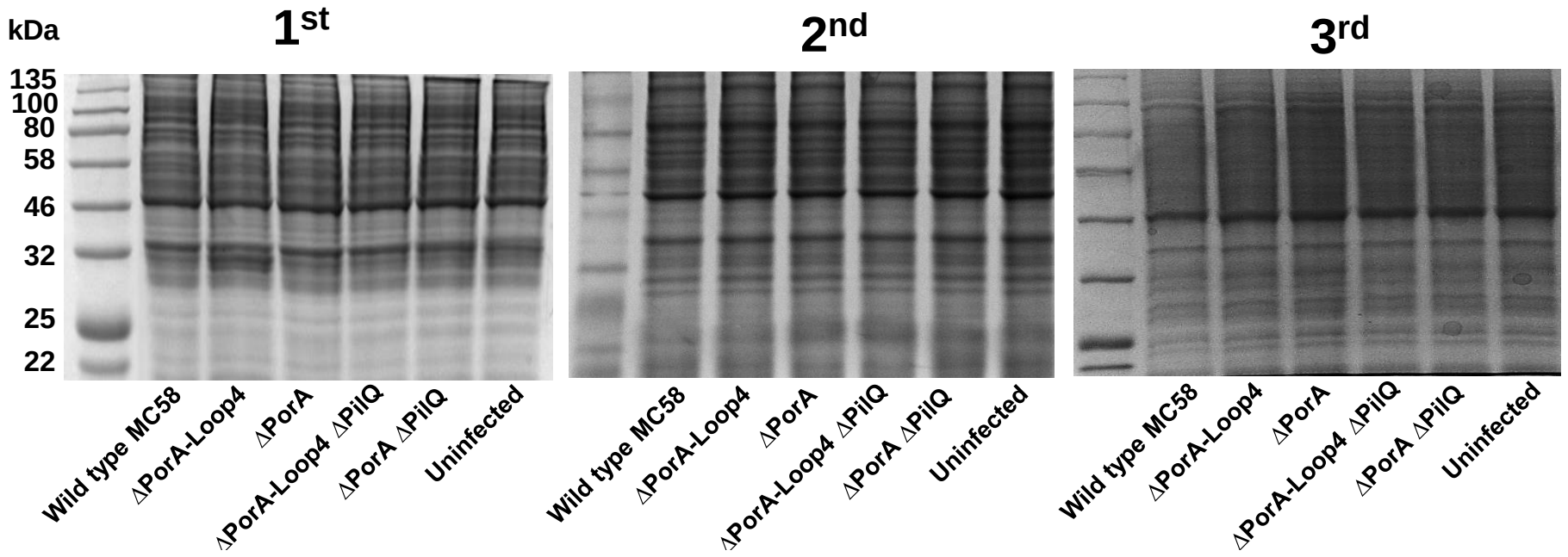

Figure 5.2: SDS-PAGE of lysates from infected HBMECs. Protein lysates were separated on 10% acrylamide gels. Images were obtained from three independent experiments (1st-3rd).

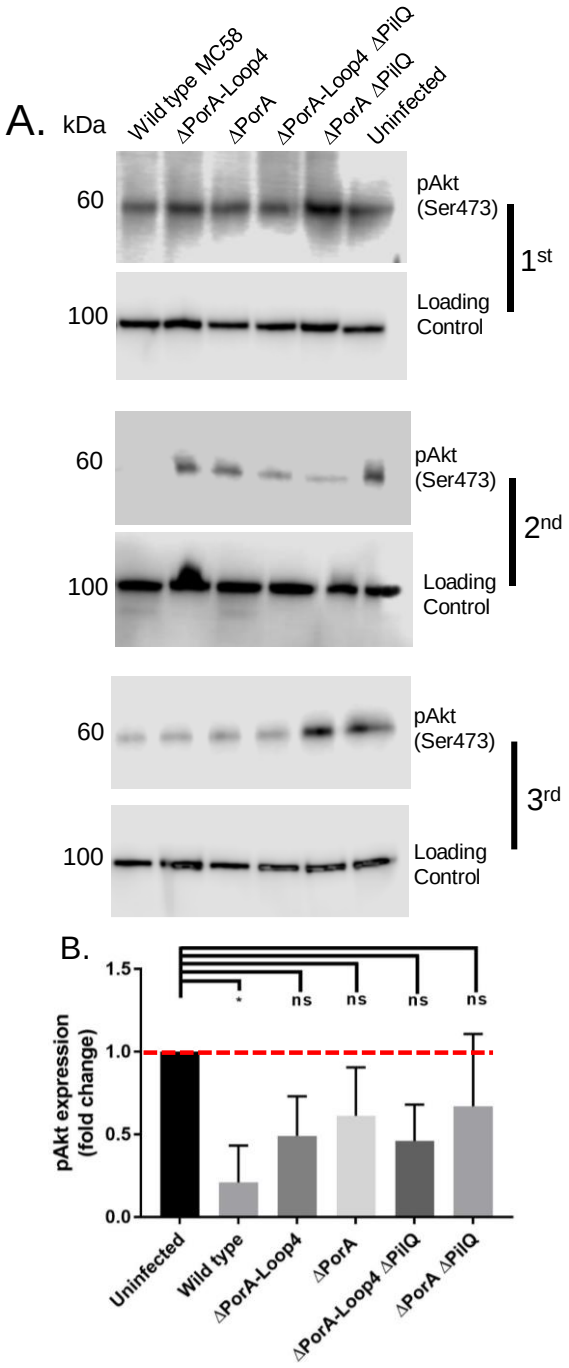

Figure 5.3: Immunoblot images (A) and densitometry analysis (B) of pAkt (Ser473) level in infected-HBMECs. HBMECs were infected with either *N. meningitidis* wild-type MC58 or its mutants (ΔPorA-Loop4, ΔPorA, ΔPorA-Loop4 ΔPilQ, ΔPorA ΔPilQ) at MOI 100. The HBMECs were left to associate with the bacteria for 8 h and lysed. Representative images were obtained from three independent experiments (1^{st}-3^{rd}). Alpha actinin was used as loading control in all immunoblots. Band intensities were quantified by Image J software. All data were normalised to the uninfected as the control and adjusted to the loading control densities. Significant difference compared to the uninfected cells are indicated (*p≤0.05, ns: not significant, one-way ANOVA Dunnet's test applied post hoc).

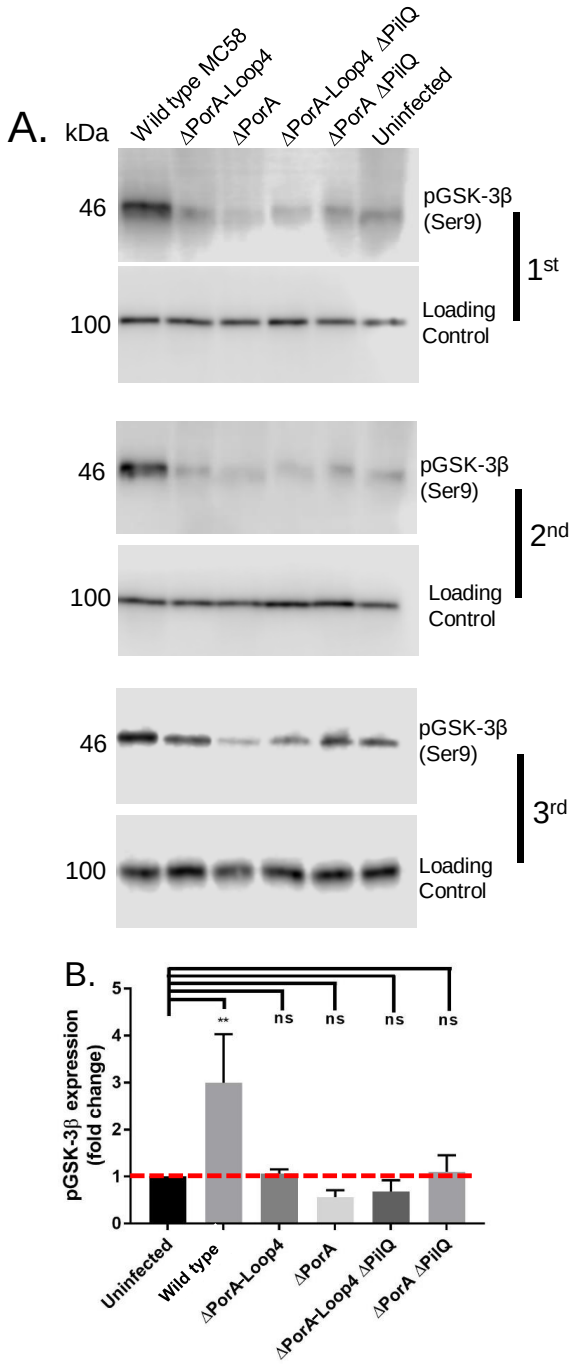

Figure 5.4: Immunoblot images (A) and densitometry analysis (B) of pGSK-3β (Ser9) level in infected-HBMECs. HBMECs were infected with either *N. meningitidis* wild-type MC58 or its mutants (ΔPorA-Loop4, ΔPorA, ΔPorA-Loop4 ΔPilQ, ΔPorA ΔPilQ) at MOI 100. The HBMECs were left to associate with the bacteria for 8 h and lysed. Representative images were obtained from three independent experiments (1^{st}-3^{rd}). Alpha actinin was used as loading control in all immunoblots. Band intensities were quantified by Image J software. All data were normalised to the uninfected as the control and adjusted to the loading control densities. Significant difference compared to the uninfected cells are indicated (**p≤0.01, ns: not significant, one-way ANOVA Dunnet's test applied post hoc).

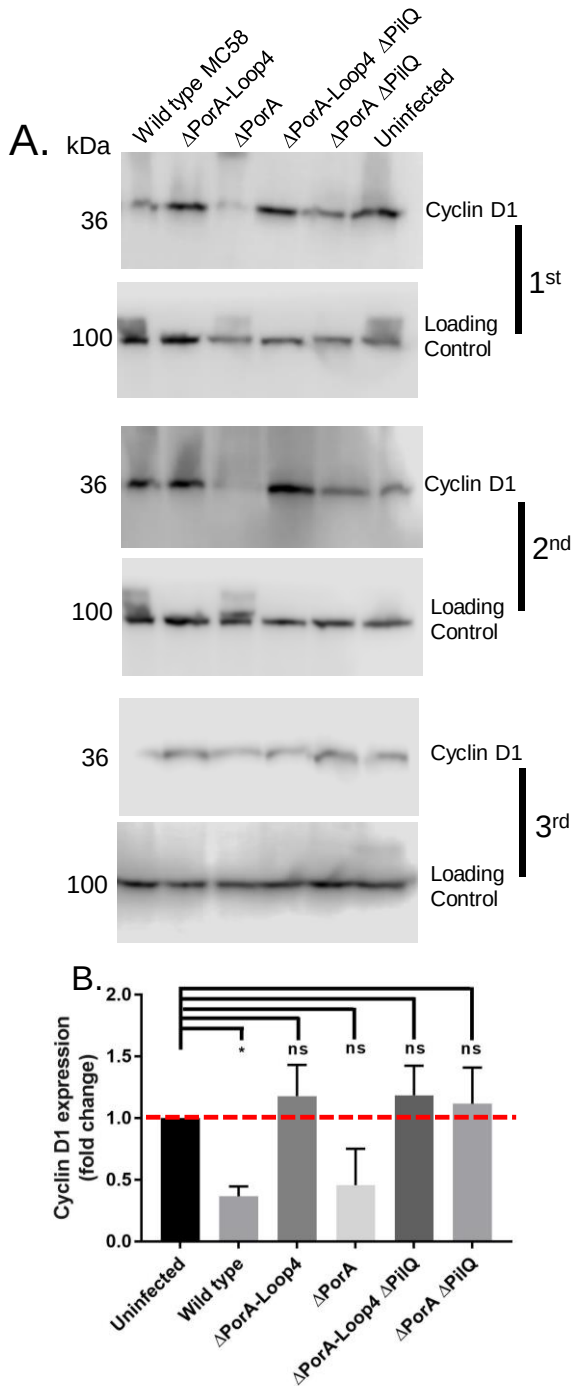

Figure 5.5: Immunoblot images (A) and densitometry analysis (B) of Cyclin D1 expression in infected-HBMECs. HBMECs were infected with either *N. meningitidis* wild-type MC58 or its mutants (ΔPorA-Loop4, ΔPorA, ΔPorA-Loop4 ΔPilQ, ΔPorA ΔPilQ) at MOI 100. The HBMECs were left to associate with the bacteria for 8 h and lysed. Representative images were obtained from three independent experiments (1st-3rd). Alpha actinin was used as loading control in all immunoblots. Band intensities were quantified by Image J software. All data were normalised to the uninfected as the control and adjusted to the loading control densities. Significant difference compared to the uninfected cells are indicated (*p≤0.05, ns: not significant, one-way ANOVA Dunnet's test applied post hoc).

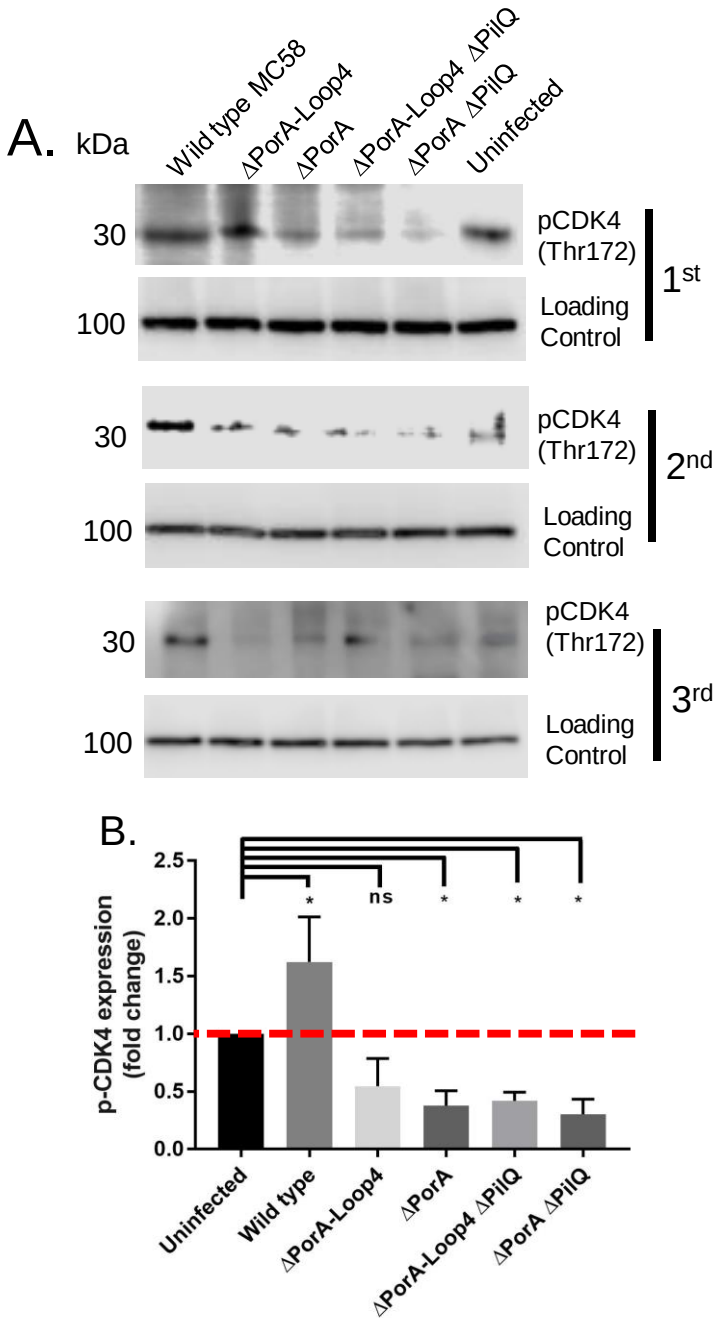

Figure 5.6: Immunoblot images (A) and densitometry analysis (B) of pCDK4 (Thr172) level in infected-HBMECs. HBMECs were infected with either *N. meningitidis* wild-type MC58 or its mutants (ΔPorA-Loop4, ΔPorA, ΔPorA-Loop4 ΔPilQ, ΔPorA ΔPilQ) at MOI 100. The HBMECs were left to associate with the bacteria for 8 h and lysed. Representative images were obtained from three independent experiments (1st-3rd). Alpha actinin was used as loading control in all immunoblots. Band intensities were quantified by Image J software. All data were normalised to the uninfected as the control and adjusted to the loading control densities. Significant difference compared to the uninfected cells are indicated (*p≤0.05, ns: not significant, one-way ANOVA Dunnet's test applied post hoc).

Table 5.1 represents the summary of perturbation of pAkt (Ser473), pGSK-3β (Ser9), Cyclin D1, and pCDK4 (Thr172) after HBMECs were treated with the peptide of PorA-Loop4 (results of Chapter 3 and 4) and after HBMECs were infected with the wild-type MC58 and its derivative mutants (ΔPorA-Loop4, ΔPorA, ΔPorA-Loop4 ΔPilQ and ΔPorA ΔPilQ). Similar changes in expression of pAkt (Ser473), pGSK-3β (Ser9), Cyclin D1, and pCDK4 (Thr172) were observed in cells infected with wild-type meningococci as were previously observed in cells treated with synthetic PorA-Loop4.

Table 5.1: The perturbation of key proteins' expression in the PI3K/Akt pathway after HBMECs were treated with the peptide of PorA-Loop4, or infected with the wild-type MC58 and its mutants (ΔPorA-Loop4, ΔPorA, ΔPorA-Loop4 ΔPilQ and ΔPorA ΔPilQ). +: upregulated, - : downregulated, ns: not significant to the untreated/uninfected cells.

	PorA-Loop4	Wild type	ΔPorA-Loop4	ΔPorA	ΔPorA-Loop4 ΔPilQ	ΔPorA ΔPilQ
pAkt (Ser473)	-	-	ns	ns	ns	ns
pGSK-3β (Ser9)	+	+	ns	ns	ns	ns
Cyclin D1	-	-	ns	ns	ns	ns
pCDK4 (Thr172)	+	+	ns	-	-	-

In cells infected with the wild-type *N. meningitidis* MC58, levels of pAkt (Ser473) were significantly reduced compared to uninfected cells ($p \leq 0.05$). By contrast, in cells infected with mutants lacking either PorA or PorA-Loop4, either alone or combined with a PilQ mutation, pAkt (Ser473) levels did not differ significantly from uninfected cells ($p > 0.05$).

The levels of pGSK-3β (Ser9) were increased in cells infected with the wild type ($p \leq 0.01$). By contrast, the levels of pGSK-3β (Ser9) in the cells infected with ΔPorA-Loop4, ΔPorA, ΔPorA-Loop4 ΔPilQ, and ΔPorA ΔPilQ did not differ significantly from uninfected cells ($p > 0.05$).

The downregulation of Cyclin D1 ($p \leq 0.05$) was observed in cells infected with the wild type. However, Cyclin D1 expression in the cells infected with ΔPorA-Loop4, ΔPorA, ΔPorA-Loop4 ΔPilQ, and ΔPorA ΔPilQ did not differ significantly from uninfected cells ($p > 0.05$). Overall, the data

suggest that PorA has a role in the perturbation of pAkt (Ser473), pGSK-3β (Ser9), and Cyclin D1.

The levels of pCDK4 (Thr172) were increased in cells infected with the wild type ($p \leq 0.05$), while the levels pCDK4 (Thr172) in cells infected with the ΔPorA-Loop4 did not differ significantly from uninfected cells ($p > 0.05$). However, cells infected with ΔPorA, ΔPorA-Loop4 ΔPilQ, and ΔPorA ΔPilQ had a decrease level of pCDK4 (Thr172) which were the opposite from cells infected with the wild type. These data showed that the upregulation the pCDK4 (Thr172) was caused mainly by the Loop4, not by other parts of the PorA nor by PilQ.

5.4 Localisation of pAkt (Ser473), pGSK-3β (Ser9), Cyclin D1, and pCDK4 (Thr172) in the infected HBMECs

The data described above suggested that the exposure of HBMECs to PorA-Loop4 peptide or infection of these cells with wild-type *N. meningitidis* MC58 caused similar perturbation of levels of pAkt (Ser473), pGSK-3β (Ser9), Cyclin D1, and pCDK4 (Thr172). These effects were not observed however, in cells infected with meningococcal mutants lacking either PorA or PorA-Loop4. To confirm these results, the localisation of pAkt (Ser473), pGSK-3β (Ser9), Cyclin D1, and pCDK4 (Thr172) were observed in the uninfected cells, and cells infected with the wild type and ΔPorA-Loop4 using confocal microscopy.

Cells were grown up on coverslips, associated with either *N. meningitidis* MC58 wild type or MC58 ΔPorA-Loop4 at MOI of 100 for 8 h. The infected cells were then fixed and stained for each investigated protein (Alexa Fluor, red) and DNA content (DAPI, blue). The fluorescence pattern across the cell surface were then imaged using confocal microscopy Zeiss LSM700 (63x objective, scale bar = 50 μm). The uninfected cells was also monitored as control. Representative images for pAkt (Ser473), pGSK-3β (Ser9), Cyclin D1, and pCDK4 (Thr172) are shown in Figure 5.7, Figure 5.8, Figure 5.9, and Figure 5.10, respectively. The images were obtained from three independent experiments.

Figure 5.7 shows the diffuse pattern of pAkt (Ser473) which primarily localised in the cytoplasmic regions. Cells infected with the wild type exhibited less overall fluorescence than uninfected cells, while cells infected with the PorA-Loop4 mutant strain displayed a similar pattern to uninfected cells. These images confirmed the immunoblots results as the wild type caused the downregulation of pAkt (Ser473), while the mutational loss of PorA-Loop4 abrogated the effect caused by wild-type meningococci.

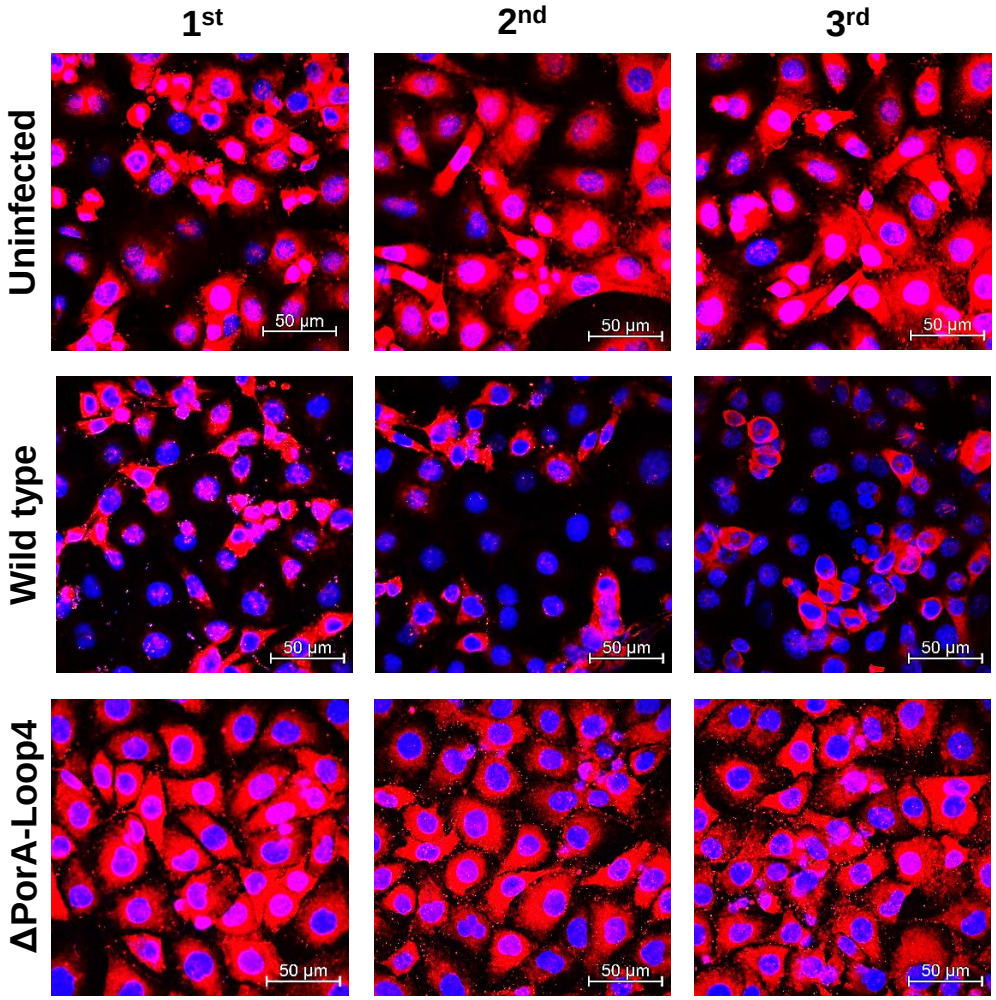

Figure 5.7: Immunofluorescence microscopy of pAkt (Ser473) in the uninfected, MC58 wild-type-infected, and ΔPorA-Loop4-infected HBMECs. HBMECs were associated with either *N. meningitidis* MC58 wild type or MC58 ΔPorA-Loop4 at MOI of 100 for 8 h. The infected monolayers on coverslips were fixed with 4% paraformaldehyde and stained with anti-pAkt (Ser473) (193H12, 1:200) followed by secondary Alexa antibody (Alexa 680, red). Coverslips were mounted with ProLong Gold anti-fade with DAPI (blue). Images were acquired using a Zeiss LSM700. Representative images were obtained from three independent experiments (1^{st}-3^{rd}). Scale bar = 50 µm.

Figure 5.8 shows a diffuse pattern of the pGSK-3β (Ser9), which localised in the cytoplasmic regions. Cells infected with the wild type exhibited more overall fluorescence, although the pattern of fluorescence was similar to that seen in uninfected cells. Cells infected with the PorA-Loop4 mutant strain displayed a similar pattern and overall fluorescence levels to those observed in the uninfected cells.

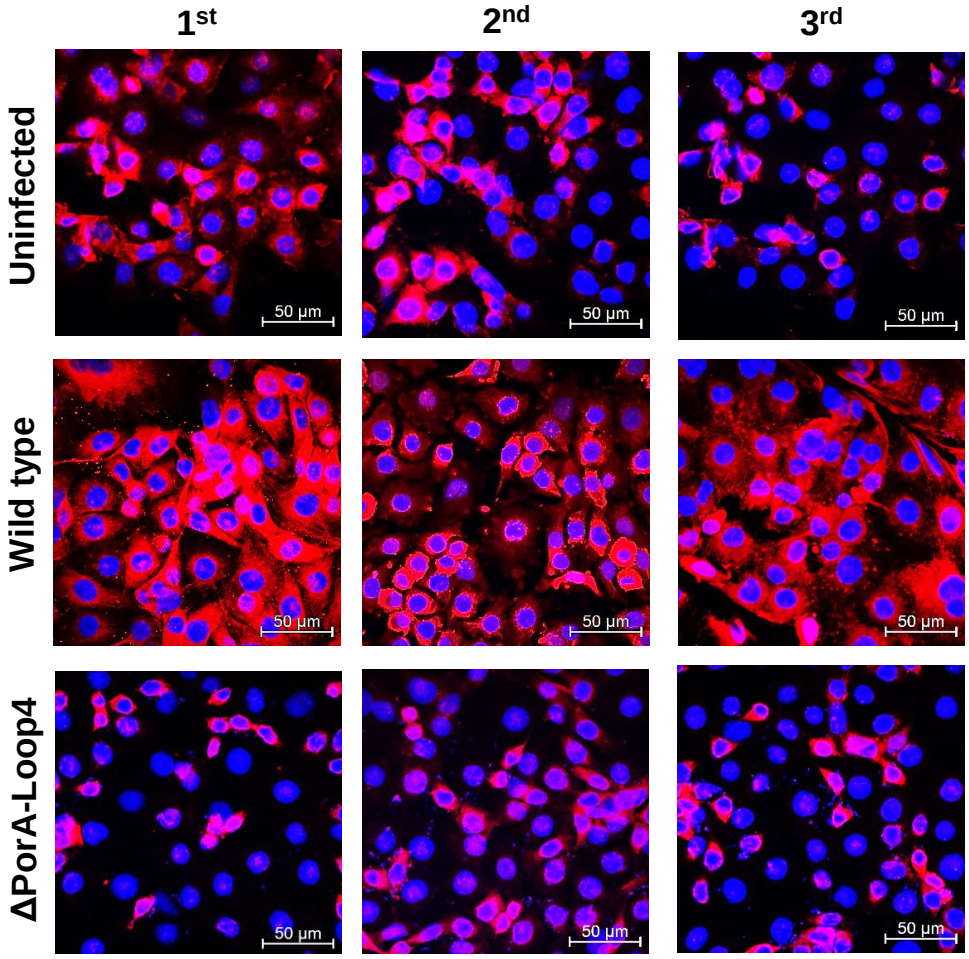

Figure 5.8: Immunofluorescence microscopy of pGSK-3β (Ser9) in the uninfected, MC58 wild-type-infected, and ΔPorA-Loop4-infected HBMECs. HBMECs were associated with either *N. meningitidis* MC58 wild type or MC58 ΔPorA-Loop4 at MOI of 100 for 8 h. The infected monolayers on coverslips were fixed with 4% paraformaldehyde and stained with anti-pGSK-3β (Ser9) (D3A4, 1:200) followed by secondary Alexa antibody (Alexa 680, red). Coverslips were mounted with ProLong Gold anti-fade with DAPI (blue). Images were acquired using a Zeiss LSM700. Representative images were obtained from three independent experiments (1^{st}-3^{rd}). Scale bar = 50 µm.

Figure 5.9 shows diffuse pattern of Cyclin D1 which primarily localised in the cytoplasmic regions. Cells infected with wild-type meningococci showed very little cytoplasmic Cyclin D1. By contrast, cells infected with the PorA-Loop4 mutant strain displayed similar pattern to the uninfected cells.

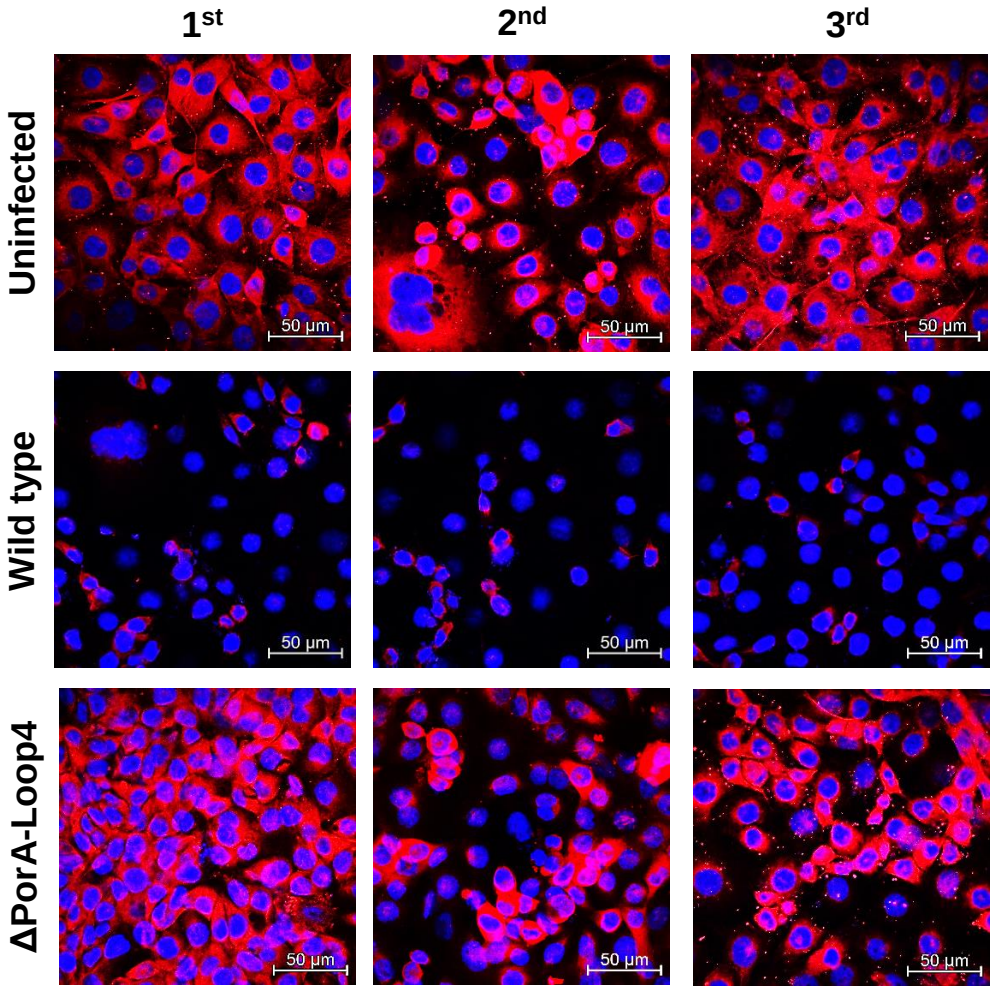

Figure 5.9: Immunofluorescence microscopy of Cyclin D1 in the uninfected, MC58 wild-type-infected, and ΔPorA-Loop4-infected HBMECs. HBMECs were associated with either *N. meningitidis* MC58 wild type or MC58 ΔPorA-Loop4 at MOI of 100 for 8 h. The infected monolayers on coverslips were fixed with 4% paraformaldehyde and stained with anti-Cyclin D1 (N1C3, 1:500) followed by secondary Alexa antibody (Alexa 680, red). Coverslips were mounted with ProLong Gold anti-fade with DAPI (blue). Images were acquired using a Zeiss LSM700. Representative images were obtained from three independent experiments (1^{st}-3^{rd}). Scale bar = 50 µm.

Figure 5.10 shows the diffuse pattern of pCDK4 (Thr172). The localisation were observed in cytoplasmic and nuclear regions. Cells infected with the wild type showed the higher diffuse pattern of pCDK4 (Thr172) and spread into the cytoplasmic regions. The cells infected with the PorA-Loop4 mutant strain displayed similar pattern to the uninfected cells.

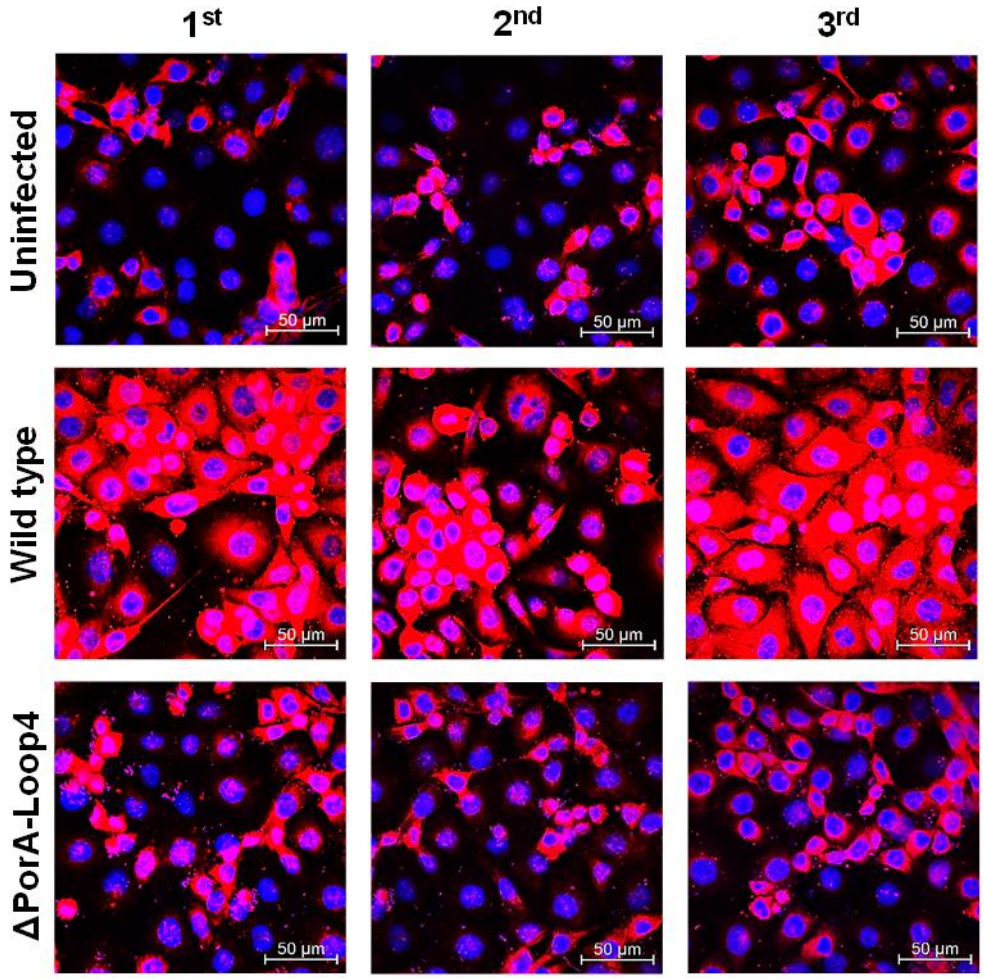

Figure 5.10: Immunofluorescence microscopy of pCDK4 (Thr172) in the uninfected, MC58 wild-type-infected, and ΔPorA-Loop4-infected HBMECs. HBMECs were associated with either *N. meningitidis* MC58 wild type or MC58 ΔPorA-Loop4 at MOI of 100 for 8h. The infected monolayers on coverslips were fixed with 4% paraformaldehyde and stained with anti-pCDK4 (Thr172) (PA5-64482, 1:300) followed by secondary Alexa antibody (Alexa 680, red). Coverslips were mounted with ProLong Gold anti-fade with DAPI (blue). Images were acquired using a Zeiss LSM700. Representative images were obtained from three independent experiments (1^{st}-3^{rd}). Scale bar = 50 µm.

Overall, the observation from confocal microscopy confirmed the previous immunoblotting results. However, there were no specific localisation of the four investigated proteins surrounding the bacterial colonies.

5.5 Discussion

In the previous chapter, it was shown that the PorA-Loop4 peptide caused the perturbation of PI3K/Akt pathway via Akt/GSK-3β/Cyclin D1/CDK4. Here, intact bacterial cells were used; the *N. meningitidis* MC58 wild type and its isogenic strains (ΔPorA-Loop4, ΔPorA, ΔPorA-Loop4 ΔPilQ, and ΔPorA ΔPilQ) were used to infect HBMECs and levels of Akt/GSK-3β/Cyclin D1/CDK4 were determined after infection. All strains were obtained from the previous study (Abouseada, 2010). All mutants retained the wild-type growth rates (data not shown).

However, spontaneous mutation could cause other phenotypic changes in meningococci. Such changes might affect the interaction between meningococcal PorA and LAMR on the surface of HBMECs. The abrogation of PorA-Loop4 did not perturb the expression of PorA or the ability of the protein to correctly localise to the meningococcal outer membrane (Abouseada et al., 2012). However, the encapsulation assays for the mutants have not been performed and possible effects of changes in expression of this phase-variable surface component on LAMR binding cannot therefore be completely ruled out.

The binding of *N. meningitidis* MC58 wild type and ΔPorA-Loop4 to each isoform of LAMR, 37LRP or 67LR, have been quantified in previous study using immunofluorescence microscopy (Vassey, 2014). The data showed that the abrogation of PorA-Loop4 reduced the recruitment of 37LRP. However, the binding of other isogenic strains to the two isoforms have not been assessed. Future studies are required to confirm the interaction of each isogenic strain to 67LR or 37LRP due to its possible phenotypic changes.

Similar perturbation of pAkt (Ser473), pGSK-3β (Ser9), Cyclin D1, and pCDK4 (Thr172) were observed in PorA-Loop4 treated cells and cells infected with wild-type meningococci, demonstrating that the PorA-Loop4 effects were not an artefact of the synthetic peptide. The PorA-Loop4 mutant infected cells did not show any significant perturbation compared to uninfected cells, demonstrating that the effect observed in HBMECs treated with wild-type meningococci was mediated by PorA-Loop4. These findings

suggest that the PorA-Loop4 has a significant role in causing the perturbation of these key proteins involved in the PI3K/Akt pathway. As PorA-Loop4 preferentially binds to 37LRP, the PorA-Loop4:37LRP interaction may block this pathway thus causing perturbation in Akt, GSK-3β, Cyclin D1, and CDK4.

Both meningococcal PorA and PilQ bind to LAMR in HBMECs (Orihuela et al., 2009). PilQ supports the meningococcal binding to the host cells by its interaction with 37LRP and Gal-3 (Figure 1.8) (Alqahtani et al., 2014). While PilQ is known to bind to LAMR, the data presented here indicate that only PorA, and specifically its fourth extracellular loop, mediate the observed effects on the PI3K/Akt pathway via Akt/GSK-3β/Cyclin D1.

However, the perturbation of pCDK4 (Thr172) was quite different from the other investigated proteins. HBMECs infected with ΔPorA-Loop4 showed unaltered expression of pCDK4 (Thr172) compared to uninfected cells. While HBMECs infected with ΔPorA, ΔPorA-Loop4 ΔPilQ, and ΔPorA ΔPilQ caused the downregulation of pCDK4 (Thr172) which are the opposite from the effect caused by the wild type. It suggest that the upregulation the pCDK4 (Thr172) was caused by the Loop4, not by other parts of the PorA nor by the PilQ. The reason for the observed reduction of pCDK4 (Thr172) in the mutant cells lacking PorA-Loop4 is not clear.

In this study, pAkt (Ser473) was mainly observed in the cytoplasmic regions. The phosphorylation of Akt at Ser473 by mTORC2 occurs in the plasma membrane (Manning and Toker, 2017), but recent reports provided evidence that there were endomembrane pools of PIP3 and PI3,4P2 in the cytoplasmic regions that directly contribute to Akt activation (Manning and Toker, 2017, Jethwa et al., 2015). The meningococcal infection to HBMECs lead to depletion of the pAkt (Ser473) in the membrane, as the diffuse pattern in the wild-type infected cells were localised nearer to the nuclear regions. The termination of Akt signalling involves PHLPP to dephosphorylate Akt directly at Ser473, resulting in inhibition of kinase activity and promotion of apoptosis (Manning and Toker, 2017, Gao et al., 2005). As there was no observed localisation of pAkt (Ser473) surrounding bacterial colonies, it is possible that meningococci stimulate PHLPP to dephosphorylate Akt.

The pGSK-3β (Ser9) was also observed throughout the cytoplasm. This was expected as the GSK-3β has traditionally been considered to be largely a cytosolic protein (Beurel et al., 2015). However, GSK-3β is also present within the nucleus (Bijur and Jope, 2001).

The Cyclin D1 was also observed throughout the cytoplasm. Cyclin D1 does not contain a nuclear localisation signal (NLS) and its sequestration

may result in accumulation within the cytoplasm (Alao, 2007). Cytoplasmic Cyclin D1 is transported into the nucleus in association with CDK4 and possibly various transcription factors (Alao, 2007). In this study, in wild-type infected cells cytoplasmic Cyclin D1 was greatly reduced. It is possible that the cytoplasmic Cyclin D1 was degraded, and meningococci might possibly stimulate proteins which degrade the Cyclin D1 (e.g. Dyrk1B).

The pCDK4 (Thr172) was observed in the nuclear and cytoplasmic regions. CDK4 in complex with Cyclin D1 is phosphorylated at Thr172 by CAK which localises to the nucleus (Diehl and Sherr, 1997). Although the Cyclin D1/CDK4 complex does not contain an NLS, their nuclear location has been shown to depend on their association with Cip/Kip family proteins (p21 and p27), which possess a classical bipartite nuclear localisation signal (Reynisdottir and Massague, 1997). However, Bockstaele et al found that subcellular localisation of CDK4 does not affect its Thr172 phosphorylation (Bockstaele et al., 2006b). The nuclear translocation of CDK4 is not the rate-limiting step of CDK4 phosphorylation by nuclear CAK. They found similar proportions of nuclear and cytoplasmic pCDK4 (Thr172) bound to p27.

It is conceivable that the observed changes in signalling proteins may occur at the site of meningococcal microcolony formation. This might have indicated that signalling complexes occurred containing these proteins. Immunofluorescence data, however, show no evidence of this and the signalling molecules were observed throughout the cytoplasm. This might be explained by events occurring at the site of meningococcal attachment, followed by diffusion of the signalling molecules, or alternatively, by changes in as yet unidentified signalling molecules lying upstream of the molecules under study.

In the previous study, the exposure of PorA-Loop4 caused a decrease of cells in the S phase by 24%, and an increase in the G_1 by 23% (Vassey, 2014). However, the immunofluorescence images in current results suggest that more cells are expressing the target proteins so are affected by the PorA-Loop4. The Loop4 may cause a more generalised effect on pAkt (Ser473), pGSK-3β (Ser9), Cyclin D1, pCDK4 (Thr172) as shown by changes in protein localisation, but then fewer cells actually going into cell cycle arrest. This may be due to variation in LAMR receptor expression or another step required to trigger cell cycle arrest.

The heterologous expression of PorA-Loop4 in meningococcal strains should also be considered in future studies. The discrepancies in some assays

for the effects of deletion of PorA-Loop4 or the whole of PorA could be clarified by adding PorA-Loop4 peptide to the mutant-infected cells. This would reveal if there are differences between the effects of the synthetic peptide and the native meningococcal PorA-Loop4 on HBMECs.

So far, the physiological relevance between the peptide concentration and the amount of PorA present on the bacterial surface has not been estimated. The expression level of PorA on the surface of *N. meningitidis* strain MC58 has not been assessed. Also, the data is not available from other reports. It should be noted that PorA is subject to phase variation. Since expression of the *porA* gene may vary over time, the peptide concentration used in assays may not always represent the amount of native PorA expressed on the surface of meningococci.

Chapter 6 – General Discussion

6.1 Study Objectives

The work described in this thesis aimed to explore the possible intracellular pathways influenced by the meningococcal PorA-Loop4 following its interaction with the 37LRP in HBMECs. Specifically, this work focused on the perturbations of levels of key proteins in the PI3K/Akt pathway (including Akt, GSK-3β, Cyclin D1, and CDK4) caused by the treatment of PorA-Loop4 peptide in HBMECs.

6.2 Main findings

The exposure of HBMECs to PorA-Loop4 peptide caused a decreased level of Cyclin D1 and increased level of CDK4 at mRNA level. The PorA-Loop4 peptide also caused a decreased level of Cyclin D1 and increased level of pCDK4 (Thr172) in HBMECs at protein level. The downregulation of Cyclin D1 at the mRNA and protein levels might lead to G_1 arrest. The lack of Cyclin D1 might influence the formation of the Cyclin D1/CDK4 complex which is required for the cell cycle progression at G_1 phase. The effect of PorA-Loop4 on Cyclin D1 and pCDK4 (Thr172) was PI3K-dependent (at both mRNA and protein levels).

Further, the study was extended to investigate the effect of PorA-Loop4 on Akt and GSK-3β as these proteins affect the Cyclin D1 in the PI3K/Akt pathway. It was shown that PorA-Loop4 caused the downregulation of pAkt (Ser473) and the upregulation of pGSK-3β (Ser9) at the protein levels in HBMECs. The PorA-Loop4's effect on pGSK-3β (Ser9) appeared to be dependent to Akt, and the downregulation of Cyclin D1 was independent of GSK-3β. Figure 6.1 shows the schematic summary of PorA-Loop4's effect in the PI3K/Akt pathway. Experiments to investigate the perturbation effect on Akt/GSK-3β/Cyclin D1/CDK4 in bacterial-infected HBMECs showed that the effects of PorA-Loop4 were reproduced in cells interacting with meningococci, and the lack of such perturbations in cells infected with mutants lacking PorA-Loop4 demonstrated that the observed effects were indeed mediated by this extracellular loop of PorA.

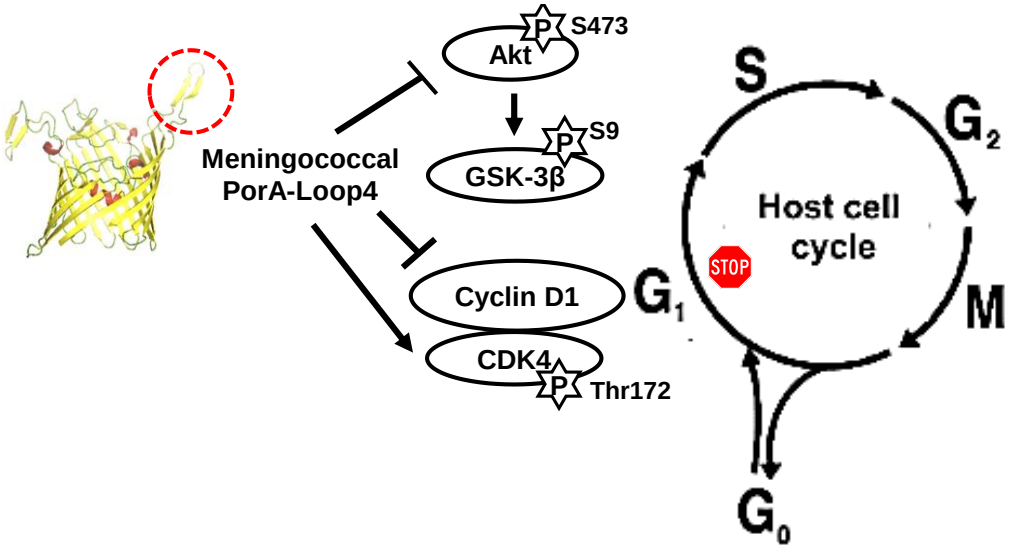

Figure 6.1: Meningococcal PorA-Loop4 causes the perturbation of PI3K/Akt pathway via Akt/GSK-3β/Cyclin D1/CDK4. Exposure of HBMECs (10^6 cells) to PorA-Loop4 peptide (50 μM) caused downregulations of pAkt (Ser473) and Cyclin D1 and upregulations of pGSK-3β (Ser9) and pCDK4 (Thr172) at the protein level 24 h post treatment. The PorA-Loop4's effect on pGSK-3β (Ser9) appeared to be dependent to Akt, and the downregulation of Cyclin D1 was independent of GSK-3β. The degradation of Cyclin D1 caused by the PorA-Loop4 possibly leads the G_1 arrest. ➔ : stimulation, ⊣ : inhibition.

So far, limited reports have been published on the meningococcal alteration of PI3K/Akt/GSK-3β/Cyclin D1/CDK4 pathways. Lambotin et al. previously reported that meningococci hijack the PI3K/Rac1-GTPase signalling pathway via meningococcal LOS to cause membrane protrusion and facilitate the bacterial uptake in non-phagocytic cells (Lambotin et al., 2005). Also, meningococcal infection of strain MC58 has been reported to cause a downregulation of Akt at mRNA level (Schubert-Unkmeir et al., 2007).

In regards to G_1-arrest caused by meningococci, work in other labs has shown blockades at other points in the cell cycle. Oosthyusen et al. reported that Opa and Opc of *N. meningitidis* MC58 caused the S-arrest in HBMECs and caused an increase in expression of p21 and Cyclin G2 (Oosthuysen et al., 2016). The cel -cycle arrest effect were thought to be associated with the preservation of post-injury restoration of endothelial barrier integrity following the bacterial infection.

Von Papen et al. have reported that meningococcal infection from pathogenic and carriage isolates caused decreased expression of Cyclin D1 and increased expression of Cyclin E and p21 at the protein level, leading to

G_1 arrest 24 h post infection (von Papen et al., 2016). However, the report did not attribute the G_1 arrest effect to any cyclomodulin(s) and was based on epithelial cells (Detroit 562 and NP69).

The findings of cell cycle blockade in both G_1 (Vassey, 2014, von Papen et al., 2016) and S phase (Oosthuysen et al., 2016) caused by meningococcal infection suggest that there may be functional redundancy showing the importance of cell cycle blockade during meningococcal interactions with host cells. In addition, given that cell cycle blockade were also caused by meningococcal infection from carriage isolates (von Papen et al., 2016), it is possible that cell cycle arrest has a role during carriage stage of meningococci, as meningococcal disease is probably not important to the long term survival and dissemination of these organisms. Thus, it is likely that the effects on HBMEC cells, and the likely role they might play in disease, are probably a reflection of mechanisms important during interaction of cells of the nasopharynx during carriage.

Some results in the current study are still in the areas of uncertainty and require more studies. The upregulation of pCDK4 (Thr172) caused by the PorA-Loop4 raises many questions in regards to the G_1-arrest effects. The activated CDK4 in complex with Cyclin D1 leads to phosphorylation of the specific site of pRb and thus the passage through the R point (Bockstaele et al., 2006a). Subsequent phosphorylation of pRb by the Cyclin E/CDK2 complex in the late G_1 phase fully dissociates Rb from the HDAC-repressor complex, permits transcription of genes required for DNA replication, and induces the progression from the G_1 to the S-phase.

However, in a recent report, pCDK4 (Thr172) was also found in a complex with p16 or p27 (Bockstaele et al., 2006b). p16 binds to catalytic domain of CDK4/6 preventing cyclin association (Hall et al., 1995, Sherr and Roberts, 1995, Pavletich, 1999). p27 functions not only to inhibit CDK4 activity (Polyak et al., 1994) but also target the CyclinD1/CDK4 complex to the nucleus (Reynisdottir and Massague, 1997). Bockstaele et al found that the Thr172 phosphorylation of CDK4 appeared to be relatively stable, which could allow the re-association with p16 of some phosphorylated CDK4 released by the rapid turnover of labile D-type cyclins (Bockstaele et al., 2006b). Indeed, some Thr172 phosphorylation persisted in CDK4 bound to either p16 or p27, even after disappearance of Cyclin D1.

Given that PorA-Loop4 caused decreased levels of Cyclin D1, the upregulation of pCDK4 (Thr172) seemed to be associated with the p27. The assumption was based on our finding that the pCDK4 (Th172) in MC58 wild-

type infected HBMECs were localised in both nuclear and cytoplasmic regions, as p27 are localised in both regions. Von papen et. al also mentioned in their report that staining revealed punctate p27 foci in cells exposed to meningococci, along with p27 localisation in the nuclear region (von Papen et al., 2016).

A future study investigating the effect of PorA-Loop4 on p27 expression in both endogenous and CDK4-bound complex form would be required to test our current hypothesis. In addition, future study investigating the effect of PorA-Loop4 in the downstream of the G_1/S checkpoint signalling pathway (e.g. Cyclin E, CDK2, pRb and E2F) would also provide a better understanding of the G_1-arrest mechanism caused by the PorA-Loop4.

The upregulation of pGSK-3β (Ser9) caused by the PorA-Loop4 also raises many questions, as the decrease of pAkt (Ser473) might lead to the lack of phosphorylation of GSK-3β on Ser9. Further, it was shown that the PorA-Loop4's effect on pGSK-3β (Ser9) appeared to be dependent on Akt activity. PorA-Loop4 might upregulate other kinases which phosphorylate the Ser9 of GSK-3β such that it would overcome the decreased kinase activity of Akt. This assumption was based on the fact that many kinases phosphorylate GSK-3β on Ser9 including PKA, PKC, p70-S6 kinase, and other kinases (Beurel et al., 2015). A future study investigating the effect of PorA-Loop4 on non-phosphorylated GSK-3β and pGSK-3β (Tyr216) would fill gaps in the current findings as pGSK-3β (Tyr216) directly affects Cyclin D1 in the PI3K/Akt pathway.

PorA-Loop4 was also observed affecting the Cyclin D1 independently from GSK-3β activity. Based on the fact that another kinase, Mirk/Dyrk1B, may serve to regulate Cyclin D1 stability in situations where GSK-3β activity is absent, and that it induces nuclear export and degradation of Cyclin D1 (Zou et al., 2004), the PorA-Loop4 seems to downregulate Cyclin D1 via Mirk/Dyrk1B. Future studies are required to investigate the effect of PorA-Loop4 on Mirk/Dyrk1B in particular or the effect of PorA-Loop4 on cytoplasmic Cyclin D1 degradation in general.

The experimental work in this thesis has focused on the role of PorA-Loop4 peptide originally derived from serogroup B strain MC58. According to the MRF database (2010-2015), there were 2395 meningococcal isolates of serogroup B, W, Y circulated in the UK with diverse PorA sequences. It raises questions whether other PorA-Loop4 sequences or PorA molecules from different strains/isolates would exert similar effects.

Investigating the cellular effects of a range of peptides with other PorA-Loop4 sequences would provide more insights to the current findings.

In the previous study, nine different PorA molecules (including PorA from strain MC58) known to be in circulation in the UK from 2010-2013 were tested for their capabilities to bind rLR (Vassey, 2014). Results showed that all nine molecules were able to bind rLR and no significant differences in LAMR binding were observed ($p>0.05$). The results suggest that the PorA-LAMR interaction is not driven specifically by the Loop4 sequence found in strain MC58. To enhance this study further a much wider range of PorA-Loop4 peptides or PorA molecules should be tested for their LAMR binding capacity and their cellular effects. So far, the data from Neisseria PorA typing database (http://pubmlst.org/neisseria/PorA/) showed serogroup B, W, and Y as the three most prevalent frequent serogroups causing IMD in the UK. Ten most frequently occurring PorA-Loop4 sequences from 2395 meningococcal isolates of serogroup B, W, Y circulated in the UK (2010-2015) are presented in Appendix V. Given that nowadays serogroup W and Y cases are increasing in the UK, studying the Loop4 variants from these serogroups (Loop4 variant 2 from serogroup W, Loop4 variant 10-1 from serogroup Y) would provide more understanding to the current study.

Many bacterial pathogens block the cell cycle progression of host cells usually for survival, growth, colonisation and invasion. The pathogenic bacteria produce multiple compounds termed as cyclomodulins to alter the cell cycle progression of host cells, impairing essential cellular functions and impeding host cell division.

A closely related pathogen to meningococcus*, N. gonorrhoea,* has been reported to cause G_1 arrest through the decrease of Cyclin B1, Cyclin D1, and Cyclin E (Jones et al., 2007). Yet, the report did not associate the G_1 arrest effect to any cyclomodulin(s). Immunoblotting and flow cytometry analysis showed that the infection with *N. gonorrhoea* strain MS11 P^+ (piliated Opa- phenotypes, MOI 100) for 24 h reduced the protein levels of Cyclin B1, Cyclin D1, and Cyclin E in epithelial cells by 10%, 20%, and 30%, respectively. Flow cytometry confirmed that a 24 h gonococcal infection caused G_1 arrest and decreased the number of cells in the S phase by 40%.

Other pathogenic bacteria that produce cyclomodulins causing the G_1-arrest are presented in Table 6.1. Most are toxins that damage the DNA and cause apoptosis. The cyclomodulins that cause the G_1 arrest through a decrease of Cyclin D1 are subtilase toxin (SubAB), anthrax toxin, cholera toxin (CTX), and Panton–Valentine leukocidin (PVL).

Table 6.1: Bacterial cyclomodulins causing G_1 arrest, modified from El-Aouhar Filho et al., (2017).

Cyclomodulins	Types	Species
Cycle inhibiting factor (CIF)	Cysteine protease	*E. coli* (EHEC, EPEC) *Yersinia pseudotuberculosis* *Pseudomonas* sp. *Enterobacter* sp. *Serratia* sp.
T-glutamyl transpeptidase (GGT)	Enzyme	*Helicobacter pylori*
Cytolethal Distending Toxin (CDT)	Three globular toxin	*E. coli* *H. hepaticus* *Salmonella enterica* serovar Typhimurium
Subtilase AB (SubAB)	AB5 toxin	*E. coli* (STEC)
Anthrax toxin (Edema toxin/Lethal toxin)	Tripartite toxin	*Bacillus anthracis*
Cholera toxin (CTX)	AB5 toxin Oligomeric complex	*Vibrio cholerae*
Adenylate Cyclase Toxin (ACT)	AB5 toxin	*Bordetella pertussis*
Vacuolating cytotoxin (VacA)	Pore-forming toxin	*H. pylori*
Panton–Valentine leukocidin (PVL)	β-pore-forming toxin	*S. aureus*
Mycolactone	Macrolide	*M. ulcerans*

Shiga Toxin-producing *E. coli* (STEC) non-O157 strains produce the SubAB that play a role in the pathogenesis of haemolytic uremic syndrome (HUS) (Paton et al., 2004, Irino et al., 2010). The SubAB have been reported to bind integrin α2β1 at the surface of Vero cells (green monkey kidney epithelial cells) (Yahiro et al., 2006). Immunoblotting and flow cytometry showed that the SubAB toxin internalise into the Vero cells by endocytosis, traffic through Golgi to the endoplasmic reticulum. The SubAB cleaves the chaperone BiP that activates PERK and eIF2α, leading to a translation inhibition, downregulation of Cyclin D1, and finally the G_1 arrest (Morinaga et al., 2008).

Anthrax edema toxin (ET) of *B. anthracis* and adenylate cyclase toxin (ACT) of *B. pertussis* induce production of ubiquitous second messenger, cAMP, at non-lethal concentrations, followed by inactivation of the c-Raf/MEK/ERK cascade and G_1 arrest (Gray and Hewlett, 2011). The ET and ACT at 1-10 ng ml^{-1} inhibit the murine reticulum cell sarcoma J774 cell proliferation without cytotoxicity. Analysis by flow cytometry revealed that treatment with either ET or ACT to J774 cells for 24 h caused a higher proportion of cells in G_1 phase (30% of those treated with ET and 23% with ACT) and a decrease in S phase. Immunoblotting showed that ET or ACT caused downregulation of phosphorylated ERK 1/2 and Cyclin D1, and upregulation of phospho-CREB and p27. PD98059, a MEK inhibitor, elicits a comparable reduction in Cyclin D1 to that produced by the two toxins and blocks proliferation.

Lethal toxin (LT), the other catalytic subunit of the anthrax toxin, directly inactivates the N-terminal end of MEK. Ha et al showed that the LT resides inside cell and continuously cleaves MEK1 for prolong periods (~4–5 days) in murine macrophage cell line RAW246.7 cells and prevents TNFα production (Ha et al., 2007a). The inactivation of MEK leads to inhibition of ERK, followed by downregulation of Cyclin D1, Cyclin D2, and checkpoint kinase 1 (Ha et al., 2007b). The perturbation would lead to a cell cycle arrest as it was observed in LT-treated monocytic cell lines (Ha et al., 2007b). The G_1 arrest may trigger necrosis in monocytes and macrophage cells causing severe defects in immune responses to *B. anthracis* in host.

V. cholerae produce CTX to bind GM1 gangliosides receptor at the cell membrane (van Heyningen, 1974). The binding of CTX B subunit (CTB) to GM1 on the intestinal cells (enterocytes) leading to endocytosis, cleavage of CTX A1 subunit (Nitulescu et al.) which then catalyses ADP-ribosylation of the Gs alpha subunit ($G_{\alpha s}$) of the G protein, thereby stimulating adenylate

cyclase to produce cAMP (O'Neal et al., 2005). High cAMP level disrupt the electrolyte balance causing a drastic efflux of ions and water from enterocytes, leading to watery diarrhoea (Nichols et al., 2015). Li et al reported that CTX induces accumulation of C6 rat glioma cells in the G_1 phase through the downregulation of Cyclin D1 and CDK2 and the upregulation of p27 and p21 (Li et al., 2007b). Moreover, using two human bladder cell lines, T24 and UM-UC-3, it was demonstrated that CTX inactivates the c-Raf/MEK/ERK cascade, via the PKA-dependent c-Raf phosphorylation at Ser43. This results in the downregulation of Cyclin D1, CDK4, and CDK6 followed by the G_1 arrest (Zheng et al., 2014).

PVL of *S. aureus* is responsible for leukocyte destruction and necrotic haemorrhagic pneumonia, a highly lethal infection that essentially affects healthy children and young adults. LukS-PV subunit of PVL had been reported to bind human complement C5A receptor (Spaan et al., 2013). It was observed that the LukS-PV subunit inhibits the proliferation of the human acute myeloid leukemia cell line THP-1 (Bu et al., 2013). The flow cytometry analysis revealed that the LukS-PV-treated THP-1 cells had a reduced number of S-phase cells while increasing the number of G_0/G_1-phase cells. The G_1 arrest was associated with the inhibition of Cyclin D1 in a dose- and time-dependent manner.

Overall, most cyclomodulins that delay the G_1 phase via downregulation of Cyclin D1 are associated with the MAPK/ERK pathway involving cAMP, PKA, and CREB. Given that the upregulation of pGSK-3β (Ser9) in HBMECs caused by the PorA-Loop4 might be associated with PKA, the MAPK/ERK pathway is also involved.

Interestingly, the recovery from the G_1 arrest in the LT-treated cells is facilitated by the PI3K/Akt pathway via upregulation of pGSK-3β (Ser9) (Ha et al., 2007b). Pre-treatment of THP-1 cells with LT or the GSK-3β-specific inhibitor SB-216763, or transfection with dominant active mutant Akt or degradation-defected mutant Cyclin D1 protected cells from LT-induced cell-cycle arrest. Based on this report, the upregulation of pGSK-3β (Ser9) in PorA-Loop4-treated HBMECs might be associated with the recovery mechanism from the G_1 arrest. Yet, the time-dependent experiments of the PorA-Loop4 treatment should be performed to confirm this assumption.

Current work only observed the effect of PorA-Loop4 in the endothelial cell line HBMEC. The variability of LAMR expression on the surface of different cell line might affect the PorA-Loop4:37LRP interaction and the following effect in the PI3K/Akt pathway and G_1 arrest. RNA-sequencing

analysis of *RPSA/LAMR* gene expression in 27 different human tissue showed that the gene is expressed lowest in liver; the LAMR is expressed lower in brain than in colon or lung (Fagerberg et al., 2014). So far, the study by Vassey had observed the PorA-Loop4-induced G_1 arrest in three different cell lines including epithelial cell lines (HCT116, Detroit 562) and endothelial cell line (HBMEC) (Vassey, 2014). Future study are required to confirm the PorA-loop4's inhibition of the PI3K/Akt pathway in the epithelial cell lines.

Based on current findings and the previous published reports, our group suggest that meningococcal PorA potentially dysregulate host cell processes during disease progression to facilitate long term colonisation. The PorA-Loop4:37LRP interaction with the cells in the local micro-environment is likely to influence normal turnover and renewal of endothelium by stalling the cell cycle via altered expression of the cell cycle regulators and PI3K/Akt pathway which ultimately allowing the bacteria to initiate a sustained colonisation.

6.3 Conclusions

In summary, the work presented in this thesis has shown that the exposure of PorA-Loop4 peptide in HBMECs caused the perturbation of PI3K/Akt pathway via Akt/GSK-3β/Cyclin D1/CDK4. Our current findings have implications for the currently known molecular mechanisms involved in the interaction of *N. meningitidis* with brain vascular cells. A thorough understanding of PorA interaction with LAMR and its effect in the PI3K/Akt pathway may provide another strategy for the development of interventions against meningococcal infection, and possibly against infections with other Gram-negative bacteria. Given that LAMR is a subject to extensive research in relation to cancer, the thorough understanding of PorA-Loop4:37LRP including the trafficking and downstream signalling pathway may offer not only an approach to interfere the meningococcal infection but also an alternative tool for treatment of cancers.

References

ABOUSEADA, N. M., ASSAFI, M. S., MAHDAVI, J., OLDFIELD, N. J., WHELDON, L. M., WOOLDRIDGE, K. G. & ALA'ALDEEN, D. A. 2012. Mapping the laminin receptor binding domains of *Neisseria meningitidis* PorA and *Haemophilus influenzae* OmpP2. *PLoS One,* 7**,** e46233.

ABOUSEADA, N. M. A. 2010. *Role of 37/67-kDa laminin receptor in binding of bacteria causing meningitis.* PhD, University of Nottingham.

ABUKHDEIR, A. M. & PARK, B. H. 2008. P21 and p27: roles in carcinogenesis and drug resistance. *Expert Rev Mol Med,* 10**,** e19.

ACHOUAK, W., HEULIN, T. & PAGÈS, J.-M. 2001. Multiple facets of bacterial porins. *FEMS Microbiol Lett,* 199**,** 1-7.

AGARWAL, E., CHAUDHURI, A., LEIPHRAKPAM, P. D., HAFERBIER, K. L., BRATTAIN, M. G. & CHOWDHURY, S. 2014. Akt inhibitor MK-2206 promotes anti-tumor activity and cell death by modulation of AIF and Ezrin in colorectal cancer. *BMC Cancer,* 14**,** 145.

AKACHE, B., GRIMM, D., PANDEY, K., YANT, S. R., XU, H. & KAY, M. A. 2006. The 37/67-kilodalton laminin receptor is a receptor for adeno-associated virus serotypes 8, 2, 3, and 9. *J Virol,* 80**,** 9831-6.

ALA'ALDEEN, D. A. & TURNER, D. P. J. 2006. *Neisseria meningitidis*. *In:* GILLESPIE, S. H. & HAWKEY, P. M. (eds.) *Principles and Practice of Clinical Bacteriology.* Chichester: John Wiley & Sons.

ALAMRO, M., BIDMOS, F. A., CHAN, H., OLDFIELD, N. J., NEWTON, E., BAI, X., AIDLEY, J., CARE, R., MATTICK, C., TURNER, D. P., NEAL, K. R., ALA'ALDEEN, D. A., FEAVERS, I., BORROW, R. & BAYLISS, C. D. 2014. Phase variation mediates reductions in expression of surface proteins during persistent meningococcal carriage. *Infect Immun,* 82**,** 2472-84.

ALAO, J. P. 2007. The regulation of cyclin D1 degradation: roles in cancer development and the potential for therapeutic invention. *Mol Cancer,* 6**,** 24.

ALBANESE, C., JOHNSON, J., WATANABE, G., EKLUND, N., VU, D., ARNOLD, A. & PESTELL, R. G. 1995. Transforming p21ras mutants and c-Ets-2 activate the cyclin D1 promoter through distinguishable regions. *J Biol Chem,* 270**,** 23589-97.

ALQAHTANI, F., MAHDAVI, J., WHELDON, L. M., VASSEY, M., PIRINCCIOGLU, N., ROYER, P. J., QARANI, S. M., MORROLL, S., STOOF, J., HOLLIDAY, N. D., TEO, S. Y., OLDFIELD, N. J., WOOLDRIDGE, K. G. & ALA'ALDEEN, D. A. 2014. Deciphering the complex three-way interaction between the non-integrin laminin receptor, galectin-3 and *Neisseria meningitidis*. *Open Biol,* 4.

ALT, J. R., CLEVELAND, J. L., HANNINK, M. & DIEHL, J. A. 2000. Phosphorylation-dependent regulation of cyclin D1 nuclear export and cyclin D1-dependent cellular transformation. *Genes Dev,* 14**,** 3102-14.

ANDERSEN, B., STEIGERWALT, A., O'CONNOR, S., HOLLIS, D., WEYANT, R., WEAVER, R. & BRENNER, D. 1993. *Neisseria weaveri* sp. nov., formerly CDC group M-5, a gram-negative bacterium associated with dog bite wounds. *J Clin Microbiol,* 31**,** 2456-2466.

ARELLANO, M. & MORENO, S. 1997. Regulation of CDK/cyclin complexes during the cell cycle. *Int J Biochem Cell Biol,* 29**,** 559-73.

BARTLEY, S. N., TZENG, Y.-L., HEEL, K., LEE, C. W., MOWLABOCCUS, S., SEEMANN, T., LU, W., LIN, Y.-H., RYAN, C. S. & PEACOCK, C. 2013. Attachment and invasion of *Neisseria meningitidis* to host cells is

related to surface hydrophobicity, bacterial cell size and capsule. *PloS One,* 8**,** e55798.

BASERGA, R. 1976. *Multiplication and division in mammalian cells,* New York, M. Dekker

BASOLO, F., POLLINA, L., PACINI, F., FONTANINI, G., MENARD, S., CASTRONOVO, V. & BEVILACQUA, G. 1996. Expression of the Mr 67,000 laminin receptor is an adverse prognostic indicator in human thyroid cancer: an immunohistochemical study. *Clin Cancer Res,* 2**,** 1777-1780.

BEAGLEHOLE, R., IRWIN, A. & PRENTICE, T. 2004. The World Health Report : 2004 : Changing History. *In:* BEAGLEHOLE, R. (ed.). Geneva: World Health Organization.

BÉKONDI, C., BERNEDE, C., PASSONE, N., MINSSART, P., KAMALO, C., MBOLIDI, D. & GERMANI, Y. 2006. Primary and opportunistic pathogens associated with meningitis in adults in Bangui, Central African Republic, in relation to human immunodeficiency virus serostatus. *Int J Infect Dis,* 10**,** 387-395.

BENSON, H., BRENNWASSER, R. & D'ANDREA, D. 1928. *Neisseria subflava* (Bergey) meningitis in an infant. *J Infect Dis***,** 516-524.

BERNAL-MIZRACHI, L., LOVLY, C. M. & RATNER, L. 2006. The role of NF-{kappa}B-1 and NF-{kappa}B-2-mediated resistance to apoptosis in lymphomas. *Proc Natl Acad Sci U S A,* 103**,** 9220-5.

BERNARD, S. C., SIMPSON, N., JOIN-LAMBERT, O., FEDERICI, C., LARAN-CHICH, M. P., MAISSA, N., BOUZINBA-SEGARD, H., MORAND, P. C., CHRETIEN, F., TAOUJI, S., CHEVET, E., JANEL, S., LAFONT, F., COUREUIL, M., SEGURA, A., NIEDERGANG, F., MARULLO, S., COURAUD, P. O., NASSIF, X. & BOURDOULOUS, S. 2014. Pathogenic *Neisseria meningitidis* utilizes CD147 for vascular colonization. *Nat Med,* 20**,** 725-31.

BERTOLI, C., SKOTHEIM, J. M. & DE BRUIN, R. A. M. 2013. Control of cell cycle transcription during G1 and S phases. *Nat Rev Mol Cell Biol,* 14**,** 518-528.

BESSON, A., GURIAN-WEST, M., SCHMIDT, A., HALL, A. & ROBERTS, J. M. 2004. p27Kip1 modulates cell migration through the regulation of RhoA activation. *Genes Dev,* 18**,** 862-876.

BEUREL, E., GRIECO, S. F. & JOPE, R. S. 2015. Glycogen synthase kinase-3 (GSK3): regulation, actions, and diseases. *Pharmacol Ther,* 148**,** 114-31.

BEVANGER, L., BERGH, K., GISNAS, G., CAUGANT, D. A. & FROHOLM, L. O. 1998. Identification of nasopharyngeal carriage of an outbreak strain of *Neisseria meningitidis* by pulsed-field gel electrophoresis versus phenotypic methods. *J Med Microbiol,* 47**,** 993-8.

BIJUR, G. N. & JOPE, R. S. 2001. Proapoptotic stimuli induce nuclear accumulation of glycogen synthase kinase-3 beta. *J Biol Chem,* 276**,** 37436-42.

BILUKHA, O. & ROSENSTEIN, N. E. 2005. Prevention and control of meningococcal disease; recommendations of the Advisory Committee on Immunization Practices (ACIP).

BIRTLES, A., HARDY, K., GRAY, S. J., HANDFORD, S., KACZMARSKI, E. B., EDWARDS-JONES, V. & FOX, A. J. 2005. Multilocus sequence typing of *Neisseria meningitidis* directly from clinical samples and application of the method to the investigation of meningococcal disease case clusters. *J Clin Microbiol,* 43**,** 6007-14.

BITTER, W., KOSTER, M., LATIJNHOUWERS, M., DE COCK, H. & TOMMASSEN, J. 1998. Formation of oligomeric rings by XcpQ and PilQ, which are involved in protein transport across the outer membrane of *Pseudomonas aeruginosa*. *Mol Microbiol,* 27**,** 209-219.

BJERRE, A., BRUSLETTO, B., ØVSTEBØ, R., JOØ, G. B., KIERULF, P. & BRANDTZAEG, P. 2003. Identification of meningococcal LPS as a major monocyte activator in IL-10 depleted shock plasmas and CSF by blocking the CD14-TLR4 receptor complex. *J Endotoxin Res,* 9**,** 155-163.

BOCKSTAELE, L., COULONVAL, K., KOOKEN, H., PATERNOT, S. & ROGER, P. P. 2006a. Regulation of CDK4. *Cell Div,* 1**,** 25.

BOCKSTAELE, L., KOOKEN, H., LIBERT, F., PATERNOT, S., DUMONT, J. E., DE LAUNOIT, Y., ROGER, P. P. & COULONVAL, K. 2006b. Regulated activating Thr172 phosphorylation of cyclin-dependent kinase 4(CDK4): its relationship with cyclins and CDK "inhibitors". *Mol Cell Biol,* 26**,** 5070-85.

BOGACHEK, M. V., PROTOPOPOVA, E. V., LOKTEV, V. B., ZAITSEV, B. N., FAVRE, M., SEKATSKII, S. K. & DIETLER, G. 2008. Immunochemical and single molecule force spectroscopy studies of specific interaction between the laminin binding protein and the West Nile virus surface glycoprotein E domain II. *J Mol Recognit,* 21**,** 55-62.

BOSLEGO, J., GARCIA, J., CRUZ, C., ZOLLINGER, W., BRANDT, B., RUIZ, S., MARTINEZ, M., ARTHUR, J., UNDERWOOD, P. & SILVA, W. 1995. Efficacy, safety, and immunogenicity of a meningococcal group B (15: P1. 3) outer membrane protein vaccine in Iquique, Chile. *Vaccine,* 13**,** 821-829.

BOVRE, K., FROHOLM, L. O., GAUSTAD, P., HOLTEN, E. & HOIBY, E. A. 1983. Some agent characteristics and their coexistence related to occurrence and severity of systemic meningococcal disease in Norway, Winter 1981-1982. *NIPH Ann,* 6**,** 75-84.

BOVRE, K. & HOLTEN, E. 1970. *Neisseria elongata* sp.nov., a rod-shaped member of the genus Neisseria. Re-evaluation of cell shape as a criterion in classification. *J Gen Microbiol,* 60**,** 67-75.

BRANDTZAEG, P. 2006. Pathogenesis and pathophysiology of invasive meningococcal disease. *In:* FROSCH, M. & MAIDEN, M. C. J. (eds.) *Handbook of meningococcal disease.* Weinheim: Wiley-VCH.

BRANDTZAEG, P., BJERRE, A., ØVSTEBØ, R., BRUSLETTO, B., JOØ, G. B. & KIERULF, P. 2001. Invited review: *Neisseria meningitidis* lipopolysaccharides in human pathology. *J Endotoxin Res,* 7**,** 401-420.

BRANDTZAEG, P., KIERULF, P., GAUSTAD, P., SKULBERG, A., BRUUN, J. N., HALVORSEN, S. & SØRENSEN, E. 1989. Plasma endotoxin as a predictor of multiple organ failure and death in systemic meningococcal disease. *J Infect Dis,* 159**,** 195-204.

BRANDTZAEG, P. & VAN DEUREN, M. 2012. Classification and pathogenesis of meningococcal infections. *Methods Mol Biol,* 799**,** 21-35.

BRANHAM, S. E. 1953. Serological relationships among meningococci. *Bacteriol Rev,* 17**,** 175-88.

BRANHAM, S. E. 1930. A new meningococcus-like organism (*Neisseria flavescens* n. sp.) from epidemic meningitis. *Ann Intern Med*, 4, 101.

BRATCHER, H. B., CORTON, C., JOLLEY, K. A., PARKHILL, J. & MAIDEN, M. C. 2014. A gene-by-gene population genomics platform: de novo assembly, annotation and genealogical analysis of 108 representative *Neisseria meningitidis* genomes. *BMC Genomics,* 15**,** 1138.

BREHM, A., MISKA, E. A., MCCANCE, D. J., REID, J. L., BANNISTER, A. J. & KOUZARIDES, T. 1998. Retinoblastoma protein recruits histone deacetylase to repress transcription. *Nature,* 391**,** 597.

BRISSAC, T., MIKATY, G., DUMENIL, G., COUREUIL, M. & NASSIF, X. 2012. The meningococcal minor pilin PilX is responsible for type IV pilus conformational changes associated with signaling to endothelial cells. *Infect Immun,* 80**,** 3297-306.

BRÖKER, M., COOPER, B., DETORA, L. M. & STODDARD, J. J. 2011. Critical appraisal of a quadrivalent CRM197 conjugate vaccine against meningococcal serogroups A, C W-135 and Y (Menveo®) in the context of treatment and prevention of invasive disease. *Infect Drug Resist,* 4**,** 137.

BROUWER, M. C., TUNKEL, A. R. & VAN DE BEEK, D. 2010. Epidemiology, diagnosis, and antimicrobial treatment of acute bacterial meningitis. *Clin Microbiol Rev,* 23**,** 467-92.

BROWN, N. R., NOBLE, M. E. M., ENDICOTT, J. A., GARMAN, E. F., WAKATSUKI, S., MITCHELL, E., RASMUSSEN, B., HUNT, T. & JOHNSON, L. N. 1995. The crystal structure of cyclin A. *Structure,* 3**,** 1235-1247.

BU, S., XIE, Q., CHANG, W., HUO, X., CHEN, F. & MA, X. 2013. LukS-PV induces mitochondrial-mediated apoptosis and G0/G1 cell cycle arrest in human acute myeloid leukemia THP-1 cells. *Int J Biochem Cell Biol,* 45**,** 1531-1537.

BUCHKOVICH, K., DUFFY, L. A. & HARLOW, E. 1989. The retinoblastoma protein is phosphorylated during specific phases of the cell cycle. *Cell,* 58**,** 1097-1105.

BURKHARDT, J., VONCK, J. & AVERHOFF, B. 2011. Structure and function of PilQ, a secretin of the DNA transporter from the thermophilic bacterium Thermus thermophilus HB27. *J Biol Chem,* 286**,** 9977-84.

BUTO, S., TAGLIABUE, E., ARDINI, E., MAGNIFICO, A., GHIRELLI, C., VAN DEN BRULE, F., CASTRONOVO, V., COLNAGHI, M. I., SOBEL, M. E. & MENARD, S. 1998. Formation of the 67-kDa laminin receptor by acylation of the precursor. *J Cell Biochem,* 69**,** 244-51.

CANTLEY, L. C. 2004. The role of phosphoinositide 3-kinase in human disease. *Harvey Lect,* 100**,** 103-22.

CAPECCHI, B., ADU-BOBIE, J., DI MARCELLO, F., CIUCCHI, L., MASIGNANI, V., TADDEI, A., RAPPUOLI, R., PIZZA, M. & ARICO, B. 2005. *Neisseria meningitidis* NadA is a new invasin which promotes bacterial adhesion to and penetration into human epithelial cells. *Mol Microbiol,* 55**,** 687-98.

CARBONE, A., GLOGHINI, A., COLOMBATTI, A., CASTRONOVO, V. & MENARD, S. 1995. Expression of the monomeric 67-kd laminin-binding protein in human lymphomas as defined by MLuC5 monoclonal antibody and paraffin section immunohistochemistry. *Hum Pathol,* 26**,** 541-6.

CARNERO, A. & HANNON, G. 1998. The INK4 family of CDK inhibitors. *Cyclin Dependent Kinase (CDK) Inhibitors.* Springer.

CARPENTER, C. L., DUCKWORTH, B. C., AUGER, K. R., COHEN, B., SCHAFFHAUSEN, B. S. & CANTLEY, L. C. 1990. Purification and characterization of phosphoinositide 3-kinase from rat liver. *J Biol Chem,* 265**,** 19704-11.

CASTRONOVO, V., CLAYSMITH, A. P., BARKER, K. T., CIOCE, V., KRUTZSCH, H. C. & SOBEL, M. E. 1991. Biosynthesis of the 67 kDa high affinity laminin receptor. *Biochem Biophys Res Commun,* 177**,** 177-83.

CAUGANT, D. A., FRØHOLM, L. O., BØVRE, K., HOLTEN, E., FRASCH, C. E., MOCCA, L. F., ZOLLINGER, W. D. & SELANDER, R. K. 1986. Intercontinental spread of a genetically distinctive complex of clones of *Neisseria meningitidis* causing epidemic disease. *Pro Natl Acad Sci U S A,* 83**,** 4927-4931.

CAUGANT, D. A. & MAIDEN, M. C. 2009. Meningococcal carriage and disease--population biology and evolution. *Vaccine,* 27 Suppl 2**,** B64-70.

CAUGANT, D. A., TZANAKAKI, G. & KRIZ, P. 2007. Lessons from meningococcal carriage studies. *FEMS Microbiol Rev,* 31**,** 52-63.

CELL SIGNALING TECHNOLOGY. 2012. *Cell Cycle G1/S Checkpoint Signaling Interactive Pathway* [Online]. London: Cell Signaling Technology. Available: https://media.cellsignal.com/www/pdfs/science/pathways/Cell_Cycle_G1S.pdf [Accessed 7 February 2019].

CENTERS FOR DISEASE CONTROL AND PREVENTION 1993. Coccidioidomycosis--United States, 1991-1992. *MMWR Morb Mortal Wkly Rep,* 42**,** 21-4.

CENTERS FOR DISEASE CONTROL AND PREVENTION 2011a. Laboratory Methods for the Diagnosis of Meningitis Caused by *Neisseria meningitidis*, *Streptococcus pneumoniae*, and *Haemophilus influenzae. In:* MAYER, L. (ed.) 2nd ed. Geneva: WHO Press.

CENTERS FOR DISEASE CONTROL AND PREVENTION 2011b. Recommendation of the Advisory Committee on Immunization Practices (ACIP) for use of quadrivalent meningococcal conjugate vaccine (MenACWY-D) among children aged 9 through 23 months at increased risk for invasive meningococcal disease. *MMWR Morb Mortal Wkly Rep,* 60**,** 1391-2.

CHAMOT-ROOKE, J., MIKATY, G., MALOSSE, C., SOYER, M., DUMONT, A., GAULT, J., IMHAUS, A. F., MARTIN, P., TRELLET, M., CLARY, G., CHAFEY, P., CAMOIN, L., NILGES, M., NASSIF, X. & DUMENIL, G. 2011. Posttranslational modification of pili upon cell contact triggers *N. meningitidis* dissemination. *Science,* 331**,** 778-82.

CHANG, F., LEE, J. T., NAVOLANIC, P. M., STEELMAN, L. S., SHELTON, J. G., BLALOCK, W. L., FRANKLIN, R. A. & MCCUBREY, J. A. 2003. Involvement of PI3K/Akt pathway in cell cycle progression, apoptosis, and neoplastic transformation: a target for cancer chemotherapy. *Leukemia,* 17**,** 590-603.

CHEN, C., EDELSTEIN, L. C. & GELINAS, C. 2000. The Rel/NF-kappaB family directly activates expression of the apoptosis inhibitor Bcl-x(L). *Mol Cell Biol,* 20**,** 2687-95.

CHEN, L., MA, Y., QIAN, L. & WANG, J. 2013. Sumoylation regulates nuclear localization and function of zinc finger transcription factor ZIC3. *Biochim Biophys Acta Mol Cell Res,* 1833**,** 2725-2733.

CHEN, T., BELLAND, R. J., WILSON, J. & SWANSON, J. 1995. Adherence of pilus-Opa+ gonococci to epithelial cells in vitro involves heparan sulfate. *J Exp Med,* 182**,** 511-517.

CHEN, T. & GOTSCHLICH, E. C. 1996. CGM1a antigen of neutrophils, a receptor of gonococcal opacity proteins. *Proc Natl Acad Sci U S A,* 93**,** 14851-14856.

CHORNER, P. M. & MOOREHEAD, R. A. 2018. A-674563, a putative AKT1 inhibitor that also suppresses CDK2 activity, inhibits human NSCLC cell growth more effectively than the pan-AKT inhibitor, MK-2206. *PLoS One,* 13**,** e0193344.

CHUNG, J. W., HONG, S. J., KIM, K. J., GOTI, D., STINS, M. F., SHIN, S., DAWSON, V. L., DAWSON, T. M. & KIM, K. S. 2003. 37-kDa laminin receptor precursor modulates cytotoxic necrotizing factor 1-mediated RhoA activation and bacterial uptake. *J Biol Chem,* 278**,** 16857-62.

CLAASSEN, I., MEYLIS, J., VAN DER LEY, P., PEETERS, C., BRONS, H., ROBERT, J., BORSBOOM, D., VAN DER ARK, A., VAN STRAATEN, I., ROHOLL, P., KUIPERS, B. & POOLMAN, J. 1996. Production, characterization and control of a *Neisseria meningitidis* hexavalent class 1 outer membrane protein containing vesicle vaccine. *Vaccine,* 14**,** 1001-8.

COHN, A. C., MACNEIL, J. R., HARRISON, L. H., HATCHER, C., THEODORE, J., SCHMIDT, M., PONDO, T., ARNOLD, K. E., BAUMBACH, J., BENNETT, N., CRAIG, A. S., FARLEY, M., GERSHMAN, K., PETIT, S.,

LYNFIELD, R., REINGOLD, A., SCHAFFNER, W., SHUTT, K. A., ZELL, E. R., MAYER, L. W., CLARK, T., STEPHENS, D. & MESSONNIER, N. E. 2010. Changes in *Neisseria meningitidis* disease epidemiology in the United States, 1998-2007: implications for prevention of meningococcal disease. *Clin Infect Dis,* 50**,** 184-91.

COLE, A., FRAME, S. & COHEN, P. 2004. Further evidence that the tyrosine phosphorylation of glycogen synthase kinase-3 (GSK3) in mammalian cells is an autophosphorylation event. *Biochem J,* 377**,** 249-55.

COLLINS, R. F., DAVIDSEN, L., DERRICK, J. P., FORD, R. C. & TØNJUM, T. 2001. Analysis of the PilQ secretin from *Neisseria meningitidis* by transmission electron microscopy reveals a dodecameric quaternary structure. *J Bacteriol,* 183**,** 3825-3832.

COLNAGHI, M. I. 1994. The simultaneous expression of c-erbB-2 oncoprotein and laminin receptor on primary breast tumors has a predicting potential analogous to that of the lymph node status. *Antigen and Antibody Molecular Engineering in Breast Cancer Diagnosis and Treatment.* Springer.

COQUERET, O. 2003. New roles for p21 and p27 cell-cycle inhibitors: a function for each cell compartment? *Trends Cell Biol,* 13**,** 65-70.

CORLESS, C. E., GUIVER, M., BORROW, R., EDWARDS-JONES, V., FOX, A. J. & KACZMARSKI, E. B. 2001. Simultaneous detection of *Neisseria meningitidis, Haemophilus influenzae,* and *Streptococcus pneumoniae* in suspected cases of meningitis and septicemia using real-time PCR. *J Clin Microbiol,* 39**,** 1553-8.

COUREUIL, M., LECUYER, H., SCOTT, M. G., BOULARAN, C., ENSLEN, H., SOYER, M., MIKATY, G., BOURDOULOUS, S., NASSIF, X. & MARULLO, S. 2010. Meningococcus Hijacks a beta2-adrenoceptor/beta-Arrestin pathway to cross brain microvasculature endothelium. *Cell,* 143**,** 1149-60.

COUREUIL, M., MIKATY, G., MILLER, F., LECUYER, H., BERNARD, C., BOURDOULOUS, S., DUMENIL, G., MEGE, R. M., WEKSLER, B. B., ROMERO, I. A., COURAUD, P. O. & NASSIF, X. 2009. Meningococcal type IV pili recruit the polarity complex to cross the brain endothelium. *Science,* 325**,** 83-7.

CROSS, D. A., ALESSI, D. R., COHEN, P., ANDJELKOVICH, M. & HEMMINGS, B. A. 1995. Inhibition of glycogen synthase kinase-3 by insulin mediated by protein kinase B. *Nature,* 378**,** 785-9.

CROXEN, M. A. & FINLAY, B. B. 2010. Molecular mechanisms of *Escherichia coli* pathogenicity. *Nat Rev Microbiol,* 8**,** 26.

D'ERRICO, A., GARBISA, S., LIOTTA, L., CASTRONOVO, V., STETLER-STEVENSON, W. & GRIGIONI, W. 1991. Augmentation of type IV collagenase, laminin receptor, and Ki67 proliferation antigen associated with human colon, gastric, and breast carcinoma progression. *Mod Pathol,* 4**,** 239-246.

DA COSTA DIAS, B., JOVANOVIC, K., GONSALVES, D., MOODLEY, K., REUSCH, U., KNACKMUSS, S., PENNY, C., WEINBERG, M. S., LITTLE, M. & WEISS, S. F. 2013. Anti-LRP/LR specific antibody IgG1-iS18 and knock-down of LRP/LR by shRNAs rescue cells from Abeta42 induced cytotoxicity. *Sci Rep,* 3**,** 2702.

DA COSTA DIAS, B., JOVANOVIC, K., GONSALVES, D. & WEISS, S. F. 2011. Structural and mechanistic commonalities of amyloid-beta and the prion protein. *Prion,* 5**,** 126-37.

DAWSON, K. G., EMERSON, J. C. & BURNS, J. L. 1999. Fifteen years of experience with bacterial meningitis. *Pediatr Infect Dis J,* 18**,** 816-822.

DE RYCKE, J. & OSWALD, E. 2001. Cytolethal distending toxin (CDT): a bacterial weapon to control host cell proliferation? *FEMS Microbiol Lett,* 203**,** 141-8.

DE SMEDT, T., PAJAK, B., MURAILLE, E., LESPAGNARD, L., HEINEN, E., DE BAETSELIER, P., URBAIN, J., LEO, O. & MOSER, M. 1996. Regulation of dendritic cell numbers and maturation by lipopolysaccharide in vivo. *J Exp Med,* 184**,** 1413-24.

DE VRIES, F. P., COLE, R., DANKERT, J., FROSCH, M. & VAN PUTTEN, J. P. 1998. *Neisseria meningitidis* producing the Opc adhesin binds epithelial cell proteoglycan receptors. *Mol Microbiol,* 27**,** 1203-1212.

DEGHMANE, A. E., GIORGINI, D., LARRIBE, M., ALONSO, J. M. & TAHA, M. K. 2002. Down-regulation of pili and capsule of *Neisseria meningitidis* upon contact with epithelial cells is mediated by CrgA regulatory protein. *Mol Microbiol,* 43**,** 1555-64.

DEL TORDELLO, E., VACCA, I., RAM, S., RAPPUOLI, R. & SERRUTO, D. 2014. *Neisseria meningitidis* NalP cleaves human complement C3, facilitating degradation of C3b and survival in human serum. *Proc Natl Acad Sci U S A,* 111**,** 427-32.

DERRICK, J. P., URWIN, R., SUKER, J., FEAVERS, I. M. & MAIDEN, M. C. 1999. Structural and evolutionary inference from molecular variation in Neisseria porins. *Infect Immun,* 67**,** 2406-13.

DEVOE, I. W. 1982. The meningococcus and mechanisms of pathogenicity. *Microbiol Rev,* 46**,** 162-90.

DI GIOVANNI, C., GROTTESI, A. & LAVECCHIA, A. 2012. Conformational switch of a flexible loop in human laminin receptor determines laminin-1 interaction. *Eur Biophys J,* 41**,** 353-8.

DIEHL, J. A., CHENG, M., ROUSSEL, M. F. & SHERR, C. J. 1998. Glycogen synthase kinase-3beta regulates cyclin D1 proteolysis and subcellular localization. *Genes Dev,* 12**,** 3499-511.

DIEHL, J. A. & SHERR, C. J. 1997. A dominant-negative cyclin D1 mutant prevents nuclear import of cyclin-dependent kinase 4 (CDK4) and its phosphorylation by CDK-activating kinase. *Mol Cell Biol,* 17**,** 7362-74.

DIGIACOMO, V., GANDO, I. A., VENTICINQUE, L., HURTADO, A. & MERUELO, D. 2015. The Transition of the 37-Kda Laminin Receptor (Rpsa) to Higher Molecular Weight Species: Sumoylation or Artifact? *Cell Mol Biol Lett,* 20**,** 571-85.

DIGIACOMO, V. & MERUELO, D. 2015. Looking into laminin receptor: critical discussion regarding the non-integrin 37/67-kDa laminin receptor/RPSA protein. *Biol Rev Camb Philos Soc*.

DIGIACOMO, V. & MERUELO, D. 2016. Looking into laminin receptor: critical discussion regarding the non-integrin 37/67-kDa laminin receptor/RPSA protein. *Biol Rev Camb Philos Soc,* 91**,** 288-310.

DINITTO, J. P. & LAMBRIGHT, D. G. 2006. Membrane and juxtamembrane targeting by PH and PTB domains. *Biochim Biophys Acta,* 1761**,** 850-67.

DOLAN-LIVENGOOD, J. M., MILLER, Y. K., MARTIN, L. E., URWIN, R. & STEPHENS, D. S. 2003. Genetic basis for nongroupable *Neisseria meningitidis*. *J Infect Dis,* 187**,** 1616-28.

DOULET, N., DONNADIEU, E., LARAN-CHICH, M. P., NIEDERGANG, F., NASSIF, X., COURAUD, P. O. & BOURDOULOUS, S. 2006. *Neisseria meningitidis* infection of human endothelial cells interferes with leukocyte transmigration by preventing the formation of endothelial docking structures. *J Cell Biol,* 173**,** 627-37.

DUENSING, T. D. & VAN PUTTEN, J. P. 1998. Vitronectin binds to the gonococcal adhesin OpaA through a glycosaminoglycan molecular bridge. *Biochem J,* 334**,** 133-139.

DULL, P. M., ABDELWAHAB, J., SACCHI, C. T., BECKER, M., NOBLE, C. A., BARNETT, G. A., KAISER, R. M., MAYER, L. W., WHITNEY, A. M., SCHMINK, S., AJELLO, G. W., DOLAN-LIVENGOOD, J., STEPHENS, D. S., CETRON, M. S., POPOVIC, T. & ROSENSTEIN, N. E. 2005. *Neisseria meningitidis* serogroup W-135 carriage among US travelers to the 2001 Hajj. *J Infect Dis,* 191**,** 33-9.

DURONIO, R. J. & XIONG, Y. 2013. Signaling pathways that control cell proliferation. *Cold Spring Harb Perspect Biol,* 5**,** a008904.

EDWARDS, M. S. & BAKER, C. J. 1981. Complications and sequelae of meningococcal infections in children. *J Pediatr,* 99**,** 540-5.

EL-AOUAR FILHO, R. A., NICOLAS, A., DE PAULA CASTRO, T. L., DEPLANCHE, M., DE CARVALHO AZEVEDO, V. A., GOOSSENS, P. L., TAIEB, F., LINA, G., LE LOIR, Y. & BERKOVA, N. 2017. Heterogeneous Family of Cyclomodulins: Smart Weapons That Allow Bacteria to Hijack the Eukaryotic Cell Cycle and Promote Infections. *Front Cell Infect Microbiol,* 7**,** 208.

EUROPEAN MEDICINES AGENCY 2017. Trumenba, meningococcal group B vaccine (recombinant, adsorbed). *European Public Assesement Report.* London: European Medicines Agency.

EVANS, T., ROSENTHAL, E. T., YOUNGBLOM, J., DISTEL, D. & HUNT, T. 1983. Cyclin: a protein specified by maternal mRNA in sea urchin eggs that is destroyed at each cleavage division. *Cell,* 33**,** 389-396.

FAGERBERG, L., HALLSTROM, B. M., OKSVOLD, P., KAMPF, C., DJUREINOVIC, D., ODEBERG, J., HABUKA, M., TAHMASEBPOOR, S., DANIELSSON, A., EDLUND, K., ASPLUND, A., SJOSTEDT, E., LUNDBERG, E., SZIGYARTO, C. A., SKOGS, M., TAKANEN, J. O., BERLING, H., TEGEL, H., MULDER, J., NILSSON, P., SCHWENK, J. M., LINDSKOG, C., DANIELSSON, F., MARDINOGLU, A., SIVERTSSON, A., VON FEILITZEN, K., FORSBERG, M., ZWAHLEN, M., OLSSON, I., NAVANI, S., HUSS, M., NIELSEN, J., PONTEN, F. & UHLEN, M. 2014. Analysis of the human tissue-specific expression by genome-wide integration of transcriptomics and antibody-based proteomics. *Mol Cell Proteomics,* 13**,** 397-406.

FEIL, E. J., MAIDEN, M. C., ACHTMAN, M. & SPRATT, B. G. 1999. The relative contributions of recombination and mutation to the divergence of clones of *Neisseria meningitidis*. *Mol Biol Evol,* 16**,** 1496-502.

FIEBELKORN, K. R., CRAWFORD, S. A. & JORGENSEN, J. H. 2005. Mutations in folP associated with elevated sulfonamide MICs for *Neisseria meningitidis* clinical isolates from five continents. *Antimicrob Agents Chemother,* 49**,** 536-40.

FINNE, J., BITTER-SUERMANN, D., GORIDIS, C. & FINNE, U. 1987. An IgG monoclonal antibody to group B meningococci cross-reacts with developmentally regulated polysialic acid units of glycoproteins in neural and extraneural tissues. *J Immunol,* 138**,** 4402-7.

FISHER, R. P. & MORGAN, D. O. 1994. A novel cyclin associates with M015/CDK7 to form the CDK-activating kinase. *Cell,* 78**,** 713-724.

FLEIGE, S. & PFAFFL, M. W. 2006. RNA integrity and the effect on the real-time qRT-PCR performance. *Mol Aspects Med,* 27**,** 126-39.

FORMISANO, P., RAGNO, P., PESAPANE, A., ALFANO, D., ALBEROBELLO, A. T., REA, V. E., GIUSTO, R., ROSSI, F. W., BEGUINOT, F., ROSSI, G. & MONTUORI, N. 2012. PED/PEA-15 interacts with the 67 kD laminin receptor and regulates cell adhesion, migration, proliferation and apoptosis. *J Cell Mol Med,* 16**,** 1435-46.

FRAME, S., COHEN, P. & BIONDI, R. M. 2001. A Common Phosphate Binding Site Explains the Unique Substrate Specificity of GSK3 and Its Inactivation by Phosphorylation. *Mol Cell,* 7**,** 1321-1327.

FREDRIKSEN, J. H., ROSENQVIST, E., WEDEGE, E., BRYN, K., BJUNE, G., FROHOLM, L. O., LINDBAK, A. K., MOGSTER, B., NAMORK, E., RYE, U. & ET AL. 1991. Production, characterization and control of MenB-vaccine "Folkehelsa": an outer membrane vesicle vaccine against group B meningococcal disease. *NIPH Ann,* 14**,** 67-79; discussion 79-80.

FRIEDRICHS, B., SIEGEL, S., KLOESS, M., BARSOUM, A., COGGIN, J., ROHRER, J., JAKOB, I., TIEMANN, M., HEIDORN, K. & SCHULTE, C. 2008. Humoral immune responses against the immature laminin receptor protein show prognostic significance in patients with chronic lymphocytic leukemia. *J Immunol,* 180**,** 6374-6384.

FRYE, S. A., ASSALKHOU, R., COLLINS, R. F., FORD, R. C., PETERSSON, C., DERRICK, J. P. & TONJUM, T. 2006. Topology of the outer-membrane secretin PilQ from *Neisseria meningitidis*. *Microbiology,* 152**,** 3751-64.

FURTADO, G. C., SLOWIK, M., KLEINMAN, H. K. & JOINER, K. A. 1992. Laminin enhances binding of *Toxoplasma gondii* tachyzoites to J774 murine macrophage cells. *Infect Immun,* 60**,** 2337-42.

GALDIERO, M., VITIELLO, M. & GALDIERO, S. 2003. Eukaryotic cell signaling and transcriptional activation induced by bacterial porins. *FEMS Microbiol Lett,* 226**,** 57-64.

GALDIERO, S., FALANGA, A., CANTISANI, M., TARALLO, R., DELLA PEPA, M. E., D'ORIANO, V. & GALDIERO, M. 2012. Microbe-host interactions: structure and role of Gram-negative bacterial porins. *Curr Protein Pept Sci,* 13**,** 843-54.

GANIERE, J. P., ESCANDE, F., ANDRE-FONTAINE, G., LARRAT, M. & FILLONEAU, C. 1995. Characterization of group EF-4 bacteria from the oral cavity of dogs. *Vet Microbiol,* 44**,** 1-9.

GAO, T., FURNARI, F. & NEWTON, A. C. 2005. PHLPP: a phosphatase that directly dephosphorylates Akt, promotes apoptosis, and suppresses tumor growth. *Mol Cell,* 18**,** 13-24.

GASPARINI, R. & PANATTO, D. 2011. Meningococcal glycoconjugate vaccines. *Hum Vaccin,* 7**,** 170-182.

GENIN, S. & BOUCHER, C. A. 1994. A superfamily of proteins involved in different secretion pathways in gram-negative bacteria: modular structure and specificity of the N-terminal domain. *Mol Gen Genet,* 243**,** 112-8.

GEORGE, K. M., CHATTERJEE, D., GUNAWARDANA, G., WELTY, D., HAYMAN, J., LEE, R. & SMALL, P. L. 1999. Mycolactone: a polyketide toxin from *Mycobacterium ulcerans* required for virulence. *Science,* 283**,** 854-7.

GERMAIN, D., RUSSELL, A., THOMPSON, A. & HENDLEY, J. 2000. Ubiquitination of free cyclin D1 is independent of phosphorylation on threonine 286. *J Biol Chem,* 275**,** 12074-9.

GIRARD, F., STRAUSFELD, U., FERNANDEZ, A. & LAMB, N. J. 1991. Cyclin A is required for the onset of DNA replication in mammalian fibroblasts. *Cell,* 67**,** 1169-1179.

GIVANT-HORWITZ, V., DAVIDSON, B. & REICH, R. 2004. Laminin-induced signaling in tumor cells: the role of the M(r) 67,000 laminin receptor. *Cancer Res,* 64**,** 3572-9.

GLOTZER, M., MURRAY, A. W. & KIRSCHNER, M. W. 1991. Cyclin is degraded by the ubiquitin pathway. *Nature,* 349**,** 132.

GOC, A., AL-HUSEIN, B., KATSANEVAS, K., STEINBACH, A., LOU, U., SABBINENI, H., DEREMER, D. L. & SOMANATH, P. R. 2014. Targeting Src-mediated Tyr216 phosphorylation and activation of GSK-3 in prostate cancer cells inhibit prostate cancer progression in vitro and in vivo. *Oncotarget,* 5**,** 775-87.

GOLD, R., LEPOW, M. L., GOLDSCHNEIDER, I., DRAPER, T. L. & GOTSCHLICH, E. C. 1975. Clinical evaluation of group A and group C meningococcal polysaccharide vaccines in infants. *J Clin Invest,* 56**,** 1536-47.

GOLDSCHNEIDER, I., GOTSCHLICH, E. C. & ARTENSTEIN, M. S. 1969. Human immunity to the meningococcus: I. The role of humoral antibodies. *J Exp Med,* 129**,** 1307-1326.

GOLEBIOWSKI, F., MATIC, I., TATHAM, M. H., COLE, C., YIN, Y., NAKAMURA, A., COX, J., BARTON, G. J., MANN, M. & HAY, R. T. 2009. System-wide changes to SUMO modifications in response to heat shock. *Sci Signal,* 2**,** ra24.

GORRINGE, A. R. & PAJON, R. 2012. Bexsero: a multicomponent vaccine for prevention of meningococcal disease. *Hum Vaccin Immunother,* 8**,** 174-83.

GOTSCHLICH, E. C., GOLDSCHNEIDER, I. & ARTENSTEIN, M. S. 1969. Human immunity to the meningococcus: IV. Immunogenicity of group A and group C meningococcal polysaccharides in human volunteers. *J Exp Med,* 129**,** 1367-1384.

GRAY, M. C. & HEWLETT, E. L. 2011. Cell cycle arrest induced by the bacterial adenylate cyclase toxins from *Bacillus anthracis* and *Bordetella pertussis*. *Cell Microbiol,* 13**,** 123-34.

GREENWOOD, B. 1999. Meningococcal meningitis in Africa. *Trans R Soc Trop Med Hyg,* 93**,** 341-353.

GREENWOOD, B., BRADLEY, A., SMITH, A. & WALL, R. 1987. Mortality from meningococcal disease during an epidemic in The Gambia, West Africa. *Trans R Soc Trop Med Hyg,* 81**,** 536-538.

GRIFFISS, J., BRANDT, B., ALTIERI, P., PIER, G. & BERMAN, S. 1981. Safety and immunogenicity of group Y and group W135 meningococcal capsular polysaccharide vaccines in adults. *Infect Immun,* 34**,** 725-732.

HA, S.-D., NG, D., LAMOTHE, J., VALVANO, M. A., HAN, J. & KIM, S. O. 2007a. Mitochondrial proteins Bnip3 and Bnip3L are involved in anthrax lethal toxin-induced macrophage cell death. *J Biol Chem,* 282**,** 26275-26283.

HA, S. D., NG, D., PELECH, S. L. & KIM, S. O. 2007b. Critical role of the phosphatidylinositol 3-kinase/Akt/glycogen synthase kinase-3 signaling pathway in recovery from anthrax lethal toxin-induced cell cycle arrest and MEK cleavage in macrophages. *J Biol Chem,* 282**,** 36230-9.

HAAS, R. & MEYER, T. F. 1986. The repertoire of silent pilus genes in *Neisseria gonorrhoeae*: evidence for gene conversion. *Cell,* 44**,** 107-15.

HACKETT, S., GUIVER, M., MARSH, J., SILLS, J., THOMSON, A., KACZMARSKI, E. & HART, C. 2002. Meningococcal bacterial DNA load at presentation correlates with disease severity. *Arch Dis Child,* 86**,** 44-46.

HADWIGER, J. A., WITTENBERG, C., RICHARDSON, H. E., DE BARROS LOPES, M. & REED, S. I. 1989. A family of cyclin homologs that control the G1 phase in yeast. *Proc Natl Acad Sci U S A,* 86**,** 6255-6259.

HAHNE, S. J. M., GRAY, S. J., AGUILERA, J. F., CROWCROFT, N. S., NICHOLS, T., KACZMARSKI, E. B. & RAMSAY, M. E. 2002. W135 meningococcal disease in England and Wales associated with Hajj 2000 and 2001. *Lancet,* 359**,** 582-583.

HALL, M., BATES, S. & PETERS, G. 1995. Evidence for different modes of action of cyclin-dependent kinase inhibitors: p15 and p16 bind to kinases, p21 and p27 bind to cyclins. *Oncogene,* 11**,** 1581-1588.

HAMMERSCHMIDT, S., HILSE, R., VAN PUTTEN, J. P., GERARDY-SCHAHN, R., UNKMEIR, A. & FROSCH, M. 1996a. Modulation of cell surface sialic acid expression in *Neisseria meningitidis* via a transposable genetic element. *EMBO J,* 15**,** 192-8.

HAMMERSCHMIDT, S., MULLER, A., SILLMANN, H., MUHLENHOFF, M., BORROW, R., FOX, A., VAN PUTTEN, J., ZOLLINGER, W. D., GERARDY-SCHAHN, R. & FROSCH, M. 1996b. Capsule phase variation in *Neisseria meningitidis* serogroup B by slipped-strand mispairing in the polysialyltransferase gene (siaD): correlation with bacterial invasion and the outbreak of meningococcal disease. *Mol Microbiol,* 20**,** 1211-20.

HAN, X. Y., HONG, T. & FALSEN, E. 2006. *Neisseria bacilliformis* sp. nov. isolated from human infections. *J Clin Microbiol,* 44**,** 474-9.

HANKINS, W. A., GWALTNEY JR, J. M., HENDLEY, J. O., FARQUHAR, J. D. & SAMUELSON, J. S. 1982. Clinical and serological evaluation of a meningococcal polysaccharide vaccine groups A, C, Y, and W135. *Proc Natl Acad Sci U S A,* 169**,** 54-057.

HARPER, J. W., ELLEDGE, S. J., KEYOMARSI, K., DYNLACHT, B., TSAI, L.-H., ZHANG, P., DOBROWOLSKI, S., BAI, C., CONNELL-CROWLEY, L. & SWINDELL, E. 1995. Inhibition of cyclin-dependent kinases by p21. *Mol Biol Cell,* 6**,** 387-400.

HARWOOD, C. A., STEVENS, J. C., ORTON, D., BULL, R. C., PAIGE, D., LESSING, M. P., MORTIMER, P. S., MARSDEN, R. A. & CERIO, R. 2005. Chronic meningococcaemia: a forgotten meningococcal disease. *Br J Dermatol,* 153**,** 669-71.

HAUCK, L., HARMS, C., GROTHE, D., AN, J., GERTZ, K., KRONENBERG, G., DIETZ, R., ENDRES, M. & VON HARSDORF, R. 2007. Critical role for FoxO3a-dependent regulation of p21CIP1/WAF1 in response to statin signaling in cardiac myocytes. *Circ Res,* 100**,** 50-60.

HEMMINGS, B. A. & RESTUCCIA, D. F. 2012. PI3K-PKB/Akt pathway. *Cold Spring Harb Perspect Biol,* 4**,** a011189.

HENGST, L. & REED, S. 1998. Inhibitors of the Cip/Kip family. *Cyclin Dependent Kinase (CDK) Inhibitors.* Springer.

HILL, D. M., LUCIDARME, J., GRAY, S. J., NEWBOLD, L. S., URE, R., BREHONY, C., HARRISON, O. B., BRAY, J. E., JOLLEY, K. A., BRATCHER, H. B., PARKHILL, J., TANG, C. M., BORROW, R. & MAIDEN, M. C. 2015. Genomic epidemiology of age-associated meningococcal lineages in national surveillance: an observational cohort study. *Lancet Infect Dis,* 15**,** 1420-8.

HIRAI, H., SOOTOME, H., NAKATSURU, Y., MIYAMA, K., TAGUCHI, S., TSUJIOKA, K., UENO, Y., HATCH, H., MAJUMDER, P. K., PAN, B. S. & KOTANI, H. 2010. MK-2206, an allosteric Akt inhibitor, enhances antitumor efficacy by standard chemotherapeutic agents or molecular targeted drugs in vitro and in vivo. *Mol Cancer Ther,* 9**,** 1956-67.

HOFFMAN, O. & WEBER, R. J. 2009. Pathophysiology and treatment of bacterial meningitis. *Ther Adv Neurol Disord,* 2**,** 1-7.

HOLLIS, D. G., WIGGINS, G. L. & WEAVER, R. E. 1969. *Neisseria lactamicus* sp. n., a lactose-fermenting species resembling *Neisseria meningitidis*. *Appl Microbiol,* 17**,** 71-7.

HOPPER, S., VASQUEZ, B., MERZ, A., CLARY, S., WILBUR, J. S. & SO, M. 2000. Effects of the immunoglobulin A1 protease on *Neisseria gonorrhoeae* trafficking across polarized T84 epithelial monolayers. *Infect Immun,* 68**,** 906-11.

HOUDOUIN, V., BONACORSI, S., BIDET, P., BLANCO, J., DE LA ROCQUE, F., COHEN, R., AUJARD, Y. & BINGEN, E. 2008. Association between mortality of *Escherichia coli* meningitis in young infants and non-virulent clonal groups of strains. *Clin Microbiol Infect,* 14**,** 685-690.

HU, H., JUVEKAR, A., LYSSIOTIS, C. A., LIEN, E. C., ALBECK, J. G., OH, D., VARMA, G., HUNG, Y. P., ULLAS, S., LAURING, J., SETH, P., LUNDQUIST, M. R., TOLAN, D. R., GRANT, A. K., NEEDLEMAN, D. J., ASARA, J. M., CANTLEY, L. C. & WULF, G. M. 2016. Phosphoinositide 3-Kinase Regulates Glycolysis through Mobilization of Aldolase from the Actin Cytoskeleton. *Cell,* 164**,** 433-46.

HUNG, M. C. & CHRISTODOULIDES, M. 2013. The biology of *Neisseria* adhesins. *Biology (Basel),* 2**,** 1054-109.

IMBEAUD, S., GRAUDENS, E., BOULANGER, V., BARLET, X., ZABORSKI, P., EVENO, E., MUELLER, O., SCHROEDER, A. & AUFFRAY, C. 2005. Towards standardization of RNA quality assessment using user-independent classifiers of microcapillary electrophoresis traces. *Nucleic Acids Res,* 33**,** e56.

IMHAUS, A. F. & DUMENIL, G. 2014. The number of *Neisseria meningitidis* type IV pili determines host cell interaction. *EMBO J,* 33**,** 1767-83.

IRINO, K., VIEIRA, M. A. M., GOMES, T. A. T., GUTH, B. E. C., NAVES, Z. V. F., OLIVEIRA, M. G., DOS SANTOS, L. F., GUIRRO, M., TIMM, C. D. & PIGATTO, C. P. 2010. Subtilase cytotoxin-encoding subAB operon found exclusively among Shiga toxin-producing *Escherichia coli* strains. *J Clin Microbiol,* 48**,** 988-990.

IRWIN, S. W., AVERIL, N., CHENG, C. Y. & SCHRYVERS, A. B. 1993. Preparation and analysis of isogenic mutants in the transferrin receptor protein genes, tbpA and tbpB, from *Neisseria meningitidis*. *Mol Microbiol,* 8**,** 1125-1133.

JACINTO, E., FACCHINETTI, V., LIU, D., SOTO, N., WEI, S., JUNG, S. Y., HUANG, Q., QIN, J. & SU, B. 2006. SIN1/MIP1 maintains rictor-mTOR complex integrity and regulates Akt phosphorylation and substrate specificity. *Cell,* 127**,** 125-37.

JACKERS, P., MINOLETTI, F., BELOTTI, D., CLAUSSE, N., SOZZI, G., SOBEL, M. E. & CASTRONOVO, V. 1996. Isolation from a multigene family of the active human gene of the metastasis-associated multifunctional protein 37LRP/p40 at chromosome 3p21.3. *Oncogene,* 13**,** 495-503.

JAMIESON, K. V., WU, J., HUBBARD, S. R. & MERUELO, D. 2008. Crystal structure of the human laminin receptor precursor. *J Biol Chem,* 283**,** 3002-5.

JEFFREY, P. D., RUSSO, A. A., POLYAK, K., GIBBS, E., HURWITZ, J., MASSAGUÉ, J. & PAVLETICH, N. P. 1995. Mechanism of CDK activation revealed by the structure of a cyclinA-CDK2 complex. *Nature,* 376**,** 313.

JEN, F. E., WARREN, M. J., SCHULZ, B. L., POWER, P. M., SWORDS, W. E., WEISER, J. N., APICELLA, M. A., EDWARDS, J. L. & JENNINGS, M. P. 2013. Dual pili post-translational modifications synergize to mediate meningococcal adherence to platelet activating factor receptor on human airway cells. *PLoS Pathog,* 9**,** e1003377.

JENNINGS, H. J. 1983. Capsular polysaccharides as human vaccines. *Adv Carbohydr Chem Biochem,* 41**,** 155-208.

JETHWA, N., CHUNG, G. H., LETE, M. G., ALONSO, A., BYRNE, R. D., CALLEJA, V. & LARIJANI, B. 2015. Endomembrane PtdIns (3, 4, 5) P3 activates the PI3K–Akt pathway. *J Cell Sci,* 128**,** 3456-3465.

JIAO, P., ZHOU, Y. S., YANG, J. X., ZHAO, Y. L., LIU, Q. Q., YUAN, C. & WANG, F. Z. 2013. MK-2206 induces cell cycle arrest and apoptosis in HepG2 cells and sensitizes TRAIL-mediated cell death. *Mol Cell Biochem,* 382**,** 217-24.

JOLLEY, K. A., BRAY, J. E. & MAIDEN, M. C. J. 2018. Open-access bacterial population genomics: BIGSdb software, the PubMLST.org website and their applications. *Wellcome Open Res,* 3**,** 124.

JOLLEY, K. A., BREHONY, C. & MAIDEN, M. C. 2007. Molecular typing of meningococci: recommendations for target choice and nomenclature. *FEMS Microbiol Rev,* 31**,** 89-96.

JONES, A., JONSSON, A. B. & ARO, H. 2007. *Neisseria gonorrhoeae* infection causes a G1 arrest in human epithelial cells. *FASEB J,* 21**,** 345-55.

JOPE, R. S. & JOHNSON, G. V. 2004. The glamour and gloom of glycogen synthase kinase-3. *Trends Biochem Sci,* 29**,** 95-102.

JOVANOVIC, K., LOOS, B., DA COSTA DIAS, B., PENNY, C. & WEISS, S. F. 2014. High resolution imaging study of interactions between the 37 kDa/67 kDa laminin receptor and APP, beta-secretase and gamma-secretase in Alzheimer's disease. *PLoS One,* 9**,** e100373.

KAHLER, C. M., MARTIN, L. E., SHIH, G. C., RAHMAN, M. M., CARLSON, R. W. & STEPHENS, D. S. 1998. The (alpha2-->8)-linked polysialic acid capsule and lipooligosaccharide structure both contribute to the ability of serogroup B *Neisseria meningitidis* to resist the bactericidal activity of normal human serum. *Infect Immun,* 66**,** 5939-47.

KALLSTROM, H., ISLAM, M. S., BERGGREN, P. O. & JONSSON, A. B. 1998. Cell signaling by the type IV pili of pathogenic *Neisseria*. *J Biol Chem,* 273**,** 21777-82.

KALLSTROM, H., LISZEWSKI, M. K., ATKINSON, J. P. & JONSSON, A. B. 1997. Membrane cofactor protein (MCP or CD46) is a cellular pilus receptor for pathogenic *Neisseria*. *Mol Microbiol,* 25**,** 639-47.

KANEDA, Y., KINOSHITA, K., SATO, M., SAEKI, Y., YAMADA, R., WATAYA-KANEDA, M. & TANAKA, K. 1998. The induction of apoptosis in HeLa cells by the loss of LBP-p40. *Cell Death Differ,* 5**,** 20-8.

KANOVA, E., JIMENEZ-MUNGUIA, I., MAJEROVA, P., TKACOVA, Z., BHIDE, K., MERTINKOVA, P., PULZOVA, L., KOVAC, A. & BHIDE, M. 2018. Deciphering the Interactome of *Neisseria meningitidis* With Human Brain Microvascular Endothelial Cells. *Front Microbiol,* 9**,** 2294.

KATO, J., MATSUSHIME, H., HIEBERT, S. W., EWEN, M. E. & SHERR, C. J. 1993. Direct binding of cyclin D to the retinoblastoma gene product (pRb) and pRb phosphorylation by the cyclin D-dependent kinase CDK4. *Genes Dev,* 7**,** 331-331.

KATO, J. Y., MATSUOKA, M., STROM, D. K. & SHERR, C. J. 1994. Regulation of cyclin D-dependent kinase 4 (cdk4) by cdk4-activating kinase. *Mol Cell Biol,* 14**,** 2713-21.

KATTNER, C., TOUSSI, D. N., ZAUCHA, J., WETZLER, L. M., RUPPEL, N., ZACHARIAE, U., MASSARI, P. & TANABE, M. 2014. Crystallographic analysis of *Neisseria meningitidis* PorB extracellular loops potentially implicated in TLR2 recognition. *J Struct Biol,* 185**,** 440-7.

KAZMIN, D. A., HOYT, T. R., TAUBNER, L., TEINTZE, M. & STARKEY, J. R. 2000. Phage display mapping for peptide 11 sensitive sequences binding to laminin-1. *J Mol Biol,* 298**,** 431-45.

KENDRICK, N. 2014. A gene's mRNA level does not usually predict its protein level. *In:* KENDRICK LABS, I. (ed.). Madison.

KEYSERLING, H., PAPA, T., KORANYI, K., RYALL, R., BASSILY, E., BYBEL, M. J., SULLIVAN, K., GILMET, G. & REINHARDT, A. 2005. Safety, immunogenicity, and immune memory of a novel meningococcal (groups A, C, Y, and W-135) polysaccharide diphtheria toxoid conjugate vaccine (MCV-4) in healthy adolescents. *Arch Pediatr Adolesc Med,* 159**,** 907-913.

KHAIRALLA, A. S., OMER, S. A., MAHDAVI, J., ASLAM, A., DUFAILU, O. A., SELF, T., JONSSON, A. B., GEORG, M., SJOLINDER, H., ROYER, P. J., MARTINEZ-POMARES, L., GHAEMMAGHAMI, A. M., WOOLDRIDGE, K. G., OLDFIELD, N. J. & ALA'ALDEEN, D. A. 2015. Nuclear trafficking, histone cleavage and induction of apoptosis by the meningococcal App and MspA autotransporters. *Cell Microbiol,* 17**,** 1008-20.

KIERBEL, A., GASSAMA-DIAGNE, A., ROCHA, C., RADOSHEVICH, L., OLSON, J., MOSTOV, K. & ENGEL, J. 2007. *Pseudomonas aeruginosa* exploits a PIP3-dependent pathway to transform apical into basolateral membrane. *J Cell Biol,* 177**,** 21-7.

KIM, K., LI, L., KOZLOWSKI, K., SUH, H. S., CAO, W. & BALLERMANN, B. J. 2005a. The protein phosphatase-1 targeting subunit TIMAP regulates LAMR1 phosphorylation. *Biochem Biophys Res Commun,* 338**,** 1327-34.

KIM, K. J., CHUNG, J. W. & KIM, K. S. 2005b. 67-kDa laminin receptor promotes internalization of cytotoxic necrotizing factor 1-expressing *Escherichia coli* K1 into human brain microvascular endothelial cells. *J Biol Chem,* 280**,** 1360-1368.

KING, R. W., JACKSON, P. K. & KIRSCHNER, M. W. 1994. Mitosis in transition. *Cell,* 79**,** 563-571.

KINOSHITA, K., KANEDA, Y., SATO, M., SAEKI, Y., WATAYA-KANEDA, M. & HOFFMANN, A. 1998. LBP-p40 binds DNA tightly through associations with histones H2A, H2B, and H4. *Biochem Biophys Res Commun,* 253**,** 277-82.

KIRSCH, E. A., BARTON, R. P., KITCHEN, L. & GIROIR, B. P. 1996. Pathophysiology, treatment and outcome of meningococcemia: a review and recent experience. *Pediatr Infect Dis J,* 15**,** 967-979.

KNAPP, J. S., TOTTEN, P. A., MULKS, M. H. & MINSHEW, B. H. 1984. Characterization of *Neisseria cinerea*, a nonpathogenic species isolated on Martin-Lewis medium selective for pathogenic *Neisseria* spp. *J Clin Microbiol,* 19**,** 63-7.

KOLB-MAURER, A., UNKMEIR, A., KAMMERER, U., HUBNER, C., LEIMBACH, T., STADE, A., KAMPGEN, E., FROSCH, M. & DIETRICH, G. 2001. Interaction of *Neisseria meningitidis* with human dendritic cells. *Infect Immun,* 69**,** 6912-22.

KONG, D. & YAMORI, T. 2007. ZSTK474 is an ATP-competitive inhibitor of class I phosphatidylinositol 3 kinase isoforms. *Cancer Sci,* 98**,** 1638-42.

KONG, D. X. & YAMORI, T. 2010. ZSTK474, a novel phosphatidylinositol 3-kinase inhibitor identified using the JFCR39 drug discovery system. *Acta Pharmacol Sin,* 31**,** 1189-97.

KOPAN, R. 2012. Notch signaling. *Cold Spring Harb Perspect Biol,* 4.

KRACHLER, A. M., WOOLERY, A. R. & ORTH, K. 2011. Manipulation of kinase signaling by bacterial pathogens. *J Cell Biol,* 195**,** 1083-92.

KUNICK, C., LAUENROTH, K., LEOST, M., MEIJER, L. & LEMCKE, T. 2004. 1-Azakenpaullone is a selective inhibitor of glycogen synthase kinase-3 beta. *Bioorg Med Chem Lett,* 14**,** 413-6.

KURZAI, O., SCHMITT, C., CLAUS, H., VOGEL, U., FROSCH, M. & KOLB-MAURER, A. 2005. Carbohydrate composition of meningococcal lipopolysaccharide modulates the interaction of *Neisseria meningitidis* with human dendritic cells. *Cell Microbiol,* 7**,** 1319-34.

LAFORCE, F. M. & OKWO-BELE, J.-M. 2011. Eliminating epidemic group A meningococcal meningitis in Africa through a new vaccine. *Health Aff (Millwood),* 30**,** 1049-1057.

LAMBOTIN, M., HOFFMANN, I., LARAN-CHICH, M. P., NASSIF, X., COURAUD, P. O. & BOURDOULOUS, S. 2005. Invasion of endothelial cells by *Neisseria meningitidis* requires cortactin recruitment by a phosphoinositide-3-kinase/Rac1 signalling pathway triggered by the lipo-oligosaccharide. *J Cell Sci,* 118**,** 3805-16.

LAROCHELLE, S., PANDUR, J., FISHER, R. P., SALZ, H. K. & SUTER, B. 1998. Cdk7 is essential for mitosis and for in vivo Cdk-activating kinase activity. *Genes Dev,* 12**,** 370-81.

LEE, M.-H., REYNISDOTTIR, I. & MASSAGUE, J. 1995. Cloning of p57KIP2, a cyclin-dependent kinase inhibitor with unique domain structure and tissue distribution. *Genes Dev,* 9**,** 639-649.

LEEVERS, S. J., VANHAESEBROECK, B. & WATERFIELD, M. D. 1999. Signalling through phosphoinositide 3-kinases: the lipids take centre stage. *Curr Opin Cell Biol,* 11**,** 219-25.

LEGGIADRO, R. J., BADDOUR, L. M., FRASCH, C. E., LAFRAIN, J. F., GAIA, S. M. & THOMAS, J. A. 1989. Invasive meningococcal disease: secondary spread in a day-care center. *South Med J,* 82**,** 511-3.

LEMMON, M. A. & SCHLESSINGER, J. 2010. Cell signaling by receptor tyrosine kinases. *Cell,* 141**,** 1117-34.

LESOT, H., KUHL, U. & MARK, K. 1983. Isolation of a laminin-binding protein from muscle cell membranes. *EMBO J,* 2**,** 861-5.

LEWIS, L. A., GRAY, E., WANG, Y. P., ROE, B. A. & DYER, D. W. 1997. Molecular characterization of hpuAB, the haemoglobin-haptoglobin-utilization operon of *Neisseria meningitidis*. *Mol Microbiol,* 23**,** 737-49.

LEWIS, L. A., VU, D. M., GRANOFF, D. M. & RAM, S. 2014. Inhibition of the alternative pathway of nonhuman infant complement by porin B2 contributes to virulence of *Neisseria meningitidis* in the infant rat model. *Infect Immun,* 82**,** 2574-84.

LEWIS, S., SADARANGANI, M., HOE, J. C. & POLLARD, A. J. 2009. Challenges and progress in the development of a serogroup B meningococcal vaccine. *Expert Rev Vaccines,* 8**,** 729-745.

LI, L., KOZLOWSKI, K., WEGNER, B., RASHID, T., YEUNG, T., HOLMES, C. & BALLERMANN, B. J. 2007a. Phosphorylation of TIMAP by glycogen synthase kinase-3beta activates its associated protein phosphatase 1. *J Biol Chem,* 282**,** 25960-9.

LI, Y., YIN, W., WANG, X., ZHU, W., HUANG, Y. & YAN, G. 2007b. Cholera toxin induces malignant glioma cell differentiation via the PKA/CREB pathway. *Proc Natl Acad Sci U S A,* 104**,** 13438-43.

LIAO, Y. & HUNG, M. C. 2010. Physiological regulation of Akt activity and stability. *Am J Transl Res,* 2**,** 19-42.

LIN, D. I., BARBASH, O., KUMAR, K. G., WEBER, J. D., HARPER, J. W., KLEIN-SZANTO, A. J., RUSTGI, A., FUCHS, S. Y. & DIEHL, J. A. 2006. Phosphorylation-dependent ubiquitination of cyclin D1 by the SCF(FBX4-alphaB crystallin) complex. *Mol Cell,* 24**,** 355-66.

LINGAPPA, J. R., AL-RABEAH, A. M., HAJJEH, R., MUSTAFA, T., FATANI, A., AL-BASSAM, T., BADUKHAN, A., TURKISTANI, A., AL-HAMDAN, N., AL-JEFFRI, M., AL MAZROU, Y., PERKINS, B. A., POPOVIC, T., MAYER, L. W. & ROSENSTEIN, N. E. 2003. Serogroup W-135 meningococcal disease during the Hajj, 2000. *Emerg Infect Dis,* 9**,** 665-671.

LIU, J.-L., GAO, G.-R., ZHANG, X., CAO, S.-F., GUO, C.-L., WANG, X., TONG, L.-J., DING, J., DUAN, W.-H. & MENG, L.-H. 2014. DW09849, a Selective Phosphatidylinositol 3-Kinase (PI3K) Inhibitor, Prevents PI3K Signaling and Preferentially Inhibits Proliferation of Cells Containing the Oncogenic Mutation p110α (H1047R). *J Pharmacol Exp Ther,* 348**,** 432-441.

LIU, J. & KIPREOS, E. T. 2000-2003. The evolution of CDK-activating kinases. *Madame Curie Bioscience Database [internet].* Austin (TX): Landes Bioscience.

LIU, Y., BEYER, A. & AEBERSOLD, R. 2016. On the Dependency of Cellular Protein Levels on mRNA Abundance. *Cell,* 165**,** 535-50.

LIVAK, K. J. & SCHMITTGEN, T. D. 2001. Analysis of relative gene expression data using real-time quantitative PCR and the 2(-Delta Delta C(T)) Method. *Methods,* 25**,** 402-8.

LOCHHEAD, P. A., KINSTRIE, R., SIBBET, G., RAWJEE, T., MORRICE, N. & CLEGHON, V. 2006. A chaperone-dependent GSK3beta transitional intermediate mediates activation-loop autophosphorylation. *Mol Cell,* 24**,** 627-33.

LUDWIG, G. V., KONDIG, J. P. & SMITH, J. F. 1996. A putative receptor for Venezuelan equine encephalitis virus from mosquito cells. *J Virol,* 70**,** 5592-9.

MADICO, G., WELSCH, J. A., LEWIS, L. A., MCNAUGHTON, A., PERLMAN, D. H., COSTELLO, C. E., NGAMPASUTADOL, J., VOGEL, U., GRANOFF, D. M. & RAM, S. 2006. The meningococcal vaccine candidate GNA1870 binds the complement regulatory protein factor H and enhances serum resistance. *J Immunol,* 177**,** 501-10.

MAEHAMA, T. & DIXON, J. E. 1998. The tumor suppressor, PTEN/MMAC1, dephosphorylates the lipid second messenger, phosphatidylinositol 3,4,5-trisphosphate. *J Biol Chem,* 273**,** 13375-8.

MAIDEN, M. C., BYGRAVES, J. A., FEIL, E., MORELLI, G., RUSSELL, J. E., URWIN, R., ZHANG, Q., ZHOU, J., ZURTH, K., CAUGANT, D. A., FEAVERS, I. M., ACHTMAN, M. & SPRATT, B. G. 1998. Multilocus sequence typing: a portable approach to the identification of clones within populations of pathogenic microorganisms. *Proc Natl Acad Sci U S A,* 95**,** 3140-5.

MAIDEN, M. C., STUART, J. M. & GROUP, U. M. C. 2002. Carriage of serogroup C meningococci 1 year after meningococcal C conjugate polysaccharide vaccination. *Lancet,* 359**,** 1829-1830.

MALINOFF, H. L. & WICHA, M. S. 1983. Isolation of a cell surface receptor protein for laminin from murine fibrosarcoma cells. *J Cell Biol,* 96**,** 1475-9.

MALYGIN, A. A., BABAYLOVA, E. S., LOKTEV, V. B. & KARPOVA, G. G. 2011. A region in the C-terminal domain of ribosomal protein SA required for binding of SA to the human 40S ribosomal subunit. *Biochimie,* 93**,** 612-7.

MANNING, B. D. & TOKER, A. 2017. AKT/PKB Signaling: Navigating the Network. *Cell,* 169**,** 381-405.

MANUEL L, F. G., RAMOS, J. M., NÚÑEZ, A., CUENCA, M. & DE GÓRGOLAS, M. 1997. Focal infections due to non-typhi *Salmonella* in patients with AIDS: report of 10 cases and review. *Clin Infect Dis,* 25**,** 690-697.

MANZA, L. L., CODREANU, S. G., STAMER, S. L., SMITH, D. L., WELLS, K. S., ROBERTS, R. L. & LIEBLER, D. C. 2004. Global shifts in protein sumoylation in response to electrophile and oxidative stress. *Chem Res Toxicol,* 17**,** 1706-15.

MARCHES, O., LEDGER, T. N., BOURY, M., OHARA, M., TU, X., GOFFAUX, F., MAINIL, J., ROSENSHINE, I., SUGAI, M., DE RYCKE, J. & OSWALD, E. 2003. Enteropathogenic and enterohaemorrhagic *Escherichia coli* deliver a novel effector called Cif, which blocks cell cycle G2/M transition. *Mol Microbiol,* 50**,** 1553-67.

MARTIGNONE, S., MENARD, S., BUFALINO, R., CASCINELLI, N., PELLEGRINI, R., TAGLIABUE, E., ANDREOLA, S., RILKE, F. & COLNAGHI, M. I. 1993. Prognostic significance of the 67-kilodalton laminin receptor expression in human breast carcinomas. *J Natl Cancer Inst,* 85**,** 398-402.

MARUVADA, R. & KIM, K. S. 2011. Extracellular loops of the *Eschericia coli* outer membrane protein A contribute to the pathogenesis of meningitis. *J Infect Dis,* 203**,** 131-40.

MASSARI, P., GUNAWARDANA, J., LIU, X. & WETZLER, L. M. 2010. Meningococcal porin PorB prevents cellular apoptosis in a toll-like receptor 2- and NF-kappaB-independent manner. *Infect Immun,* 78**,** 994-1003.

MASSARI, P., HENNEKE, P., HO, Y., LATZ, E., GOLENBOCK, D. T. & WETZLER, L. M. 2002. Cutting edge: Immune stimulation by neisserial porins is toll-like receptor 2 and MyD88 dependent. *J Immunol,* 168**,** 1533-1537.

MASSARI, P., KING, C. A., HO, A. Y. & WETZLER, L. M. 2003. Neisserial PorB is translocated to the mitochondria of HeLa cells infected with *Neisseria meningitidis* and protects cells from apoptosis. *Cell Microbiol,* 5**,** 99-109.

MASSARI, P., VISINTIN, A., GUNAWARDANA, J., HALMEN, K. A., KING, C. A., GOLENBOCK, D. T. & WETZLER, L. M. 2006. Meningococcal porin PorB binds to TLR2 and requires TLR1 for signaling. *J Immunol,* 176**,** 2373-80.

MCNEIL, L. K., ZAGURSKY, R. J., LIN, S. L., MURPHY, E., ZLOTNICK, G. W., HOISETH, S. K., JANSEN, K. U. & ANDERSON, A. S. 2013. Role of factor H binding protein in *Neisseria meningitidis* virulence and its potential as a vaccine candidate to broadly protect against meningococcal disease. *Microbiol Mol Biol Rev,* 77**,** 234-52.

MEDEMA, R. H., KOPS, G. J., BOS, J. L. & BURGERING, B. M. 2000. AFX-like Forkhead transcription factors mediate cell-cycle regulation by Ras and PKB through p27kip1. *Nature,* 404**,** 782-7.

MÉNARD, S., TAGLIABUE, E. & COLNAGHI, M. I. 1998. The 67 kDa laminin receptor as a prognostic factor in human cancer. *Breast Cancer Res Treat,* 52**,** 137-145.

MEYER, J., BRISSAC, T., FRAPY, E., OMER, H., EUPHRASIE, D., BONAVITA, A., NASSIF, X. & BILLE, E. 2016. Characterization of MDAPhi, a temperate filamentous bacteriophage of *Neisseria meningitidis*. *Microbiology,* 162**,** 268-82.

MILLAR, J. W., SIESS, E. E., FELDMAN, H. A., SILVERMAN, C. & FRANK, P. 1963. In vivo and in vitro resistance to sulfadiazine in strains of *Neisseria meningitidis*. *Jama,* 186**,** 139-141.

MILLER, E., SALISBURY, D. & RAMSAY, M. 2001. Planning, registration, and implementation of an immunisation campaign against meningococcal serogroup C disease in the UK: a success story. *Vaccine,* 20**,** S58-S67.

MILLER, J. M., BINNICKER, M. J., CAMPBELL, S., CARROLL, K. C., CHAPIN, K. C., GILLIGAN, P. H., GONZALEZ, M. D., JERRIS, R. C., KEHL, S. C. & PATEL, R. 2018. A guide to utilization of the microbiology laboratory for diagnosis of infectious diseases: 2018 update by the Infectious Diseases Society of America and the American Society for Microbiology. *Clin Infect Dis,* 67**,** e1-e94.

MINETTI, C. A., BLAKE, M. S. & REMETA, D. P. 1998. Characterization of the structure, function, and conformational stability of PorB class 3 protein from *Neisseria meningitidis*. A porin with unusual physicochemical properties. *J Biol Chem,* 273**,** 25329-38.

MITTAL, R., KRISHNAN, S., GONZALEZ-GOMEZ, I. & PRASADARAO, N. V. 2011. Deciphering the roles of outer membrane protein A extracellular loops in the pathogenesis of *Escherichia coli* K1 meningitis. *J Biol Chem,* 286**,** 2183-2193.

MONTANARI, P., BOZZA, G., CAPECCHI, B., CAPRONI, E., BARRILE, R., NORAIS, N., CAPITANI, M., SALLESE, M., CECCHINI, P. & CIUCCHI, L. 2012. Human heat shock protein (Hsp) 90 interferes with *Neisseria meningitidis* adhesin A (NadA)-mediated adhesion and invasion. *Cell Microbiol,* 14**,** 368-385.

MONTUORI, N., MÜLLER, F., DE RIU, S., FENZI, G., SOBEL, M. E., ROSSI, G. & VITALE, M. 1999. Laminin receptors in differentiated thyroid tumors: restricted expression of the 67-kilodalton laminin receptor in follicular carcinoma cells. *J Clin Endocrinol Metab,* 84**,** 2086-2092.

MORGAN, D. O. 1995. Principles of CDK regulation. *Nature,* 374**,** 131.
MORINAGA, N., YAHIRO, K., MATSUURA, G., MOSS, J. & NODA, M. 2008. Subtilase cytotoxin, produced by Shiga-toxigenic *Escherichia coli*, transiently inhibits protein synthesis of Vero cells via degradation of BiP and induces cell cycle arrest at G1 by downregulation of cyclin D1. *Cell Microbiol,* 10**,** 921-9.
MORRISON, D. K. 2012. MAP kinase pathways. *Cold Spring Harb Perspect Biol,* 4**,** a011254.
MUENZNER, P., DEHIO, C., FUJIWARA, T., ACHTMAN, M., MEYER, T. F. & GRAY-OWEN, S. D. 2000. Carcinoembryonic antigen family receptor specificity of *Neisseria meningitidis* Opa variants influences adherence to and invasion of proinflammatory cytokine-activated endothelial cells. *Infect Immun,* 68**,** 3601-3607.
MULLER, A., GUNTHER, D., DUX, F., NAUMANN, M., F.MEYER, T. & RUDEL, T. 1999. Neisserial porin (PorB) causes rapid calcium influx in target cells and induces apoptosis by the activation of cysteine proteases. *EMBO J,* 18**,** 339-352.
MUSSMANN, R., GEESE, M., HARDER, F., KEGEL, S., ANDAG, U., LOMOW, A., BURK, U., ONICHTCHOUK, D., DOHRMANN, C. & AUSTEN, M. 2007. Inhibition of GSK3 promotes replication and survival of pancreatic beta cells. *J Biol Chem,* 282**,** 12030-7.
NADEL, S. & KROLL, J. S. 2007. Diagnosis and management of meningococcal disease: the need for centralized care. *FEMS Microbiol Rev,* 31**,** 71-83.
NAGAHARA, H., VOCERO-AKBANI, A. M., SNYDER, E. L., HO, A., LATHAM, D. G., LISSY, N. A., BECKER-HAPAK, M., EZHEVSKY, S. A. & DOWDY, S. F. 1998. Transduction of full-length TAT fusion proteins into mammalian cells: TAT-p27 Kip1 induces cell migration. *Nat Med,* 4**,** 1449.
NAGATA, S. 1997. Apoptosis by death factor. *Cell,* 88**,** 355-65.
NAGELE, V., HEESEMANN, J., SCHIELKE, S., JIMENEZ-SOTO, L. F., KURZAI, O. & ACKERMANN, N. 2011. *Neisseria meningitidis* adhesin NadA targets beta1 integrins: functional similarity to Yersinia invasin. *J Biol Chem,* 286**,** 20536-46.
NAUMANN, M., RUDEL, T. & MEYER, T. F. 1999. Host cell interactions and signalling with *Neisseria gonorrhoeae*. *Curr Opin Microbiol,* 2**,** 62-70.
NEDELEC, J., BOURCRAUT, J., GARNIER, J. & ROUGON, G. 1990. Evidence for autoimmune antibodies directed against embryonic neural cell adhesion molecules (N-CAM) in patients with group B meningitis. *J Neuroimmunol,* 29**,** 49-56.
NEISSER, A. 1879. Über eine der Gonorrhoe eigentümliche Micrococcus Form. *Centralblatt für medizinische Wissenschaf,* 17**,** 497-500.
NICHOLS, J. M., MAIELLARO, I., ABI-JAOUDE, J., CURCI, S. & HOFER, A. M. 2015. "Store-operated" cAMP signaling contributes to Ca2+-activated Cl- secretion in T84 colonic cells. *Am J Physiol Gastrointest Liver Physiol,* 309**,** G670-9.
NIGROVIC, L. E., KUPPERMANN, N., MALLEY, R. & PEDIATRICS, B. M. S. G. O. T. P. E. M. C. R. C. O. T. A. A. O. 2008. Children with bacterial meningitis presenting to the emergency department during the pneumococcal conjugate vaccine era. *Acad Emerg Med,* 15**,** 522-528.
NITULESCU, G. M., MARGINA, D., JUZENAS, P., PENG, Q., OLARU, O. T., SALOUSTROS, E., FENGA, C., SPANDIDOS, D. A., LIBRA, M. & TSATSAKIS, A. M. 2016. Akt inhibitors in cancer treatment: The long journey from drug discovery to clinical use (Review). *Int J Oncol,* 48**,** 869-885.

NOUGAYREDE, J. P., TAIEB, F., DE RYCKE, J. & OSWALD, E. 2005. Cyclomodulins: bacterial effectors that modulate the eukaryotic cell cycle. *Trends Microbiol,* 13**,** 103-10.

NUDELMAN, Y. & TUNKEL, A. R. 2009. Bacterial meningitis. *Drugs,* 69**,** 2577-2596.

NUSSE, R. 2012. Wnt signaling. *Cold Spring Harb Perspect Biol,* 4.

O'DONOHUE, M. F., CHOESMEL, V., FAUBLADIER, M., FICHANT, G. & GLEIZES, P. E. 2010. Functional dichotomy of ribosomal proteins during the synthesis of mammalian 40S ribosomal subunits. *J Cell Biol,* 190**,** 853-66.

O'NEAL, C. J., JOBLING, M. G., HOLMES, R. K. & HOL, W. G. 2005. Structural basis for the activation of cholera toxin by human ARF6-GTP. *Science,* 309**,** 1093-1096.

OHGA, S., AOKI, T., OKADA, K., AKEDA, H., FUJIOKA, K., OHSHIMA, A., MORI, T., MINAMISHIMA, I. & UEDA, K. 1994. Cerebrospinal fluid concentrations of interleukin-1 beta, tumour necrosis factor-alpha, and interferon gamma in bacterial meningitis. *Arch Dis Child,* 70**,** 123-5.

OHTSUBO, M., THEODORAS, A. M., SCHUMACHER, J., ROBERTS, J. M. & PAGANO, M. 1995. Human cyclin E, a nuclear protein essential for the G1-to-S phase transition. *Mol Cell Biol,* 15**,** 2612-2624.

OKAMOTO, K. & BEACH, D. 1994. Cyclin G is a transcriptional target of the p53 tumor suppressor protein. *EMBO J,* 13**,** 4816-4822.

OLDFIELD, N. J. & ALA'ALDEEN, D. A. A. 2012. *Neisseria and Moraxella: Meningitis, septicaemia, gonorrhoea, respiratory infections*.

OLDFIELD, N. J., BLAND, S. J., TARAKTSOGLOU, M., DOS RAMOS, F. J., ROBINSON, K., WOOLDRIDGE, K. G. & ALA'ALDEEN, D. A. 2007. T-cell stimulating protein A (TspA) of *Neisseria meningitidis* is required for optimal adhesion to human cells. *Cell Microbiol,* 9**,** 463-78.

OLDFIELD, N. J., MATAR, S., BIDMOS, F. A., ALAMRO, M., NEAL, K. R., TURNER, D. P., BAYLISS, C. D. & ALA'ALDEEN, D. A. 2013. Prevalence and phase variable expression status of two autotransporters, NalP and MspA, in carriage and disease isolates of *Neisseria meningitidis*. *PLoS One,* 8**,** e69746.

OOSTHUYSEN, W. F., MUELLER, T., DITTRICH, M. T. & SCHUBERT-UNKMEIR, A. 2016. *Neisseria meningitidis* causes cell cycle arrest of human brain microvascular endothelial cells at S phase via p21 and cyclin G2. *Cell Microbiol,* 18**,** 46-65.

ORIHUELA, C. J., MAHDAVI, J., THORNTON, J., MANN, B., WOOLDRIDGE, K. G., ABOUSEADA, N., OLDFIELD, N. J., SELF, T., ALA'ALDEEN, D. A. & TUOMANEN, E. I. 2009. Laminin receptor initiates bacterial contact with the blood brain barrier in experimental meningitis models. *J Clin Invest,* 119**,** 1638-46.

OVIEDO-BOYSO, J., CORTES-VIEYRA, R., HUANTE-MENDOZA, A., YU, H. B., VALDEZ-ALARCON, J. J., BRAVO-PATINO, A., CAJERO-JUAREZ, M., FINLAY, B. B. & BAIZABAL-AGUIRRE, V. M. 2011. The phosphoinositide-3-kinase-Akt signaling pathway is important for *Staphylococcus aureus* internalization by endothelial cells. *Infect Immun,* 79**,** 4569-77.

ØVSTEBØ, R., BRANDTZAEG, P., BRUSLETTO, B., HAUG, K. B. F., LANDE, K., HØIBY, E. A. & KIERULF, P. 2004. Use of robotized DNA isolation and real-time PCR to quantify and identify close correlation between levels of *Neisseria meningitidis* DNA and lipopolysaccharides in plasma and cerebrospinal fluid from patients with systemic meningococcal disease. *J Clin Microbiol,* 42**,** 2980-2987.

PALOMO, V., SOTERAS, I., PEREZ, D. I., PEREZ, C., GIL, C., CAMPILLO, N. E. & MARTINEZ, A. 2011. Exploring the binding sites of glycogen

synthase kinase 3. Identification and characterization of allosteric modulation cavities. *J Med Chem,* 54**,** 8461-70.
PANDEY, M. K. & DEGRADO, T. R. 2016. Glycogen Synthase Kinase-3 (GSK-3)-Targeted Therapy and Imaging. *Theranostics,* 6**,** 571-93.
PARDEE, A., DUBROW, R., HAMLIN, J. & KLETZIEN, R. 1978. Animal cell cycle. *Annu Rev Biochem,* 47**,** 715-750.
PATHAN, N., FAUST, S. N. & LEVIN, M. 2003. Pathophysiology of meningococcal meningitis and septicaemia. *Arch Dis Child,* 88**,** 601-7.
PATON, A. W., SRIMANOTE, P., TALBOT, U. M., WANG, H. & PATON, J. C. 2004. A new family of potent AB(5) cytotoxins produced by Shiga toxigenic *Escherichia coli*. *J Exp Med,* 200**,** 35-46.
PAULOVICH, A. G. & HARTWELL, L. H. 1995. A checkpoint regulates the rate of progression through S phase in *S. cerevisiae* in response to DNA damage. *Cell,* 82**,** 841-847.
PAVLETICH, N. P. 1999. Mechanisms of cyclin-dependent kinase regulation: structures of Cdks, their cyclin activators, and Cip and INK4 inhibitors. *J Mol Biol,* 287**,** 821-828.
PELLEGRINI, R., MARTIGNONE, S., MÉNARD, S. & COLNAGHI, M. I. 1994. Laminin receptor expression and function in small-cell lung carcinoma. *Int J Cancer,* 57**,** 116-120.
PENG, J., MARSHALL, N. F. & PRICE, D. H. 1998. Identification of a Cyclin Subunit Required for the Function of *Drosophila* P-TEFb. *J Biol Chem,* 273**,** 13855-13860.
PERKINS-BALDING, D., RATLIFF-GRIFFIN, M. & STOJILJKOVIC, I. 2004. Iron transport systems in *Neisseria meningitidis*. *Microbiol Mol Biol Rev,* 68**,** 154-71.
PETTERSSON, A., MAAS, A. & TOMMASSEN, J. 1994. Identification of the iroA gene product of *Neisseria meningitidis* as a lactoferrin receptor. *J Bacteriol,* 176**,** 1764-6.
PETTERSSON, A., MAAS, A., VAN WASSENAAR, D., VAN DER LEY, P. & TOMMASSEN, J. 1995. Molecular characterization of FrpB, the 70-kilodalton iron-regulated outer membrane protein of *Neisseria meningitidis*. *Infect Immun,* 63**,** 4181-4184.
PETTERSSON, A., PRINZ, T., UMAR, A., VAN DER BIEZEN, J. & TOMMASSEN, J. 1998. Molecular characterization of LbpB, the second lactoferrin-binding protein of *Neisseria meningitidis*. *Mol Microbiol,* 27**,** 599-610.
PINES, J. 1991. Cyclins: wheels within wheels. *Cell Growth Differ,* 2**,** 305-310.
PINES, J. 1995. Cyclins and cyclin-dependent kinases: theme and variations. *Adv Cancer Res.* Elsevier.
POLLARD, A. J. 2011. Infectious disease: childhood meningitis may be preventable if we can afford it. *Nat Rev Neurol,* 7**,** 539-40.
POLYAK, K., LEE, M.-H., ERDJUMENT-BROMAGE, H., KOFF, A., ROBERTS, J. M., TEMPST, P. & MASSAGUÉ, J. 1994. Cloning of p27Kip1, a cyclin-dependent kinase inhibitor and a potential mediator of extracellular antimitogenic signals. *Cell,* 78**,** 59-66.
PRESCOTT, D. M. 1976. The cell cycle and the control of cellular reproduction. *Adv Genet.* Elsevier.
PRINCE, S. M., ACHTMAN, M. & DERRICK, J. P. 2002. Crystal structure of the OpcA integral membrane adhesin from *Neisseria meningitidis*. *Proc Natl Acad Sci U S A,* 99**,** 3417-3421.
PRINZ, T., MEYER, M., PETTERSSON, A. & TOMMASSEN, J. 1999. Structural characterization of the lactoferrin receptor from *Neisseria meningitidis*. *J Bacteriol,* 181**,** 4417-9.
PROTOPOPOVA, E. V., SOROKIN, A. V., KONOVALOVA, S. N., KACHKO, A. V., NETESOV, S. V. & LOKTEV, V. B. 1999. Human laminin binding

protein as a cell receptor for the tick-borne encephalitis virus. *Zentralbl Bakteriol,* 289**,** 632-638.

PUBLIC HEALTH ENGLAND 2015. New meningococcal vaccination programme expected to save lives. *The MenACWY vaccination programme is beginning with the vaccination of teenagers aged between 17 and 18 years old.* London: PHE Press Office, infections.

PUBLIC HEALTH ENGLAND 2018. Invasive meningococcal disease in England: annual laboratory confirmed reports for epidemiological year 2017 to 2018. *Health Protection Report.* London: PHE publications.

QARANI, S. 2015. *Investigation of the role of the non-integrin laminin receptor in the pathogenesis of bacterial meningitis.* PhD, University of Nottingham.

RAMSAY, M., KACZMARSKI, E., RUSH, M., MALLARD, R., FARRINGTON, P. & WHITE, J. 1997. Changing patterns of case ascertainment and trends in meningococcal disease in England and Wales. *Commun Dis Rep CDR Rev,* 7**,** R49-54.

RAO, C. N., CASTRONOVO, V., SCHMITT, M. C., WEWER, U. M., CLAYSMITH, A. P., LIOTTA, L. A. & SOBEL, M. E. 1989. Evidence for a precursor of the high-affinity metastasis-associated murine laminin receptor. *Biochemistry,* 28**,** 7476-86.

RAO, N. C., BARSKY, S. H., TERRANOVA, V. P. & LIOTTA, L. A. 1983. Isolation of a tumor cell laminin receptor. *Biochem Biophys Res Commun,* 111**,** 804-8.

READ, R. C. 2014. *Neisseria meningitidis*; clones, carriage, and disease. *Clin Microbiol Infect,* 20**,** 391-5.

RECHSTEINER, M. & ROGERS, S. W. 1996. PEST sequences and regulation by proteolysis. *Trends Biochem Sci,* 21**,** 267-271.

REYNISDOTTIR, I. & MASSAGUE, J. 1997. The subcellular locations of p15(Ink4b) and p27(Kip1) coordinate their inhibitory interactions with cdk4 and cdk2. *Genes Dev,* 11**,** 492-503.

RICKERT, P., SEGHEZZI, W., SHANAHAN, F., CHO, H. & LEES, E. 1996. Cyclin C/CDK8 is a novel CTD kinase associated with RNA polymerase II. *Oncogene,* 12**,** 2631-2640.

RIEGER, R., LASMEZAS, C. I. & WEISS, S. 1999. Role of the 37 kDa laminin receptor precursor in the life cycle of prions. *Transfus Clin Biol,* 6**,** 7-16.

RIOU, J.-Y. & GUIBOURDENCHE, M. 1987. *Neisseria polysaccharea* sp. nov. *Int J Syst Evol Microbiol,* 37**,** 163-165.

ROBBINS, J. B. 1978. Vaccines for the prevention of encapsulated bacterial diseases: current status, problems and prospects for the future. *Immunochemistry,* 15**,** 839-54.

ROSENSTEIN, N. E., PERKINS, B. A., STEPHENS, D. S., LEFKOWITZ, L., CARTTER, M. L., DANILA, R., CIESLAK, P., SHUTT, K. A., POPOVIC, T. & SCHUCHAT, A. 1999. The changing epidemiology of meningococcal disease in the United States, 1992–1996. *J Infect Dis,* 180**,** 1894-1901.

ROSENSTEIN, N. E., PERKINS, B. A., STEPHENS, D. S., POPOVIC, T. & HUGHES, J. M. 2001. Meningococcal disease. *N Engl J Med,* 344**,** 1378-88.

ROUPHAEL, N. G. & STEPHENS, D. S. 2012. *Neisseria meningitidis*: biology, microbiology, and epidemiology. *Methods Mol Biol,* 799**,** 1-20.

RUIJTER, J. M., RAMAKERS, C., HOOGAARS, W. M., KARLEN, Y., BAKKER, O., VAN DEN HOFF, M. J. & MOORMAN, A. F. 2009. Amplification efficiency: linking baseline and bias in the analysis of quantitative PCR data. *Nucleic Acids Res,* 37**,** e45.

SAARINEN, M., TAKALA, A. K., KOSKENNIEMI, E., KELA, E., RONNBERG, P. R., PEKKANEN, E., KIISKI, P. & ESKOLA, J. 1995. Spectrum of 2,836 cases of invasive bacterial or fungal infections in children: results of prospective nationwide five-year surveillance in Finland. Finnish Pediatric Invasive Infection Study Group. *Clin Infect Dis,* 21**,** 1134-44.

SANJUAN, X., FERNANDEZ, P. L., MIQUEL, R., MUNOZ, J., CASTRONOVO, V., MENARD, S., PALACIN, A., CARDESA, A. & CAMPO, E. 1996. Overexpression of the 67-kD laminin receptor correlates with tumour progression in human colorectal carcinoma. *J Pathol,* 179**,** 376-80.

SASAKI, T., FASSLER, R. & HOHENESTER, E. 2004. Laminin: the crux of basement membrane assembly. *J Cell Biol,* 164**,** 959-63.

SATOH, K., NARUMI, K., ABE, T., SAKAI, T., KIKUCHI, T., TANAKA, M., SHIMO-OKA, T., UCHIDA, M., TEZUKA, F., ISEMURA, M. & NUKIWA, T. 1999. Diminution of 37-kDa laminin binding protein expression reduces tumour formation of murine lung cancer cells. *Br J Cancer,* 80**,** 1115-22.

SATOH, K., NARUMI, K., ISEMURA, M., SAKAI, T., ABE, T., MATSUSHIMA, K., OKUDA, K. & MOTOMIYA, M. 1992. Increased expression of the 67kDa-laminin receptor gene in human small cell lung cancer. *Biochem Biophys Res Commun,* 182**,** 746-52.

SCARSELLI, M., SERRUTO, D., MONTANARI, P., CAPECCHI, B., ADU-BOBIE, J., VEGGI, D., RAPPUOLI, R., PIZZA, M. & ARICO, B. 2006. *Neisseria meningitidis* NhhA is a multifunctional trimeric autotransporter adhesin. *Mol Microbiol,* 61**,** 631-44.

SCHEIMAN, J., JAMIESON, K. V., ZIELLO, J., TSENG, J. C. & MERUELO, D. 2010a. Extraribosomal functions associated with the C terminus of the 37/67 kDa laminin receptor are required for maintaining cell viability. *Cell Death Dis,* 1**,** e42.

SCHEIMAN, J., TSENG, J. C., ZHENG, Y. & MERUELO, D. 2010b. Multiple functions of the 37/67-kd laminin receptor make it a suitable target for novel cancer gene therapy. *Mol Ther,* 18**,** 63-74.

SCHUBERT-UNKMEIR, A., KONRAD, C., SLANINA, H., CZAPEK, F., HEBLING, S. & FROSCH, M. 2010. *Neisseria meningitidis* induces brain microvascular endothelial cell detachment from the matrix and cleavage of occludin: a role for MMP-8. *PLoS Pathog,* 6**,** e1000874.

SCHUBERT-UNKMEIR, A., SOKOLOVA, O., PANZNER, U., EIGENTHALER, M. & FROSCH, M. 2007. Gene expression pattern in human brain endothelial cells in response to *Neisseria meningitidis*. *Infect Immun,* 75**,** 899-914.

SERRUTO, D., ADU-BOBIE, J., SCARSELLI, M., VEGGI, D., PIZZA, M., RAPPUOLI, R. & ARICO, B. 2003. *Neisseria meningitidis* App, a new adhesin with autocatalytic serine protease activity. *Mol Microbiol,* 48**,** 323-34.

SHARIP, A., SORVILLO, F., REDELINGS, M. D., MASCOLA, L., WISE, M. & NGUYEN, D. M. 2006. Population-based analysis of meningococcal disease mortality in the United States: 1990-2002. *Pediatr Infect Dis J,* 25**,** 191-4.

SHAW, F. W. 1932. The pathogenicity of *Neisseria sicca*. *Science,* 75**,** 488-488.

SHENKER, B. J. & DATAR, S. 1995. *Fusobacterium nucleatum* inhibits human T-cell activation by arresting cells in the mid-G1 phase of the cell cycle. *Infect Immun,* 63**,** 4830-6.

SHERR, C. J. 1994. G1 phase progression: cycling on cue. *Cell,* 79**,** 551-555.

SHERR, C. J. 1995. D-type cyclins. *Trends Biochem Sci,* 20**,** 187-190.

SHERR, C. J. & ROBERTS, J. M. 1995. Inhibitors of mammalian G1 cyclin-dependent kinases. *Genes Dev,* 9**,** 1149-1163.

SHIN, S. J., LEE, S. E., BOO, J. H., KIM, M., YOON, Y. D., KIM, S. I. & MOOK-JUNG, I. 2004. Profiling proteins related to amyloid deposited brain of Tg2576 mice. *Proteomics,* 4**,** 3359-68.

SIERRA, G., CAMPA, H., VARCACEL, N., GARCIA, I., IZQUIERDO, P., SOTOLONGO, P., CASANUEVA, G., RICO, C., RODRIGUEZ, C. & TERRY, M. 1991. Vaccine against group B *Neisseria meningitidis*: protection trial and mass vaccination results in Cuba. *NIPH annals,* 14**,** 195-207; discussion 208-10.

SIMONEAU, S., HAIK, S., LEUCHT, C., DORMONT, D., DESLYS, J. P., WEISS, S. & LASMEZAS, C. 2003. Different isoforms of the non-integrin laminin receptor are present in mouse brain and bind PrP. *Biol Chem,* 384**,** 243-6.

SPAAN, ANDRÁS N., HENRY, T., VAN ROOIJEN, WILLEMIEN J. M., PERRET, M., BADIOU, C., AERTS, PIET C., KEMMINK, J., DE HAAS, CARLA J. C., VAN KESSEL, KOK P. M., VANDENESCH, F., LINA, G. & VAN STRIJP, JOS A. G. 2013. The Staphylococcal Toxin Panton-Valentine Leukocidin Targets Human C5a Receptors. *Cell Host Microbe,* 13**,** 584-594.

SPINOSA, M. R., PROGIDA, C., TALA, A., COGLI, L., ALIFANO, P. & BUCCI, C. 2007. The *Neisseria meningitidis* capsule is important for intracellular survival in human cells. *Infect Immun,* 75**,** 3594-603.

STEIN, J., MILEWSKI, W. M., HARA, M., STEINER, D. F. & DEY, A. 2011. GSK-3 inactivation or depletion promotes beta-cell replication via down regulation of the CDK inhibitor, p27 (Kip1). *Islets,* 3**,** 21-34.

STEPHENS, D. S. 2009. Biology and pathogenesis of the evolutionarily successful, obligate human bacterium *Neisseria meningitidis*. *Vaccine,* 27 Suppl 2**,** B71-7.

STEPHENS, D. S., GREENWOOD, B. & BRANDTZAEG, P. 2007. Epidemic meningitis, meningococcaemia, and *Neisseria meningitidis*. *Lancet,* 369**,** 2196-2210.

STEPHENS, D. S., HOFFMAN, L. H. & MCGEE, Z. A. 1983. Interaction of *Neisseria meningitidis* with human nasopharyngeal mucosa: attachment and entry into columnar epithelial cells. *J Infect Dis,* 148**,** 369-376.

STOJILJKOVIC, I., HWA, V., DE SAINT MARTIN, L., O'GAORA, P., NASSIF, X., HEFFRON, F. & SO, M. 1995. The *Neisseria meningitidis* haemoglobin receptor: its role in iron utilization and virulence. *Mol Microbiol,* 15**,** 531-41.

STRAUSS, J. H., WANG, K. S., SCHMALJOHN, A. L., KUHN, R. J. & STRAUSS, E. G. 1994. Host-cell receptors for Sindbis virus. *Arch Virol Suppl,* 9**,** 473-84.

SUIZU, F., HIRAMUKI, Y., OKUMURA, F., MATSUDA, M., OKUMURA, A. J., HIRATA, N., NARITA, M., KOHNO, T., YOKOTA, J., BOHGAKI, M., OBUSE, C., HATAKEYAMA, S., OBATA, T. & NOGUCHI, M. 2009. The E3 ligase TTC3 facilitates ubiquitination and degradation of phosphorylated Akt. *Dev Cell,* 17**,** 800-10.

SUSANTAD, T. & SMITH, D. R. 2008. siRNA-mediated silencing of the 37/67-kDa high affinity laminin receptor in Hep3B cells induces apoptosis. *Cell Mol Biol Lett,* 13**,** 452-64.

SWE, K. S., NAGEL, G., VAN DER WESTHUIZEN, M. & HOOSEN, A. 2008. *Salmonella typhimurium* meningitis in an adult patient with AIDS. *J Clin Pathol,* 61**,** 138-139.

SWIATKOWSKI, P., NIKOLAEVA, I., KUMAR, G., ZUCCO, A., AKUM, B. F., PATEL, M. V., D'ARCANGELO, G. & FIRESTEIN, B. L. 2017. Role of Akt-independent mTORC1 and GSK3beta signaling in sublethal NMDA-induced injury and the recovery of neuronal electrophysiology and survival. *Sci Rep,* 7**,** 1539.

TAGLIABUE, E. & PASTORINO, U. 1996. Re: Killing of laminin receptor-positive human lung cancers by tumor-infiltrating lymphocytes bearing gamma delta + T-cell receptors. *J Natl Cancer Inst,* 88**,** 1241-2.

TAKAHASHI-YANAGA, F. & SASAGURI, T. 2008. GSK-3beta regulates cyclin D1 expression: a new target for chemotherapy. *Cell Signal,* 20**,** 581-9.

TALA, A., PROGIDA, C., DE STEFANO, M., COGLI, L., SPINOSA, M. R., BUCCI, C. & ALIFANO, P. 2008. The HrpB-HrpA two-partner secretion system is essential for intracellular survival of *Neisseria meningitidis*. *Cell Microbiol,* 10**,** 2461-82.

TAN, L. K., CARLONE, G. M. & BORROW, R. 2010. Advances in the development of vaccines against *Neisseria meningitidis*. *New England J Med,* 362**,** 1511-1520.

TETTELIN, H., SAUNDERS, N. J., HEIDELBERG, J., JEFFRIES, A. C., NELSON, K. E., EISEN, J. A., KETCHUM, K. A., HOOD, D. W., PEDEN, J. F., DODSON, R. J., NELSON, W. C., GWINN, M. L., DEBOY, R., PETERSON, J. D., HICKEY, E. K., HAFT, D. H., SALZBERG, S. L., WHITE, O., FLEISCHMANN, R. D., DOUGHERTY, B. A., MASON, T., CIECKO, A., PARKSEY, D. S., BLAIR, E., CITTONE, H., CLARK, E. B., COTTON, M. D., UTTERBACK, T. R., KHOURI, H., QIN, H., VAMATHEVAN, J., GILL, J., SCARLATO, V., MASIGNANI, V., PIZZA, M., GRANDI, G., SUN, L., SMITH, H. O., FRASER, C. M., MOXON, E. R., RAPPUOLI, R. & VENTER, J. C. 2000. Complete genome sequence of *Neisseria meningitidis* serogroup B strain MC58. *Science,* 287**,** 1809-15.

THEILEN, U., WILSON, L., WILSON, G., BEATTIE, J. O., QURESHI, S., SIMPSON, D. & GUIDELINE DEVELOPMENT, G. 2008. Management of invasive meningococcal disease in children and young people: summary of SIGN guidelines. *BMJ,* 336**,** 1367-70.

THEPPARIT, C. & SMITH, D. R. 2004. Serotype-specific entry of dengue virus into liver cells: identification of the 37-kilodalton/67-kilodalton high-affinity laminin receptor as a dengue virus serotype 1 receptor. *J Virol,* 78**,** 12647-56.

THIGPEN, M. C., WHITNEY, C. G., MESSONNIER, N. E., ZELL, E. R., LYNFIELD, R., HADLER, J. L., HARRISON, L. H., FARLEY, M. M., REINGOLD, A., BENNETT, N. M., CRAIG, A. S., SCHAFFNER, W., THOMAS, A., LEWIS, M. M., SCALLAN, E. & SCHUCHAT, A. 2011. Bacterial meningitis in the United States, 1998-2007. *N Engl J Med,* 364**,** 2016-25.

THONGTAN, T., WIKAN, N., WINTACHAI, P., RATTANARUNGSAN, C., SRISOMSAP, C., CHEEPSUNTHORN, P. & SMITH, D. R. 2012. Characterization of putative Japanese encephalitis virus receptor molecules on microglial cells. *J Med Virol,* 84**,** 615-23.

TOHGO, A., TAKASAWA, S., MUNAKATA, H., YONEKURA, H., HAYASHI, N. & OKAMOTO, H. 1994. Structural determination and characterization of a 40 kDa protein isolated from rat 40 S ribosomal subunit. *FEBS Lett,* 340**,** 133-8.

TØNJUM, T. 2005. Family Neisseriaceae and genus *Neisseria*. *In:* GARRITY, G. (ed.) *Bergey's manual of systematic bacteriology: the proteobacteria.* New York: Springer Verlag.

TONJUM, T., CAUGANT, D. A., DUNHAM, S. A. & KOOMEY, M. 1998. Structure and function of repetitive sequence elements associated with a highly polymorphic domain of the *Neisseria meningitidis* PilQ protein. *Mol Microbiol,* 29**,** 111-24.

TUNKEL, A. R., HARTMAN, B. J., KAPLAN, S. L., KAUFMAN, B. A., ROOS, K. L., SCHELD, W. M. & WHITLEY, R. J. 2004. Practice guidelines for the management of bacterial meningitis. *Clin Infect Dis,* 39**,** 1267-84.

TURK, D. 1984. The pathogenicity of *Haemophilus influenzae*. *J Med Microbiol,* 18**,** 1-16.

TURNER, D. P., MARIETOU, A. G., JOHNSTON, L., HO, K. K., ROGERS, A. J., WOOLDRIDGE, K. G. & ALA'ALDEEN, D. A. 2006. Characterization of MspA, an immunogenic autotransporter protein that mediates adhesion to epithelial and endothelial cells in *Neisseria meningitidis*. *Infect Immun,* 74**,** 2957-64.

TZENG, Y. L., THOMAS, J. & STEPHENS, D. S. 2016. Regulation of capsule in *Neisseria meningitidis*. *Crit Rev Microbiol,* 42**,** 759-72.

TZIVION, G., DOBSON, M. & RAMAKRISHNAN, G. 2011. FoxO transcription factors; Regulation by AKT and 14-3-3 proteins. *Biochim Biophys Acta,* 1813**,** 1938-45.

UMBAUGH, C. S. & FIGUEIREDO, M. L. 2018. Lysines residing in putative Small Ubiquitin-like MOdifier (SUMO) motifs regulate fate and function of 37KDa laminin receptor. *Biochimie,* 156**,** 92-99.

UMEDA, D., YANO, S., YAMADA, K. & TACHIBANA, H. 2008. Green tea polyphenol epigallocatechin-3-gallate signaling pathway through 67-kDa laminin receptor. *J Biol Chem,* 283**,** 3050-8.

UNKMEIR, A., LATSCH, K., DIETRICH, G., WINTERMEYER, E., SCHINKE, B., SCHWENDER, S., KIM, K. S., EIGENTHALER, M. & FROSCH, M. 2002. Fibronectin mediates Opc-dependent internalization of *Neisseria meningitidis* in human brain microvascular endothelial cells. *Mol Microbiol,* 46**,** 933-946.

VAN DE BEEK, D., BROUWER, M. C., THWAITES, G. E. & TUNKEL, A. R. 2012. Advances in treatment of bacterial meningitis. *Lancet,* 380**,** 1693-1702.

VAN DE BEEK, D., DE GANS, J., SPANJAARD, L., WEISFELT, M., REITSMA, J. B. & VERMEULEN, M. 2004. Clinical features and prognostic factors in adults with bacterial meningitis. *N Engl J Med,* 351**,** 1849-59.

VAN DE BEEK, D., DE GANS, J., TUNKEL, A. R. & WIJDICKS, E. F. 2006. Community-acquired bacterial meningitis in adults. *N Engl J Med,* 354**,** 44-53.

VAN DE BEEK, D., DRAKE, J. M. & TUNKEL, A. R. 2010. Nosocomial bacterial meningitis. *N Engl J Med,* 362**,** 146-154.

VAN DEN BRULE, F., BERCHUCK, A., BAST, R., LIU, F.-T., GILLET, C., SOBEL, M. & CASTRONOVO, V. 1994. Differential expression of the 67-kD laminin receptor and 31-kD human laminin-binding protein in human ovarian carcinomas. *Eur J Cancer,* 30**,** 1096-1099.

VAN DEN HEUVEL, S. & DYSON, N. J. 2008. Conserved functions of the pRB and E2F families. *Nat Rev Mol Cell Biol,* 9**,** 713-24.

VAN DER ENDE, A., HOPMAN, C. & DANKERT, J. 1999. Deletion of porA by recombination between clusters of repetitive extragenic palindromic sequences in *Neisseria meningitidis*. *Infect Immun,* 67**,** 2928-2934.

VAN DER LEY, P., HECKELS, J. E., VIRJI, M., HOOGERHOUT, P. & POOLMAN, J. T. 1991. Topology of outer membrane porins in pathogenic *Neisseria* spp. *Infect Immun,* 59**,** 2963-71.

VAN DER LEY, P., VAN DER BIEZEN, J., SUTMULLER, R., HOOGERHOUT, P. & POOLMAN, J. T. 1996. Sequence variability of FrpB, a major iron-regulated outer-membrane protein in the pathogenic neisseriae. *Microbiology,* 142 (Pt 11)**,** 3269-74.

VAN HEYNINGEN, S. 1974. Cholera Toxin: Interaction of Subunits with Ganglioside GM1. *Science,* 183**,** 656-657.

VAN PUTTEN, J. & PAUL, S. 1995. Binding of syndecan-like cell surface proteoglycan receptors is required for *Neisseria gonorrhoeae* entry into human mucosal cells. *EMBO J,* 14**,** 2144-2154.

VAN SORGE, N. M. & DORAN, K. S. 2012. Defense at the border: the blood-brain barrier versus bacterial foreigners. *Future Microbiol,* 7**,** 383-94.

VASSEY, M. 2014. *The meningococcal outer membrane protein PorA and the human laminin receptor.* PhD, The University of Nottingham.

VENTICINQUE, L., JAMIESON, K. V. & MERUELO, D. 2011. Interactions between laminin receptor and the cytoskeleton during translation and cell motility. *PLoS One,* 6**,** e15895.

VERMEULEN, K., VAN BOCKSTAELE, D. R. & BERNEMAN, Z. N. 2003. The cell cycle: a review of regulation, deregulation and therapeutic targets in cancer. *Cell Prolif,* 36**,** 131-49.

VERON, M., THIBAULT, P. & SECOND, L. *Neisseria mucosa* (*Diplococcus mucosus* Lingelsheim). I. Bacteriological description and study of its pathogenicity. Annales de l'Institut Pasteur, 1959. 497-510.

VETTER, V., BAXTER, R., DENIZER, G., SAFADI, M. A., SILFVERDAL, S. A., VYSE, A. & BORROW, R. 2016. Routinely vaccinating adolescents against meningococcus: targeting transmission & disease. *Expert Rev Vaccines,* 15**,** 641-58.

VIACAVA, P., NACCARATO, A. G., COLLECCHI, P., MENARD, S., CASTRONOVO, V. & BEVILACQUA, G. 1997. The spectrum of 67-kD laminin receptor expression in breast carcinoma progression. *J Pathol,* 182**,** 36-44.

VIRJI, M. 2009. Pathogenic neisseriae: surface modulation, pathogenesis and infection control. *Nat Rev Microbiol,* 7**,** 274-86.

VIRJI, M., EVANS, D., HADFIELD, A., GRUNERT, F., TEIXEIRA, A. M. & WATT, S. M. 1999. Critical determinants of host receptor targeting by *Neisseria meningitidis* and *Neisseria gonorrhoeae*: identification of Opa adhesiotopes on the N-domain of CD66 molecules. *Mol Microbiol,* 34**,** 538-551.

VIRJI, M., MAKEPEACE, K. & MOXON, E. R. 1994. Distinct mechanisms of interactions of Opc-expressing meningococci at apical and basolateral surfaces of human endothelial cells; the role of integrins in apical interactions. *Mol Microbiol,* 14**,** 173-184.

VIRJI, M., SAUNDERS, J. R., SIMS, G., MAKEPEACE, K., MASKELL, D. & FERGUSON, D. J. 1993. Pilus-facilitated adherence of *Neisseria meningitidis* to human epithelial and endothelial cells: modulation of adherence phenotype occurs concurrently with changes in primary amino acid sequence and the glycosylation status of pilin. *Mol Microbiol,* 10**,** 1013-28.

VIRJI, M., WATT, S. M., BARKER, S., MAKEPEACE, K. & DOYONNAS, R. 1996. The N-domain of the human CD66a adhesion molecule is a target for Opa proteins of *Neisseria meningitidis* and *Neisseria gonorrhoeae*. *Mol Microbiol,* 22**,** 929-939.

VITIELLO, M., FINAMORE, E., CANTISANI, M., BEVILACQUA, P., INCORONATO, N., FALANGA, A., GALDIERO, E. & GALDIERO, M. 2011. P2 porin and loop L7 from *Haemophilus influenzae* modulate expression of IL-6 and adhesion molecules in astrocytes. *Microbiol Immunol,* 55**,** 347-56.

VOGEL, U. 2010. Molecular epidemiology of meningococci: application of DNA sequence typing. *Int J Med Microbiol,* 300**,** 415-20.

VOGEL, U., TAHA, M. K., VAZQUEZ, J. A., FINDLOW, J., CLAUS, H., STEFANELLI, P., CAUGANT, D. A., KRIZ, P., ABAD, R., BAMBINI, S., CARANNANTE, A., DEGHMANE, A. E., FAZIO, C., FROSCH, M., FROSI, G., GILCHRIST, S., GIULIANI, M. M., HONG, E., LEDROIT, M., LOVAGLIO, P. G., LUCIDARME, J., MUSILEK, M., MUZZI, A., OKSNES,

J., RIGAT, F., ORLANDI, L., STELLA, M., THOMPSON, D., PIZZA, M., RAPPUOLI, R., SERRUTO, D., COMANDUCCI, M., BOCCADIFUOCO, G., DONNELLY, J. J., MEDINI, D. & BORROW, R. 2013. Predicted strain coverage of a meningococcal multicomponent vaccine (4CMenB) in Europe: a qualitative and quantitative assessment. *Lancet Infect Dis,* 13**,** 416-25.

VON PAPEN, M., OOSTHUYSEN, W. F., BECAM, J., CLAUS, H. & SCHUBERT-UNKMEIR, A. 2016. Disease and Carrier Isolates of *Neisseria meningitidis* Cause G1 Cell Cycle Arrest in Human Epithelial Cells. *Infect Immun,* 84**,** 2758-70.

WAAGE, A., HALSTENSEN, A. & ESPEVIK, T. 1987. Association between tumour necrosis factor in serum and fatal outcome in patients with meningococcal disease. *Lancet,* 1**,** 355-7.

WAAGE, A., HALSTENSEN, A., SHALABY, R., BRANDTZAEG, P., KIERULF, P. & ESPEVIK, T. 1989. Local production of tumor necrosis factor alpha, interleukin 1, and interleukin 6 in meningococcal meningitis. Relation to the inflammatory response. *J Exp Med,* 170**,** 1859-67.

WALKER, D. H. & MALLER, J. L. 1991. Role for cyclin A in the dependence of mitosis on completion of DMA replication. *Nature,* 354**,** 314.

WALTREGNY, D., DE LEVAL, L., MÉNARD, S., DE LEVAL, J. & CASTRONOVO, V. 1997. Independent prognostic value of the 67-kd laminin receptor in human prostate cancer. *J Natl Cancer Inst,* 89**,** 1224-1227.

WANG, K. S., KUHN, R. J., STRAUSS, E. G., OU, S. & STRAUSS, J. H. 1992. High-affinity laminin receptor is a receptor for Sindbis virus in mammalian cells. *J Virol,* 66**,** 4992-5001.

WANG, X., DING, J. & MENG, L.-H. 2015. PI3K isoform-selective inhibitors: next-generation targeted cancer therapies. *Acta Pharmacol Sin,* 36**,** 1170-1176.

WANG, X., SJOLINDER, M., GAO, Y., WAN, Y. & SJOLINDER, H. 2016a. Immune Homeostatic Macrophages Programmed by the Bacterial Surface Protein NhhA Potentiate Nasopharyngeal Carriage of *Neisseria meningitidis*. *MBio,* 7**,** e01670-15.

WANG, Y., LIU, J., QIU, Y., JIN, M., CHEN, X., FAN, G., WANG, R. & KONG, D. 2016b. ZSTK474, a specific class I phosphatidylinositol 3-kinase inhibitor, induces G1 arrest and autophagy in human breast cancer MCF-7 cells. *Oncotarget,* 7**,** 19897-909.

WANG, Y. A., ELSON, A. & LEDER, P. 1997. Loss of p21 increases sensitivity to ionizing radiation and delays the onset of lymphoma in atm-deficient mice. *Proc Natl Acad Sci U S A,* 94**,** 14590-14595.

WEICHSELBAUM, A. 1887. Ueber die Aetiologie der akuten meningitis cerebro-spinalis. *Fortschr. Med,* 5**,** 573-583, 620-626.

WEINBERG, R. A. 2014. *The Biology of Cancer,* New York, Garland Science, Taylor & Francis Group, LLC.

WEIS, N. & LIND, I. 1998. Epidemiological markers in *Neisseria meningitidis*: an estimate of the performance of genotyping vs phenotyping. *Scand J Infect Dis,* 30**,** 69-75.

WELSCH, J. A. & RAM, S. 2008. Factor H and neisserial pathogenesis. *Vaccine,* 26 Suppl 8**,** I40-I45.

WEWER, U. M., LIOTTA, L. A., JAYE, M., RICCA, G. A., DROHAN, W. N., CLAYSMITH, A. P., RAO, C. N., WIRTH, P., COLIGAN, J. E., ALBRECHTSEN, R. & ET AL. 1986. Altered levels of laminin receptor mRNA in various human carcinoma cells that have different abilities to bind laminin. *Proc Natl Acad Sci U S A,* 83**,** 7137-41.

WEYLER, L., ENGELBRECHT, M., MATA FORSBERG, M., BREHWENS, K., VARE, D., VIELFORT, K., WOJCIK, A. & ARO, H. 2014. Restriction endonucleases from invasive *Neisseria gonorrhoeae* cause double-

strand breaks and distort mitosis in epithelial cells during infection. *PLoS One,* 9**,** e114208.

WHITMAN, M., DOWNES, C. P., KEELER, M., KELLER, T. & CANTLEY, L. 1988. Type I phosphatidylinositol kinase makes a novel inositol phospholipid, phosphatidylinositol-3-phosphate. *Nature,* 332**,** 644-6.

WILDER-SMITH, A., GOH, K. T., BARKHAM, T. & PATON, N. I. 2003. Hajj-associated outbreak strain of *Neisseria meningitidis* serogroup W135: Estimates of the attack rate in a defined population and the risk of invasive disease developing. *Clin Infect Dis,* 36**,** 679-683.

WLODARCHAK, N. & XING, Y. 2016. PP2A as a master regulator of the cell cycle. *Crit Rev Biochem Mol Biol,* 51**,** 162-84.

WORLD HEALTH ORGANIZATION 2006. Outbreak News. Meningococcal disease, African meningitis belt, epidemic season 2006. *Wkly Epidemiol Rec,* 81**,** 117-128.

WORLD HEALTH ORGANIZATION. 2014. *Number of suspected meningitis cases and deaths reported* [Online]. WHO. Available: https://www.who.int/gho/epidemic_diseases/meningitis/suspected_cases_deaths/en/ [Accessed 18 April 2019].

WORLD HEALTH ORGANIZATION 2015a. Meningococcal disease control in countries of the African meningitis belt, 2014. *Wkly Epidemiol Rec,* 90**,** 123-31.

WORLD HEALTH ORGANIZATION 2015b. World Health Statistics 2015. Geneva: WHO.

XUE, G. & HEMMINGS, B. A. 2013. PKB/Akt-dependent regulation of cell motility. *J Natl Cancer Inst,* 105**,** 393-404.

YAHIRO, K., MORINAGA, N., SATOH, M., MATSUURA, G., TOMONAGA, T., NOMURA, F., MOSS, J. & NODA, M. 2006. Identification and characterization of receptors for vacuolating activity of subtilase cytotoxin. *Mol Microbiol,* 62**,** 480-490.

YANG, K., GUO, Y., STACEY, W. C., HARWALKAR, J., FRETTHOLD, J., HITOMI, M. & STACEY, D. W. 2006a. Glycogen synthase kinase 3 has a limited role in cell cycle regulation of cyclin D1 levels. *BMC Cell Biol,* 7**,** 33.

YANG, K., HITOMI, M. & STACEY, D. W. 2006b. Variations in cyclin D1 levels through the cell cycle determine the proliferative fate of a cell. *Cell Div,* 1**,** 32-32.

YAZDANKHAH, S. P. & CAUGANT, D. A. 2004. *Neisseria meningitidis*: an overview of the carriage state. *J Med Microbiol,* 53**,** 821-32.

YU, J., ZHANG, Y., MCILROY, J., RORDORF-NIKOLIC, T., ORR, G. A. & BACKER, J. M. 1998. Regulation of the p85/p110 phosphatidylinositol 3'-kinase: stabilization and inhibition of the p110alpha catalytic subunit by the p85 regulatory subunit. *Mol Cell Biol,* 18**,** 1379-87.

ZELLE-RIESER, C., BARSOUM, A. L., SALLUSTO, F., RAMONER, R., ROHRER, J. W., HOLTL, L., BARTSCH, G., COGGIN, J. H. & THURNHER, M. 2001. Expression and immunogenicity of oncofetal antigen-immature laminin receptor in human renal cell carcinoma. *J Urol,* 165**,** 1705-1709.

ZHENG, X., OU, Y., SHU, M., WANG, Y., ZHOU, Y., SU, X., ZHU, W., YIN, W., LI, S., QIU, P., YAN, G., ZHANG, J., HU, J. & XU, D. 2014. Cholera toxin, a typical protein kinase A activator, induces G1 phase growth arrest in human bladder transitional cell carcinoma cells via inhibiting the c-Raf/MEK/ERK signaling pathway. *Mol Med Rep,* 9**,** 1773-9.

ZHONG, J. 2016. RAS and downstream RAF-MEK and PI3K-AKT signaling in neuronal development, function and dysfunction. *Biol Chem,* 397**,** 215-22.

ZHOU, L., XIE, M., ZHOU, J. Q. & TAO, L. 2006. 67-kDa Laminin Receptor in Human Laryngeal Squamous Cell Carcinoma. *Laryngoscope,* 116**,** 28-32.

ZHU, H., WANG, Q., WEN, L., XU, J., SHAO, Z., CHEN, M., CHEN, M., REEVES, P. R., CAO, B. & WANG, L. 2012. Development of a multiplex PCR assay for detection and genogrouping of *Neisseria meningitidis*. *J Clin Microbiol,* 50**,** 46-51.

ZHU, P., KLUTCH, M. J., BASH, M. C., TSANG, R. S., NG, L. K. & TSAI, C. M. 2002. Genetic diversity of three lgt loci for biosynthesis of lipooligosaccharide (LOS) in *Neisseria* species. *Microbiology,* 148**,** 1833-44.

ZOU, Y., EWTON, D. Z., DENG, X., MERCER, S. E. & FRIEDMAN, E. 2004. Mirk/dyrk1B kinase destabilizes cyclin D1 by phosphorylation at threonine 288. *J Biol Chem,* 279**,** 27790-8.

ZUGHAIER, S. M., LINDNER, B., HOWE, J., GARIDEL, P., KOCH, M. H., BRANDENBURG, K. & STEPHENS, D. S. 2007. Physicochemical characterization and biological activity of lipooligosaccharides and lipid A from *Neisseria meningitidis*. *J Endotoxin Res,* 13**,** 343-57.

Appendix I – Commonly used buffers and solutions

Sodium carbonate buffer (coating buffer): 9.3 g of Sodium Carbonate (Na_2CO_3) and 1 g Sodium Bicarbonate (NaH_2CO_3), made up to 1L with dH_2O, pH adjusted at 9.4.

Sodium dodecyl sulphate (SDS)-separating (resolving) buffer (Buffer A): 181.7 g Tris base, 40 ml 10% (w/v) SDS, made up to 1L with dH_2O, pH adjusted at 8.8.

SDS-stacking buffer (Buffer B): 60.6 g Tris base, 40 ml 10% (w/v) SDS, made up to 1L with dH_2O, pH adjusted at 6.8.

SDS-running buffer (10x): 30.3 g Tris base, 144 g Glycine, 10 g SDS made up to 1L with dH_2O.

SDS-sample buffer (5x): 1 g SDS, 5 ml Glycerol, Bromophenol Blue 25 mg, Tris base 150 mg, 1 ml 2-mercaptoethanol, made up to 10 ml with dH_2O, pH adjusted at 6.8.

10% Acrylamide mini gels

- **Separating (resolving) gel master mix:** 2.5 ml Buffer A, 3.3 ml Acrylamide/Bis-acrylamide (30%, w/v), 4.1 ml dH_2O, 30 µl 10% (w/v) Ammonium persulfate (APS), 30 µl Tetramethylethylenediamine (TEMED).

- **Stacking gel master mix:** 1.3 ml Buffer B, 1 ml Acrylamide/ Bis-acrylamide (30%, w/v), 2.7 ml dH_2O, 10 µl 10% (w/v) APS, 10 µl TEMED.

SDS-PAGE Coomassie Staining Solution: 0.6 g Coomassie Blue (Sigma-Aldrich), 250 ml methanol, 51 ml acetic acid, made up to 500 ml with dH_2O.

SDS-PAGE Destaining Solution: 250 ml methanol, 104.2 ml acetic acid, made up to 1L with dH_2O.

Semi-dry transfer buffer: 5.82 g Tris, 2.93 g Glycine, 3.75 ml 10% SDS, 200 ml methanol, made up to 1L with dH_2O, pH adjusted at 9.

Tris-buffered saline (TBS, 10x): 24 g Tris base, 88 g NaCl, made up to 1 L with dH_2O, pH adjusted at 7.6.

Phosphate buffered saline solution (PBS): prepared by dissolving 1 tablet of phosphate buffered saline (Dulbecco A, Oxoid) in 100 ml dH_2O and autoclave. (NaCl 0.116 mol, KCl 0.003 mol, Na_2HPO_4 0.008 mol, K_2HPO_4 0.001 mol, pH 7.3).

Blocking buffer (BSA): 1-5% (w/v) Bovine serum albumin (Sigma-Aldrich A3912) in PBS-T or TBS-T, sterilize by filtration (0.22 µm filter).

Blocking buffer (Milk): 5% (w/v) skimmed milk powder in TBS-T.

Washing buffer (TBS-T): 0.1% (v/v) Tween20 in TBS 1x.

Washing buffer (PBS-T): 0.05**-**0.1% (v/v) Tween20 in PBS.

Radio-immunoprecipitation assay (RIPA) buffer: 5 ml of RIPA buffer (Sigma-Aldrich) supplemented with ½ tablet of PhosSTOP cOmplete ultra protease inhibitor tablet (Roche) and ½ tablet of cOmplete mini EDTA-free protease inhibitor cocktail tablet.

Antibiotics: All antibiotics were purchased from Sigma-Aldrich, UK, prepared according to the recommended concentration, sterilised by filtration, and stored at 4°C.

Kanamycin (50 mg ml^{-1} stock solution prepared in dH_2O)
Streptomycin (50 mg ml^{-1} stock solution prepared in dH_2O)
Spectinomycin (50 mg ml^{-1} stock solution prepared in dH_2O)

Working concentration was 1000x dilution from the prepared stock.

Fibronectin solution: 1 µg ml^{-1} of bovine fibronectin (Sigma-Aldrich) in PBS, sterilised by filtration (0.22 µm filter).

Fixing solution (4% paraformaldehyde): 40 g of paraformaldehyde powder was added to the pre-heated 800 mL of PBS at 60^{o}C. pH was slowly adjusted at 6.9 by 1 N NaOH, final volume made up to 1L with PBS.

Permeabilization solution: 0.5 g of BSA in 50 ml of mixture of 0.1% of Triton X-100 (v/v) in PBS.

Appendix II – Optimisation of ELISA parameters

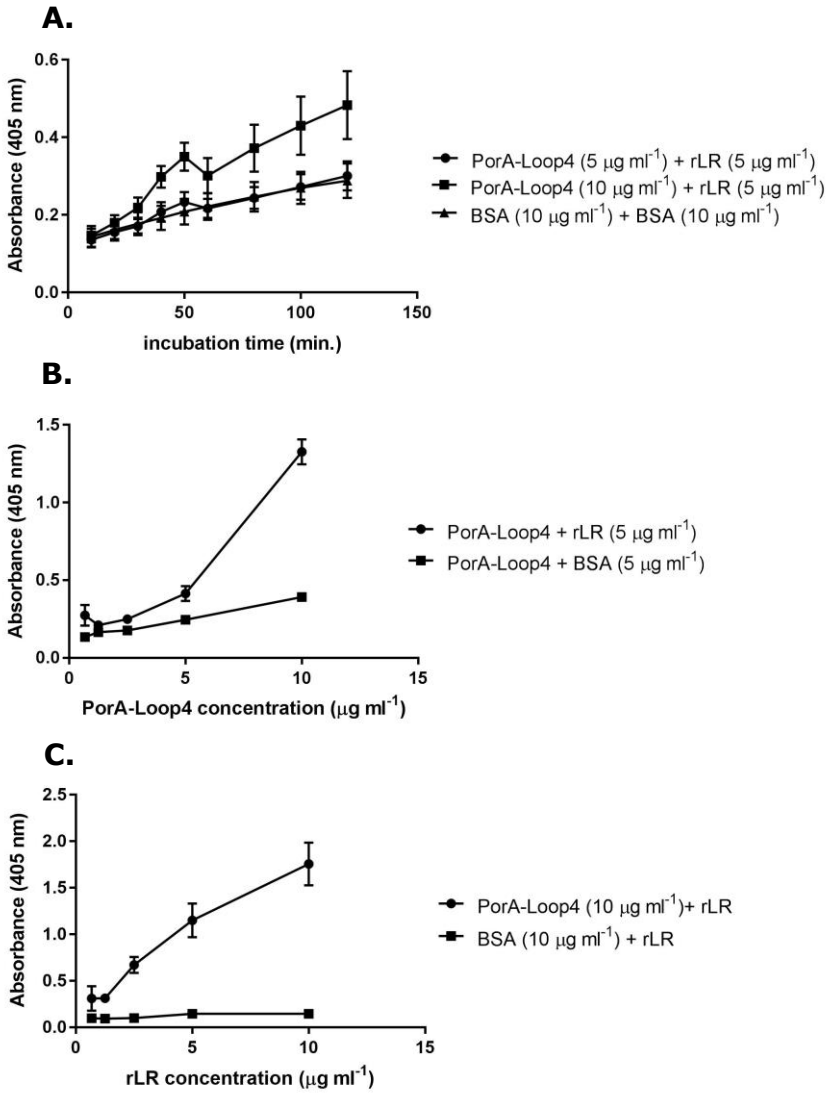

Figure A.1: Optimisation of ELISA parameters in current study. (A) Optimisation for the incubation period with phosphatase substrate. Two hours incubation of the substrate gave the highest absorbance to the assay, before entering the static phase for longer incubation (not shown in the graph). (B) Optimisation for the concentration of PorA-Loop4 peptide to coat the plate. The binding of 10 μg ml^{-1} PorA-Loop4 to the rLR showed higher absorbance than the binding from 5 μg ml^{-1} of PorA-Loop4. (C) Optimisation for the rLR concentration. The binding of the PorA-Loop4 peptide to the 5 μg ml^{-1} of rLR showed similar/static absorbance to the binding from 10 μg ml^{-1} of rLR. BSA was used as a control to measure the background absorbance. Absorbance represents average from three wells; error bars represents the SD.

Appendix III – Chromatograms of RNA samples used in Chapter 3

Figure A.2: Electrophoregram of mRNA samples extracted from PorA-Loop4 treated cells and the untreated controls for 0, 2, 4, 8, and 24 h. The two distinctive peaks at 2000 and 4000 [nt] represent the ribosomal subunits 28s and 18s from eukaryotic cells RNA.

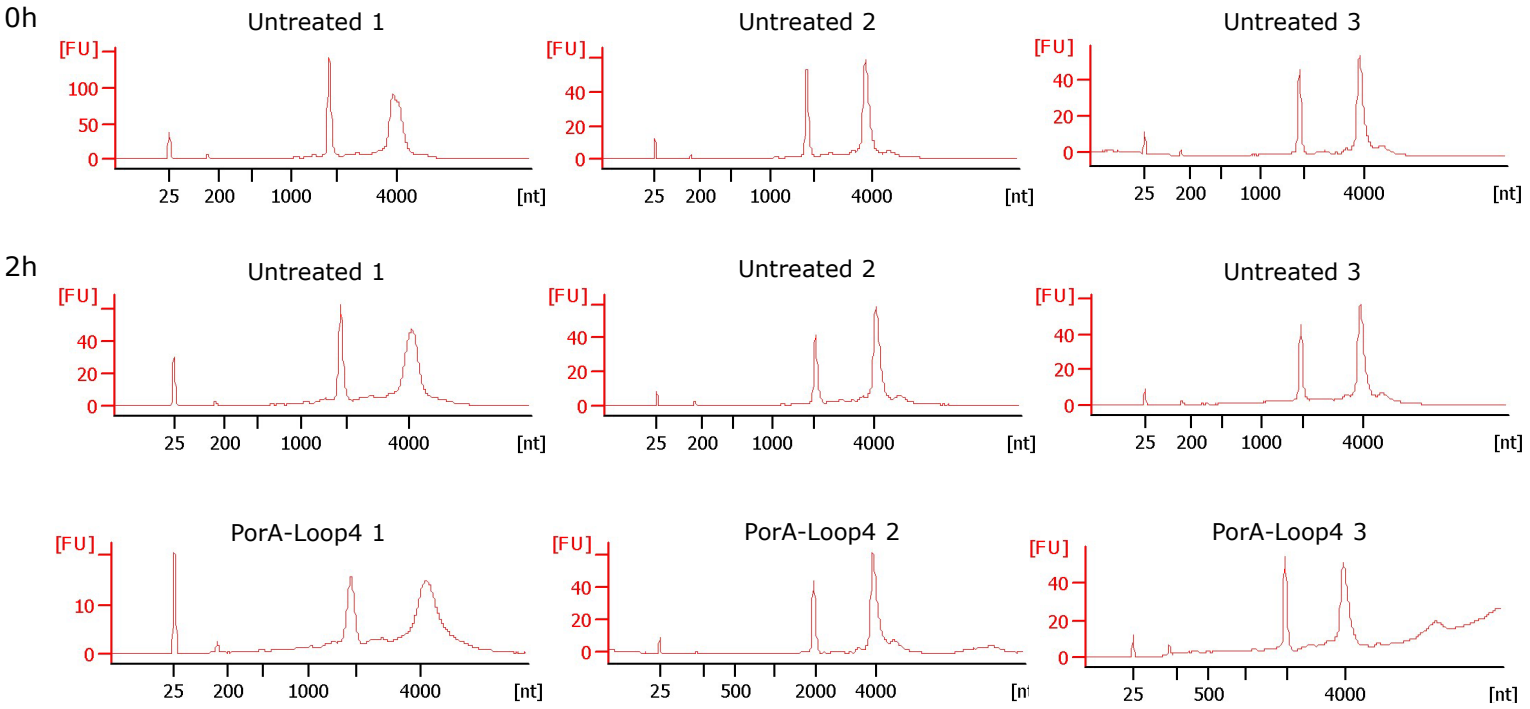

Continue to the next page

4h

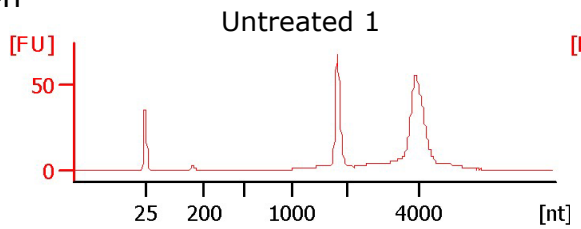

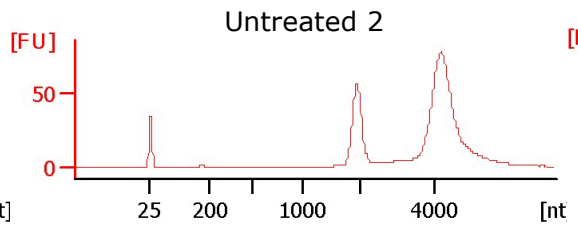

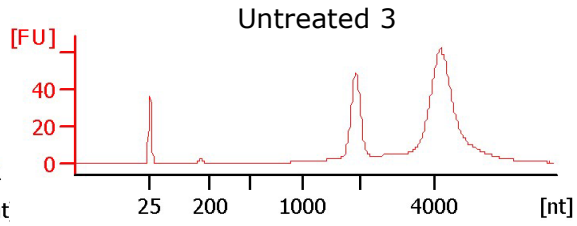

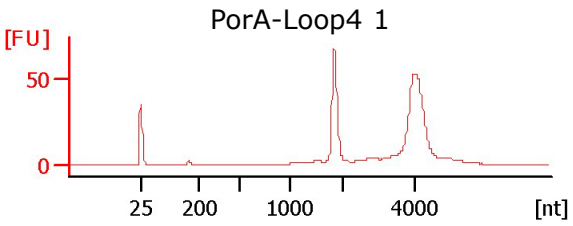

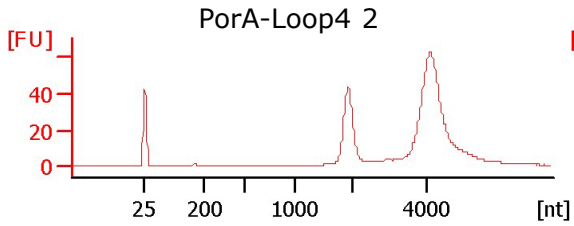

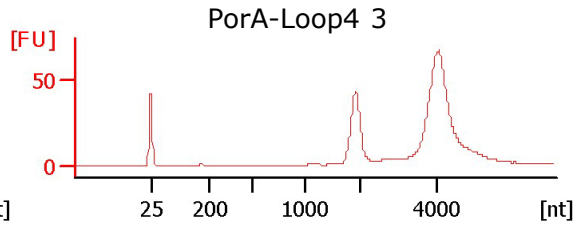

8h

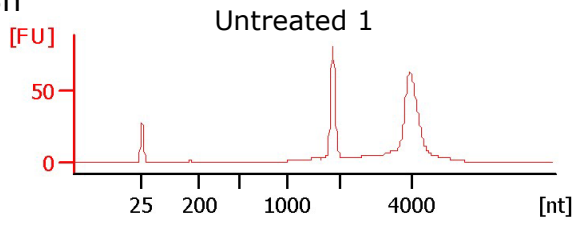

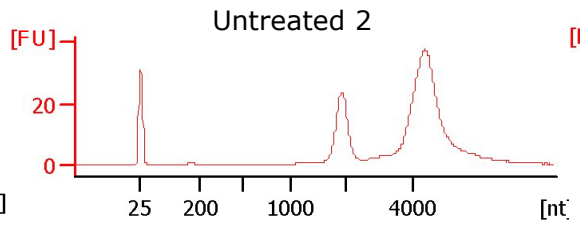

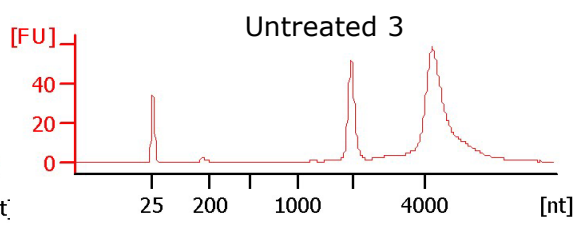

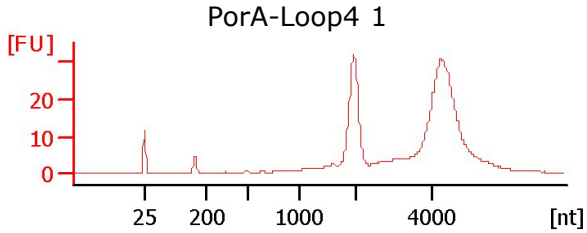

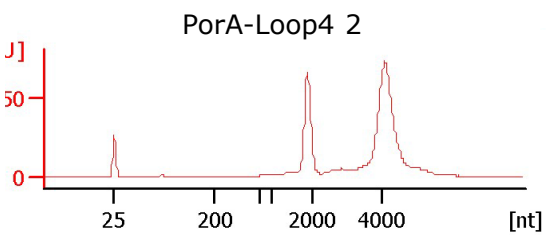

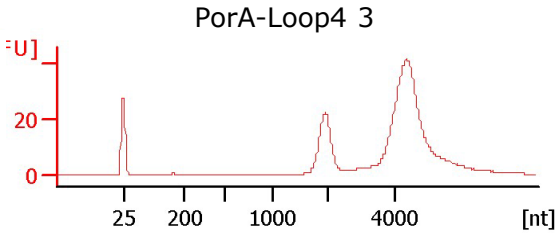

Continue to the next page

24h

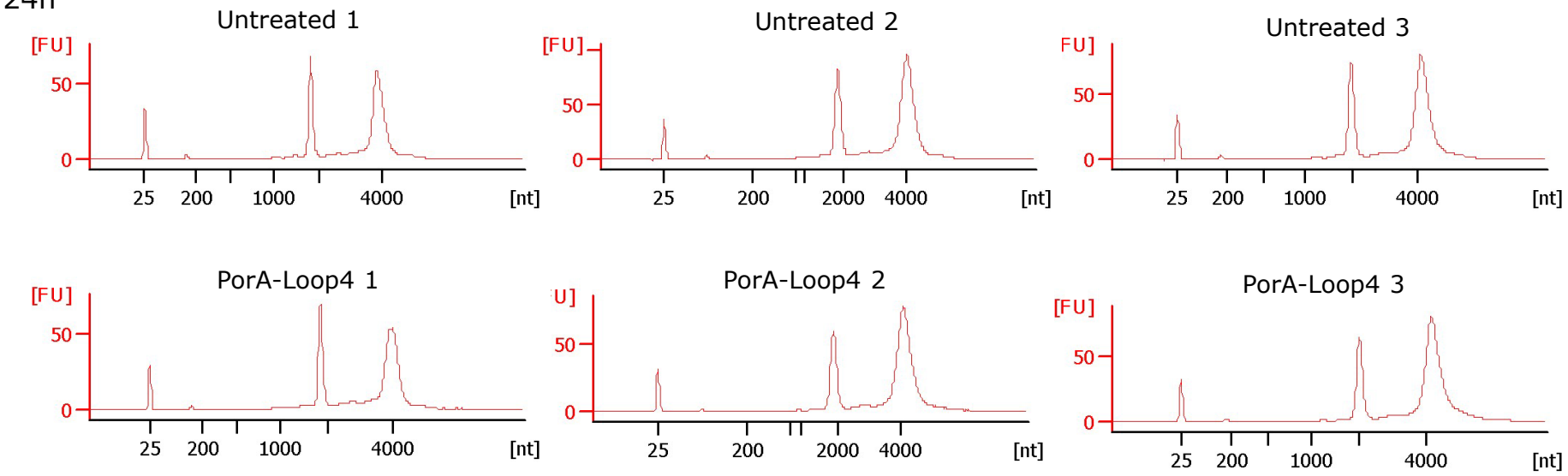
Untreated 1
[FU]
50
0
25
200
1000
4000
[nt]
Untreated 2
[FU]
50
0
25
200
2000
4000
[nt]
Untreated 3
FU]
50
0
25
200
1000
4000
[nt]
PorA-Loop4 1
[FU]
50
0
25
200
1000
4000
[nt]
PorA-Loop4 2
U]
50
0
25
200
2000
4000
[nt]
PorA-Loop4 3
[FU]
50
0
25
200
1000
4000
[nt]

Appendix IV – RIN, pseudo-image gels and chromatograms from RNA samples used in Chapter 4

Table A.1: 28S/18s ratio and RIN values of RNA samples used in Chapter 4.

Incubation time (h)	Samples	Replicate	28S/18S ratio	RIN
0	Untreated	1	1.9	9.8
		2	1.8	9.9
		3	1.7	10
2	Untreated	1	2.1	9.6
		2	2.1	9.9
		3	1.9	8.7
	PorA-Loop4	1	2.5	9.3
		2	2.0	10
		3	1.9	10
	ZSTK474	1	1.5	9
		2	3.1	10
		3	2.2	10
	PorA-Loop4 + ZSTK474	1	2	10
		2	1.7	9.9
		3	2.1	10
4	Untreated	1	1.8	9.8
		2	2.7	10
		3	2.5	10
	PorA-Loop4	1	1.7	9.8
		2	2.8	10
		3	3.0	10
	ZSTK474	1	1.8	8.2
		2	2.8	10
		3	2.8	10
	PorA-Loop4 + ZSTK474	1	1.8	9.8
		2	2.9	10
		3	3.5	10

Continue to the next page

Table A.1 (continued)

Incubation time (h)	Samples	Replicate	28S/18S ratio	RIN
8	Untreated	1	2.1	9.6
		2	2.1	9.9
		3	1.9	8.7
	PorA-Loop4	1	2.5	9.3
		2	2.0	10
		3	1.9	10
	ZSTK474	1	2.5	9.9
		2	2.6	10
		3	2.6	10
	PorA-Loop4 + ZSTK474	1	2	9.6
		2	2.7	10
		3	3.1	10
24	Untreated	1	1.8	9.8
		2	2.7	10
		3	2.5	10
	PorA-Loop4	1	1.7	9.8
		2	2.8	10
		3	3.0	10
	ZSTK474	1	2	9.9
		2	2.5	10
		3	2.8	10
	PorA-Loop4 + ZSTK474	1	2	9.7
		2	2.4	10
		3	2.3	10

Figure A.3: Pseudo-gel images of RNA samples used in Chapter 4. Figure A-E represent quality of samples from HBMECs treated with PorA-Loop4 peptide, ZSTK474, both PorA-Loop4 peptide and ZSTK474, and untreated controls for 0, 2, 4, 8, and 24h, respectively from three independent experiments. Each RNA sample was extracted from 1 x 10^6 cells of HBMECs using RNeasy® Mini Kit (Qiagen). Bands in 2000 and 4000 nt represent 18S and 28S RNA, respectively.

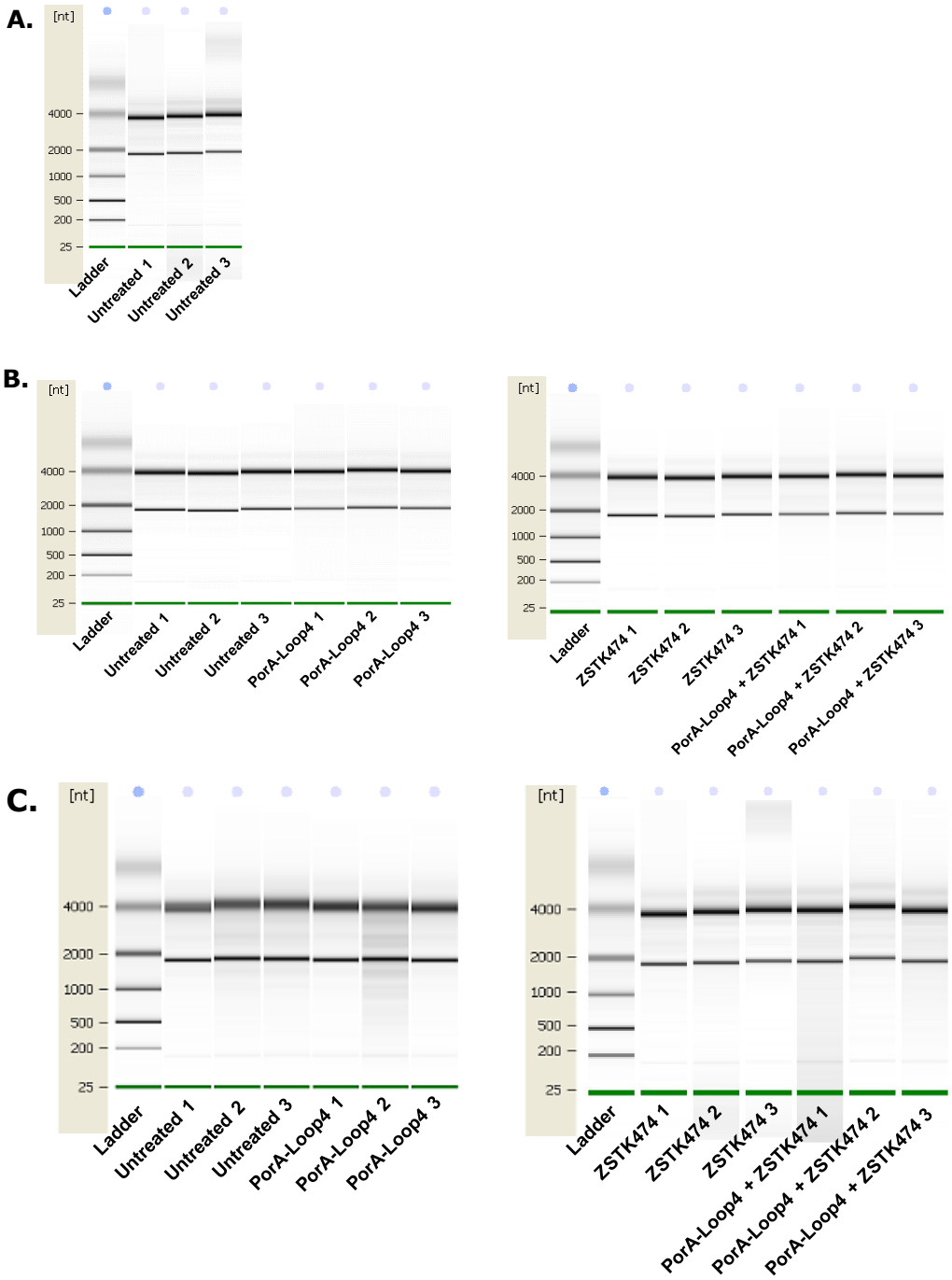

Continue to the next page

D.

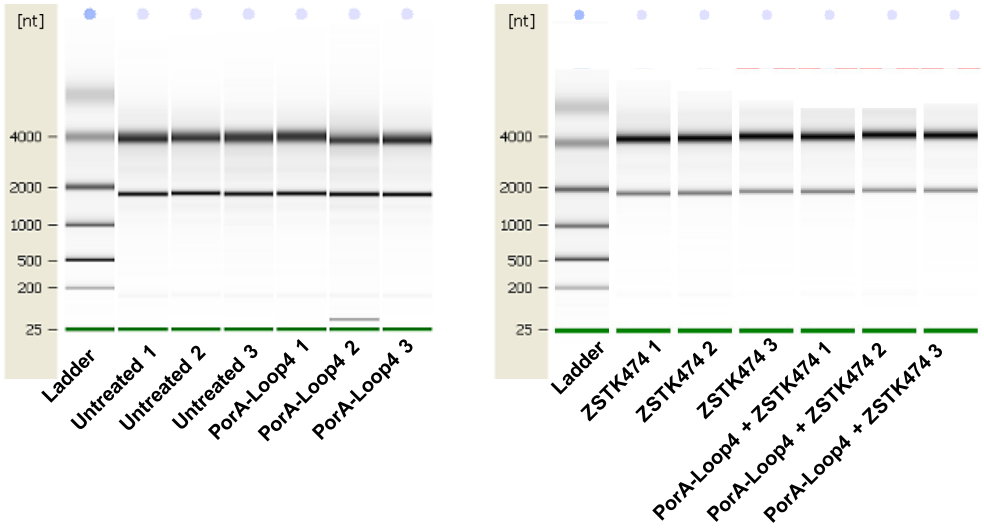
[nt]
4000
2000
1000
500
200
25
Ladder
Untreated 1
Untreated 2
Untreated 3
PorA-Loop4 1
PorA-Loop4 2
PorA-Loop4 3
[nt]
4000
2000
1000
500
200
25
Ladder
ZSTK474 1
ZSTK474 2
ZSTK474 3
PorA-Loop4 + ZSTK474 1
PorA-Loop4 + ZSTK474 2
PorA-Loop4 + ZSTK474 3

E.

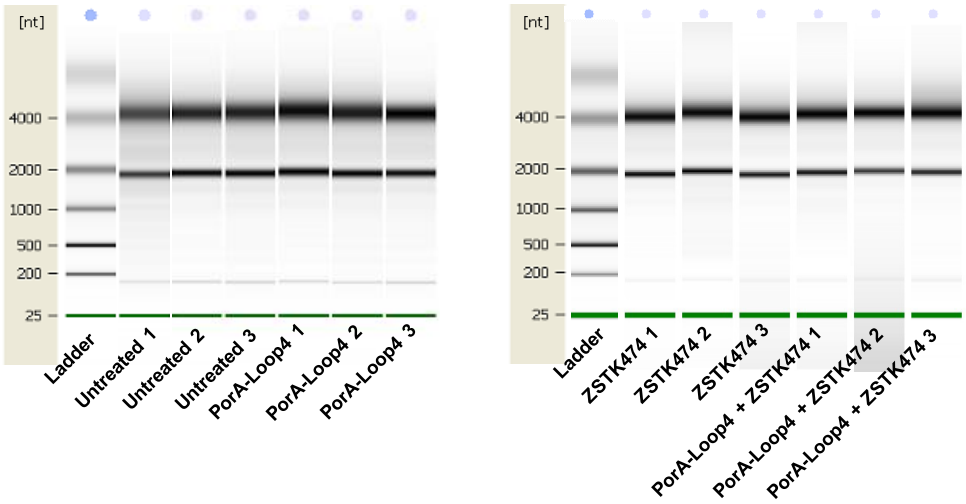
[nt]
4000
2000
1000
500
200
25
Ladder
Untreated 1
Untreated 2
Untreated 3
PorA-Loop4 1
PorA-Loop4 2
PorA-Loop4 3
[nt]
4000
2000
1000
500
200
25
Ladder
ZSTK474 1
ZSTK474 2
ZSTK474 3
PorA-Loop4 + ZSTK474 1
PorA-Loop4 + ZSTK474 2
PorA-Loop4 + ZSTK474 3

Figure A.4: Electrophoregram of mRNA samples extracted from treated cells and the untreated for 0, 2, 4, 8, and 24 h. The cells were treated either with PorA-Loop4 peptide, ZSTK474, or both PorA-Loop4 peptide and ZSTK474. The two distinctive peaks at 2000 and 4000 [nt] represent the ribosomal subunits 28s and 18s from eukaryotic cells RNA.

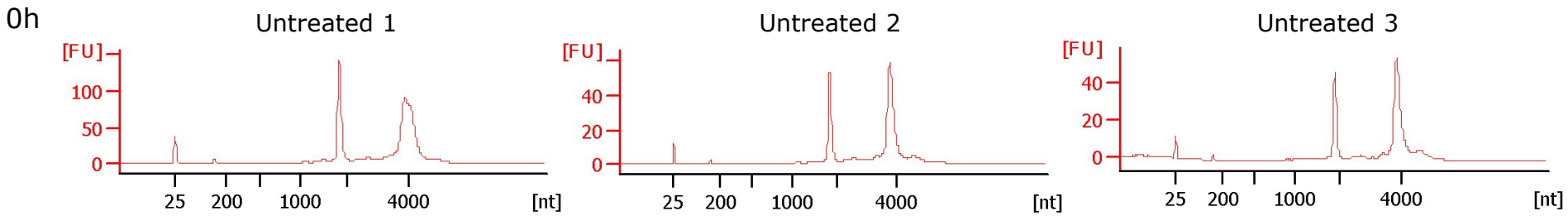

Continue to the next page

2h

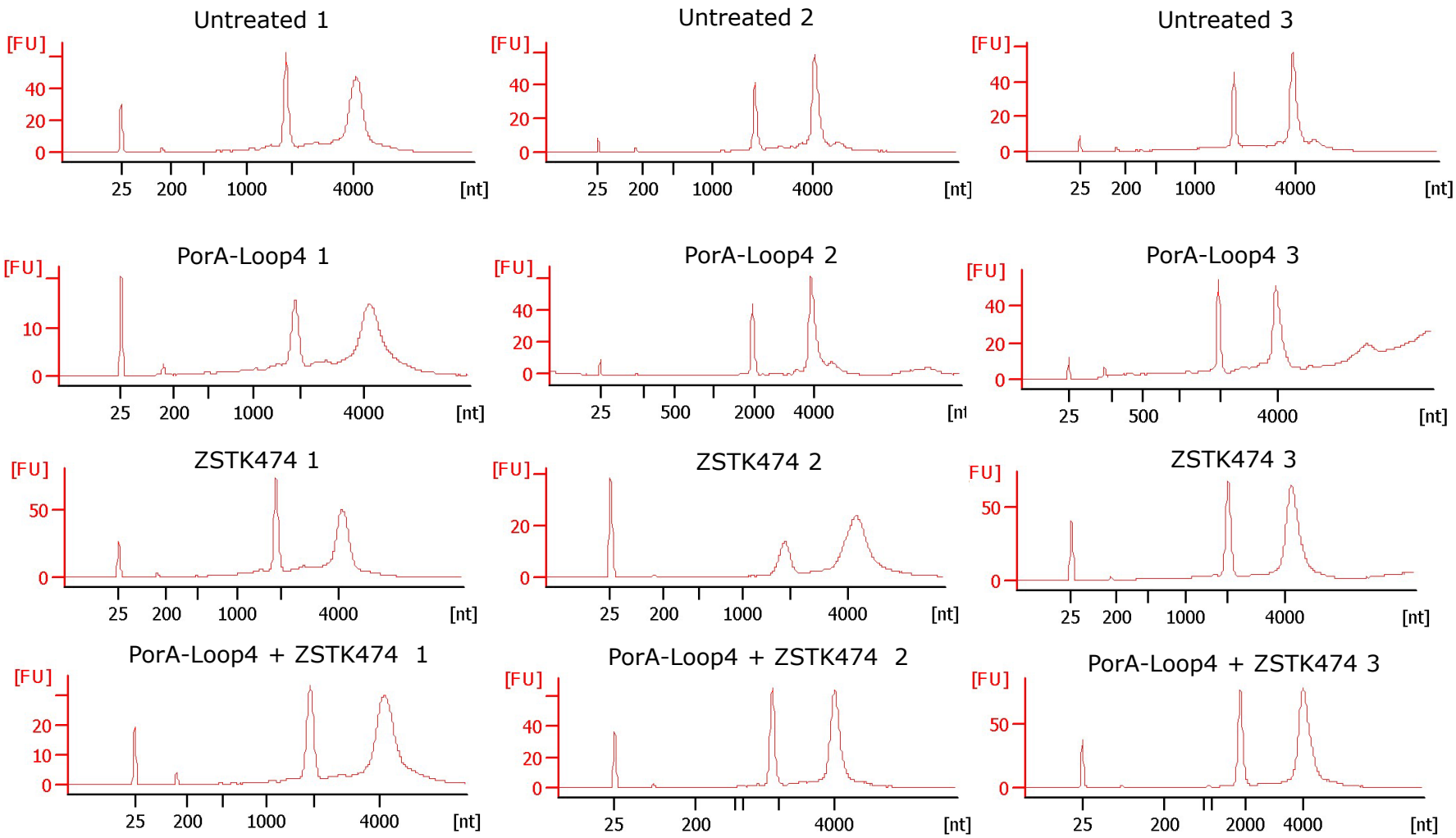

Continue to the next page

4h

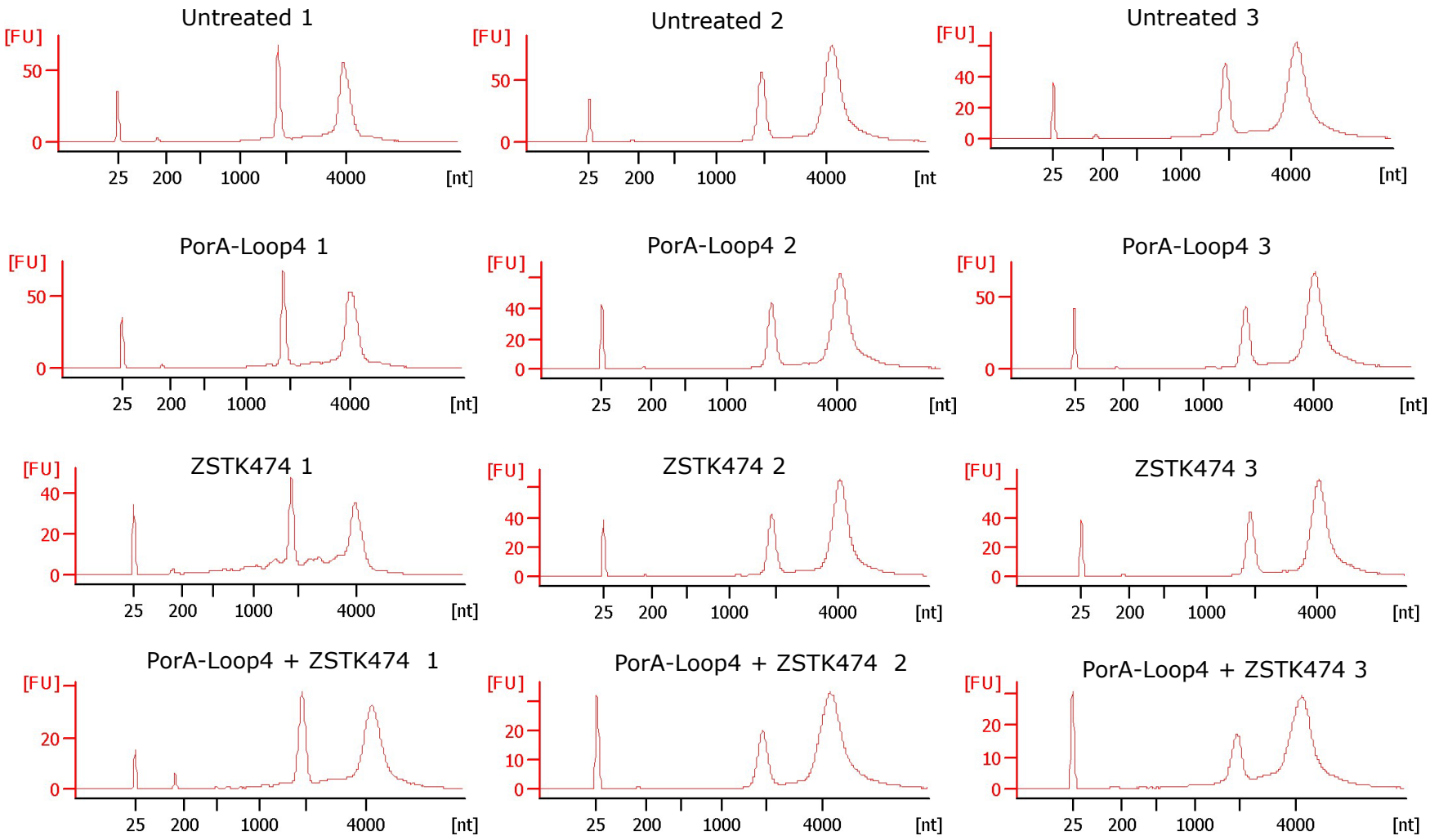

Continue to the next page

8h

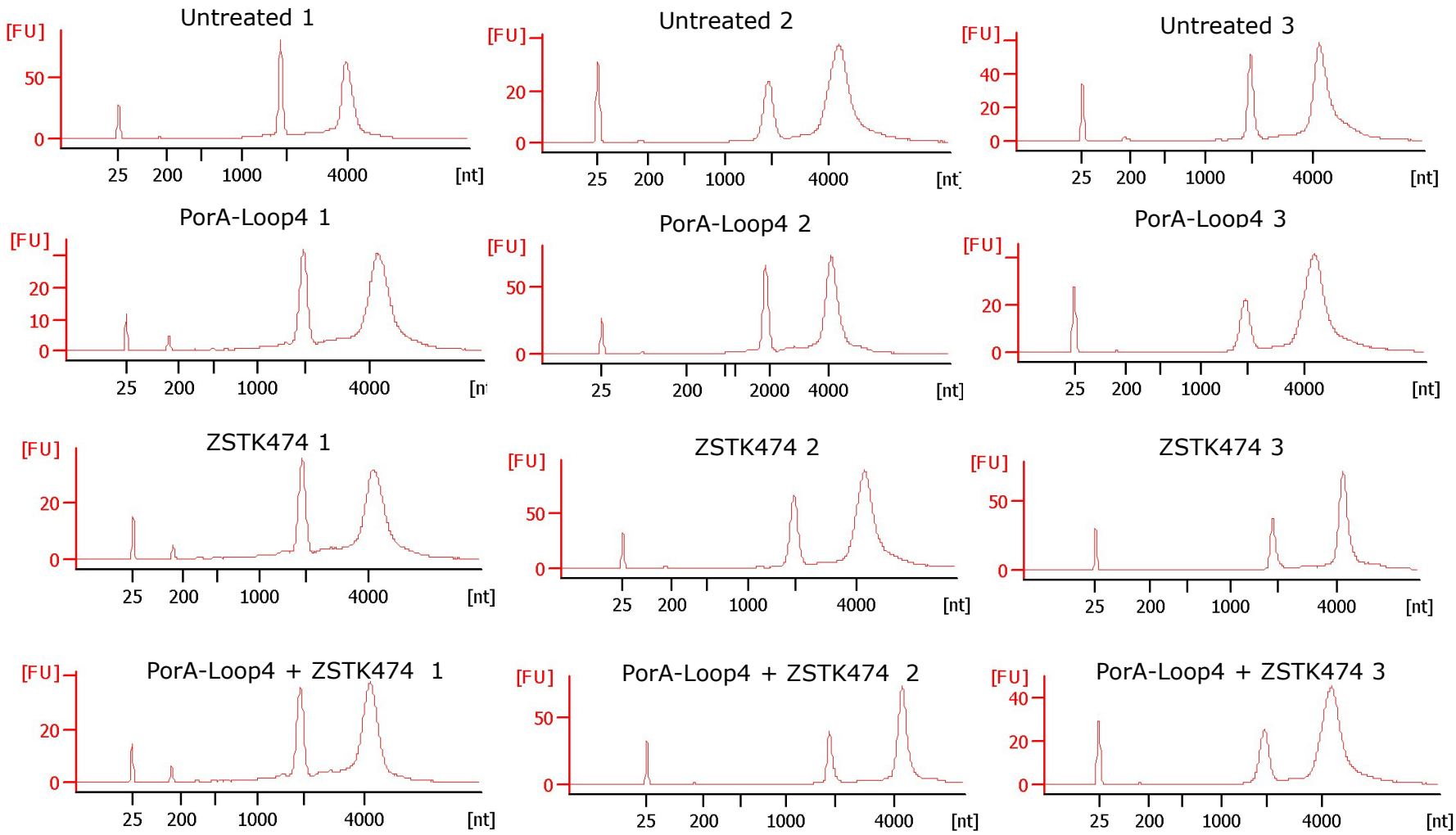

Continue to the next page

24h

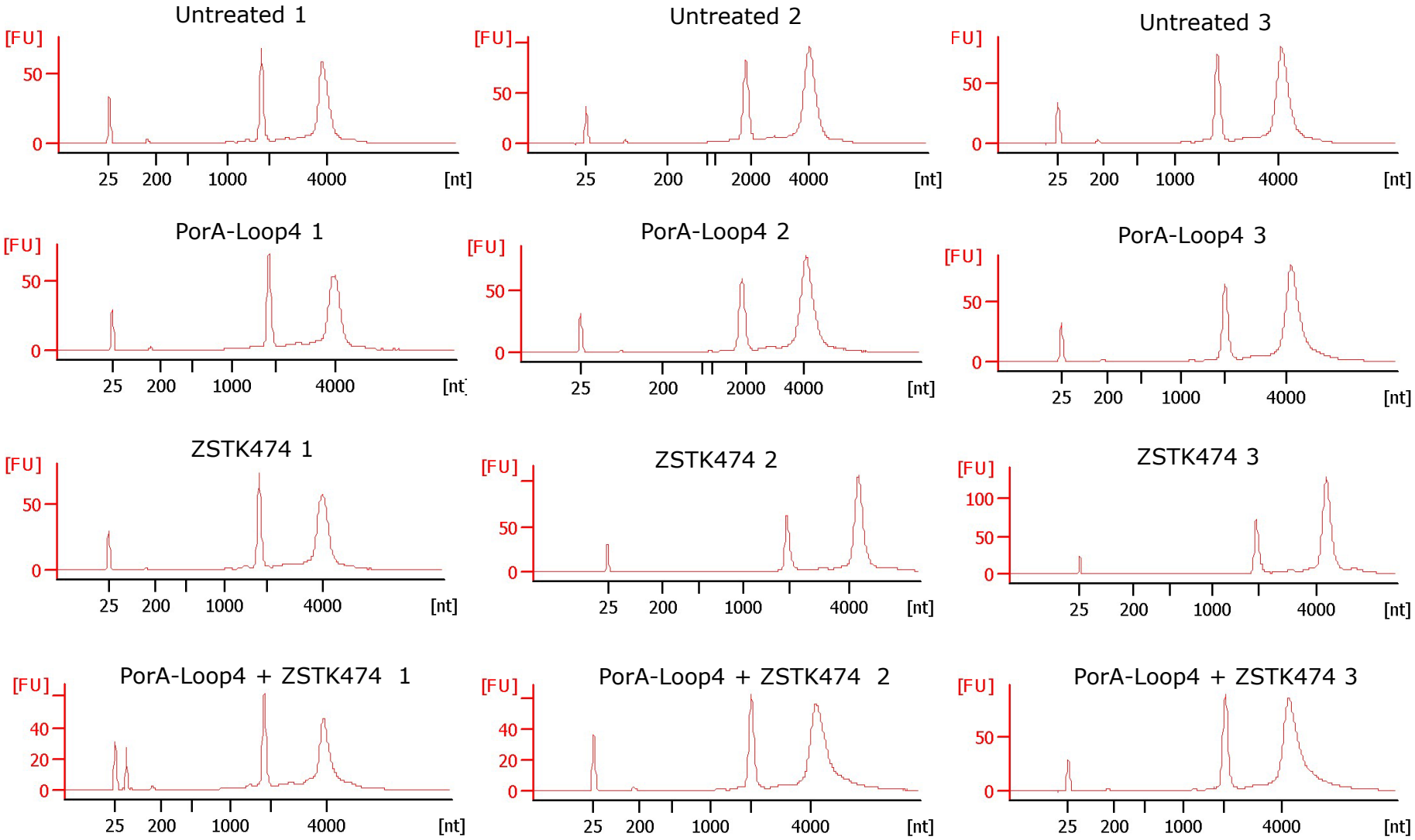
Untreated 1
Untreated 2
Untreated 3
PorA-Loop4 1
PorA-Loop4 2
PorA-Loop4 3
ZSTK474 1
ZSTK474 2
ZSTK474 3
PorA-Loop4 + ZSTK474 1
PorA-Loop4 + ZSTK474 2
PorA-Loop4 + ZSTK474 3
[FU]
[nt]
25
200
1000
2000
4000

Appendix V – Most frequent PorA-Loop4 variants circulating in the UK

Table A.2: Ten most frequent PorA-Loop4 variants from UK meningococcal isolates from serogroup B, W, and Y (2010-2015). Frequency was calculated as isolate number of the variant divided to the total number isolates per serogroup. The total number of meningococcal isolates of serogroup B, W, and Y in the current database was 2395 isolates. The % sequence identity of each variant to MC58 sequence was generated by EMBOSS WATER, pairwise sequence alignment software available on http://www.ebi.ac.uk/Tools/psa/emboss_water/. The sequences in red were the variable regions of the variants.

No.	Loop4 Variant	Sequence	% sequence identity (to MC58, variant 16-2)	Serogroup B (1619 isolates)		Serogroup W (382 isolates)		Serogroup Y (394 isolates)		Total	Frequency (%)
				No. Isolates	Frequency (%)	No. Isolates	Frequency (%)	No. Isolates	Frequency (%)		
1	2	C-PAQNSKSAYTPA**HFVQQTPKSQPTLVP**AVVGKPGS-C	70.3	22	1.36	322	84.29	2	0.51	346	14.45
2	9	C-PAQNSKSAYTPA**YVDEQSKYHA**AVVGKPGS-C	61.1	320	19.77	0	0.00	2	0.51	322	13.44
3	4	C-PIQNSKSAYTPA**HVVVNNKVATHVP**AVVGKPGS-C	75.0	304	18.78	0	0.00	0	0.00	304	12.69
4	14	C-PIQNSKSAYKPA**YVDEKKMVHA**AVVGKPGS-C	61.1	259	16.00	2	0.52	0	0.00	261	10.90
5	10-1	C-PAQNSKSAYTPA**HFVQNKQNQPPTLVP**AVVGKPGS-C	73.0	20	1.24	4	1.05	213	54.06	237	9.90
6	16	C-PIQNSKSAYTPA**YYTKDTNNNLTLVP**AVVGKPGS-C	97.2	115	7.10	3	0.79	10	2.54	128	5.34
7	10-4	C-PAQNSKSAYTPA**HFVQNKQNKQNQPPTLVP**AVVGKPGS-C	67.5	12	0.74	4	1.05	85	21.57	101	4.22
8	15	C-PIQNSKSAYTPA**HYTRQNNADVFVP**AVVGKPGS-C	77.8	86	5.31	0	0.00	0	0.00	86	3.59
9	15-11	C-PIQNSKSAYTPA**HYTRQNNIDVFVP**AVVGKPGS-C	77.8	86	5.31	0	0.00	0	0.00	86	3.59
10	3	C-PAQNSKSAYTPA**TLANGANNTIIRVP**AVVGKPGS-C	69.4	30	1.85	41	10.73	4	1.02	75	3.13